



US Army Corps
of Engineers

MISCELLANEOUS PAPER CERC-89-17

BOLSA BAY, CALIFORNIA, PROPOSED OCEAN ENTRANCE SYSTEM STUDY

Report 2

COMPREHENSIVE SHORELINE RESPONSE COMPUTER SIMULATION, BOLSA BAY, CALIFORNIA

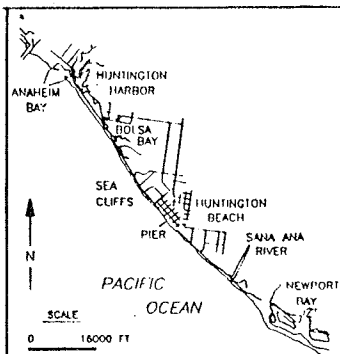
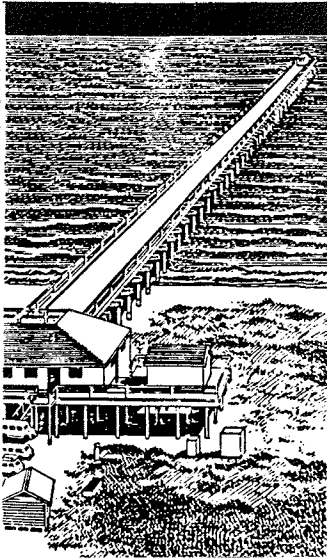
by

Mark B. Gravens

Coastal Engineering Research Center

DEPARTMENT OF THE ARMY

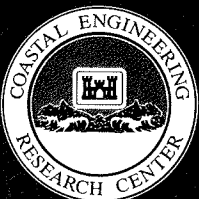
Waterways Experiment Station, Corps of Engineers
3909 Halls Ferry Road, Vicksburg, Mississippi 39180-6199



April 1990

Report 2 of a Series

Approved For Public Release; Distribution Unlimited



Prepared for State of California
State Land Commission

1807 13th Street, Sacramento, California 95814

Destroy this report when no longer needed. Do not return
it to the originator.

The findings in this report are not to be construed as an official
Department of the Army position unless so designated
by other authorized documents.

The contents of this report are not to be used for
advertising, publication, or promotional purposes.
Citation of trade names does not constitute an
official endorsement or approval of the use of
such commercial products.

Unclassified

SECURITY CLASSIFICATION OF THIS PAGE

REPORT DOCUMENTATION PAGE				Form Approved OMB No. 0704-0188	
1a. REPORT SECURITY CLASSIFICATION Unclassified			1b. RESTRICTIVE MARKINGS		
2a. SECURITY CLASSIFICATION AUTHORITY			3. DISTRIBUTION/AVAILABILITY OF REPORT Approved for public release; distribution unlimited.		
2b. DECLASSIFICATION/DOWNGRADING SCHEDULE					
4. PERFORMING ORGANIZATION REPORT NUMBER(S) Miscellaneous Paper CERC-89-17			5. MONITORING ORGANIZATION REPORT NUMBER(S)		
6a. NAME OF PERFORMING ORGANIZATION USAEWES, Coastal Engineering Research Center		6b. OFFICE SYMBOL (if applicable)	7a. NAME OF MONITORING ORGANIZATION		
6c. ADDRESS (City, State, and ZIP Code) 3909 Halls Ferry Road Vicksburg, MS 39180-6199			7b. ADDRESS (City, State, and ZIP Code)		
8a. NAME OF FUNDING/SPONSORING ORGANIZATION State of California, State Lands Commission		8b. OFFICE SYMBOL (if applicable)	9. PROCUREMENT INSTRUMENT IDENTIFICATION NUMBER		
8c. ADDRESS (City, State, and ZIP Code) 1807 13th Street Sacramento, CA 95814			10. SOURCE OF FUNDING NUMBERS		
			PROGRAM ELEMENT NO.	PROJECT NO.	TASK NO.
					WORK UNIT ACCESSION NO.
11. TITLE (Include Security Classification) Bolsa Bay, California, Proposed Ocean Entrance System Study; Report 2, Comprehensive Shoreline Response Computer Simulation, Bolsa Bay, California					
12. PERSONAL AUTHOR(S) Gravens, Mark B.					
13a. TYPE OF REPORT Report 2 of a series		13b. TIME COVERED FROM _____ TO _____		14. DATE OF REPORT (Year, Month, Day) April 1990	
				15. PAGE COUNT 240	
16. SUPPLEMENTARY NOTATION Available from National Technical Information Service, 5285 Port Royal Road, Springfield, VA 22161.					
17. COSATI CODES			18. SUBJECT TERMS (Continue on reverse if necessary and identify by block number)		
FIELD	GROUP	SUB-GROUP			
			Beach erosion Huntington Beach		
			Bolsa Chica Shoreline change		
			Coastal processes Southern California		
19. ABSTRACT (Continue on reverse if necessary and identify by block number)					
<p>This report describes an application of the shoreline change numerical model GENESIS in the assessment of potential shoreline impacts resulting from the construction of a structured inlet entrance system at Bolsa Chica, California. The methodology of shoreline change modeling, including the preliminary steps of data collection, analysis, and preparation for input to the shoreline change model is discussed, as well as interpretation of model results. In this study, three simultaneous independent wave sources (Northern Hemisphere swell, Southern Hemisphere swell, and locally generated wind sea) were used to drive the shoreline change model. In addition to estimating potential shoreline impacts, three project impact mitigation design alternatives were quantitatively investigated.</p>					
20. DISTRIBUTION/AVAILABILITY OF ABSTRACT <input checked="" type="checkbox"/> UNCLASSIFIED/UNLIMITED <input type="checkbox"/> SAME AS RPT. <input type="checkbox"/> DTIC USERS			21. ABSTRACT SECURITY CLASSIFICATION Unclassified		
22a. NAME OF RESPONSIBLE INDIVIDUAL			22b. TELEPHONE (Include Area Code)		22c. OFFICE SYMBOL

DD Form 1473, JUN 86

Previous editions are obsolete.

SECURITY CLASSIFICATION OF THIS PAGE

Unclassified

PREFACE

This report describes the procedures and results of a study to predict the long-term evolution of the shoreline along the southern California coast bounded by Anaheim Entrance to the north and Santa Ana River to the south. The study was sponsored by the California State Lands Commission (SLC) through a Memorandum of Agreement between SLC and the Department of the Army signed 2 July 1987. The study was conducted at the US Army Engineer Waterways Experiment Station's (WES) Coastal Engineering Research Center (CERC) under authority of Title III of the Intergovernmental Cooperation Act of 1968. As such, resultant study products are based on specific technical expertise only and should not be inferred to indicate support or nonsupport of any subsequent project.

The investigation reported herein was conducted between 1 June 1988 and 31 May 1989. Mr. Mark B. Gravens, Coastal Processes Branch (CPB), Research Division (RD), CERC, was principal investigator for the shoreline response modeling efforts and wrote the technical sections of the main report. Drs. Lyndell Z. Hales, CPB, RD, CERC, and Steven A. Hughes, Wave Dynamics Division, CERC, wrote sections of the report covering background information common to other Bolsa Chica Study reports. Dr. Nicholas C. Kraus, RD, CERC, provided technical guidance and review. Mr. David P. Simpson, CPB, RD, CERC, and Dr. Norman W. Scheffner, CPB, RD, CERC, made substantial editorial contributions during the preparation of this report.

During the conduct of the shoreline response study, supplementary topics for study were identified and performed by WES as authorized through an amendment to the original Memorandum of Agreement. These supplemental studies include a stability analysis of the non-navigable and navigable entrance system alternatives and an investigation into the effect the navigable entrance system would have on the surfability of the local wave break. The results of these investigations are described in Appendix C (Stability Analysis of Proposed Ocean Entrance Channels, Bolsa Chica, California) written by Dr. Steven A. Hughes, and Appendix D (Bolsa Chica Surf Climate Studies) written by Dr. William R. Dally, Florida Institute of Technology.

This investigation was performed under general supervision of Dr. James R. Houston and Mr. Charles C. Calhoun, Jr., Chief and Assistant Chief, CERC,

respectively; and direct supervision of Mr. H. Lee Butler, Chief, RD, CERC, and Mr. Bruce A. Ebersole, Chief, CPB, RD, CERC.

Project Managers during the conduct of this investigation and preparation of the report were Mr. Daniel Gorfain for SLC and Dr. Steven A. Hughes for WES.

COL Larry B. Fulton, EN, was Commander and Director during final preparation and publication of this report. Technical Director was Dr. Robert W. Whalin.

CONTENTS

	<u>Page</u>
PREFACE	1
LIST OF TABLES	5
LIST OF FIGURES	5
CONVERSION FACTORS, NON-SI TO SI (METRIC) UNITS OF MEASUREMENT	11
PART I: INTRODUCTION	12
Bolsa Chica Modeling Studies	12
Purpose of the Study	15
Scope of the Investigation	15
PART II: BACKGROUND	17
Description of the Bolsa Chica Area	17
Historical Perspective	23
Proposed Improvements	25
Previous Studies	29
Regional Geology	34
Subsidence in the Bolsa Chica Area	35
Sea Level Rise in the Bolsa Chica Area	36
PART III: SHORELINE CHANGE MODELING	43
Overview of Methodology	43
Description of the Wave Model RCPWAVE	47
Description of the Shoreline Evolution Model GENESIS	50
PART IV: SHORELINE CHANGE MODEL CALIBRATION AND VERIFICATION	53
Historical Shoreline Positions and Shoreline Movement	53
Nearshore Bathymetry	64
Analysis of Wave Data	66
Potential Longshore Sand Transport Rates	73
Selection of Wave Climatology	76
Model Calibration and Verification	78
PART V: SHORELINE CHANGE MODEL TESTS: PROPOSED NAVIGABLE ENTRANCE	89
Model Tests	89
Results	90
Shoreline Impact Mitigation: Requirements, Criteria, and Plans	130

PART VI: DISCUSSION OF RESULTS AND CONCLUSIONS	153
Summary of Model Results	153
Conclusions	154
REFERENCES	156
APPENDIX A: PRELIMINARY STUDY	A1
APPENDIX B: SOUTHERN CALIFORNIA HINDCAST	B1
APPENDIX C: STABILITY ANALYSIS OF PROPOSED OCEAN ENTRANCE CHANNELS, BOLSA CHICA, CALIFORNIA	C1
APPENDIX D: BOLSA CHICA SURF CLIMATE STUDIES	D1
APPENDIX E: NOTATION.	E1

LIST OF TABLES

<u>No.</u>		<u>Page</u>
1.	Summary of Shoreline Position Data Sets	54
2.	Shoreline Position Change, Santa Ana River to Anaheim Bay, CA (Base Year 1878)	58
3.	Shoreline Position Change, Santa Ana River to Anaheim Bay, CA (Base Year 1934)	59
4.	Shoreline Position Change, Santa Ana River to Anaheim Bay, CA (Base Year 1937)	60
5.	Shoreline Position Change, Santa Ana River to Anaheim Bay, CA (Base Year 1949)	61
6.	Shoreline Position Change, Santa Ana River to Anaheim Bay, CA (Base Years 1958 and 1963)	62
7.	Shoreline Position Change, Santa Ana River to Anaheim Bay, CA (Base Years 1967, 1969, and 1970)	63
8.	Summary of Modeled Design Alternatives.	89
C1.	Non-Navigable Entrance Tidal Prism Values	C10
C2.	Navigable Entrance Tidal Prism Values	C17
D1.	Surf Climate Classifications.	D3
D2.	Joint Probability of Wave Height and Period	D10
D3.	Probability of Breaker Angle and Direction.	D11
D4.	Joint Probability of Wind Speed and Direction	D15
D5.	Percent Occurrence of Observed Breaker Types.	D18
D6.	Peel Rates for Diffracted Waves from Physical Model	D27

LIST OF FIGURES

<u>No.</u>		<u>Page</u>
1.	Bolsa Chica, California, study region location (after Orange County Environmental Management Agency 1985)	18
2.	Bolsa Chica, California, area of interest (after Orange County Environmental Management Agency 1985).	19
3.	Present tidal inundation, Bolsa Chica, California (after Orange County Environmental Management Agency 1985)	20
4.	Land ownership, Bolsa Chica, California, region (after Orange County Environmental Management Agency 1985)	22
5.	Bolsa Bay Preferred Alternative; (a) adopted land use plan, and (b) revised land use plan	26
6.	Bolsa Bay Secondary Alternative (after Orange County Environmental Management Agency 1985)	28
7.	Historical subsidence near Huntington Beach, California (after Woodward-Clyde Consultants 1984)	37
8.	Average annual subsidence rate, 1976 to 1982, Bolsa Chica region (after Woodward-Clyde Consultants 1984)	38
9.	Average annual subsidence rate, 1976 to 1985, Bolsa Chica region (after Woodward-Clyde Consultants 1986)	39
10.	Average annual subsidence rate, 1982 to 1985, Bolsa Chica region (after Woodward-Clyde Consultants 1986)	40

11.	Schematic of eustatic sea level rise curves, (A) Rate of rise over last century projected into the future, (B), (C), (D), and (E) Hoffman et al. (1983) estimates respectively for conservative, mid-range low, mid-range high, and high rates of increase, (F) Revelle (1983), (G) Polar Research Board estimate augmented for thermal expansion (Revelle 1983) (after Dean 1986)	41
12.	Illustration of an idealized equilibrium beach profile and control volume for longshore sand transport continuity	46
13.	RCPWAVE bathymetry grid	49
14.	Angle band definition sketch	50
15.	Shoreline positions, 1878-1949	55
16.	Shoreline positions, 1949-1967	56
17.	Shoreline positions, 1967-1983	57
18.	Representative beach profiles at Bolsa Chica	65
19.	Transformation from Stations 14 and 11 to the RCPWAVE bathymetry grid	69
20.	Distribution of incident wave angles at 26.9 ft depth	70
21.	Distribution of wave period	71
22.	Distribution of wave height	72
23.	Total littoral drift rose for Anaheim Bay to Santa Ana River (20-year-long hindcast data base)	75
24.	Total littoral drift rose for Anaheim Bay to Santa Ana River (selected 10-year time history of representative wave conditions)	77
25.	Model calibration results	80
26.	Model calibration: surveyed vs. calculated shoreline change	82
27.	Average annual longshore sand transport rates for the calibration period (1963 -1970)	83
28.	Effect of the Huntington Pier boundary condition	84
29.	Model verification results	86
30.	Model verification: surveyed vs. calculated shoreline change	87
31.	Average annual longshore sand transport rates for the verification period (1970 - 1983)	88
32.	Alternative WP1A: without-project, without feeder beach	91
33.	Alternative WP1A: average annual longshore sand transport rates	92
34.	Alternative WP1B: without-project, without feeder beach, year 1 southern swell wave conditions	93
35.	Alternative WP1B: average annual longshore sand transport rates	94
36.	Alternative WP1C: without-project, without feeder beach, year 2 southern swell wave conditions	95
37.	Alternative WP1C: average annual longshore sand transport rates	96
38.	Alternative WP2A: without-project, with feeder beach	98
39.	Alternative WP2A: average annual longshore sand transport rates	99
40.	Alternative WP2B: without-project, with feeder beach, year 1 southern swell wave conditions	100
41.	Alternative WP2B: average annual longshore sand transport rates	101

42.	Alternative WP2C: without-project, with feeder beach, year 2 southern swell wave conditions	102
43.	Alternative WP2C: average annual longshore sand transport rates	103
44.	Alternative PRO1A: preferred alternative, without feeder beach	105
45.	Alternative PRO1A: average annual longshore sand transport rates	106
46.	Alternative PRO1B: preferred alternative, without feeder beach, year 1 southern swell wave conditions	107
47.	Alternative PRO1B: average annual longshore sand transport rates	108
48.	Alternative PRO1C: preferred alternative, without feeder beach, year 2 southern swell wave conditions	109
49.	Alternative PRO1C: average annual longshore sand transport rates	110
50.	Alternative PRO2A: preferred alternative, with feeder beach	112
51.	Alternative PRO2A: average annual longshore sand transport rates	113
52.	Alternative PRO2B: preferred alternative, with feeder beach, year 1 southern swell wave conditions	114
53.	Alternative PRO2B: average annual longshore sand transport rates	115
54.	Alternative PRO2C: preferred alternative, with feeder beach, year 2 southern swell wave conditions	116
55.	Alternative PRO2C: average annual longshore sand transport rates	117
56.	Alternative PUC2A: upcoast site, with feeder beach	118
57.	Alternative PUC2A: average annual longshore sand transport rates	119
58.	Alternative PUC2B: upcoast site, with feeder beach, year 1 southern swell wave conditions	120
59.	Alternative PUC2B: average annual longshore sand transport rates	121
60.	Alternative PUC2C: upcoast site, with feeder beach, year 2 southern swell wave conditions	122
61.	Alternative PUC2C: average annual longshore sand transport rates	123
62.	Alternative PDC2A: downcoast site, with feeder beach	124
63.	Alternative PDC2A: average annual longshore sand transport rates	125
64.	Alternative PDC2B: downcoast site, with feeder beach, year 1 southern swell wave conditions	126
65.	Alternative PDC2B: average annual longshore sand transport rates	127
66.	Alternative PDC2C: downcoast site, with feeder beach, year 2 southern swell wave conditions	128
67.	Alternative PDC2C: average annual longshore sand transport rates	129
68.	Predicted shoreline change from 1983 shoreline position (a) Alternative WP1A vs. Alternative PRO1A (b) Alternative WP2A vs. Alternative PRO2A.	131

69.	Predicted shoreline change from 1983 shoreline position	
	(a) Alternative WP1B vs. Alternative PRO1B	
	(b) Alternative WP2B vs. Alternative PRO2B.	132
70.	Predicted shoreline change from 1983 shoreline position	
	(a) Alternative WP1C vs. Alternative PRO1C	
	(b) Alternative WP2C vs. Alternative PRO2C.	133
71.	Alternative SM1A: sand management, without feeder beach.	137
72.	Alternative SM1A: average annual longshore sand transport rates	138
73.	Alternative SM2A: sand management, with feeder beach	139
74.	Alternative SM2A: average annual longshore sand transport rates	140
75.	Predicted shoreline change from 1983 shoreline position	
	(a) Alternative WP1A vs. Alternative SM1A	
	(b) Alternative WP2A vs. Alternative SM2A	141
76.	Alternative SM1B: sand management, without feeder beach.	142
77.	Alternative SM1B: average annual longshore sand transport rates	143
78.	Alternative SM2B: sand management, with feeder beach	144
79.	Alternative SM2B: average annual longshore sand transport rates	145
80.	Predicted shoreline change from 1983 shoreline position	
	(a) Alternative WP1B vs. Alternative SM1B	
	(b) Alternative WP2B vs. Alternative SM2B	146
81.	Alternative SM1C: sand management, without feeder beach.	147
82.	Alternative SM1C: average annual longshore sand transport rates	148
83.	Alternative SM2C: sand management, with feeder beach	149
84.	Alternative SM2C: average annual longshore sand transport rates	150
85.	Predicted shoreline change from 1983 shoreline position	
	(a) Alternative WP1C vs. Alternative SM1C	
	(b) Alternative WP2C vs. Alternative SM2C	152
A1.	Average annual longshore sand transport rate (Preliminary model with corrected input wave conditions)	A2
B1.	Wave Information Study (WIS) Phase I grid for the North Pacific (2 deg, Mercator projection).	B3
B2.	Southern California Bight study area, (10-nm grid) Meteorological stations.	B4
B3.	X'(t) and Y'(t) average response function for land station wind information mean conditions for all Januarys 1956-1975 (vertical lines represent one standard deviation)	B5
B4.	Comparison between hindcast and measured energy based wave heights and peak spectral wave periods (NDBC 46042 located 36.8N, 122.4W).	B12
B5.	Comparison between hindcast and measured energy based wave heights and peak spectral wave periods (NDBC 46028 located 35.8N, 121.9W).	B13
B6.	Comparison between hindcast and measured energy based wave heights and peak spectral wave periods (NDBC 46011 located 34.9N, 120.9W).	B14

B7.	Comparison between hindcast and measured energy based wave heights and peak spectral wave periods (NDBC 46025 located 33.7N, 119.1W)	B15
C1.	Non-navigable entrance channel alternative - conceptual layout	C5
C2.	Non-navigable ocean entrance channel cross-section.	C6
C3.	Non-navigable entrance channel - water surface elevations.	C7
C4.	Non-navigable entrance channel - water velocities.	C8
C5.	Non-navigable entrance channel - flow discharge.	C9
C6.	Non-navigable entrance channel tidal prism vs throat area, all inlets on Pacific coast.	C11
C7.	Non-navigable entrance channel tidal prism vs throat area, inlets on Pacific coast with one or no jetties	C12
C8.	Navigable entrance channel alternative - conceptual layout	C16
C9.	Navigable ocean entrance channel cross-section	C17
C10.	Navigable entrance channel - water surface elevations	C18
C11.	Navigable entrance channel - water velocities	C19
C12.	Navigable entrance channel - flow discharge	C20
C13.	Navigable entrance channel tidal prism vs throat area, inlets on Pacific coast with one or no jetties	C21
D1.	Schematic diagram of obliquely incident waves arriving at the surf zone. Due to angle between wave crests and bottom contours, break point translates along the beach at a finite speed	D4
D2.	Schematic diagram of normally incident waves breaking over irregular bottom topography (crescentic bar). Two break points form and translate in opposite directions	D6
D3.	Schematic diagram of obliquely incident waves reflecting from a shore-normal structure. Point where wave crests superimpose steepens to form a "bowl" that translates opposite to the direction of incident waves	D7
D4.	Histograms of maximum breaking wave height for Bolsa Chica generated from LEO data. Mean height is 2.2 ft in (4a) and 2.4 ft in (4b)	D12
D5.	Histograms of mean wave period for Bolsa Chica. Average value in (5a) is 13.2 s and in (5b) 13.1 s	D13
D6.	Histograms of wind speed generated from LEO data	D16
D7.	Histograms of wind direction	D17
D8.	Averaged bottom profile for the beach at Bolsa Chica. Mean bottom slope between MLLW and -5.0 ft is approximately 1/45	D19
D9.	Histograms of Irribarren Number generated from LEO data. Most waves fall within the range of values for plunging breakers	D20
D10.	Wave rose oriented and positioned at 27 ft contour at site of proposed navigation project. Generated from one year of LEO data and transformed using linear wave theory (after Gravens, 1988).	D23
D11.	Schematic diagram of proposed navigation project and primary impacts on surf climate for dominant wave direction	D24
D12.	Shadow zone cast by offshore breakwater for the three dominant wave directions at Bolsa Chica	D25
D13.	Shadow zone cast by offshore breakwater and jetties for the two secondary wave directions.	D26

D14. Projected shoreline response (Gravens, 1988) and expected changes in local Irribarren Number due to changes in mean bottom slope. Under this particular scenario, surfing conditions should improve updrift of the project D29

CONVERSION FACTORS, NON-SI TO SI (METRIC)
UNITS OF MEASUREMENT

Non-SI units of measurement used in this report can be converted to SI (metric) units as follows:

<u>Multiply</u>	<u>By</u>	<u>To Obtain</u>
cubic yards	0.7646	cubic meters
feet	0.3048	meters
inches	2.5400	centimeters
knots (international)	0.5144	meters per second
miles (US statute)	1.6093	kilometers
miles (nautical)	1.8520	kilometers
square feet	0.0929	square meters
yards	0.9144	meters

BOLSA BAY, CALIFORNIA
PROPOSED OCEAN ENTRANCE SYSTEM STUDY

COMPREHENSIVE SHORELINE RESPONSE COMPUTER SIMULATION

BOLSA BAY, CALIFORNIA

PART I: INTRODUCTION

Bolsa Chica Modeling Studies

1. The State of California, State Lands Commission (SLC), is reviewing a plan for a new ocean entrance system as part of a multi-use project. This project involves both State and private property in the proposed development by the SLC, Signal Landmark, and others. The project, located in the Bolsa Chica area of the County of Orange, California, includes navigational, commercial, recreational, and residential uses, together with major wetlands restoration. The County of Orange approved a Land Use Plan (LUP) in 1985 as part of the Local Coastal Program for Bolsa Chica in accordance with the California Coastal Act of 1976. This same LUP was certified with conditions by the California Coastal Commission (CCC) in 1986. Part of the LUP certification requirement to satisfy those conditions include confirmation review of modeling studies of a navigable and a non-navigable ocean entrance at Bolsa Chica.

2. In order to satisfy the CCC requirements for confirmation of the LUP, the SLC requested the US Army Engineer Waterways Experiment Station (WES), through a Memorandum of Agreement executed 2 July 1987, to conduct engineering, technical, and environmental studies to assess a navigable ocean entrance system and a non-navigable ocean entrance system as conditionally approved in the LUP. Results of these studies will assist SLC and other parties which are formulating reports and plans for the proposed Bolsa Bay project that meet the criteria set forth in Policies 23 through 26 of the LUP. These services were provided to SLC by WES under authority of Title III of the Intergovernmental Cooperation Act of 1968. As such, resultant study products are based on specific technical expertise only and should not be inferred to

indicate support or non-support by the Corps of Engineers for either project involving a navigable or non-navigable ocean entrance, or for the environmental or economic aspects of these or any other subsequent project.

3. Four general categories of modeling studies of the Bolsa Chica area conducted by WES:

- a. Numerical modeling of long-term shoreline response as influenced by placement of entrance channel stabilization structures, including sand management concepts.
- b. Physical modeling of the proposed entrance channel, interior channels, and marina with regard to wave penetration, harbor oscillation, and qualitatively inferred sediment movement paths.
- c. Numerical modeling of tidal circulation, including transport and dispersion of conservative tracers, in the Bolsa Bay, Huntington Harbour, and Anaheim Bay complex.
- d. Potential impacts of various ocean entrance designs on the local wave climate and, consequently, the potential impacts on recreational surfing activities at the proposed ocean entrance.

4. Detailed results of the modeling studies are given in four separate reports. The title and a short description of each report scope are given below.

Report 1: Preliminary Shoreline Response Computer Simulation

5. This report describes numerical model simulations of long-term shoreline position change as a result of longshore movement of sediment. The model simulations were termed preliminary because of uncertainties associated with the input wave data. Shoreline change simulations covering a 10-year period over the reach of coast from Anaheim entrance southward to the Santa Ana River are compared for a variety of conditions, including a non-navigable entrance, a structured navigable entrance without sand management, and a structured navigable entrance with sand management techniques. This study was conducted to determine a reasonable range of shoreline response to construction of an entrance system, and to evaluate the potential for mitigation of any adverse effects induced by the entrance. The preliminary modeling was conducted in advance of a special Coastal Commission required "Confirmation Review" hearing on the Bolsa Chica LUP, and in advance of detailed wave hindcasts utilized during the Comprehensive Shoreline Response Computer Simulation described in the present report.

Report 2: Comprehensive Shoreline Response Computer Simulation

6. This report describes numerical model simulations of long-term shoreline change under the same conditions as tested in the preliminary modeling described in Report 1. The comprehensive modeling effort utilizes hindcast wave data obtained from the Wave Information Study (WIS) of the Corps of Engineers. These hindcast data represent the best available wave data for use in the shoreline model. Partial funding of the WIS hindcast at Bolsa Chica was provided by SLC as part of the overall Bolsa Chica Study. This report also contains a stability analysis of the proposed non-navigable entrance channel.

Report 3: Tidal Circulation and Transport Computer Simulation and Water Quality Assessment

7. This report describes numerical model simulations of tidal circulation and constituent transport in the Bolsa Bay, Huntington Harbour, and Anaheim Bay complex. A link-node model was calibrated and verified using data from the present configuration of the tidally-subjected region. The calibrated numerical model was then used to simulate a variety of proposed area developments, including increased wetlands, full tidal and muted tidal areas, marinas, and navigation channels. Modeling provided results for the proposed navigable and non-navigable entrance alternatives, with and without a navigable connector channel to Huntington Harbour from Outer Bolsa Bay. Water quality assessment is provided based on existing conditions and data, coupled with constituent transport modeling results. The transport modeling results provide estimates of water flushing and residence times which are used to project water quality parameters expected in the new wetlands configuration.

Report 4: Physical Model Simulation

8. This report describes results obtained from tests conducted in a 1-to-75 model-to-prototype scale physical model of the proposed Bolsa Bay entrance channel and marina complex. The purpose of the testing was to examine wave penetration into the marina basin and the resulting harbor oscillations, to qualitatively study current circulation and sediment transport paths in the vicinity of the structures, and to make preliminary assessment of the entrance channel design configuration. Physical model inputs included unidirectional irregular waves, steady-state flood and ebb tidal currents, and flood flows from the East Garden Grove-Wintersburg Flood Control Channel.

Purpose of the Study

9. Numerical models of shoreline change provide a means to evaluate shoreline evolution produced by the longshore transport of beach sediment. The results of the modeling effort described in this report will provide decision makers with a quantitative foundation on which to make feasibility and impact assessments of the proposed ocean entrance system at Bolsa Chica. Hence, the purpose of the Comprehensive Shoreline Response Computer Simulation Task was to utilize the best available wave data and shoreline change information to develop, calibrate, and verify a shoreline change computer model for the project coast. The model is then used to assess and quantify potential shoreline impacts of the proposed ocean entrance system at Bolsa Chica. The estimates of the magnitude of effects are sufficiently accurate to formulate conclusions regarding the ability to mitigate impacts to a prescribed level.

Scope of the Investigation

10. The scope of work for this task as outlined in the Management Plan for the Proposed Bolsa Bay, California, New Ocean Entrance System Study includes the following:

- a. Collect and review existing wave and shoreline processes data at and adjacent to the project.
- b. Develop and calibrate a shoreline response prediction model to estimate the impacts of and develop mitigation methods for the proposed navigable and non-navigable entrance channels on adjacent beaches.
- c. Identify and compare available wave data sources. Perform a nearshore wave transformation analysis using the Regional Coastal Processes WAVE (RCPWAVE) model.
- d. Calibrate and verify the GENERALized model for SIMulating Shoreline change (GENESIS) using known quantities of beach nourishment material placed on the shore and historical shoreline evolution from surveyed shoreline positions.
- e. Perform simulations with the verified shoreline response model to predict future shoreline change of the shoreline under consideration resulting from construction of a navigable entrance channel into Bolsa Bay from the Pacific Ocean.

- f. Perform simulations to assess impacts of the proposed navigable entrance channel using higher- and lower-energy intensities of the input wave time series to obtain estimates of project impact over a wider range of wave climates.

PART II: BACKGROUND

Description of the Bolsa Chica Area

11. Bolsa Chica is an unincorporated area of Orange County, California, located along the coastline approximately 9 miles* south of Long Beach and surrounded by the City of Huntington Beach (Figure 1). The Bolsa Chica project area (Figure 2) comprises approximately 1,645 acres, which includes the Bolsa Mesa and adjacent lowlands, and the shoreline adjacent to the Bay from the intersection of Warner Avenue and the Pacific Coast Highway (PCH) to the Huntington Mesa, located to the north of the intersection of Golden West Boulevard and the PCH. As discussed by the US Army Engineer District, Los Angeles (1987), the project area is bordered by bluffs on the northwest and southeast, and by the Pacific Coast Highway and Bolsa Chica Beach State Park on the southwest. Urban lands lie north and east of the project area.

12. The Bolsa lowland area is a remnant of a once-extensive tidal and river wetlands system of the mouth of the Santa Ana River which extended inland across the coastal plain to the surrounding mountains. Historically, the lowlands were frequently inundated by tidal flows through a direct natural connection to the ocean, and received fresh water from artesian wells and from local storm-water runoff. In 1899 tidal flow into the Bolsa Chica area was modified by construction of tide gates, and the natural channel to the ocean was eventually closed. The Bolsa Chica area was further modified in the 1920s by oil and gas interests, and construction of PCH. Subsequently, construction of the East Garden Grove-Wintersburg Flood Control Channel bisected the area, and its flow discharged into Outer Bolsa Bay and then into Huntington Harbour.

13. At present, tidal flow enters Outer Bolsa Bay and Inner Bolsa Bay (Figure 3) only through Huntington Harbour and Anaheim Bay. Local runoff and precipitation provide the freshwater inflow. Dirt roads and dikes criss-cross the lowland connecting drill pads, oil pumping rigs, related structures, and pipe networks. Other existing improvements include the East Garden Grove-Wintersburg Flood Control Channel, bridges that cross the channel, tide gates at the confluence of the flood control channel and Outer Bolsa Bay, and a

* A table of factors for converting non-SI units of measurements to SI (metric) units is presented on page 11.

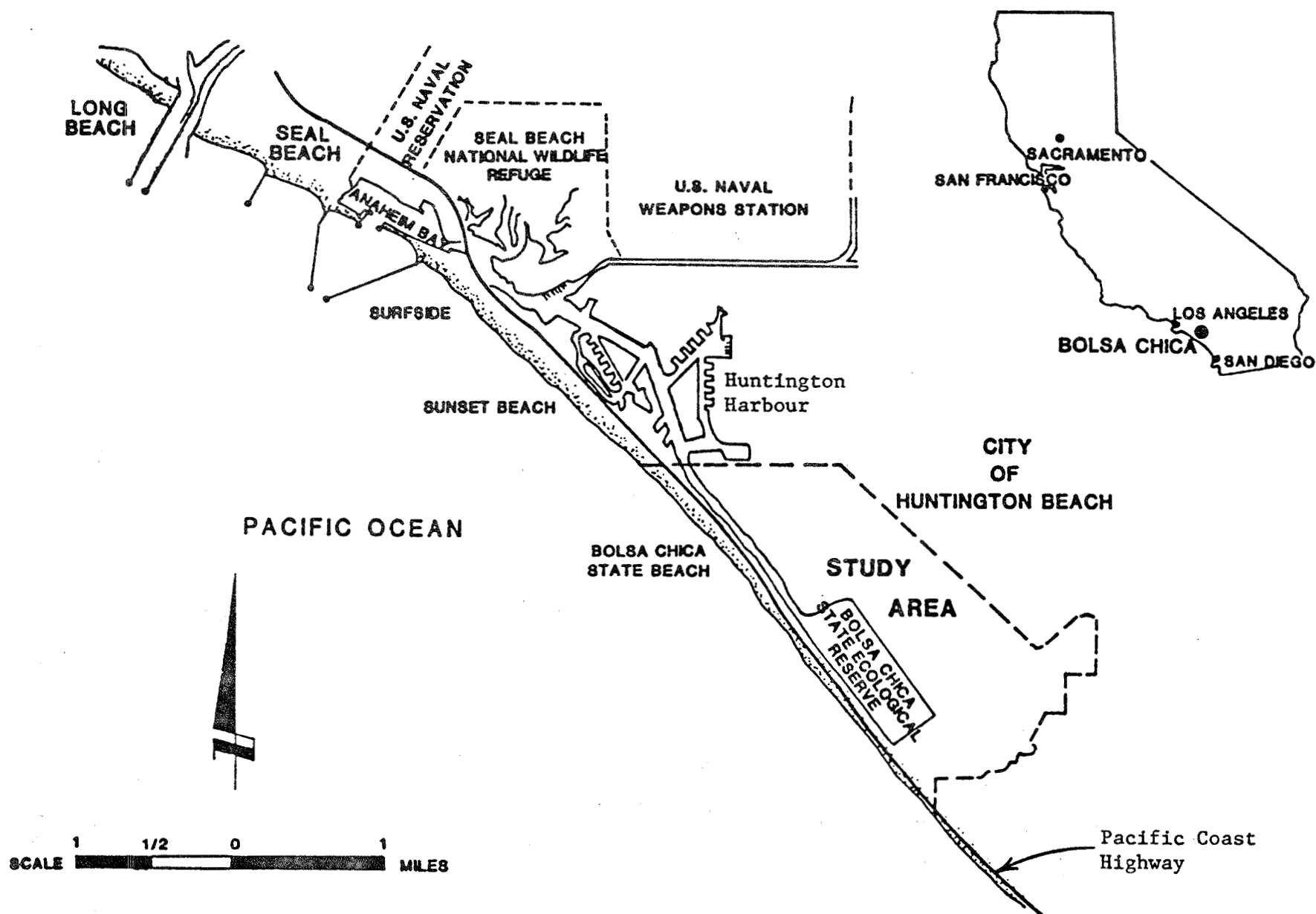
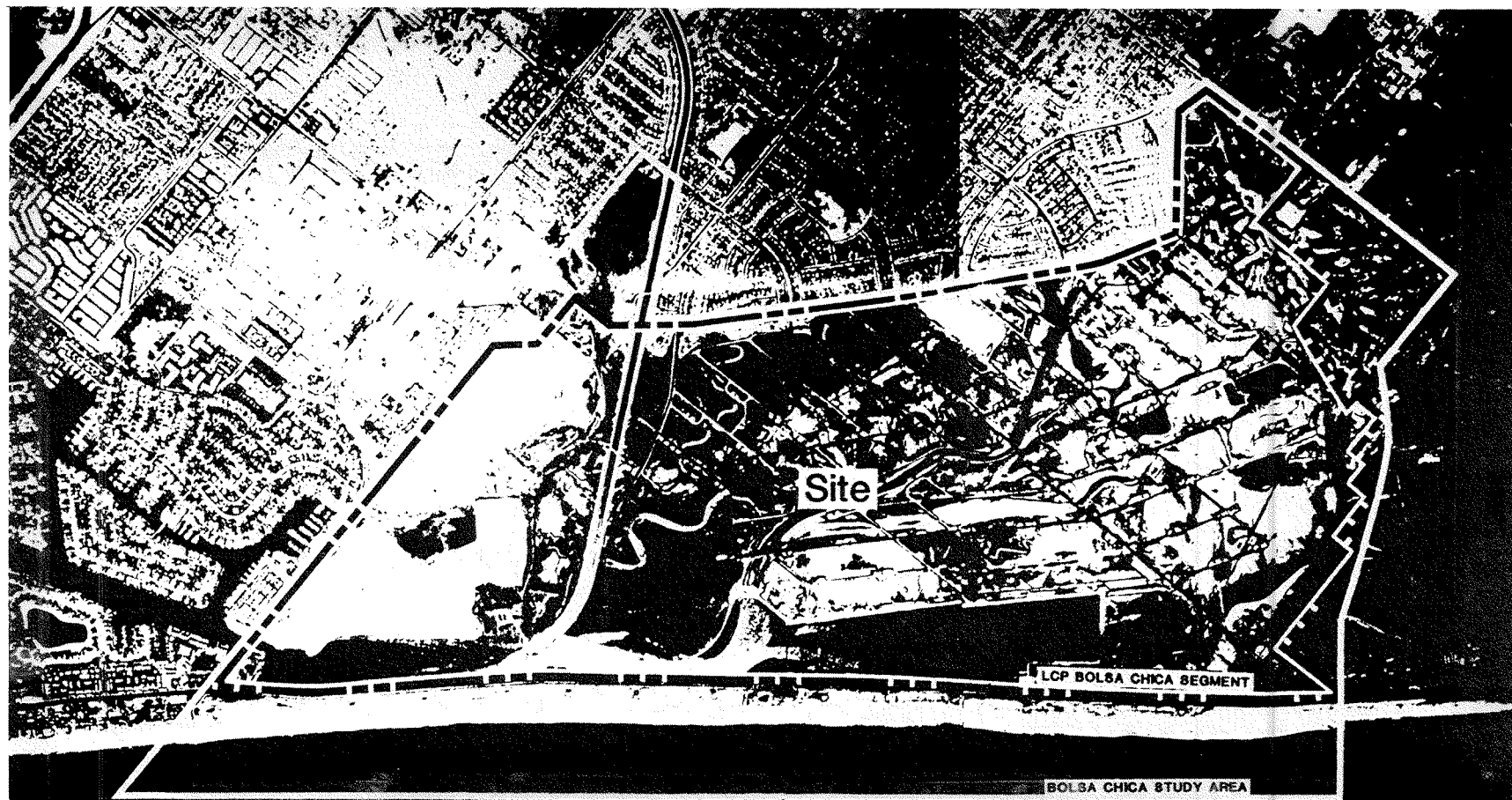


Figure 1. Bolsa Chica, California, study region location (after Orange County Environmental Management Agency 1985)



SEPTEMBER 1980

Figure 2. Bolsa Chica, California, area of interest
(after Orange County Environmental Management Agency 1985)

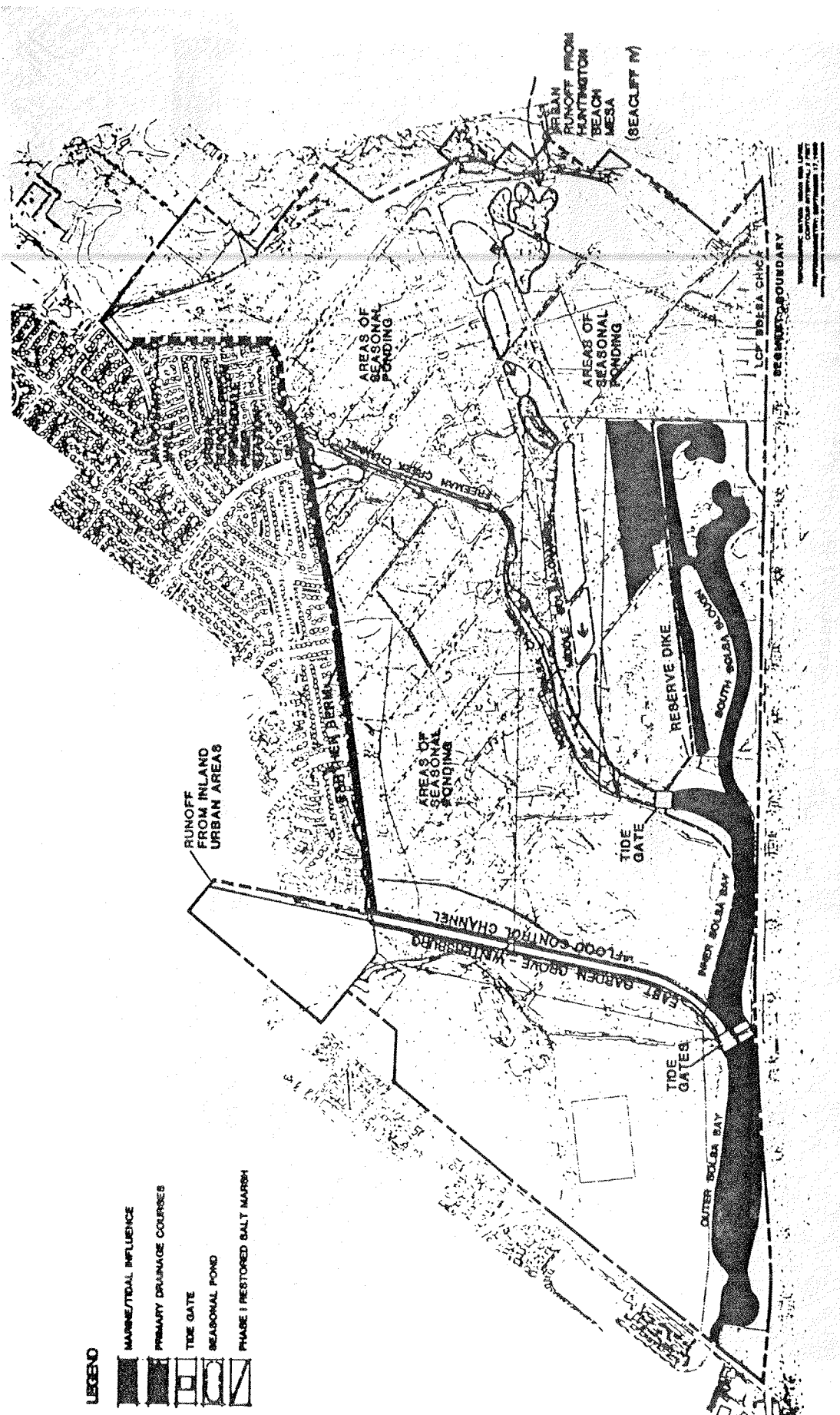


Figure 3. Present tidal inundation, Bolsa Chica, California (after Orange County Environmental Management Agency 1985)

pedestrian walkway and footpath to the Bolsa Chica State Ecological Reserve from a public parking lot adjacent to PCH.

14. The community surrounding Bolsa Chica (the City of Huntington Beach), is predominantly a medium-density residential community. Bolsa Chica State Beach, on the ocean side of Bolsa Chica across the PCH, is utilized by both residents and visitors from outside the area. Recreational beach uses include sunbathing, swimming, picnicking, surfing, and hiking and bicycling along trails located along the seaward side of the beach parking areas. There is also a private equestrian facility with training facilities located in the northerly corner of the lowland. Recreational boating opportunities in the immediate area are located in the marina at Huntington Harbour, with ocean access being provided by the entrance to Anaheim Bay.

15. A 300-acre State-owned Ecological Reserve, of which 173 acres have been restored to high quality wetlands habitats, contains a limited amount of public footpaths for nature study. Public access into the majority of the Reserve is restricted to preclude unnecessary disruptions to wildlife values and use. An additional 230 acres adjacent to the Reserve is leased to the State of California by the major landowner of the area, Signal Landmark (Figure 4). These lands would be conveyed to the State provided that the State causes the construction of a navigable ocean entrance and channel connecting to Signal lands, as part of the Bolsa Chica Land Use Plan. The Bolsa Chica lowland and existing wetlands in the Reserve provide important habitat both for migratory birds which nest, rest, and/or feed in the area, as well as resident shorebirds, waterfowl, and other vertebrate and invertebrate wildlife.

16. The County of Orange has adopted a Land Use Plan for the Bolsa Chica Project pursuant to State requirements under the California Coastal Act of 1976. The plan was certified by the Coastal Commission in January 1986, subject to review and confirmation of five elements. The certified Land Use Plan contains both urban and wildlife uses that yield more than 75 percent of the area as public use and other public open space. This certified Land Use Plan includes 915 acres of existing and restored wetlands, 86.8 acres of additional environmentally sensitive habitats, a 1300-slip public marina with land provided for an additional 400 dry-stored boats, public launch ramps, and commercial areas providing visitor-serving uses and amenities. More than 100

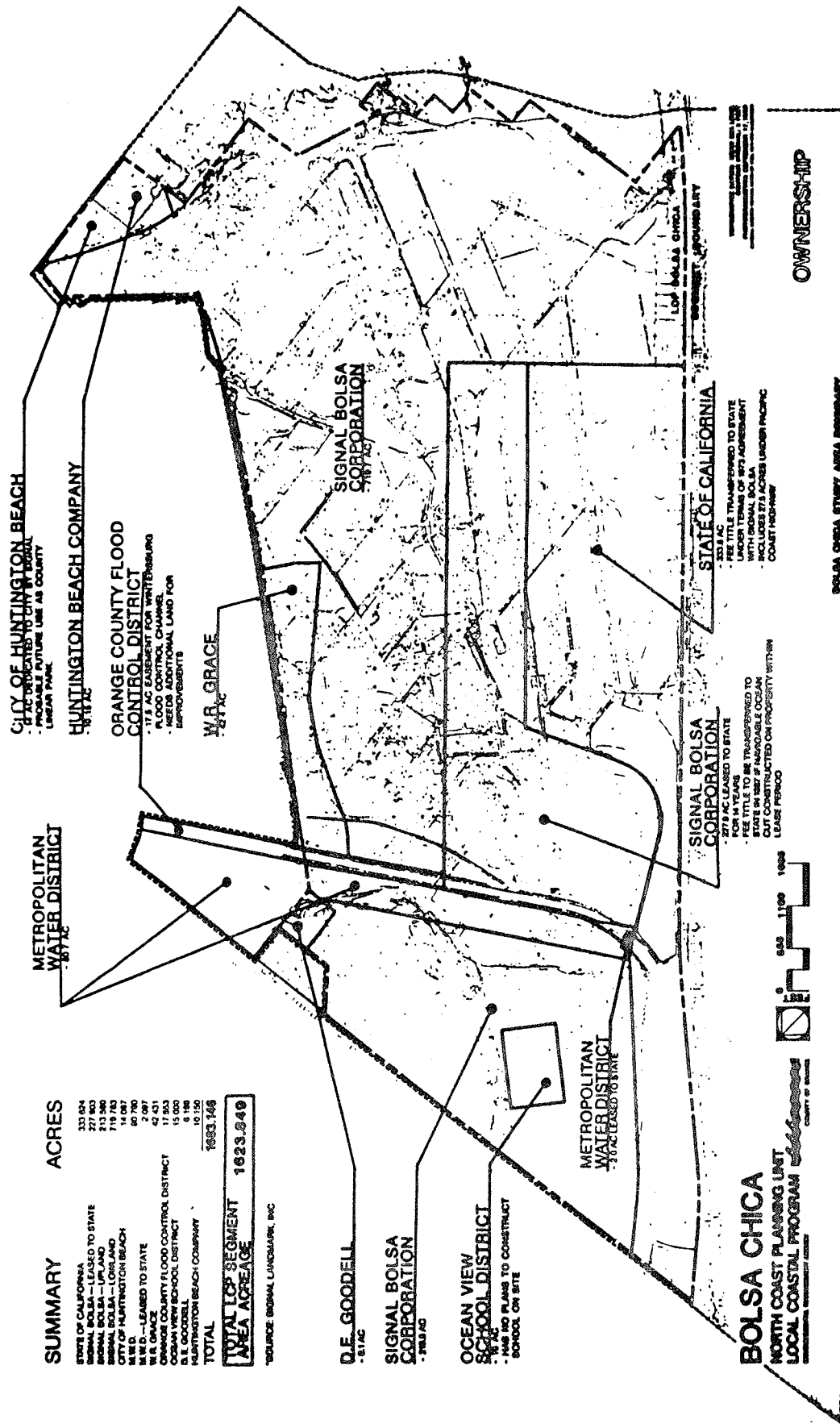


Figure 4. Land ownership, Bolsa Chica, California, region (after Orange County Environmental Management Agency 1985)

acres of navigable waters also are proposed to serve the marina-commercial complex, and to provide delivery of ocean waters to the restored wetlands areas. Flood control improvements, new public roads, hiking, bicycling and equestrian trails, public parks, and other major infrastructure are also planned. Finally, the Plan will contain residential uses, including waterfront and off-water dwelling units.

Historical Perspective

17. Involvement of the Federal government in the Bolsa Chica region was directed by Congressional resolutions in 1964 and 1976, and reaffirmed by the Water Resources Development Acts of 1986 and 1988. (The use of the phrase "Sunset Harbor" in those authorizing documents is incorrect, as no such location exists.) The 1964 resolution requested a study to determine the need for a light-draft vessel harbor at Bolsa Chica. The 1976 resolution expanded the study scope to include determination of the feasibility and desirability of providing and maintaining tidal waters and re-creating a tidal marsh. Several studies and surveys have been conducted by both the US Army Engineer District, Los Angeles (SPL), and non-Corps interests. In addition, a Corps feasibility study had been initiated in response to the 1976 Congressional authority, but has not been completed at the present time.

Congressional Resolution of 1964

18. This resolution, requested by Congressman Richard T. Hanna and adopted April 11, 1964, states:

"...Resolved by the Committee on Public Works of the House of Representatives, United States, that the Board of Engineers for Rivers and Harbors is hereby requested to review the reports on the coast of southern California, with a view to determining the need for a harbor for light-draft vessels in the Bolsa Chica-Sunset Bay area, California..."

Congressional Resolution of 1976

19. This resolution, requested by Congressman Mark W. Hannaford and adopted September 23, 1976, states:

"...Resolved by the Committee on Public Works and Transportation of the House of Representatives, United States, that the Board of Engineers for Rivers and Harbors is hereby requested to review the reports on the Coast of Southern California for Light Draft Vessels with a view to determining whether any modifications therein are warranted in the Bolsa Chica-Sunset Bay area, Califor-

nia, and to conduct a study to determine the feasibility and desirability of re-creating a tidal marsh upon the State-controlled lands in Bolsa Chica Bay for increasing its value for fish and wildlife. This study is to include evaluation and investigation of levees, jetties, breakwaters, and other works needed to provide and maintain tidal waters within the proposed marsh..."

Water Resources Development Act of 1986 (PL 99-662)

20. The following excerpt from the Water Resources Development Act of 1986 pertains to the Bolsa Chica area, although the Corps has not at present interpreted pertinent sections of the Act, nor determined how best to implement such sections thereof:

SEC. 1119: SUNSET HARBOR, CALIFORNIA

- a. "...The Secretary is directed to expedite completion of the feasibility study of the navigation project for Sunset Harbor, California,...and to submit a report to Congress on the results of such study...
- b. ...Upon execution of agreements by the State of California or Local sponsors, or both, for preservation and mitigation of wetlands areas and appropriate financial participation, the Secretary is authorized to participate with appropriate non-Federal sponsors in a project to demonstrate the feasibility of non-Federal cost sharing under provisions of Section 916 of this Act..."

21. Any and all provisions of the Water Resources Development Act of 1986 (PL 99-662) should be read with the understanding that the Department of the Army has not, at present, made any determination or interpretation with respect to this Act.

Water Resources Development Act of 1988 (PL 100-676)

22. The following excerpt from the Water Resources Development Act of 1988 pertains to the Bolsa Chica area.

SEC. 4: SUNSET HARBOR, CALIFORNIA

- f. "...The demonstration project at Sunset Harbor, California, authorized by Sec. 1119(b) of the Water Resources Development Act of 1986 (100 Stat. 4238), is modified to include wetland restoration as a purpose of such demonstration project. All costs allocated to such wetland restorations shall be paid by non-federal interests in accordance with Sec. 916 of such Act..."

Settlement Agreement of 1973

23. During preparation of this report, Signal Landmark was the major landowner in the Bolsa Chica study area, having title to 1,200 acres. W. R.

Grace Properties, Inc. owned 42 acres adjacent to the East Garden Grove-Wintersburg Flood Control Channel and the northerly boundary of the site. Slightly more than 100 acres were owned by other interests which include the Metropolitan Water District of Southern California, the Huntington Beach Company, the Ocean View School District, and Donald Goodell. The State of California holds title to 327.5 acres in addition to 230 acres that it holds pursuant to a lease with an option to acquire, subject to the provisions of the 1973 "Boundary Settlement and Land Exchange Agreement Regarding Lands in the Bolsa Chica Area, Orange County, California."

24. Under the 1973 Settlement Agreement between the State and Signal Landmark, which was signed by the governor of California on March 15, 1973, the State acquired title to a 327.5-acre parcel in the Bolsa Chica lowland. The State also acquired a lease for an additional 230 acres adjacent to the 327.5-acre parcel for a period of 14 years, which was extended to 17 years by the parties in 1984. The State has an option to acquire title to the 230-acre lease parcel if (among other conditions) a navigable ocean entrance system is constructed within a specified time period. Such a system is to consist of a navigable waterway between the Pacific Ocean and land owned by Signal Landmark in the Bolsa Chica area.

Proposed Improvements

25. The County of Orange has adopted a Land Use Plan (LUP) as part of the Local Coastal Program for the Bolsa Chica area in accordance with the California Coastal Act of 1976. This LUP includes a navigable ocean entrance system (Preferred Alternative), and a non-navigable ocean entrance system (Secondary Alternative). The principal landowner of the region, Signal Landmark, desires to implement the Preferred Alternative.

Preferred Alternative

26. The Preferred Alternative of the LUP, as depicted in Figure 5, contains the following features and acreage allocations:

- a. 915 acres of restored, high quality, fully-functioning full tidal, muted tidal, fresh, and brackish water wetlands within the study area, with emphasis on diversity of habitat and protection and recovery of endangered species.

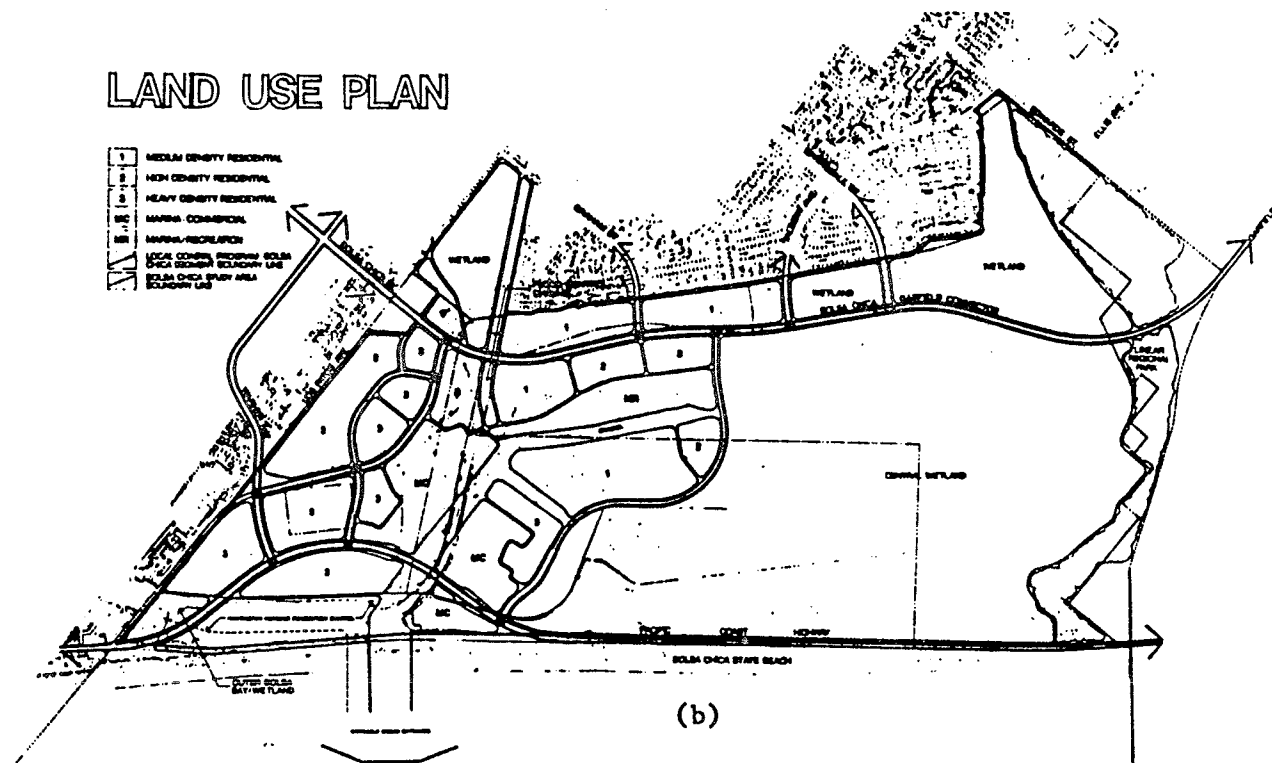
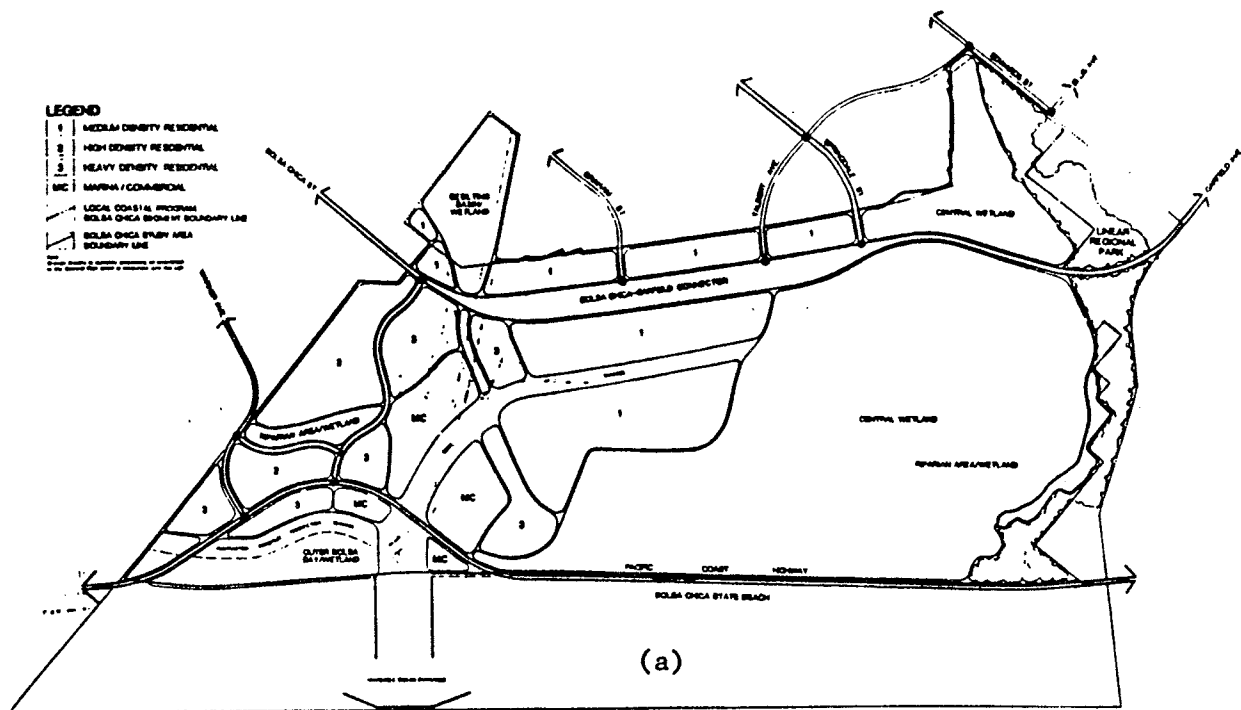


Figure 5. Bolsa Bay Preferred Alternative;
(a) adopted land use plan, and (b) revised land use plan

- b. 86 acres of existing or newly created environmentally sensitive habitat within the study area.
- c. Buffer areas between wetlands and urban development to protect environmentally sensitive habitats.
- d. A fully-navigable ocean entrance to provide a continuous, assured source of water for tidal wetlands and interior waterways, and for recreational boating ocean access from both the Bolsa Chica area and Huntington Harbour.
- e. Interior navigable waterways providing navigable connections to the Bolsa Bay marina, waterfront residential housing, and Huntington Harbour.
- f. At least 75 acres of mixed-use, marina and commercial area providing in-water berthing and dry storage for at least 1,700 boats.
- g. A realignment of the Pacific Coast Highway (PCH) from the existing PCH-Warner Avenue intersection, across Outer Bolsa Bay, Bolsa Chica Mesa, and the main entrance channel to the proposed marina.
- h. An internal roadway system connecting Bolsa Chica Street with Garfield Avenue within a corridor between 500 and 950 ft from adjacent existing neighborhoods.
- i. Creation of a 130-acre Bolsa Chica Linear Regional Park on Huntington Mesa.
- j. Approximately 500 gross acres of medium-, high-, and heavy-density residential development in the lowland and on Bolsa Chica Mesa.

Secondary Alternative

27. In certifying the LUP, the California Coastal Commission (CCC) also certified an alternative plan (Secondary Alternative), shown in Figure 6, with a non-navigable ocean entrance and different internal use configurations than the Preferred Alternative. This alternative contains 915 acres of wetlands, a non-navigable ocean entrance, and a marina along the present Warner Avenue alignment on Bolsa Chica Mesa. The CCC indicated that the Secondary Alternative could be certified as the LUP without further hearings if the proposed navigable ocean entrance were found to be infeasible pursuant to performance standards contained in the November 1984 staff report and the January 1986 certified LUP, and if the Secondary Alternative were adopted by the County of Orange as its Land Use Plan.

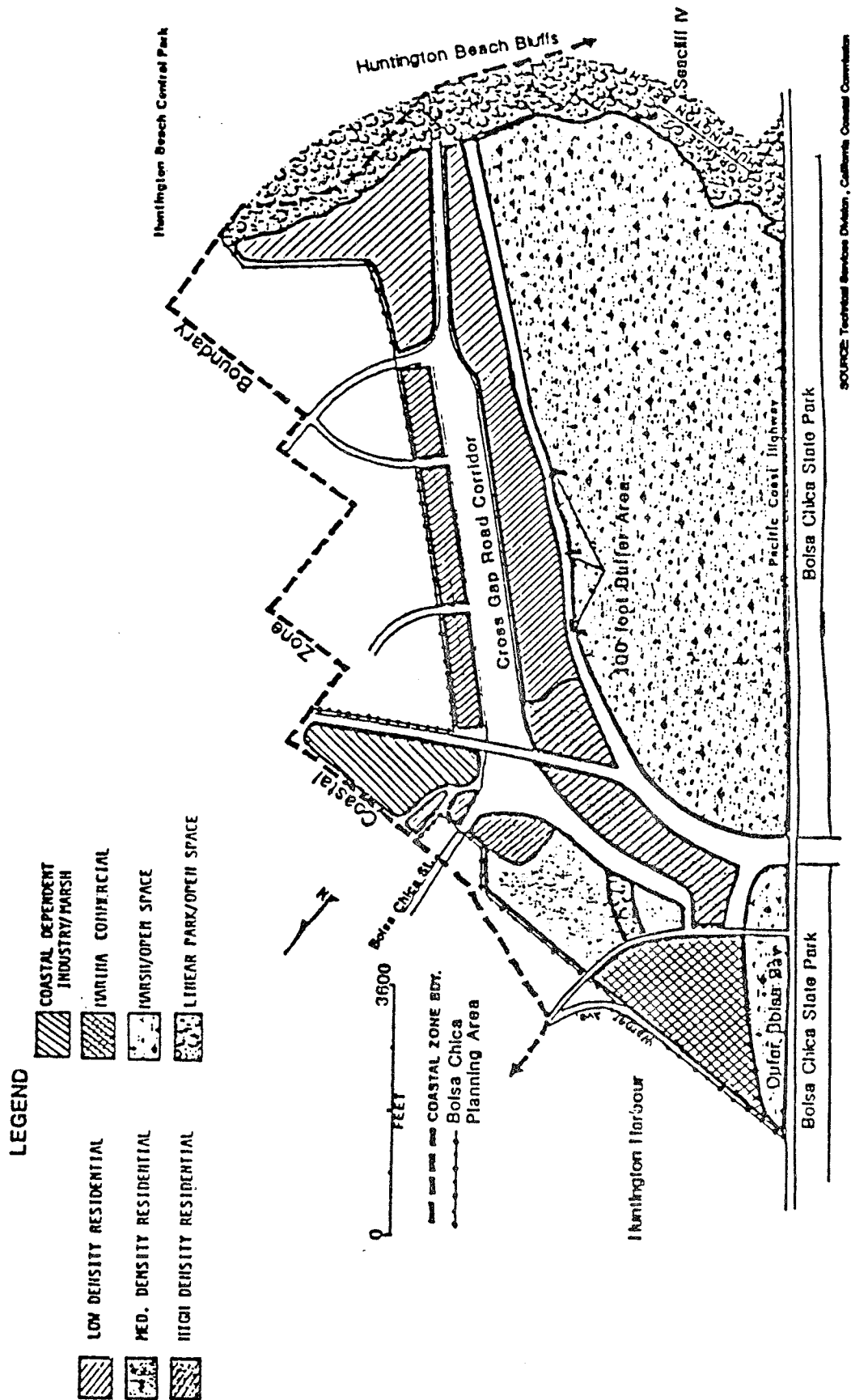


Figure 6. Bolsa Bay Secondary Alternative
(after Orange County Environmental Management Agency 1985)

Previous Studies

28. The Bolsa Chica area is located immediately adjacent to Huntington Harbour, from which navigation vessels exit to the Pacific Ocean through Anaheim Bay. The Anaheim Bay entrance is heavily utilized by Seal Beach Naval Weapons Station, and concern has existed for many years about accidental encounters between civilian and military craft in this area, where ammunition off-loading and storage are common practices. Local interests have previously requested the US Army Engineer District, Los Angeles, to investigate the practicality of the construction of a new entrance channel connecting Bolsa Chica with the Pacific Ocean.

29. The Bolsa Chica and Huntington Harbour regions are separated from the Pacific Ocean by Surfside, Sunset Beach, and Bolsa Chica State Beach. The west jetty at Anaheim Bay effectively creates a littoral cell boundary at Seal Beach for the region of coast to the north, and the east jetty is a boundary for the littoral cell between the Anaheim jetties and Newport to the south. Rivers no longer contribute significant sediment into the littoral cell between Anaheim and Newport Beach. Artificial beach nourishment at Surfside-Sunset, in amounts that average approximately 350,000 cu yd per year, has provided a feeder beach for the littoral cell that extends down the coast toward Newport Beach. Much of the nourishment is due to disposal of material excavated from the Navy channel at Anaheim and has been dictated by funds available, rather than by the optimum requirements for beach nourishment.

30. A new entrance channel to Bolsa Chica will require stabilization by a jetty system. Furthermore, interruption of downcoast movement of littoral material may require a sand bypassing system. Tidal flow through a new entrance channel also may affect tidal circulation through Huntington Harbour. These concerns are multifaceted and interrelated, and have given rise to many studies of beach processes and tidal circulation evaluations in recent years.

State of California studies

31. Following completion of the boundary settlement and land exchange agreement between the State of California and Signal Landmark, it became apparent that a plan should be developed depicting the interests of all concerned State agencies. The 1973 State budget provided funds for such a plan-

ning effort involving the Departments of Transportation, Fish and Game, Parks and Recreation, and the Department of Navigation and Ocean Development. That plan, entitled "Bolsa Chica Marsh Re-Establishment Project" (State of California, 1974), was presented by The Resources Agency. Alternative methods were evaluated for obtaining the greatest benefits for the use of public lands in Bolsa Chica and fulfilling the land settlement commitments. Each alternative included the following:

- a. Development of an additional area to provide a total of approximately 350 acres of marsh.
- b. Construction of interpretive and visitor-use facilities.
- c. Construction of a channel to the ocean to provide tidal waters to the marsh and ocean access for boats.
- d. Construction of an 1800-boat marina and small boat launching ramp.
- e. Provisions for a 300-ft wide channel connection between Signal properties and State lands.
- f. Integrated development between Bolsa Chica State Beach and the marina-ecological reserve complex.
- g. Transportation alternatives for the beach-marina-marsh complex.

Orange County studies

32. In addition to continuous water quality monitoring studies, the "Bolsa Chica Local Coastal Program Land Use Plan" was adopted by the Orange County Environmental Management Agency (1985), and it contains all suggested modifications approved by the CCC on October 23, 1985. These modifications have received the full concurrence of the major landowner, Signal Landmark. The wetlands concept plan has been reviewed by the California Department of Fish and Game (DFG), and is presently in the process of acceptance by DFG. The LUP includes the following features:

- a. 915 acres of productive and diverse wetlands and 86 acres of environmentally sensitive habitat areas.
- b. A navigable ocean entrance to provide high-quality tidal flow to the wetlands and navigable access to the ocean, new navigable waterways, a 75-acre or larger marina and commercial area with berthing and dry storage for at least 1,700 boats, launch

ramps, and coastal-dependent, visitor-serving commercial facilities.

- c. An optional navigable interior waterway connection to Huntington Harbour.

US Army Engineer District, Los Angeles, studies

33. The Corps study of the Bolsa Chica/Sunset Bay area, California, was authorized by Congressional resolutions in 1964 and 1976, and reaffirmed in the Water Resources Development Acts of 1986 and 1988. Several studies and surveys have been initiated, but a Corps feasibility study in response to the study authority has not been completed at the present time. Preliminary studies, and current indications of the desirability for both recreational boating and wetland restoration within the local community, suggest that achievement of both may be feasible. However, additional study is needed to determine (a) the engineering, economic, and environmental feasibility of specific plans for small-craft harbor development, and wetland preservation, enhancement, and restoration, and (b) the extent of Federal participation, if any, in any plan implementation.

Previous tidal circulation studies

34. Waterways Experiment Station (1981). The first hydrodynamic modeling of the tidal circulation characteristics of existing Bolsa Chica tidal areas was conducted for SPL by WES in 1981 to compare tidal elevations, velocities, and volumes of flow at specific prototype gage locations in Anaheim Bay, Huntington Harbour, Warner Avenue Bridge, Outer Bolsa Bay, and Inner Bolsa Bay (US Army Engineer Waterways Experiment Station 1981). The hydrodynamic model used in this study was a two-dimensional, depth-averaged, finite-difference approximation model developed at WES. Comparisons were made for existing conditions and seven proposed alternative plans. Prototype field data for numerical model calibration and comparison with alternatives had been obtained by Meridian Ocean Systems, Inc., at data stations during a 25-hr period over April 24-25, 1980. The primary objective of the study was to identify any impacts to the existing channel system in Huntington Harbour resulting from a new ocean entrance, marina, and wetland areas in Bolsa Chica. The tidal characteristics of the existing wetlands and new wetlands under the proposed plans, however, were not considered in that study. The conclusion reached from the study was that tidal amplitudes were not significantly alter-

ed in Anaheim Bay, Huntington Harbour, or Outer Bolsa Bay by any of the plans evaluated. Direction of flood flow under Warner Avenue Bridge with the proposed new entrance channel in place changed flow direction such that flood flow was into Huntington Harbour. Hence, a region of reduced tidal velocity was indicated in Huntington Harbour.

35. Philip Williams & Associates (1984). A study of the tidal characteristics of the existing Huntington Harbour area and seven proposed alternative designs for Bolsa Chica, and an evaluation of a self-maintained ocean entrance at Bolsa Chica, were conducted by Philip Williams & Associates (1984). Because of the significant channelization throughout the flow system, this study utilized a one-dimensional link-node model that uses the method of characteristics to solve the equations of water motion within each link. Field data previously obtained by Meridian Ocean Systems, Inc., during a 25-hr period over April 24-25, 1980, were also used in this study for calibration and comparison of results. The purpose of the study was to evaluate the impacts of proposed plans on tidal velocities in Huntington Harbour, and to determine the tidal range in the restored wetland. The study concluded that, for the case of no new ocean entrance, tidal velocities in Huntington Harbour would increase with the addition of fully tidal wetlands in Bolsa Chica. With a new ocean entrance, however, the velocities would not generally increase. The analysis of tidal range in the restored wetlands consisted of a qualitative comparison between simulated conditions with and without the new ocean entrance. The results from the analysis indicated that a small dampening and phase lag would occur to the tide in Bolsa Chica if the area were opened to full tidal action with no new ocean entrance. A maximum reduction in tidal range of about 25 percent would occur during very high spring tides. These studies also concluded that proposed restoration designs for Bolsa Chica would have sufficient tidal prism to maintain a natural channel of between 1,400 and 3,700 sq ft if the channel sides were stabilized. The channel could have widths of 200 to 450 ft, with depths from 10 to 12 ft.

36. Moffatt & Nichol, Engineers (1987). A hydraulic analysis of the Bolsa Chica wetlands was performed by Moffatt & Nichol, Engineers (1987) using a one-dimensional link-node model that was calibrated to existing conditions using field measurements taken over a 3-week period from August 16 through September 5, 1986. The study was performed to:

- a. Provide an understanding of the hydraulic response of coastal wetlands, and wetlands with a muted tide regime that is applicable to Bolsa Chica wetlands.
- b. Model the hydraulics of the existing Bolsa Chica wetlands and the tidal cell added by the California Department of Fish and Game.
- c. Develop a wetland model that is calibrated to existing conditions, and that can be used to analyze proposed wetland configurations.

The scope of the work required that the study:

- a. Describe the hydraulics of coastal wetlands as well as tide control structures that are applicable to Bolsa Chica.
- b. Outline the design approach used in the hydraulic analysis of wetlands.
- c. Modify and calibrate a numerical model to analyze the existing conditions in the Bolsa Chica wetlands.
- d. Perform a sensitivity analysis to identify the relative effect that each input value has on the results in order to indicate confidence intervals.

37. The calibrated model will be used to further analyze proposed wetland configurations for Bolsa Chica. Since results obtained for proposed configurations cannot be compared with measurements to assess accuracy, a sensitivity analysis was performed to estimate the range in which the results are most likely to fall. It was determined by this study that tide range in the wetlands is greatly affected by the type of tide control structure used. Tide control structures can be designed to provide the required tidal range and mean water level in the wetlands. This is important to achieve the desired mix of habitats. The hydraulic design comprises a large part of the wetland design. The complex calculations involved are readily solved by this numerical model in a timely and economical fashion.

Previous beach sand movement studies

38. Beach Erosion Board (1956). The Anaheim Bay jetties were completed in 1944 and serve as an effective barrier to littoral sand transport along the shore to a depth of about 20 ft. The construction of the jetties was followed by severe erosion of the beach immediately to the south of the east jetty. The eroded sand was apparently transported in a southerly direction by the dominant wave action. Erosion progressed to such a degree that extensive property damage was imminent and, late in 1947, a beach fill

was placed to restore the shore. (Subsequently, this reach of shoreline has been periodically renourished with an average annual volume of approximately 350,000 cu yd of sand made available from channel maintenance operations at Anaheim). Sand movement along the coast was correlated with dominant wave energy by this study (Caldwell 1956).

39. US Army Engineer District, Los Angeles (1978). Because of the continuing necessity to rehabilitate the Surfside-Sunset Beach region of coastline due to severe beach erosion, SPL established a monitoring program to evaluate the effectiveness of the placement procedures. One of the purposes of the effort was to determine if portions of the material disappearing from the beach was moving offshore where it would be recycled periodically to the beach. Results of the overall monitoring program were inconclusive.

40. Waterways Experiment Station (1984). The potential effects of a new entrance channel to Bolsa Chica on unstabilized adjacent shorelines was considered by WES in 1984 (Hales 1984). That study utilized a one-line numerical model for longshore sediment transport and an equivalent monthly wave climate deduced from frequency of occurrence of waves from a 3-year hindcast (1956 to 1958) by National Marine Consultants (1960) and Marine Advisors (1961). Evaluations were performed for uniform bypassing placement distributions of 300, 500, 1,000, and 2,000 ft from the east jetty at Anaheim Bay. As the distribution of the bypassed material was extended farther down coast, those computational cells nearer the east jetty experienced an increased depletion of material. The actual equilibrium shoreline orientation that develops will be in response to the effectiveness of the bypassing program and the actual wave climate.

Regional Geology

41. As discussed in House Document No. 349 (US Congress 1954), Bolsa Chica is on the edge of San Pedro Bay, approximately in the center of the Los Angeles coastal plain. This low plain is bordered on the north by the eastern Santa Monica Mountains and the Repetto Hills, on the east by the Puente Hills and the Santa Ana Mountains, on the southeast by the San Joaquin Hills, and on the south and west by the Pacific Ocean. Many of the structural features surrounding the Los Angeles coastal plain are extremely young, and the present

relief and alignment of geographic units are, to a large extent, the product of a mountain-building epoch. The gently curving arc of shoreline extending from Point Fermin on the west to the bluffs of Corona del Mar on the east is composed, in part, of disconnected stretches of barrier beach fronting slowly rising tidal marsh areas. Separating these lowlands are the friable wave-cut cliffs or bluffs at Long Beach, Seal Beach, Huntington Beach, and Newport Beach. The character of these wave-cut bluffs, and the uniform plain to which they have been shaped by the sea, indicate that each headland formerly extended seaward of the present shoreline.

42. Under natural conditions that existed over 100 years ago, the Los Angeles and San Gabriel Rivers deposited most of their sediment loads on the ocean bars at their mouths where this material became available for nourishment of the beaches. Flood-control structures in the upper reaches of these rivers, constructed during the past century, now have nearly eliminated sediment from being delivered to the beaches by the rivers.

43. The significant findings resulting from a review of the geologic history of the area under investigation may be summarized as follows:

- a. Prior to historic time, uplift and erosion of the headlands, together with subsidence and fill of low area, developed the early shoreline into a semblance of the present shore.
- b. The shoreline appears to have become relatively stable at about the beginning of historic time, and further erosion of the headlands was dependant on the balance between losses of beach material by marine erosion and wind, and the periodic supply of new material brought to the shore by streams.
- c. During historic time, the beaches adjacent to Long Beach, Seal Beach, and Huntington Beach bluffs have remained comparatively narrow, which indicates that a very close balance between loss and supply existed in these areas.

Subsidence in the Bolsa Chica Area

44. The Local Coastal Plan has identified ground subsidence as one of the geologic hazards that must be addressed in planning the Bolsa Chica development. Subsidence in the Bolsa Chica area has been evaluated by Woodward-Clyde Consultants (1984, 1986). Subsidence refers to broad scale, gradual downward changes in elevation of the land surface. Such subsidence can occur naturally and from influences by man. The natural causes could be

tectonic structural flexure of faulting, consolidation of sedimentary rocks, or highly compressible peat deposits. Man-induced subsidence has been attributed to oil and water withdrawal in many of California's oil fields and ground-water basins.

45. The major subsidence area has coincided with the limits of the Huntington Beach oil field. Historical subsidence patterns from 1933 to 1972, and from 1964 to 1969 are shown in Figure 7. The decrease in the subsidence has been attributed to water injection of oil producing zones which was initiated in 1959. Estimates of the maximum amount of subsidence have ranged up to 5 ft since 1920 when oil production began. The maximum range of subsidence from 1955 to 1968 was reported as 0.15 ft (1.8 in.) per year, but this rate decreased to 0.05 ft (0.6 in.) per year from 1968 to 1972 (California Division of Oil and Gas 1973).

46. Subsidence rates from 1976 to 1985 have been calculated by analyzing precise leveling data of benchmarks in the area obtained from the Orange County Surveyor's Office. The history of subsidence in the areas was presented for the periods from 1976 to 1982, 1976 to 1985, and 1982 to 1985. The average annual subsidence rates for these periods are presented in Figures 8 through 10, respectively. Review of these figures indicate that although subsidence is continuing across the site, it appears that in the last several years it is occurring at a lower rate. The annual subsidence over the site is estimated to continue at an average rate of 0.01 ft per year, based on the rates from 1982 to 1985. However, the subsidence in the area is considered to be primarily due to hydrocarbon withdrawal, and the rate should respond closely to oil extraction and water injection.

Sea Level Rise in the Bolsa Chica Area

47. The annual average rate of mean sea level rise along the California coast is approximately 0.005 ft per year, based on available tide gage records. A 0.5 ft per century rate is also considered the global average of sea level increase over the past century (Revelle 1983).

48. Various projections of future sea level rise have been proposed, and are illustrated in Figure 11. Work summarized by Hoffman et al. (1983) and Hoffman (1983) foresees the possibility of rates of increase with upper

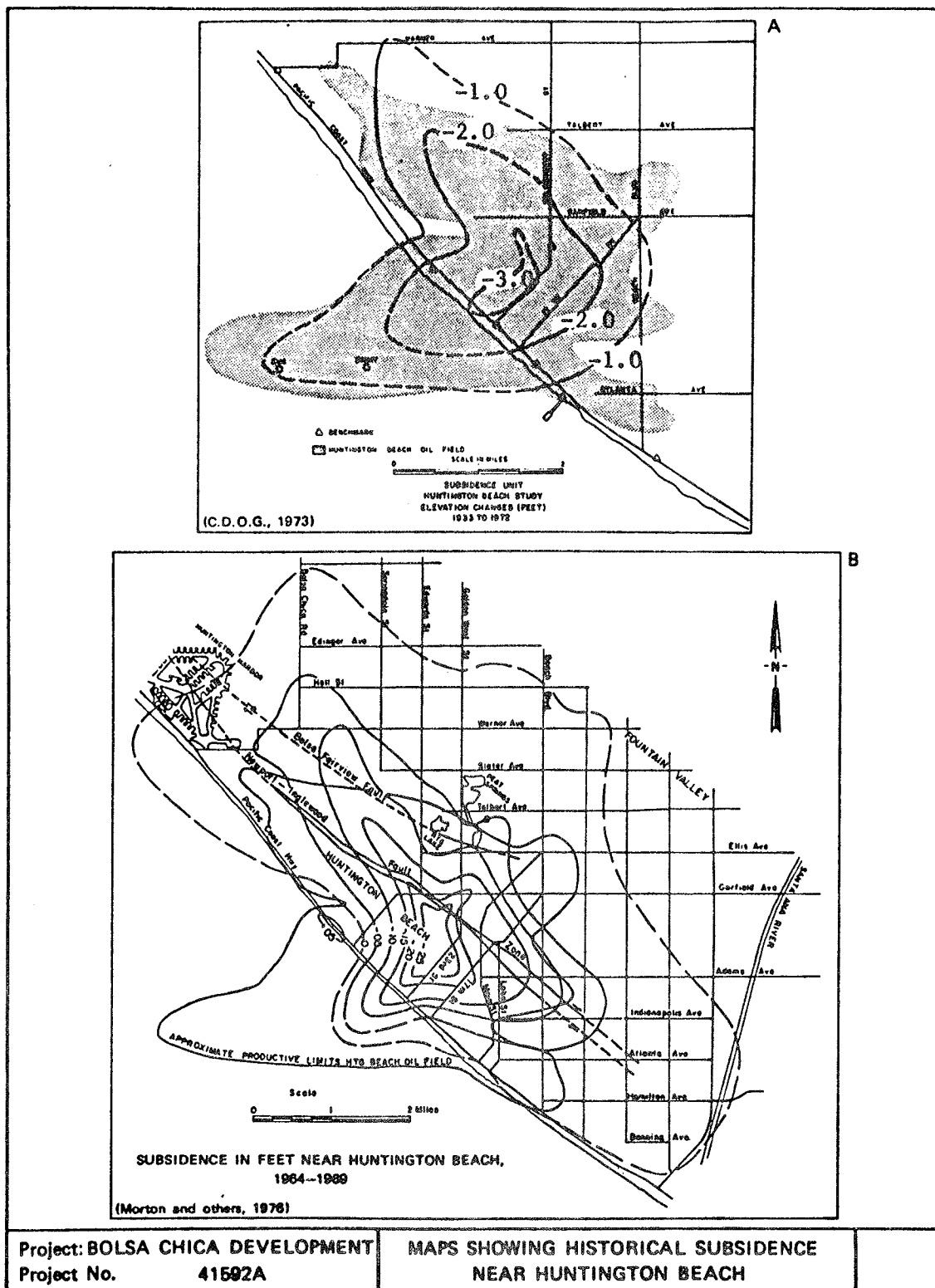


Figure 7. Historical subsidence near Huntington Beach, California
(after Woodward-Clyde Consultants 1984)

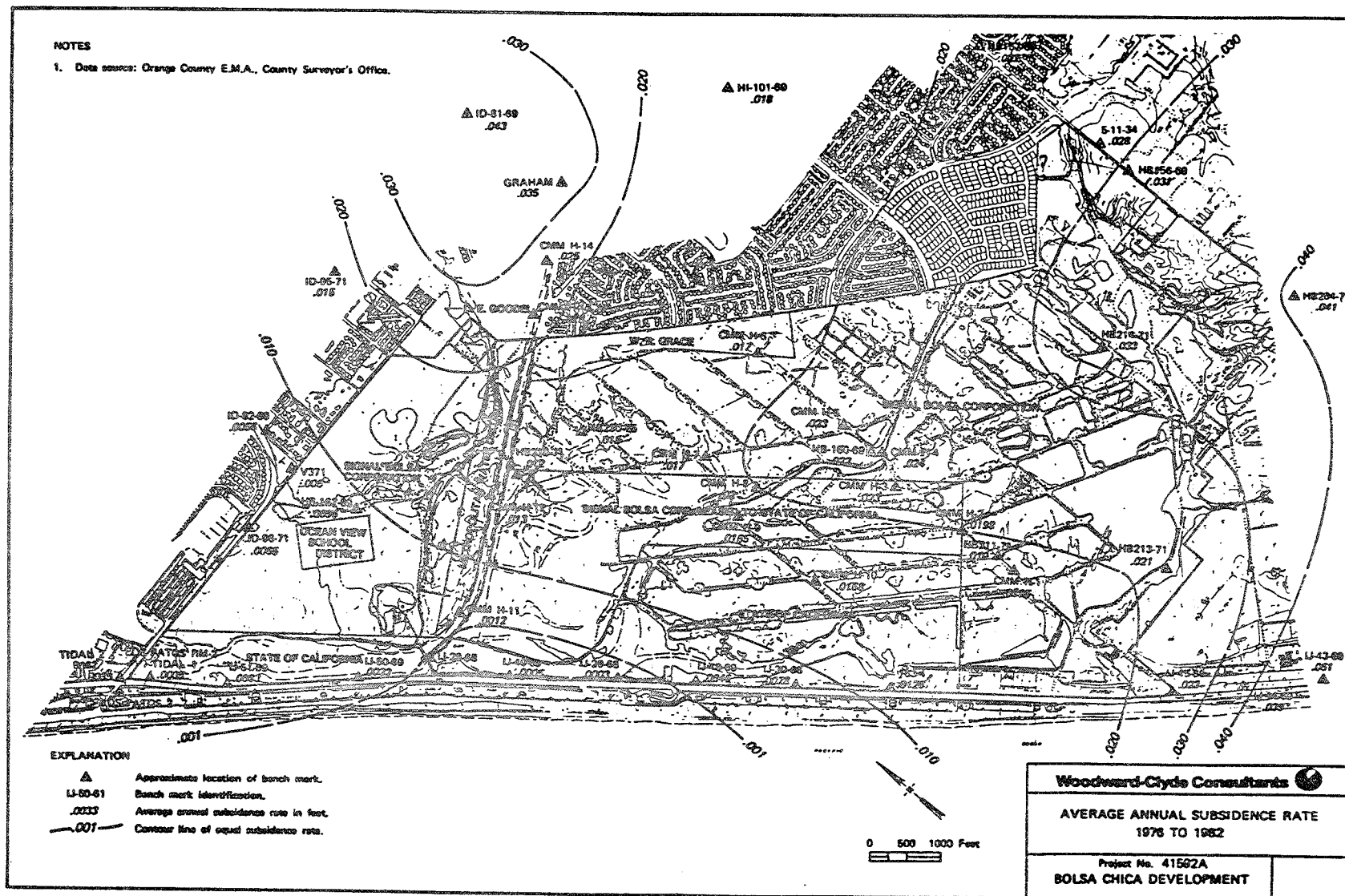


Figure 8. Average annual subsidence rate, 1976 to 1982, Bolsa Chica region
(after Woodward-Clyde Consultants 1984)

Figure 9. Average annual subsidence rate, 1976 to 1985, Bolsa Chica region (after Woodward-Clyde Consultants 1986)

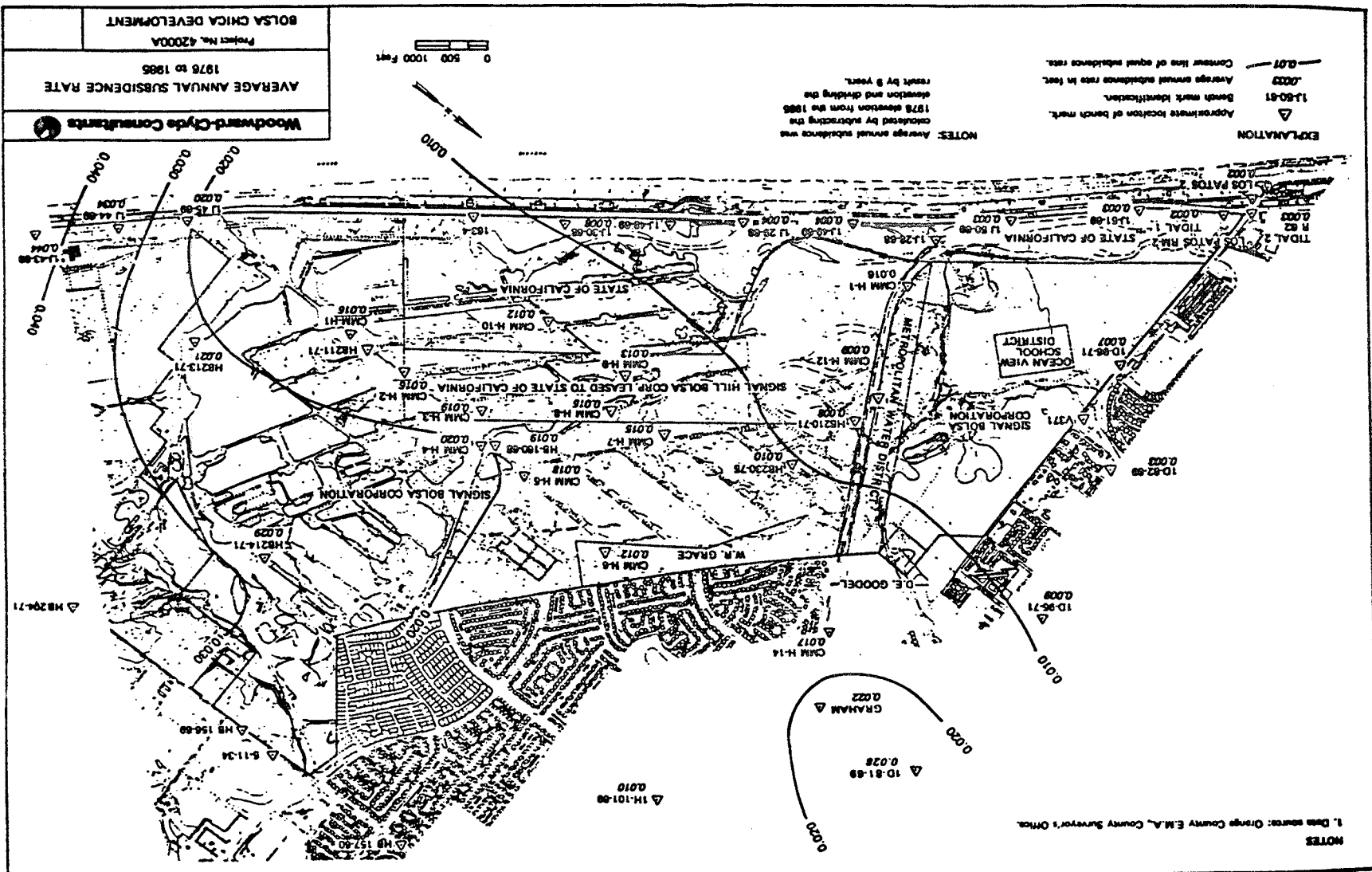
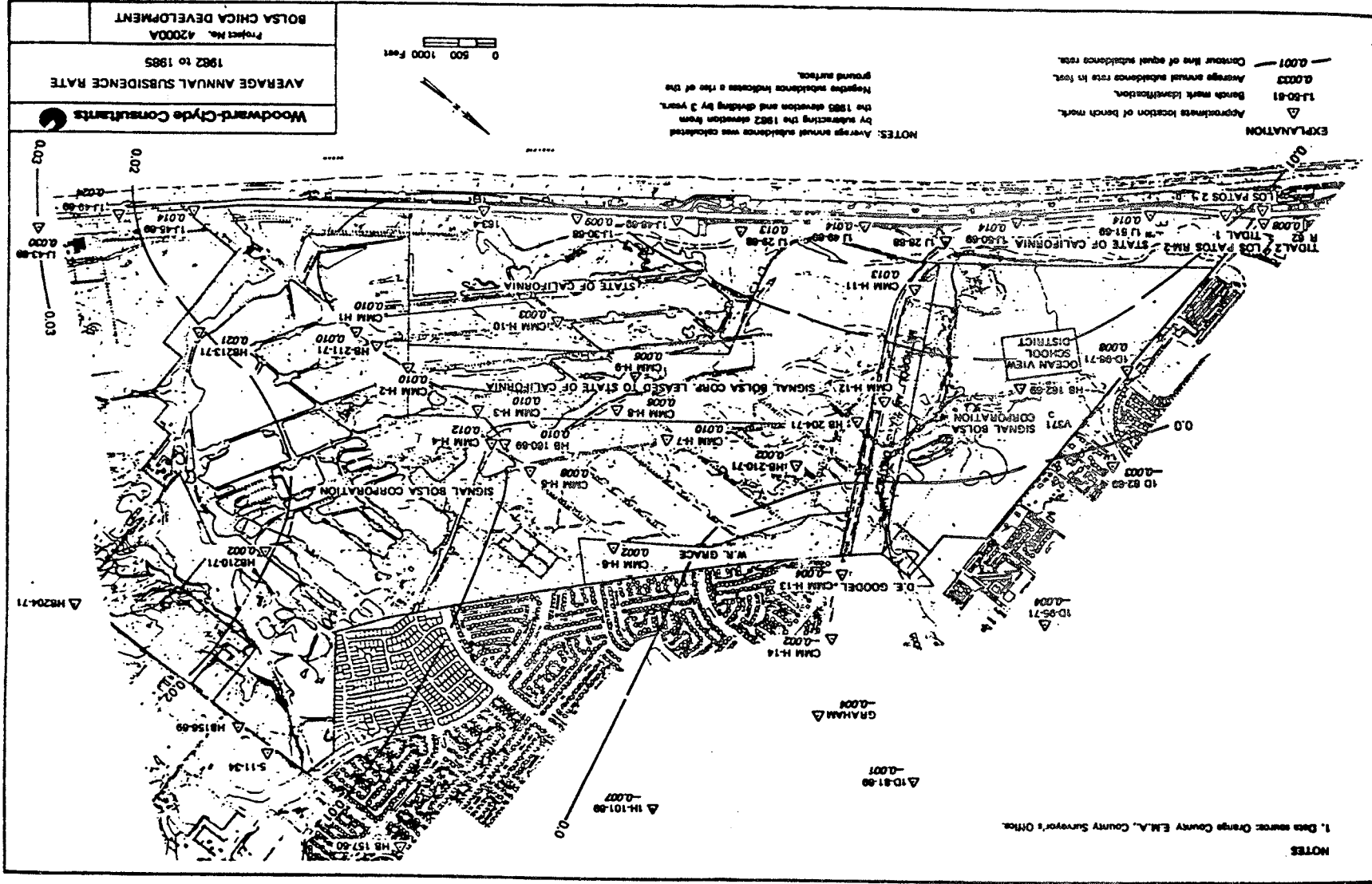


Figure 10. Average annual subsidence rate, 1982 to 1985, Bolsa Chica region (after Woodward-Clyde Consultants 1986)



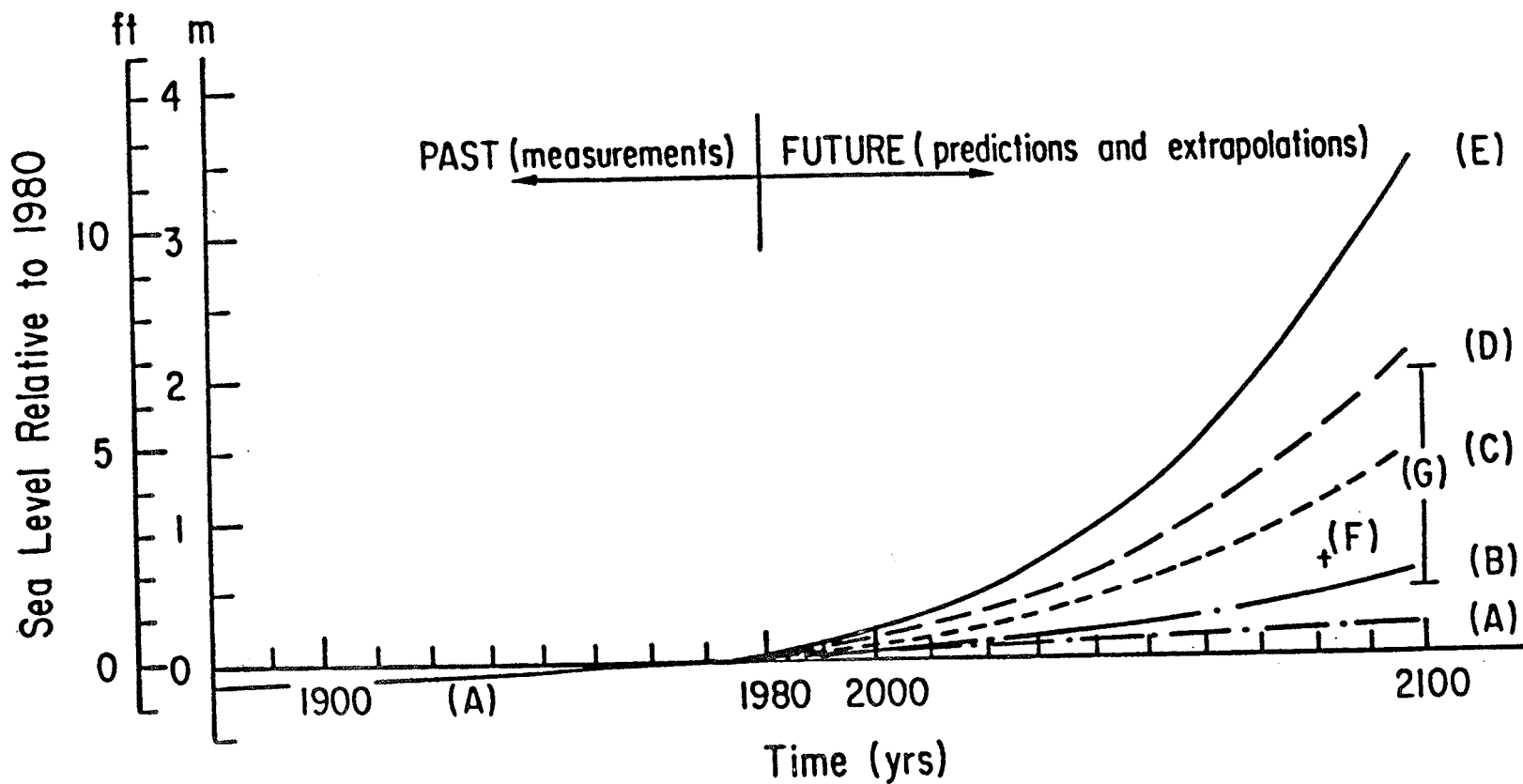


Figure 11. Schematic of eustatic sea level rise curves
 (A) Rate of rise over last century projected into the future,
 (B), (C), (D), and (E) Hoffman et al. (1983) estimates respectively for
 conservative, mid-range low, mid-range high, and high rates of increase,
 (F) Revelle (1983), (G) Polar Research Board estimate augmented for
 thermal expansion (Revelle 1983) (after Dean 1986)

limits exceeding an average of 9 ft per century over the next 120 years. These projections are based on fundamentally unverifiable computer models of global warming given past and projected increases in atmospheric carbon dioxide and other greenhouse gases, including methane and chlorofluorocarbons. These scenarios contain a large amount of uncertainty, as reflected in the wide range of estimates shown in Figure 11 (Seidel and Keyes 1983). The most recent study by the Marine Board (1987) predicts a rate of increase of 1.3 ft per century (0.013 ft per year), and is recommended for 25-year design projects. However, the historical rate of sea level rise has been only approximately 0.5 ft per century.

PART III: SHORELINE CHANGE MODELING

Overview of Methodology

Introduction

49. Numerical modeling of shoreline change has proven to be a useful engineering technique for understanding and predicting the evolution of the plan shape of sandy beaches. Mathematical models provide a concise and economical means of quantifying systematic trends in shoreline evolution commonly observed at groins, jetties, and detached breakwaters, as well as changes in shoreline position produced by coastal engineering activities such as beach nourishment and sand mining. The primary objective of shoreline change modeling is to assess the long-term impacts of planned or proposed engineering activities on the project shoreline.

Model selection

50. Shoreline and beach change are produced by the combined processes of waves, currents, wind, water level, changes in sand supply and other factors which interact in a time-dependent and nonlinear way. In the following paragraphs four classes of beach change models are discussed according to a classification system given by Kraus (1983, 1989). This classification provides a framework for evaluating the inherent or expected capabilities and limitations of available beach change models. The four classes of beach response models are:

- a. The macro-process model.
- b. The shoreline change or one-contour line model.
- c. The multi-contour line model.
- d. The 3-dimensional (3D) bathymetric change model.

51. Macro-process models provide a qualitative indication of how a shoreline will tend to evolve under a given set of constant (representative) influences (breaking wave conditions) and constraints (an assumed equilibrium profile with a depth of closure). Analytical solutions of shoreline change and the one-line numerical model operated with constant wave conditions are examples of this class of model. The macro-process model is the least sophisticated of all the beach change models and is mainly used to obtain rough indications of shoreline change. The longshore extent of macro-process models

can be any project scale under highly idealized conditions. Larson et al. (1987) provide a compendium of more than 25 analytical solutions of shoreline change derived for idealized wave and boundary conditions.

52. One-line beach change models have been verified for numerous engineering projects and have been proven capable of quantitatively predicting essential features of shoreline change that occur near coastal structures such as groins, detached breakwaters, and beach nourishment projects. A primary assumption of the shoreline change model shared with the other models is that the long-term planform shape of an open-ocean sandy coast is controlled by the incident waves and the longshore current they produce. Although it is recognized that other types of currents, as well as water level and wind also play a role in shoreline evolution, these processes are presumed to be secondary in the long-term. Also, cross-shore transport is neglected under the assumption that the beach profile maintains a constant form. Sand sources and sinks can be represented, if necessary. Since this class of model is the most commonly applied model for engineering applications and its use has been shown to produce quantitatively reliable results (e.g., Kraus 1983, Kraus and Harikai 1983, Chu et al. 1987, Hanson et al. 1988, Gravens, Scheffner, and Hubertz 1989), the shoreline change model was selected for use in the subject project investigation. A more detailed description of the shoreline model, including assumptions and computational flow, is given in the following section.

53. Multi-line models are typically an extension of the one-line model in which the planform change of certain contour lines is calculated in addition to computed changes in the shoreline contour (Bakker 1968, Perlin and Dean 1983). These models calculate both longshore and cross-shore sediment (sand) transport, and do not require the assumption of constant profile shape used in the one-line model. Although this type of model shows considerable promise for future engineering applications, significant development of lateral and shoreside boundary conditions and algorithms for the calculation of the incident wave climate would be required in order to apply it to the subject project coast. Once the required enhancements are developed, the execution time of the model is expected to be at least 100 times that of the one-line model not including the extra execution time required by an associated wave refraction model. Because of high execution cost, multi-line model simulations are limited to simulations of approximately 1 mile for a period

ranging from months to years. Finally, multi-line models have not been well verified for prototype applications and have been successfully applied to only a few engineering projects (for example, Scheffner and Rosati 1987).

54. Three-dimensional bathymetric change models are the most sophisticated and comprehensive of the beach change modeling techniques. Their purpose is to calculate, on a two-dimensional grid, local sediment transport caused by arbitrary combinations of waves, currents, and the corresponding topographic changes. This class of model requires extensive computational resources, as well as specialized operator expertise. Consequently, the spatial and temporal limits of these models are on the order of less than 1 mile and months, respectively. Three-dimensional models are still at the research development stage and cannot be economically applied to large-scale projects where long-term shoreline change is of interest.

Shoreline model theory

55. The aim of shoreline change modeling is to describe long-term evolution in shoreline position, in which the beach profile is assumed to maintain an equilibrium shape. This implies that bottom contours are parallel and that the entire profile is translated either seaward or landward for an accreting or eroding shoreline, respectively. Under this assumption it is necessary to consider the movement of only one contour line, conveniently taken to be the shoreline, as shown in Figure 12. Seasonal trends in shoreline position change are assumed to be accounted for in an average sense, thereby requiring a sufficiently long calibration interval.

56. In the model, longshore sand transport is assumed to occur uniformly over the active beach profile down to a limiting depth, called the depth of closure D . No longshore sand transport is assumed at depths greater than the depth of closure. Hence, a change in the shoreline position Δy at a certain point is related to the change in cross-sectional area ΔA at the same point according to Equation 1:

$$\Delta A = \Delta y D \quad (1)$$

where

ΔA = change in cross-sectional beach area, sq ft

Δy = change in shoreline position, ft

D = active profile (depth of closure + berm height), ft

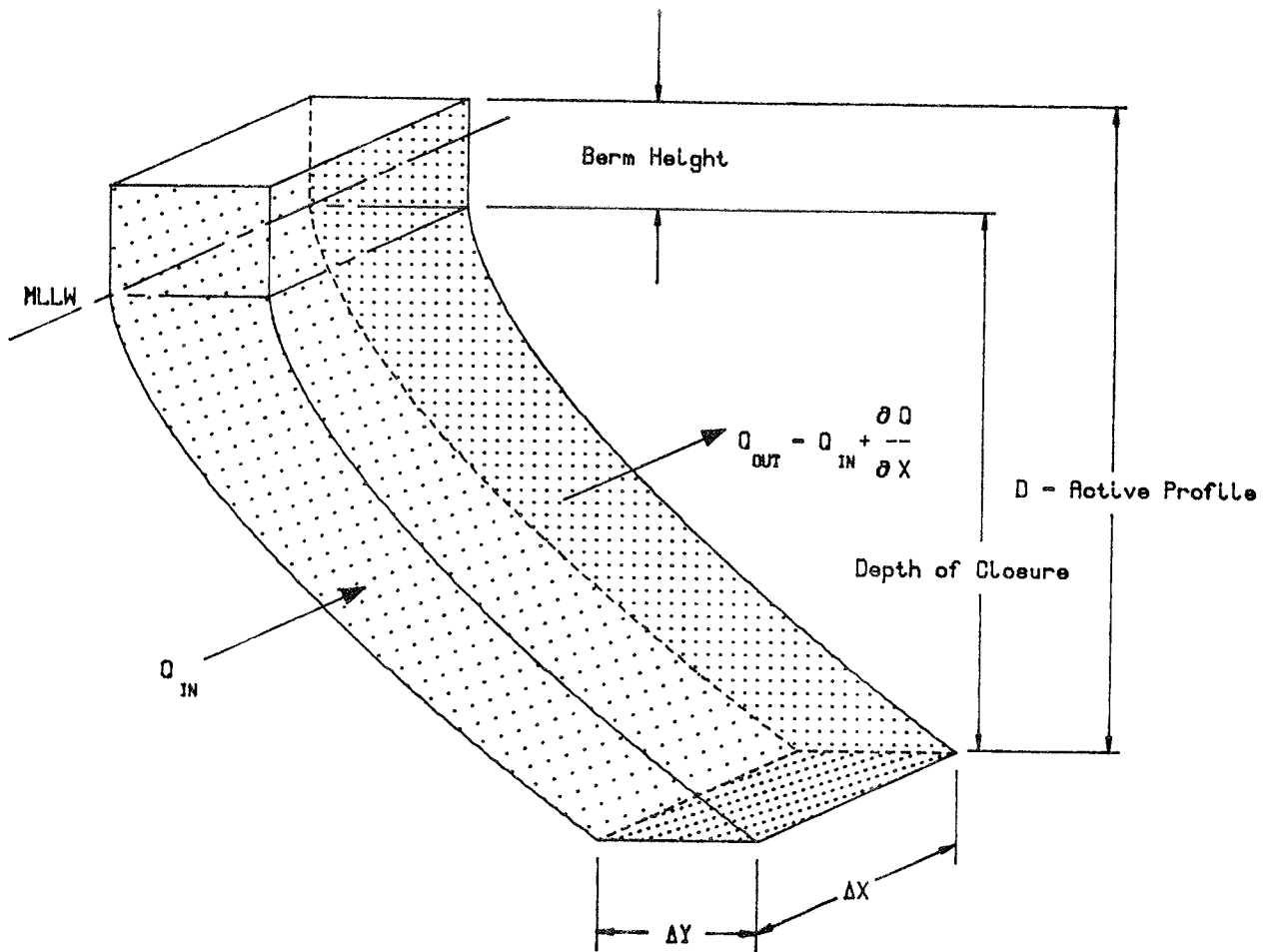


Figure 12. Illustration of an idealized equilibrium beach profile and control volume for longshore sand transport continuity

By considering a control volume of sand and formulating a mass balance during an infinitesimal interval of time, the following differential equation is obtained:

$$\frac{\partial Q}{\partial x} + \frac{\partial A}{\partial t} = 0 \quad (2)$$

where

- Q = longshore sand transport rate, cu ft/sec
- A = cross-sectional area of beach, sq ft
- x = spatial coordinate along the axis parallel to the trend of the shoreline, ft
- t = time, sec

Equation 2 requires that a variation in the longshore sand transport rate be balanced by changes in the shoreline position. Therefore, at a given time step, Δy shown in Figure 12 is equal to $(Q_{in} - Q_{out}) / (D \Delta x)$.

57. In order to solve Equation 2, it is necessary to specify an expression for the longshore sand transport rate. The predictive formula for Q used in the shoreline change model is:

$$Q = \frac{H_b^2 C_{gb}}{16(S-1)(1-a)} \left[K_1 \sin(2\alpha_{bs}) - 2 K_2 \frac{dH_b}{dx} \cot(\beta) \cos(\alpha_{bs}) \right] \quad (3)$$

where

- H_b = breaking wave height, ft
- C_{gb} = wave group speed at breaking, ft/sec
- S = ratio of sediment (quartz) density to water density ($S = 2.65$)
- a = sediment porosity ($a = 0.4$)
- α_{bs} = breaking wave angle with respect to the shoreline
- $\cot(\beta)$ = reciprocal of beach slope

The quantities K_1 and K_2 are empirical coefficients and are treated as calibration parameters.

58. The first term in Equation 3 corresponds to the "CERC formula" described in the Shore Protection Manual (SPM) (1984, Chapter 4) and provides an estimate of the sand transport produced by obliquely incident breaking waves. The second term estimates transport produced by a longshore current resulting from a variation in the breaking wave height alongshore. The first term is always dominant on an open coast, but the second term provides a significant correction if diffraction enters into the problem (Ozasa and Brampton 1980, Kraus 1983, Kraus and Harikai 1983).

59. Lateral boundary conditions are required in the solution prescribed in Equation 2. Typical boundary conditions are no sand transport, such as at a long groin or breakwater, and uniform transport, such as at a stable beach. Other boundary conditions may be formulated (Hanson and Kraus 1989).

Description of the Wave Model RCPWAVE

60. Equation 3 shows that the calculated longshore sand transport rate is dependant on the breaking wave angle with respect to the shore and the breaking wave height. Calculated shoreline change is therefore sensitive to

the input wave conditions. In order to obtain accurate estimates of the nearshore wave climate, a wave transformation model is required that calculates wave refraction, diffraction, and shoaling over a natural bathymetry. The Regional Coastal Processes WAVE (RCPWAVE) propagation model (Ebersole, Cialone, and Prater 1986) was used to model the transformation of representative classes of linear waves over a digitized bathymetry which extended from the east jetty at Anaheim Bay southward to the Santa Ana River. The finite difference solution scheme of the model requires a 2-dimensional horizontal computational grid. The grid used in this study consisted of 97 cells alongshore and 22 cells across-shore with grid cell dimensions of 600 ft alongshore and 300 ft across-shore. A plot of the RCPWAVE bathymetry grid employed in the present project is given in Figure 13. The alongshore coordinates 1 and 97 correspond to profiles along the east Anaheim Bay jetty and just south of the Santa Ana River, respectively.

61. Execution of the wave transformation model for every offshore wave condition in the simulation time series would require more extensive resources than would be justified by the accuracy of the input wave data and sophistication of the numerical models. As an alternative approach the offshore wave data were separated into seven 22.5-deg angle bands and two 11.25-deg angle bands as shown in Figure 14. A wave of unit height with a period corresponding to each wave period existing in the offshore wave data was input to RCPWAVE on the offshore boundary (at a depth equal to that applicable to the wave data) of the computational grid at an incident angle equal to the central angle of the angle band. RCPWAVE results (a wave height transformation coefficient and nearshore incident wave angle) were saved at grid points alongshore at a nominal depth of 18 ft. These values were written to a data base and keyed to the input angle band and wave period. When the shoreline change model GENESIS read the offshore wave conditions at a given time step a key was calculated in the same manner. The key was then used to identify the corresponding nearshore wave conditions along the project coast. Using this methodology, nearshore wave heights and incident angles are obtained at 600-ft intervals for input to the shoreline change model. The dashed line with the "x" symbols in Figure 13 represents the locations at which the nearshore wave conditions were saved. This procedure allows the shoreline change model to

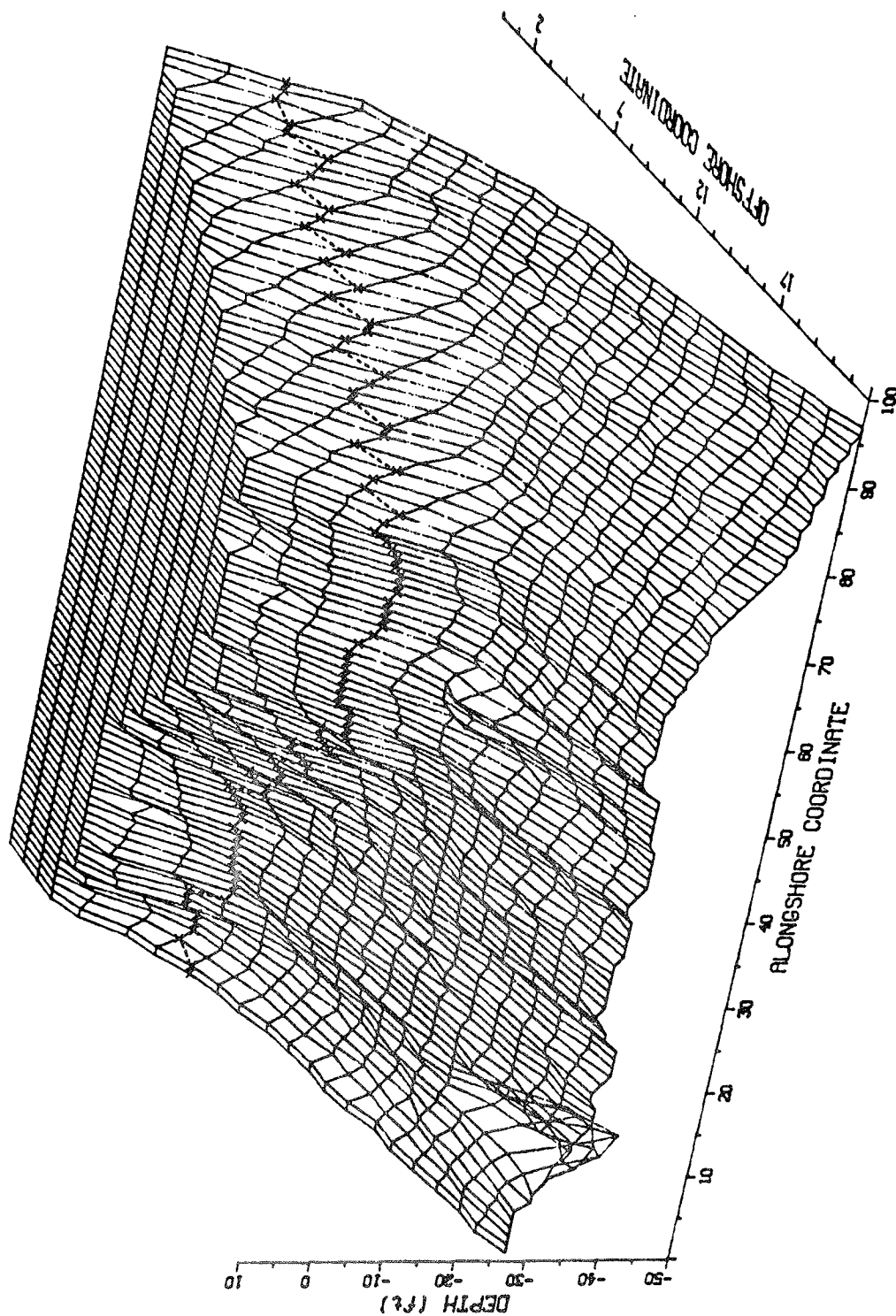


Figure 13. RCPWAVE bathymetry grid

account for effects of major bathymetric features which may cause convergence or divergence of wave energy along the coast.

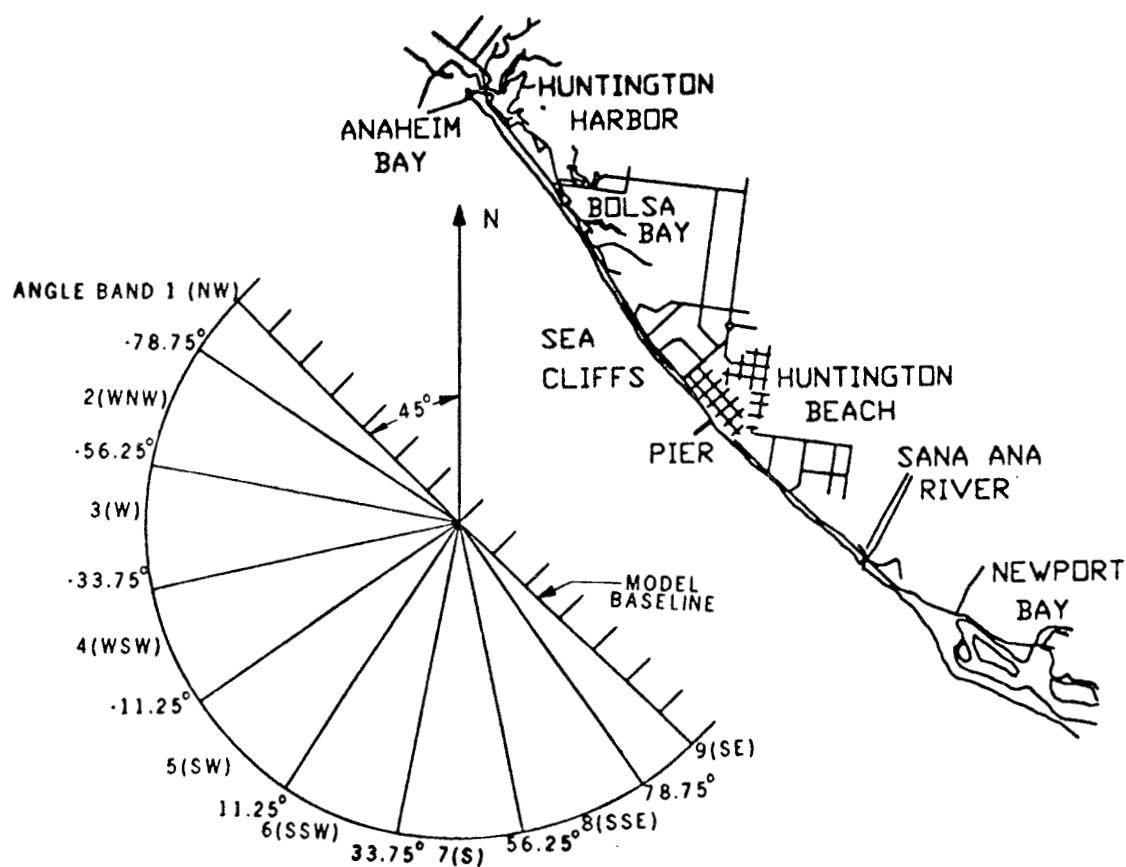


Figure 14. Angle band definition sketch

Description of the Shoreline Evolution Model GENESIS

62. The numerical model GENESIS is a one-contour line beach evolution model of the type first introduced by Pelnard-Considere (1956). The acronym GENESIS stands for GENeralized model for SIMulating SHoreline change (Hanson 1987). A detailed description of the model is provided by Hanson (1987) and Hanson and Kraus (1989). GENESIS is a generalized system of numerical models

and computer subroutines which allows simulation of long-term shoreline change under a wide variety of user-specified conditions. GENESIS has been successfully applied at numerous project sites for the purpose of evaluating proposed engineering activities or for verifying the model's ability to reproduce known shoreline changes resulting from coastal structures on the Atlantic, Gulf of Mexico, Great Lakes, and Pacific coasts (Chu et.al. 1987; Kraus et.al. 1988; Hanson, Kraus, and Gravens 1988; Gravens, Scheffner, and Hubertz 1989; Hanson, Kraus, and Nakashima 1989).

63. GENESIS calculates the longshore sand transport rate and resulting plan shape of the modeled coast. The effect of natural and artificial coastal structures such as sea cliffs, seawalls, and groins, and engineering activities such as beach fills on the longshore sand transport rate are incorporated in the model by use of appropriate boundary conditions and constraints. The diffraction effect of detached breakwaters and long groins on the local wave climate is represented.

64. GENESIS can be utilized with two types of wave inputs depending on the available data and degree of computational effort appropriate. A single offshore or deepwater wave condition can be input, and the breaking wave model within GENESIS will calculate breaking wave conditions along the modeled reach. The wave model in GENESIS is based on linear wave theory and assumption of a uniformly sloping bottom with parallel contours. Wave refraction and shoaling are iteratively calculated using Snell's Law and the assumption of wave energy conservation to satisfy a breaking criterion. For calculation points in the lee of structures located in the offshore, diffraction is also included in the calculation of breaking waves. Alternatively, a more sophisticated wave transformation model (such as RCPWAVE) which describes wave propagation over the actual offshore bathymetry can be used to perform the required wave transformations to shallow water. In this case, GENESIS retrieves the nearshore wave characteristics (output from RCPWAVE) from a data base and performs local refraction, diffraction, and shoaling calculations to obtain a breaking wave height and angle with respect to the shoreline. In either case, once the breaking wave field along the modeled reach is available, longshore sand transport rates are calculated using Equation 3, and Equation 2 is used to calculate the shoreline position.

65. GENESIS is primarily used to calculate long-term changes in shoreline position caused by the alongshore movement of sand. Cross-shore transport of sand caused, for example, by intense short-duration storm events, or seasonal changes in waves, is not modeled. However, shoreline changes resulting from these events could be superimposed on the shoreline position calculated by GENESIS to obtain a first approximation of the potential variation about the calculated shoreline position if information of the storm-induced beach change were available.

66. Details of the adaptation of GENESIS to the project coast of Bolsa Chica are provided in PART IV of this report.

PART IV: SHORELINE CHANGE MODEL CALIBRATION AND VERIFICATION

Historical Shoreline Positions and Shoreline Movement

Background

67. According to the study of Hales (1984), sand supply from the north to beaches between Anaheim Bay and the Santa Ana River was completely cut off due to the construction of the Anaheim Bay jetties in 1944. Since then, shoreline erosion has been a relatively continuous problem (US Army Engineer District, Los Angeles 1978). During the 1940's, 1,422,000 cu yd of material were placed in the Surfside-Sunset Beach area to mitigate shoreline retreat. Since that time, beach nourishment projects of varying magnitude have been conducted as needed. The average annual placed nourishment volume is approximately 350,000 cu yd.

68. Ten historical shoreline position data sets were used to characterize changes in position of the mean high-water (MHW) shoreline (+5.4 ft relative to MLLW datum) between 1878 and 1983. Table 1 gives a summary of these data sets. Map scales ranged from 1:3600 (1 in. = 300 ft) to 1:9600 (1 in. = 800 ft). Six of the shoreline data sets (1878, 1934, 1937, 1949, 1958, 1967) were constructed from a composite map illustrating MHW shoreline positions. The remaining four data sets were developed using beach and nearshore profile data at various positions alongshore. Shoreline positions were digitized at approximately 100-ft intervals from the Santa Ana River Jetty to Anaheim Bay. Shoreline positions developed from profile surveys were digitized at varying intervals determined by the survey spacing. All x-y coordinate pairs were measured relative to a baseline referenced to the California State-plane coordinate system. Since the alongshore spacing of shoreline position data was irregular, cubic spline interpolation was used to produce shoreline positions with an exact alongshore spacing of 100 ft.

69. Statistics of spatial and temporal variabilities in the shoreline position data sets were then calculated. Mean, standard deviation, and average absolute shoreline change were calculated at each point. These data yielded average amounts of shoreline movement for selected segments of the shoreline in the study area. The selected shoreline segments are as follows: Segment 1, Santa Ana River to Huntington Pier; Segment 2, Huntington Pier to

Anaheim Bay; Segment 3, Santa Ana River to Anaheim Bay (modeled reach); and Segment 4, near proposed ocean entrance site (cells 160-230).

Table 1
Summary of Shoreline Position Data Sets

<u>Date of Survey</u>	<u>Scale</u>	<u>Datum</u>	<u>File No.</u> ¹
1878 ²	1:9600	MLLW	C-949 - C-951
1934 ²	1:9600	MLLW	C-949 - C-951
1937 ²	1:9600	MLLW	C-949 - C-951
1949 ²	1:9600	MLLW	C-949 - C-951
1958 ²	1:9600	MLLW	C-949 - C-951
JUN 1963 - AUG 1963	1:3600	MLLW	902-B - 907-B
1967 ²	1:9600	MLLW	C-949 - C-951
APR 1969	1:9600	MLLW	C-921 - C-923
APR 1970	1:4800	MLLW	C-926-70-4 - C-931-70-4
DEC 1982 - JAN 1983	1:4800	MLLW	E-906 - E-910

¹ SPL file numbers.

² Month of survey not available.

Historic shoreline position change

70. Historic changes in shoreline position exhibited fairly consistent trends along two distinct shoreline segments between the Santa Ana River and Anaheim Bay. The southern stretch of shore between the Santa Ana River and Huntington Pier on the average experienced shoreline progradation between 1878 and 1983 (Figures 15-17). The northern coastal segment from Huntington Pier to Anaheim Bay was relatively stable for the same time period; however, shoreline progradation was dominant between 1934 and 1983. Additionally, changes in shoreline position were assessed for the entire length of coastline in the study area.

71. Tables 2-7 provide a summary of movement in shoreline position for each available time interval between 1878 and 1983. Positive values indicate shoreline progradation. The most obvious trend is net progradation at all segment locations for the 105-year record. Although average trends indicate accretion, local sections of coastline did experience episodes of erosion. Between the Santa Ana River and Huntington Pier, average absolute change in shoreline position was an increase (accretion) of 21.2 to 400.0 ft. This trend was also apparent for the northern shoreline section; however, in this

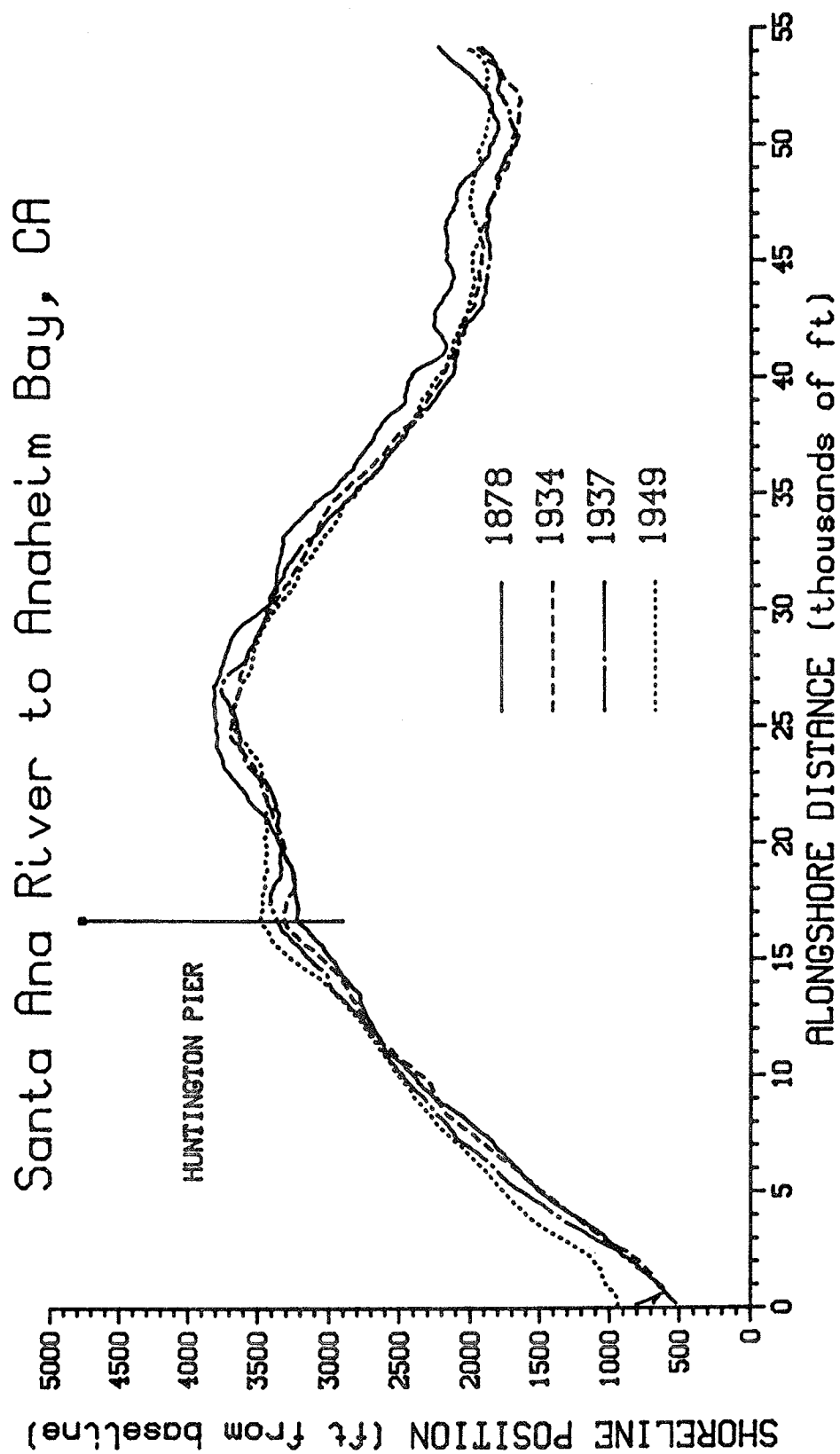


Figure 15. Shoreline positions, 1878-1949

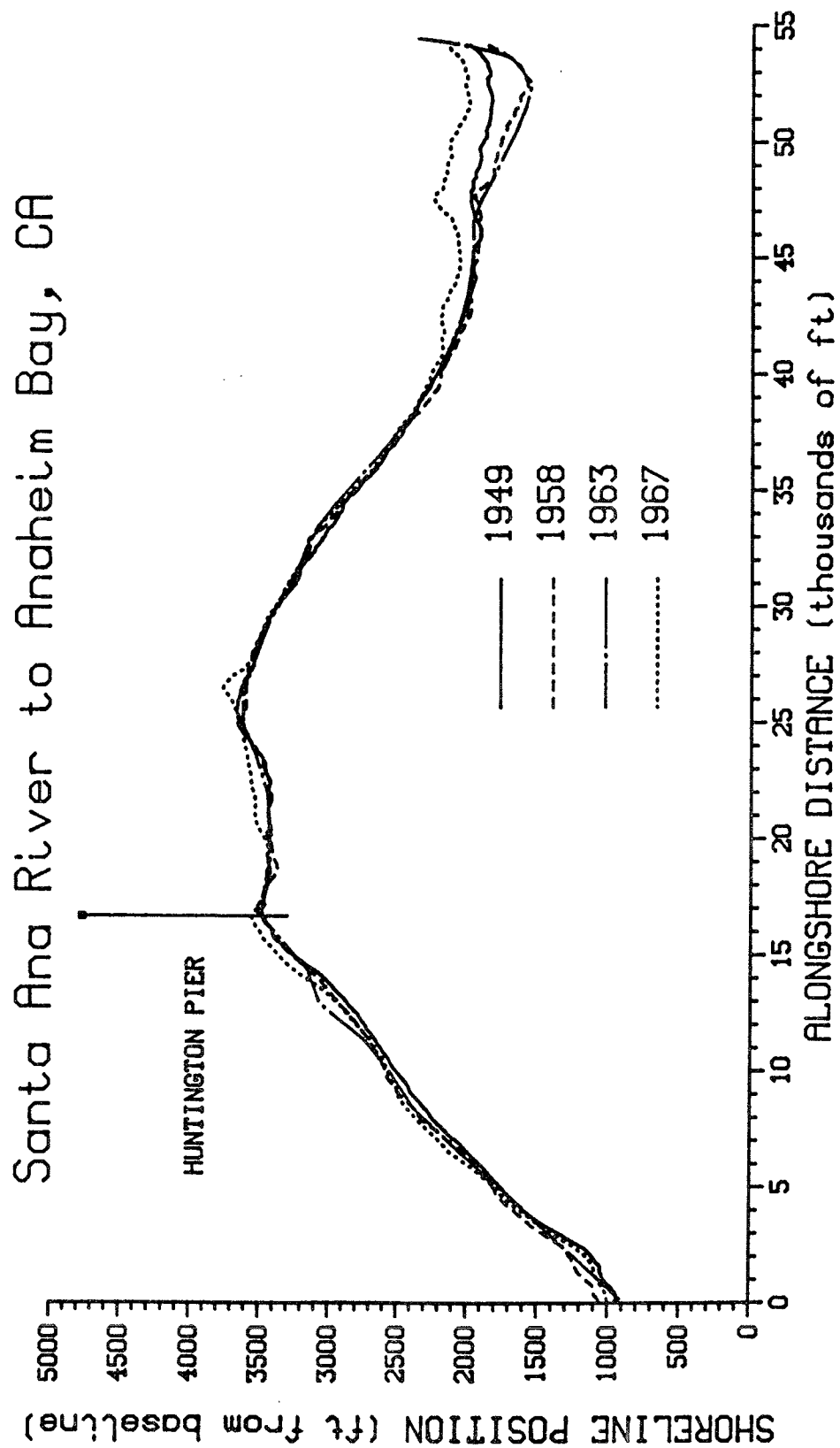


Figure 16. Shoreline positions, 1949-1967

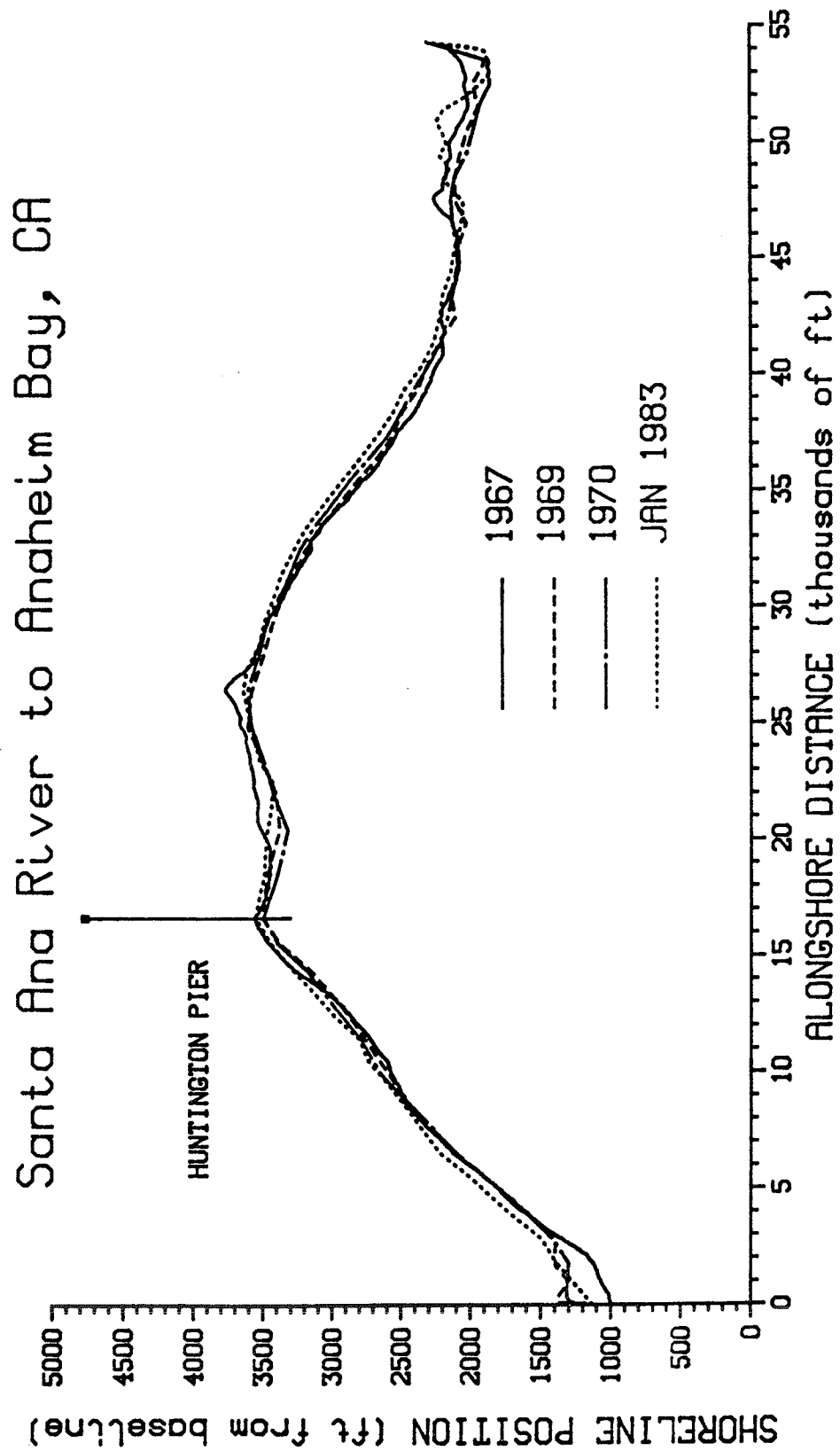


Figure 17. Shoreline positions, 1967-1983

Table 2
Shoreline Position Change, Santa Ana River to Anaheim Bay, CA
(Base Year 1878)

<u>Shoreline Movement</u>	<u>1878- 1934</u>	<u>1878- 1937</u>	<u>1878- 1949</u>	<u>1878- 1958</u>	<u>1878- 1963</u>	<u>1878- 1967</u>	<u>1878- 1969</u>	<u>1878- 1970</u>	<u>1878- 1983</u>
<u>Santa Ana River to Huntington Pier</u>									
Absolute change (ft)	21.2	105.9	224.1	296.0	288.8	301.8	327.1	337.3	400.0
Average rate (ft/yr)	0.4	1.8	3.2	3.7	3.4	3.4	3.6	3.7	3.8
Standard deviation (ft/yr)	0.9	1.1	1.4	1.5	1.0	1.2	1.7	1.4	1.2
<u>Huntington Pier to Anaheim Bay</u>									
Absolute change (ft)	-148.9	-147.6	-109.4	-140.8	-132.2	-23.2	-61.2	-57.5	-1.1
Average rate (ft/yr)	-2.7	-2.5	-1.5	-1.8	-1.6	-0.3	-0.7	-0.6	0.0
Standard deviation (ft/yr)	1.5	2.0	1.9	1.7	1.5	1.7	1.6	1.4	1.6
<u>Santa Ana River to Anaheim Bay (Modeled Reach)</u>									
Absolute change (ft)	-97.9	-71.6	-9.4	-9.7	-5.9	74.3	55.3	60.9	119.2
Average rate (ft/yr)	-1.7	-1.2	-0.1	-0.1	-0.1	0.8	0.6	0.7	1.1
Standard deviation (ft/yr)	1.9	2.6	2.8	3.0	2.7	2.3	2.6	2.4	2.3
<u>Near Proposed Ocean Entrance Site (Cells 160-230)</u>									
Absolute change (ft)	-131.2	-162.6	-152.0	-151.6	-123.8	-107.1	-87.5	-63.1	-14.9
Average rate (ft/yr)	-2.3	-2.8	-2.1	-1.9	-1.5	-1.2	-1.0	-0.7	-0.1
Standard deviation (ft/yr)	1.4	1.6	1.3	1.0	0.8	0.9	0.8	0.6	0.4

Table 3

Shoreline Position Change, Santa Ana River to Anaheim Bay, CA
(Base Year 1934)

<u>Shoreline Movement</u>	<u>1934- 1937</u>	<u>1934- 1949</u>	<u>1934- 1958</u>	<u>1934- 1963</u>	<u>1934- 1967</u>	<u>1934- 1969</u>	<u>1934- 1970</u>	<u>1934- 1983</u>
<u>Santa Ana River to Huntington Pier</u>								
Absolute change (ft)	84.7	202.9	274.8	267.6	280.6	305.9	316.1	378.8
Average rate (ft/yr)	28.2	13.5	11.5	9.2	8.5	8.7	8.8	7.7
Standard deviation (ft/yr)	14.7	6.3	5.1	2.9	2.7	4.5	3.7	2.5
<u>Huntington Pier to Anaheim Bay</u>								
Absolute change (ft)	1.3	39.5	8.1	16.7	125.7	87.6	91.3	147.8
Average rate (ft/yr)	0.4	2.6	0.3	0.6	3.8	2.5	2.5	3.0
Standard deviation (ft/yr)	19.2	6.5	3.0	2.4	4.4	3.8	3.3	3.1
<u>Santa Ana River to Anaheim Bay (Modeled Reach)</u>								
Absolute change (ft)	26.3	88.5	88.1	92.0	172.2	153.1	158.8	217.1
Average rate (ft/yr)	8.8	5.9	3.7	3.2	5.2	4.4	4.4	4.4
Standard deviation (ft/yr)	22.0	8.1	6.3	4.7	4.5	4.9	4.4	3.6
<u>Near Proposed Ocean Entrance Site (Cells 160-230)</u>								
Absolute change (ft)	-31.5	-20.8	-20.4	7.4	24.1	43.7	68.1	116.2
Average rate (ft/yr)	-10.5	-1.4	-0.8	0.3	0.7	1.2	1.9	2.4
Standard deviation (ft/yr)	12.0	3.2	1.3	0.8	2.1	1.9	1.6	1.5

Table 4
Shoreline Position Change, Santa Ana River to Anaheim Bay, CA
(Base Year 1937)

<u>Shoreline Movement</u>	<u>1937- 1949</u>	<u>1937- 1958</u>	<u>1937- 1963</u>	<u>1937- 1967</u>	<u>1937- 1969</u>	<u>1937- 1970</u>	<u>1937- 1983</u>
<u>Santa Ana River to Huntington Pier</u>							
Absolute change (ft)	118.2	190.1	182.9	195.9	221.2	231.4	294.1
Average rate (ft/yr)	9.9	9.1	7.0	6.5	6.9	7.0	6.4
Standard deviation (ft/yr)	8.5	6.3	3.9	3.1	5.4	4.6	2.9
<u>Huntington Pier to Anaheim Bay</u>							
Absolute change (ft)	38.2	6.8	15.4	124.4	86.4	90.1	146.5
Average rate (ft/yr)	3.2	0.3	0.6	4.1	2.7	2.7	3.2
Standard deviation (ft/yr)	19.2	6.5	3.0	2.4	4.4	3.8	3.3
<u>Santa Ana River to Anaheim Bay (Modeled Reach)</u>							
Absolute change (ft)	62.2	61.8	65.7	145.9	126.8	132.5	190.8
Average rate (ft/yr)	5.2	2.9	2.5	4.9	4.0	4.0	4.1
Standard deviation (ft/yr)	8.3	6.1	4.5	4.4	4.9	4.5	3.5
<u>Near Proposed Ocean Entrance Site (Cells 160-230)</u>							
Absolute change (ft)	10.7	11.1	38.9	55.5	75.1	99.5	147.7
Average rate (ft/yr)	0.9	0.5	1.5	1.9	2.3	3.0	3.2
Standard deviation (ft/yr)	4.6	1.6	1.5	2.6	2.3	2.2	2.0

Table 5

Shoreline Position Change, Santa Ana River to Anaheim Bay, CA(Base Year 1949)

<u>Shoreline Movement</u>	<u>1949- 1958</u>	<u>1949- 1963</u>	<u>1949- 1967</u>	<u>1949- 1969</u>	<u>1949- 1970</u>	<u>1949- 1983</u>
<u>Santa Ana River to Huntington Pier</u>						
Absolute change (ft)	71.9	64.7	77.7	103.0	113.2	175.9
Average rate (ft/yr)	8.0	4.6	4.3	5.2	5.4	5.2
Standard deviation (ft/yr)	4.7	4.1	1.9	4.9	3.7	1.5
<u>Huntington Pier to Anaheim Bay</u>						
Absolute change (ft)	-31.4	-22.8	86.2	48.2	51.9	108.3
Average rate (ft/yr)	-3.5	-1.6	4.8	2.4	2.5	3.2
Standard deviation (ft/yr)	7.8	6.4	3.9	3.2	3.8	2.8
<u>Santa Ana River to Anaheim Bay (Modeled Reach)</u>						
Absolute change (ft)	-0.4	3.5	83.7	64.6	70.3	128.6
Average rate (ft/yr)	0.0	0.2	4.6	3.2	3.3	3.8
Standard deviation (ft/yr)	8.8	6.5	3.5	4.0	4.0	2.6
<u>Near Proposed Ocean Entrance Site (Cells 160-230)</u>						
Absolute change (ft)	0.4	28.2	44.9	64.5	88.9	137.0
Average rate (ft/yr)	0.0	2.0	2.5	3.2	4.2	4.0
Standard deviation (ft/yr)	3.7	2.4	2.6	1.9	2.2	2.0

Table 6

Shoreline Position Change, Santa Ana River to Anaheim Bay, CA
(Base Years 1958 and 1963)

<u>Shoreline Movement</u>	<u>1958- 1963</u>	<u>1958- 1967</u>	<u>1958- 1969</u>	<u>1958- 1970</u>	<u>1958- 1983</u>	<u>1963- 1967</u>	<u>1963- 1969</u>	<u>1963- 1970</u>	<u>1963- 1983</u>
	<u>Santa Ana River to Huntington Pier</u>								
Absolute change (ft)	-7.3	5.7	31.1	41.2	104.0	13.0	38.4	48.5	111.3
Average rate (ft/yr)	-1.5	0.6	2.8	3.4	4.2	3.2	6.4	6.9	5.6
Standard deviation (ft/yr)	12.5	7.1	6.5	4.7	1.4	16.7	17.1	11.5	2.9
	<u>Huntington Pier to Anaheim Bay</u>								
Absolute change (ft)	8.6	117.6	79.5	83.2	139.7	109.0	70.9	74.6	131.1
Average rate (ft/yr)	1.7	13.1	7.2	6.9	5.6	27.3	11.8	10.7	6.6
Standard deviation (ft/yr)	7.2	13.7	9.5	8.2	4.9	35.5	20.0	15.6	7.0
	<u>Santa Ana River to Anaheim Bay (Modeled Reach)</u>								
Absolute change (ft)	3.8	84.0	65.0	70.6	128.9	80.2	61.2	66.8	125.1
Average rate (ft/yr)	0.8	9.3	5.9	5.9	5.2	20.1	10.2	9.5	6.3
Standard deviation (ft/yr)	9.2	13.4	8.9	7.5	4.2	32.9	19.3	14.6	6.1
	<u>Near Proposed Ocean Entrance Site (Cells 160-230)</u>								
Absolute change (ft)	27.8	44.5	64.1	88.5	136.6	16.7	36.3	60.7	108.8
Average rate (ft/yr)	5.6	4.9	5.8	7.4	5.5	4.2	6.0	8.7	5.4
Standard deviation (ft/yr)	4.1	6.3	4.7	4.3	3.0	12.9	7.5	5.6	3.0

Table 7

Shoreline Position Change, Santa Ana River to Anaheim Bay, CA
(Base Years 1967, 1969, and 1970)

<u>Shoreline Movement</u>	<u>1967- 1969</u>	<u>1967- 1970</u>	<u>1967- 1983</u>	<u>1969- 1970</u>	<u>1969- 1983</u>	<u>1970- 1983</u>
	<u>Santa Ana River to Huntington Pier</u>					
Absolute change (ft)	25.4	35.5	98.3	10.1	72.9	62.7
Average rate (ft/yr)	12.7	11.8	6.1	10.1	5.2	4.8
Standard deviation (ft/yr)	53.7	29.9	4.2	36.5	4.6	4.0
	<u>Huntington Pier to Anaheim Bay</u>					
Absolute change (ft)	-38.1	-34.4	22.0	3.7	60.1	56.4
Average rate (ft/yr)	-19.0	-11.5	1.4	3.7	4.3	4.3
Standard deviation (ft/yr)	34.5	28.5	6.2	43.5	4.2	5.0
	<u>Santa Ana River to Anaheim Bay (Modeled Reach)</u>					
Absolute change (ft)	-19.0	-13.4	44.9	5.6	63.9	58.3
Average rate (ft/yr)	-9.5	-4.5	2.8	5.6	4.6	4.5
Standard deviation (ft/yr)	43.7	30.9	6.1	41.6	4.3	4.8
	<u>Near Proposed Ocean Entrance Site (Cells 160-230)</u>					
Absolute change (ft)	19.6	44.0	92.2	24.4	72.6	48.2
Average rate (ft/yr)	9.8	14.7	5.8	24.4	5.2	3.7
Standard deviation (ft/yr)	21.0	15.0	3.7	25.1	3.1	1.9

region, the net rate of shoreline retreat had been decreasing. This stretch of coastline has benefitted from periodic beach nourishment since the 1940's. The dramatic decrease in the absolute amount of shoreline retreat between 1963 and 1967 was likely the result of 4,000,000 cu yd of material placed on the Surfside-Sunset Beach shoreline in 1964 (Hales 1984). Without such periodic additions of nourishment, the northern shoreline segment would probably not exhibit net accretion. The entire 10.2-mile stretch of shoreline showed a similar trend, switching from a net erosional condition between 1878 and 1934 to a net progradational shoreline from 1878 to 1983 (Table 2). Although the magnitude and direction of short-term shoreline movement varied between individual survey intervals, long-term trends in shoreline change were consistent.

72. A third coastal segment was isolated to examine shoreline movement near the proposed construction site of the ocean entrance channel (between 32,000 ft and 46,000 ft from the origin on Figures 15-17). Historic shoreline movement averaged -0.1 ft/yr between 1878 and 1983, although more recent rates of change showed an advance which averaged approximately +5 ft/yr (1963-1983, 1967-1983, 1969-1983, 1970-1983). This is similar to average trends for the entire length of shoreline. Additional shoreline position data and information on shoreline changes in the study area are provided by Signal Landmark (1988).

Nearshore Bathymetry

73. Depth contours at the project coast are generally parallel to the trend of the shoreline. At the southern end of the modeled reach (near the Santa Ana River), the profile steepens slightly. Figure 13 shows the bathymetry that was used in the wave transformation model. The bathymetry was digitized from a 1983 survey performed by SPL (Table 1). The nearshore bathymetry along this shoreline reach lends itself well to shoreline change numerical modeling because the refraction and shoaling routines in GENESIS employ straight and parallel contours to determine breaking conditions from input local nearshore wave conditions. Two profiles near the proposed entrance channel location were digitized for the years of 1970, and 1983. Plots of these profiles (Figure 18), which span 13 years, indicate that the assumption of an active profile moving parallel to itself is well satisfied.

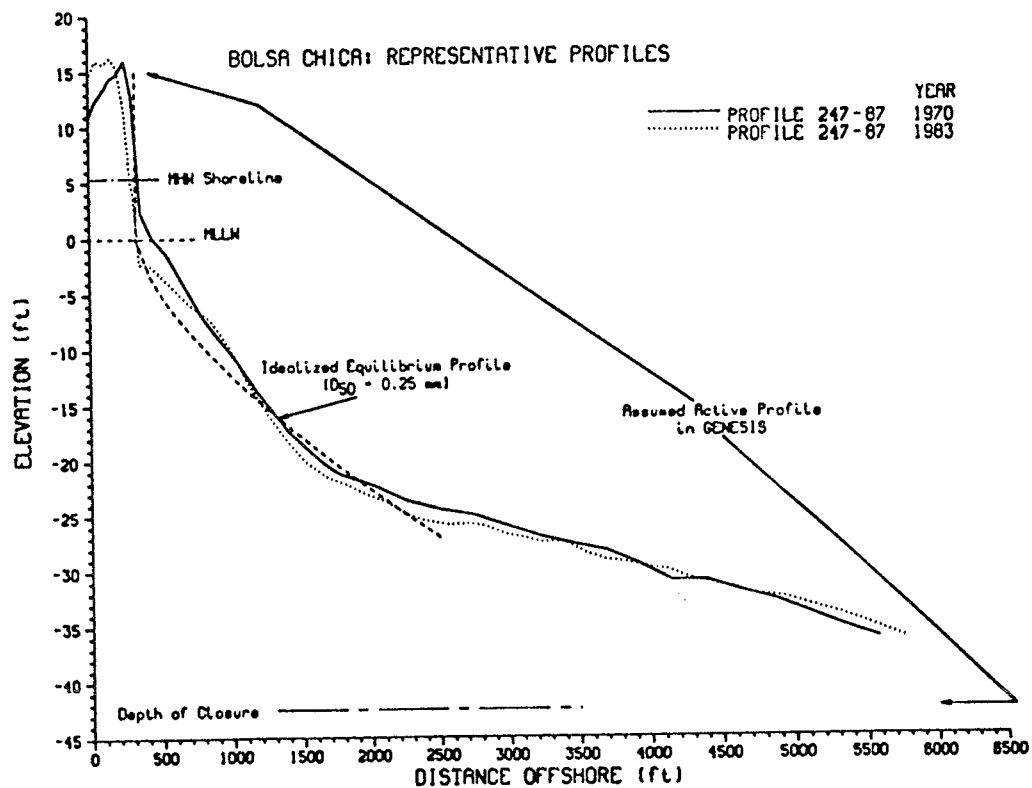
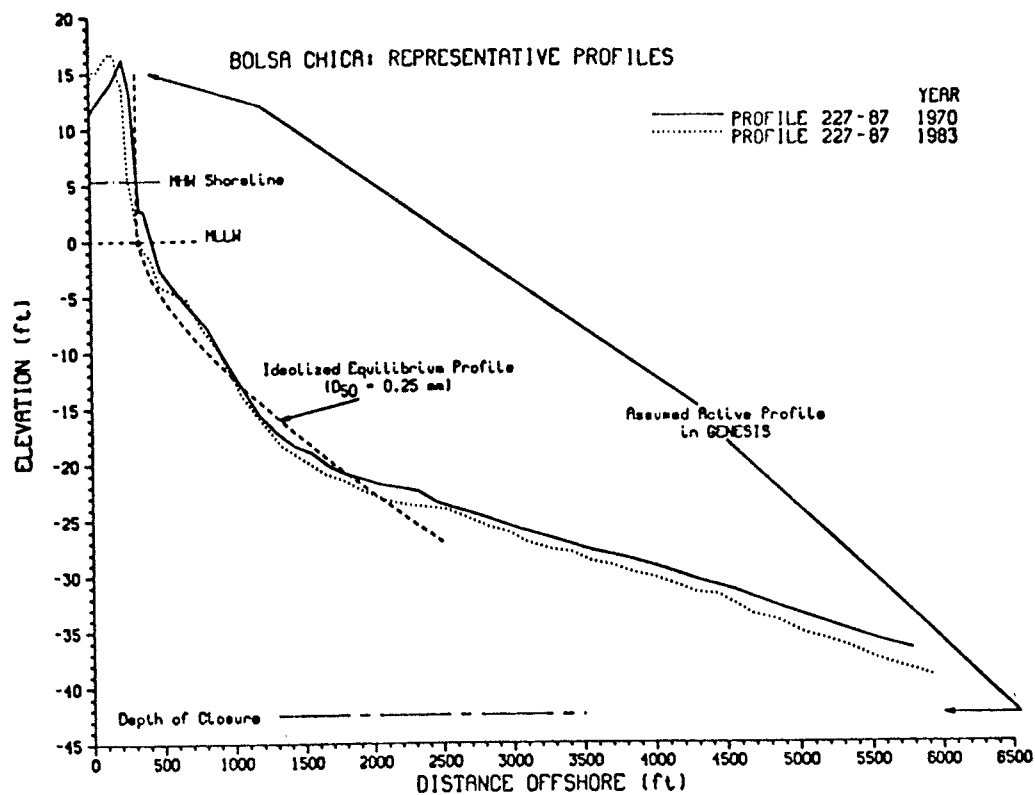


Figure 18. Representative beach profiles at Bolsa Chica

Furthermore, the idealized equilibrium profile assumed in GENESIS appears to fit the representative profiles shown in Figure 18 well to a depth of approximately 25 ft. Although the profile shape changes somewhat throughout the year due to seasonal changes in the incident waves, the effect of these seasonal changes on wave refraction and shoaling are assumed secondary in one-line modeling. The intent of using the wave model RCPWAVE and a digitized bathymetry is to incorporate into the wave refraction and shoaling calculations major bathymetric features which may focus or disperse wave energy along the project coast.

Analysis of Wave Data

74. As part of the mission of the Corps of Engineers, the Wave Information Study (WIS), performed a 20-year wind-wave hindcast for the Southern California Bight of the Pacific Coast from Point Conception, California, to the US-Mexican border. The hindcast study involved consideration of a highly complex system of forcing functions and local effects that control the wave climate. The forcing mechanisms included: large scale forcing by northern Pacific swell; synoptic east Pacific wind fields; southern hemisphere swell; and localized effects such as island sheltering and diffraction, as well as meso-scale meteorological systems such as land-sea breezes. A discussion of the hindcast methodology is provided in Appendix B, which is a reprint of the paper entitled "A Multi-Faceted Wind-Wave Hindcast Method to Describe a Southern California Wave Climate" by Jensen, Vincent, and Reinhard (1989). For the present Bolsa Chica study, the 20-year hindcast was repeated on a 5 nautical mile (nm) sub-grid of the WIS 10 nm hindcast grid. The time histories of wave conditions at Stations 14 and 11, from the 5 nm grid were used as input for the shoreline change model GENESIS. These data represent the best available wave data for the project reach.

75. Four additional sources of wave data are available for project coast. These are the Marine Advisors (MA) hindcast (Marine Advisors 1961), the National Marine Consultants (NMC) hindcast (National Marine Consultants 1960), two US Army Corps of Engineers Littoral Environment Observation (LEO) Stations (Sherlock and Szuwalski 1987), and a slope array wave gage maintained by Scripps Institution of Oceanography (SIO). The SIO gage data were used in

the Preliminary Shoreline Response Study (Gravens 1988). In the following paragraphs the various wave data sets are compared.

76. The NMC and MA hindcasts are for the years 1956, 1957, and 1958, and give percent occurrences for given deepwater wave heights and periods. These data were used for statistical comparison purposes only.

77. The LEO program had two stations on the project coast, at Bolsa Chica and Huntington Beach. The LEO program provides daily visual estimates of the breaking wave height, angle, and period, as well as other littoral environment data. LEO data are available for the Bolsa Chica station from October 1979 to May 1982, and for the Huntington Beach station from October 1979 to April 1985. A one-year-long time history of wave data was selected from the Bolsa Chica and Huntington Beach LEO stations for use in the statistical comparison of the available wave data.

78. As part of the Coastal Data Information Program sponsored by the US Army Corps of Engineers and the California Department of Boating and Waterways, SIO maintains a slope array wave gage at a water depth of 26.9 ft just offshore of Bolsa Chica (SIO reports the gage depth as 8.2 m, here converted to 26.9 ft). This wave gage has been in place since November 1980, and the longest period of continuous data is a 27-month period from February 1981 to May 1983. The next longest continuous record is 1 year and 2 months long, from June 1986 to August 1987. These two continuous records were combined to simulate a continuous 3-year time series of significant wave height, incident angle, and wave period at 6-hr intervals. This time series was used in the Preliminary Shoreline Response Study.

79. The first step in examination of the available wave data was to compare the statistics of the available data sets at the stations of interest (MA hindcast (station B), NMC hindcast (station 7), two LEO stations (Bolsa Chica, and Huntington Beach), the SIO wave gage at Sunset Beach, and the 5 nm grid hindcast wave data. Because GENESIS uses a time-step procedure to calculate shoreline change, only the LEO data, SIO gage data, and the WIS hindcast data can be readily adapted for use. The WIS hindcast is the preferred data set because it contains estimates of the significant wave height, peak spectral period, and mean direction of both sea and swell wave components at 3-hr intervals for the 20-year period January 1956 through December 1975.

80. The wave data for the two LEO stations and the MA and NMC hindcast stations were transformed to a depth of 26.9 ft (the depth of the SIO wave gage) using linear wave theory refraction and shoaling in order to compare the distribution of incident wave angles between the data sets. The time histories of wave conditions at Stations 14 and 11 from the 5 nm WIS hindcast grid were transformed from their respective depths of 88 ft and 331 ft to a depth of 26.9 ft. The transformations of the hindcast wave data included the effect of local wave energy shadowing by Point Fermin. Additionally the transformations were performed with respect to the local shoreline orientation. The hindcast stations and the assumptions of the local transformations are illustrated in Figure 19.

81. Wave roses of incident angle were plotted for each of the stations and are shown in Figure 20. In Figure 20, the percent occurrence is given for each angle band as described earlier. The distribution of incident wave angles for the NMC hindcast Station 7 is greatly different from that of the other sources. This is due to its location, which is just north of Santa Catalina Island. The directional distribution of the transformed WIS hindcast data compares well with the two LEO stations and the MA Station B hindcast. As discussed in the preliminary study (Gravens 1988) the directional distribution of SIO gage data is somewhat narrower than the other data sets. In fact, the gage data show nearly double the percentage of waves occurring in the southwest (shore perpendicular) angle band than any of the other stations.

82. Next the distribution of wave period was calculated for the LEO stations, the SIO gage data, and the transformed WIS hindcast data. The results are shown in Figure 21. All four data sources show similar distributions of wave period. Figure 22 shows the distribution of wave height for the LEO stations, the SIO gage data, and the transformed WIS hindcast data. Here it is seen that the distribution of height from the transformed WIS hindcast and the SIO gage show larger wave heights than the LEO stations; however, the distribution of wave heights for the four data sources are roughly similar.

83. Based on the above comparisons of the available wave data for the project site, the transformed WIS hindcast wave data was chosen for input to GENESIS.

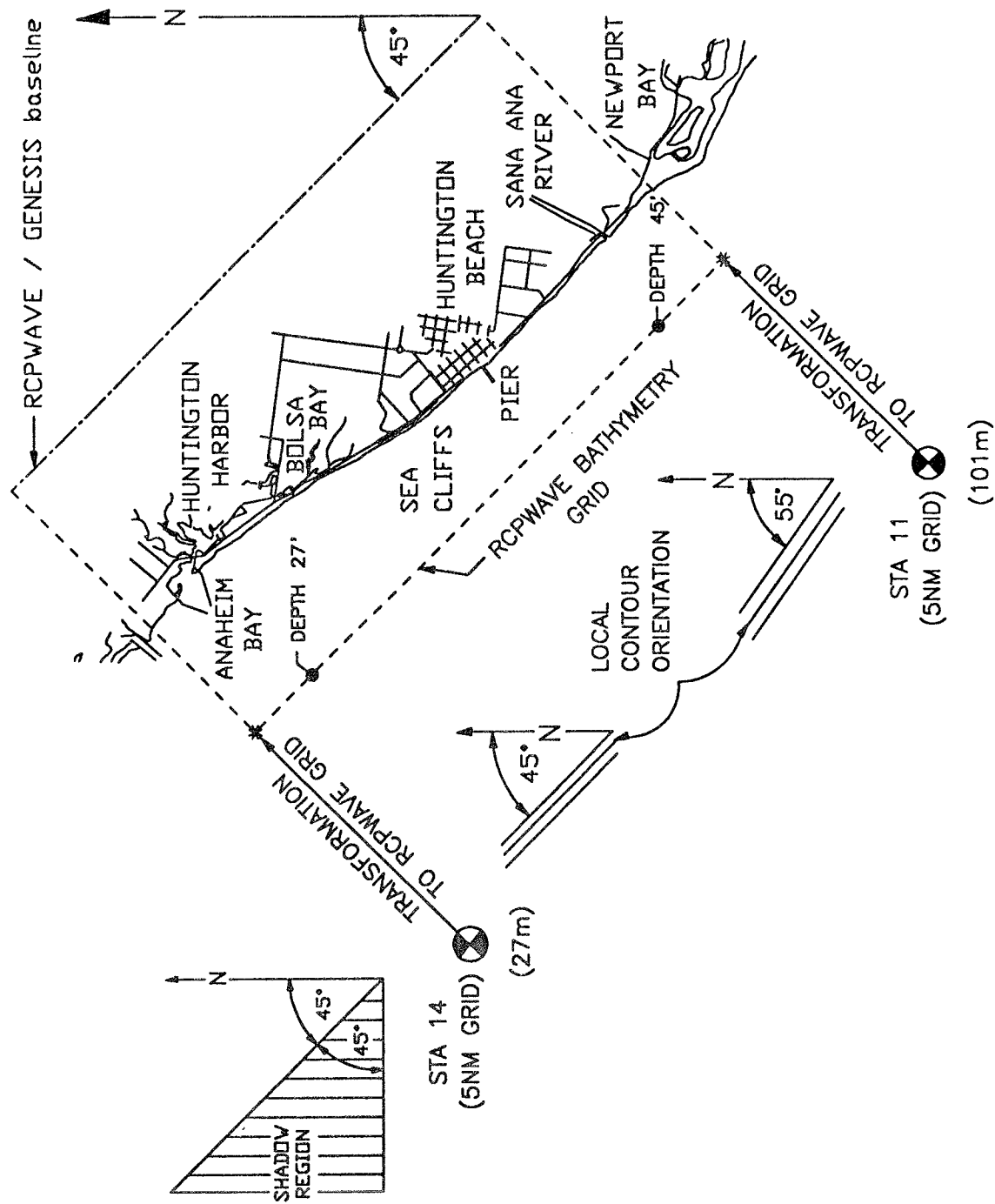
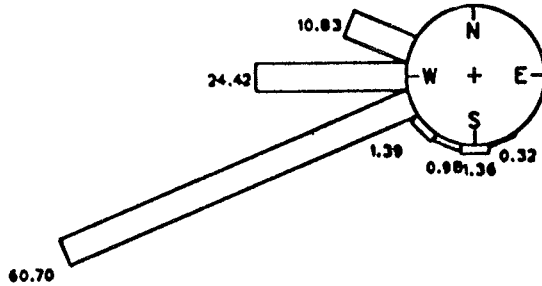
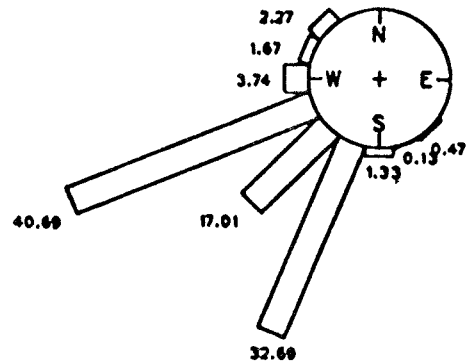


Figure 19. Transformation from Stations 14 and 11 to the RCPWAVE bathymetry grid

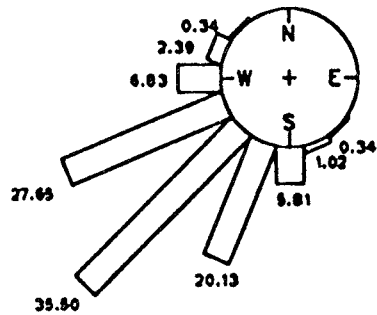
WAVE ROSE FOR NATIONAL MARINE CONSULTANTS HINDCAST
STATION 7 AT 26.9-ft. DEPTH



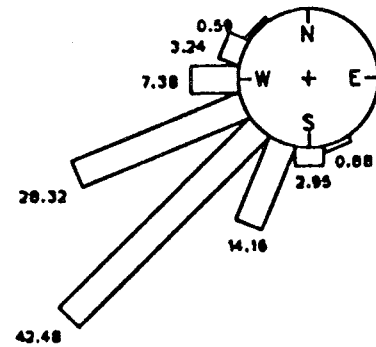
WAVE ROSE FOR MARINE ADVISORS HINDCAST
STATION B AT 26.9-ft. DEPTH



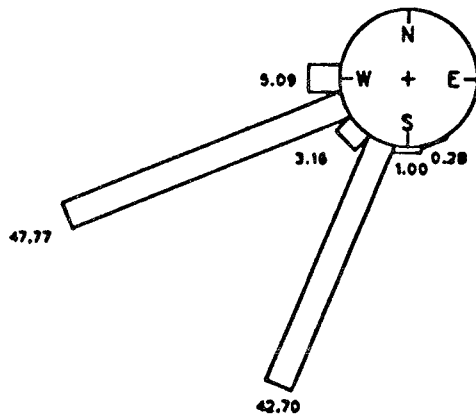
WAVE ROSE FOR BOLSA CHICA LEO STATION
AT 26.9-ft. DEPTH



WAVE ROSE FOR HUNTINGTON BEACH LEO STATION
AT 26.9-ft. DEPTH



WAVE ROSE FOR TRANSFORMED WIS HINDCAST AVERAGED
SOUTHERN SWELL (1984 & 1985) AT 26.9-ft. DEPTH



WAVE ROSE FOR SIO Sxy GAGE
AT 26.9-ft. DEPTH

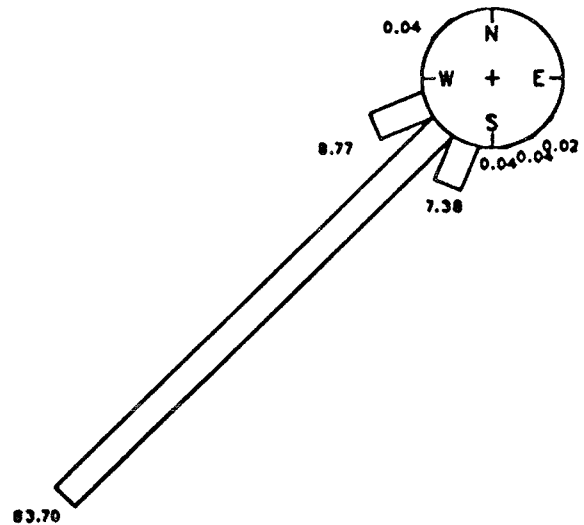


Figure 20. Distribution of incident wave angles at 26.9 ft depth

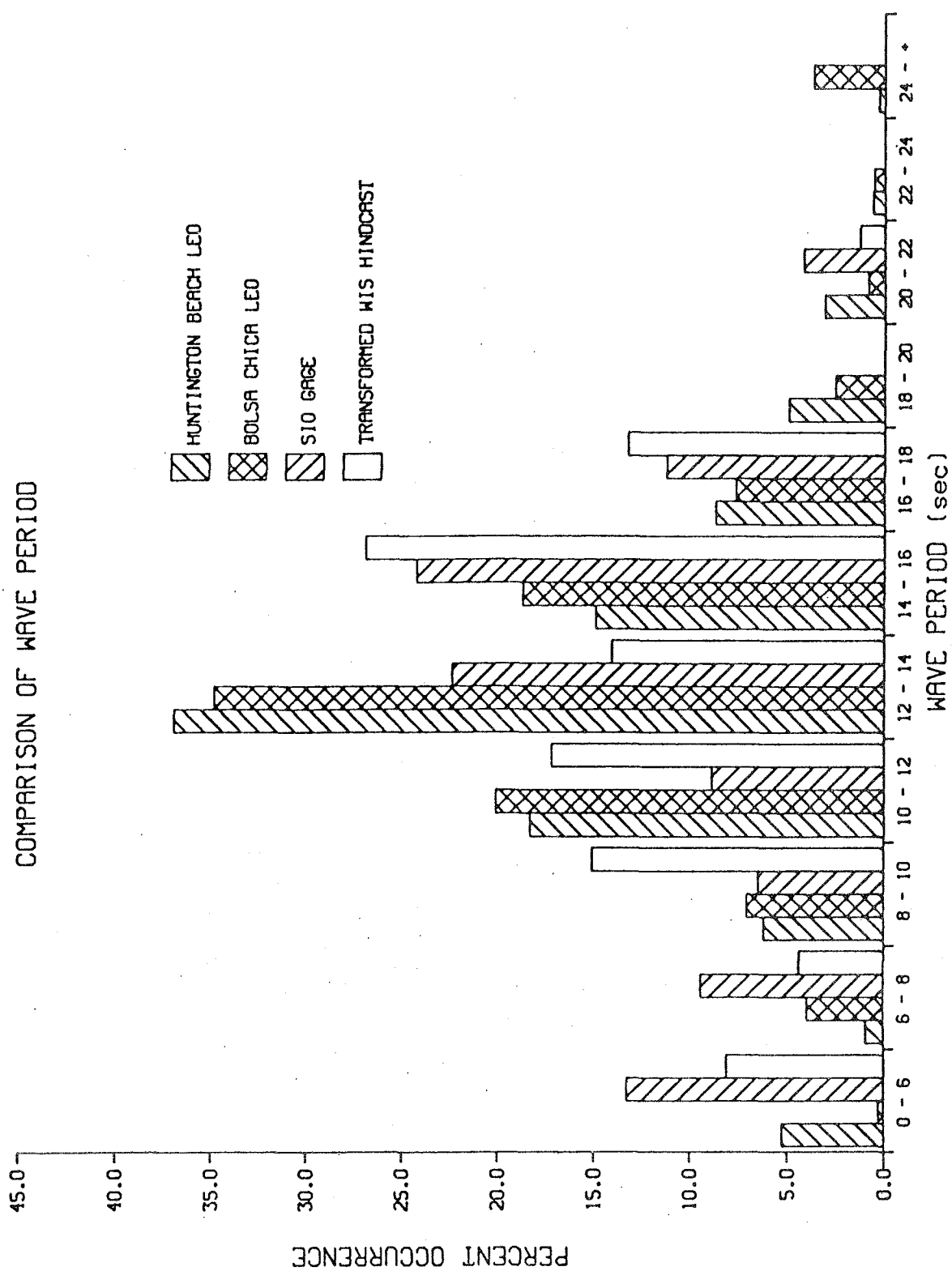


Figure 21. Distribution of wave period



Figure 22. Distribution of wave height

Potential Longshore Sand Transport Rates

84. Prior to running the shoreline response model GENESIS, estimates of the potential upcoast (northwest traveling sand) and downcoast (southwest traveling sand) sand transport rates were made for the years 1956 through 1975 using the transformed WIS hindcast wave conditions. The assumptions of the potential sand transport rate calculations include: linear wave refraction and shoaling, straight and parallel bottom contours, unlimited sand supply, and no littoral drift barriers. The transport rates were calculated using the energy flux method as described in the Shore Protection Manual (SPM, 1984) Chapter 4. These calculations were repeated for 23 shoreline orientations (representative of the surveyed shoreline orientations within the project reach) between 6 deg either side of the model baseline orientation which lies on a northwest-southeast line (45 deg counter-clockwise from north).

85. Input wave conditions for the potential sand transport rate calculations were obtained from the transformed WIS hindcast. The WIS hindcast provided wave height, period, and direction estimates for northern hemisphere sea and swell wave conditions for the 20-year period 1956 through 1975 at 3-hr intervals. WIS hindcast estimates for a third wave component, southern hemisphere generated swell, were available for the 2-year period 1984 and 1985 at 3-hr intervals. The southern swell hindcast for 1984 and 1985 will be referred to as southern hemisphere swell year 1 and year 2, respectively. The input data for the southern swell hindcast were obtained from National Data Buoy Center (NDBC) buoy No. 46024, located approximately 35 nm west of San Clemente Island.

86. The potential longshore sand transport rate calculated using year 1 of the southern swell hindcast as input was found to be approximately half the rate obtained using year 2 of the southern swell hindcast as input. This large variation in potential sand transport rates between consecutive years is not unusual and in fact was observed often in the analysis of the 20-year-long time history of northern hemisphere swell wave conditions. It is unfortunate that a longer data base of this important component of the incident wave climate in southern California is not available. The southern swell wave conditions will be utilized to band the solutions provided by the shoreline change model and to allow for an analysis of potential shoreline

changes resulting from persistent low-energy southern swell wave conditions (southern swell year 1, 1984) and high-energy southern swell wave conditions (southern swell year 2, 1985).

87. After calculating the potential upcoast and downcoast sand transport rates for each year of the 20-year northern hemisphere hindcast and for both years of the southern hemisphere swell hindcast a total average littoral drift rose (Walton and Dean 1973) was computed for the Anaheim Bay to Santa Ana River study reach. Through an analysis of the available shoreline position data it was determined that the shoreline orientation in this region varied through 13 deg (the analysis was performed in segments of 1000 ft), specifically, between 39 deg and 51 deg measured counter clockwise from north. Therefore, the total littoral drift rose shown in Figure 23 was computed for the shoreline orientations indicated by the survey data. There are 3 curves shown on the littoral drift rose shown in Figure 23, the curve with the circle symbols represents the total downcoast (southwest traveling) sand transport rate, whereas the curves with the asterisk and triangle symbols represent the total upcoast (northwest traveling) sand transport rate for year 1, and year 2 of the southern hemisphere swell, respectively.

88. To use the total littoral drift rose, first determine the orientation of coastal segment for which the sand transport rate is desired. Then using the angle of the coastal segment, enter the rose and find the total downcoast transport rate and the total upcoast transport rate; the net potential transport rate is the difference of the two. For example, assuming a shoreline orientation of 45 deg, the total downcoast sand transport rate is approximately 400,000 cu yd/year; the total upcoast sand transport rate is approximately 320,000 cu yd/year using year 1 of the southern hemisphere swell or 510,000 cu yd/year using year 2 of the southern hemisphere swell. The net sand transport rate therefore is 80,000 cu yd/year downcoast using southern swell year 1 or 110,000 cu yd/year upcoast using southern swell year 2. This figure also illustrates the sensitivity of the potential sand transport rate to the shoreline orientation. For instance, for a shoreline orientation of 40 deg the net potential sand transport rates is between 160,000 and 340,000 cu yd/year upcoast whereas for a shoreline orientation of 50 deg the net potential sand transport rate is between 140,000 cu yd/year and approximately 300,000 cu yd/year downcoast.

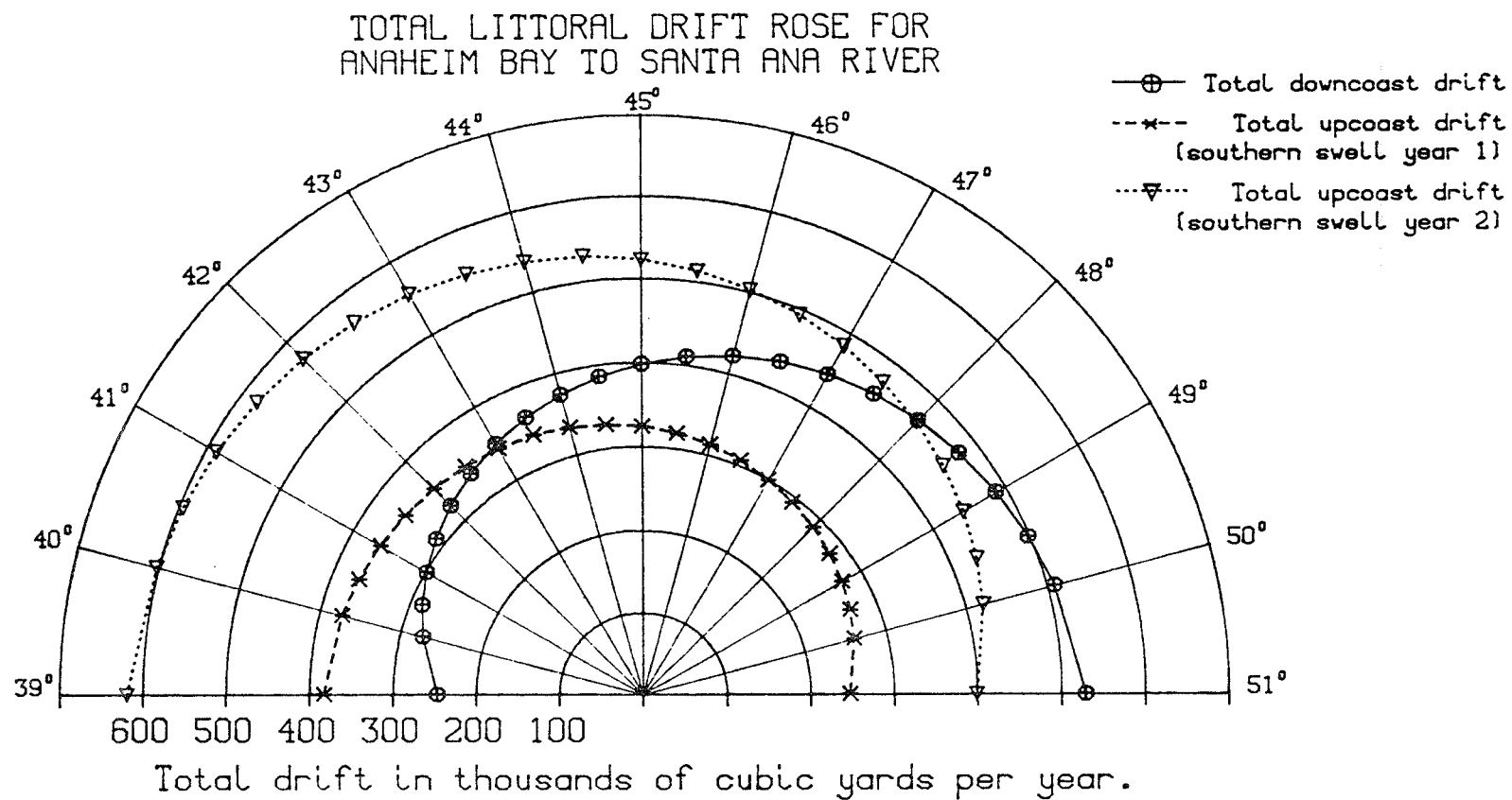


Figure 23. Total littoral drift rose for Anaheim Bay to Santa Ana River
(20-year-long hindcast data base)

Selection of Wave Climatology

89. Three parameters are used by GENESIS to describe the characteristics of the wave climate. These are the significant wave height, dominant wave period, and incident wave angle. GENESIS will be used to simulate historical shoreline changes in the model calibration and verification, and to predict future shoreline changes in the project design alternative simulations. Consequently, wave conditions input to the model must be applicable to the simulation period for shoreline change. As stated previously, the WIS northern hemisphere wave hindcast was performed for the years 1956 through 1975. The hindcast therefore, coincides with the calibration period (June 1963 through April 1970) and a portion of the verification period (April 1970 through January 1983). However, a synthetic time history of wave conditions will be required for input to GENESIS in the project design alternative simulations. The procedure used for selecting the wave conditions for the project design alternative simulations is presented in the following paragraphs.

90. GENESIS will be used to predict shoreline changes for a 10-year interval beginning immediately after project construction, which will require a 10-year-long time history of incident wave conditions. Ten years were randomly selected from the hindcast data base 1956 through 1975. A total of 20 10-year samples were taken. Then the average potential longshore sand transport rates were computed for each of the 10-year-long samples and for the entire hindcast data base. The sample which produced the average net potential sand transport rate closest to that of the hindcast data base was input to GENESIS in the design alternative simulations. A total littoral drift rose was computed for the selected 10-year time history of wave conditions and is given in Figure 24. Figures 23 and 24, show the similarity of total littoral drift curves as well as the net potential longshore sand transport rates for the randomly selected 10-year time history and the 20-year-long hindcast. Intersections of lines representing upcoast- and downcoast-directed transport indicate nodal points may occur at shoreline locations having orientations between 43 and 48 deg.

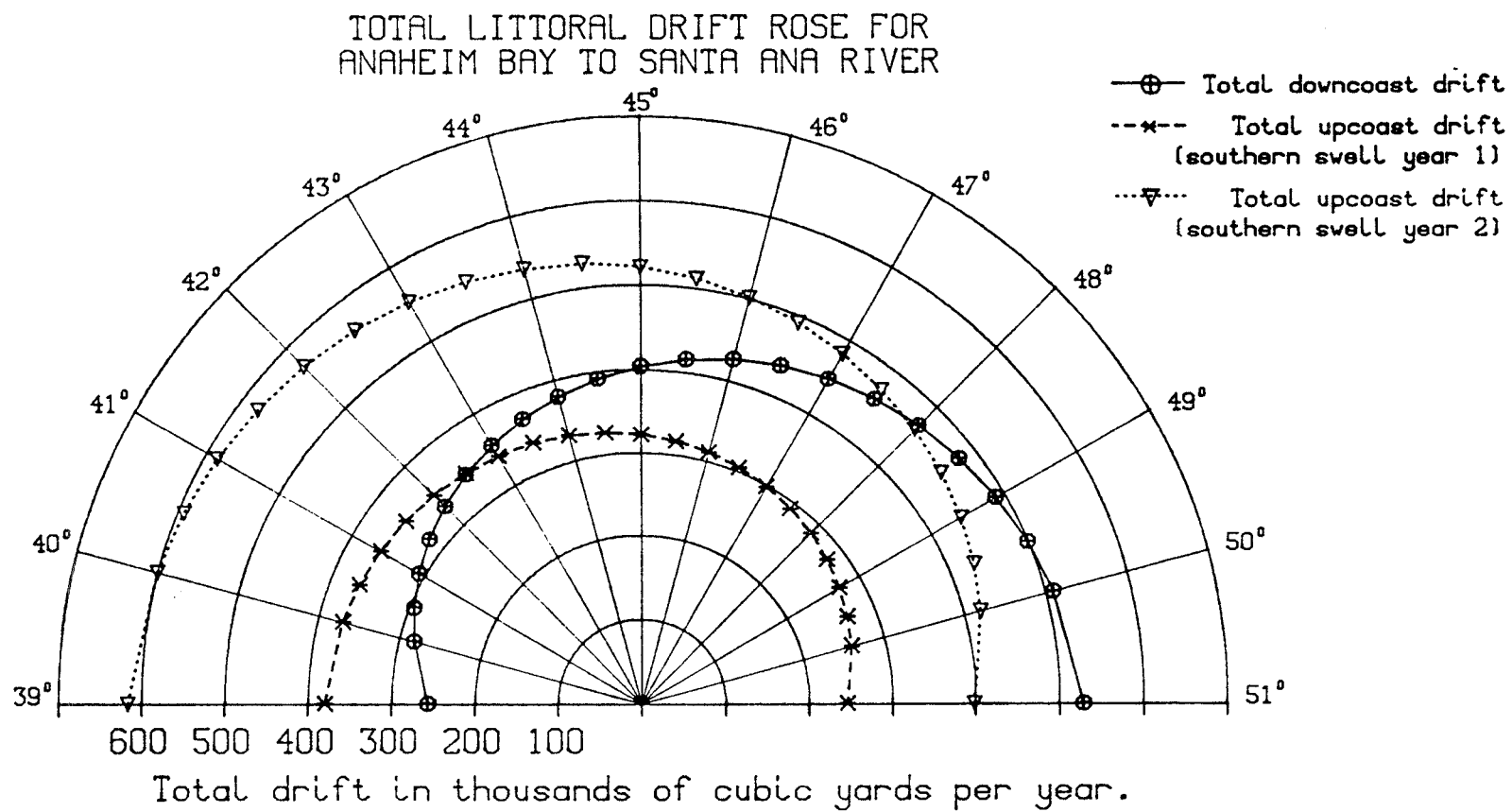


Figure 24. Total littoral drift rose for Anaheim Bay to Santa Ana River
(selected 10-year time history of representative wave conditions)

Model Calibration and Verification

91. The shoreline change numerical model GENESIS was configured for application to the project coast. The modeled reach extends from the east jetty of Anaheim Bay to the north jetty of the Santa Ana river and has 270 alongshore calculation cells (3 shoreline calculation cells for each wave refraction cell). The southern boundary condition at the Santa Ana River is simulated as a short groin (gated boundary condition see, Hanson and Kraus 1989). The implication of this boundary condition is that a portion of the calculated sand in transit at the boundary can pass into or out of the modeled reach provided that the calculated maximum depth of longshore transport at the given time step exceeds the 3-ft depth at the tip of the jetty. This boundary condition allows sand to move both into the model reach from the south and out of the model reach from the north. The sand discharge of the Santa Ana River is estimated to be insignificant and was therefore not included in the model.

92. The northern boundary condition, the east jetty of Anaheim Bay was simulated as a long non-diffracting jetty. The implication of this boundary condition is that no sand can move into the modeled reach from the north. Due to the orientation of the east Anaheim Bay jetty, waves which approach normal to the shore or from the south are reflected from the structure toward the shore at angles which may produce sand transport to the south. The importance of wave reflection from the east Anaheim Bay jetty was investigated in a desk study. The results of the study indicated that the longshore sand transport rate and resulting planform shape of the beach within about 2000 ft of the jetty could be strongly influenced by the effect of reflected waves impacting the shoreline if the incident waves are conditions which would produce reflected waves. However, because this is a localized phenomenon, having no effect on the proposed project site which is located approximately 15,000 ft from the Anaheim Bay jetty, wave reflection from the jetty was not simulated in the shoreline change model.

93. Two constraints on the sediment transport rate and shoreline change were imposed inside the modeled reach. They were the Huntington Beach Pier and the sea cliffs located between the proposed ocean entrance at Bolsa Chica and the Huntington Beach Pier. The Huntington Pier was simulated as a groin with a permeability of 5 percent. The permeability factor of 5 percent

was selected during the calibration process in which the permeability factor was varied between 0 (no permeability) and 100 percent (complete permeability) to determine the most appropriate value for this structure. The implication is that 5 percent of the transport volume which does not pass beyond the groin tip is passed through the structure. The Huntington Pier, however, does not actually function as a groin; instead it appears to reduce wave heights in a shadow region defined by the incident wave conditions. Regardless, calculated shoreline change and longshore sand transport rates within the area of interest (north of the sea cliffs) are not affected by the model constraint imposed at the pier. The sea cliffs along the Huntington Mesa were simulated as a seawall. This internal boundary condition prohibits the shoreline from eroding beyond the present position of the cliffs.

94. Several model simulations were performed for the calibration period of seven years spanning June 1963 to April 1970. The calibration parameters K_1 and K_2 in Equation 3 were varied for each calibration simulation. Values of K_1 and K_2 ranging between 0.8 and 0.2 were tested in the various calibration simulations. As a result the values $K_1 = 0.45$ and $K_2 = 0.4$ were judged to most appropriately estimate gross and net longshore sand transport rates to reproduce surveyed shoreline change. The calibration period included a massive beach fill in April 1964 which consisted of the placement of 4 million cu yd of sediment extending from the Anaheim bay jetty approximately 2 miles down coast to Warner Avenue.

95. The June 1963 surveyed shoreline was input to the model as the initial shoreline position. The calculated April 1970 shoreline position was then plotted together with the surveyed 1970 shoreline for comparison. In addition, the calculated net longshore sand transport rates were monitored and compared to previous estimates of transport rates at the project site (Caldwell 1956, Hales 1984).

96. The calibration results are given in Figure 25. The lower plot has a distorted vertical scale to resolve details of differences in shoreline position. The solid line in Figure 25 represents the initial shoreline position (June 1963 surveyed shoreline position), and the chain-dot line and dash line are the April 1970 surveyed and calculated shoreline positions, respectively. The calibration results are considered satisfactory, and it appears that the influence of natural and artificial structures within the

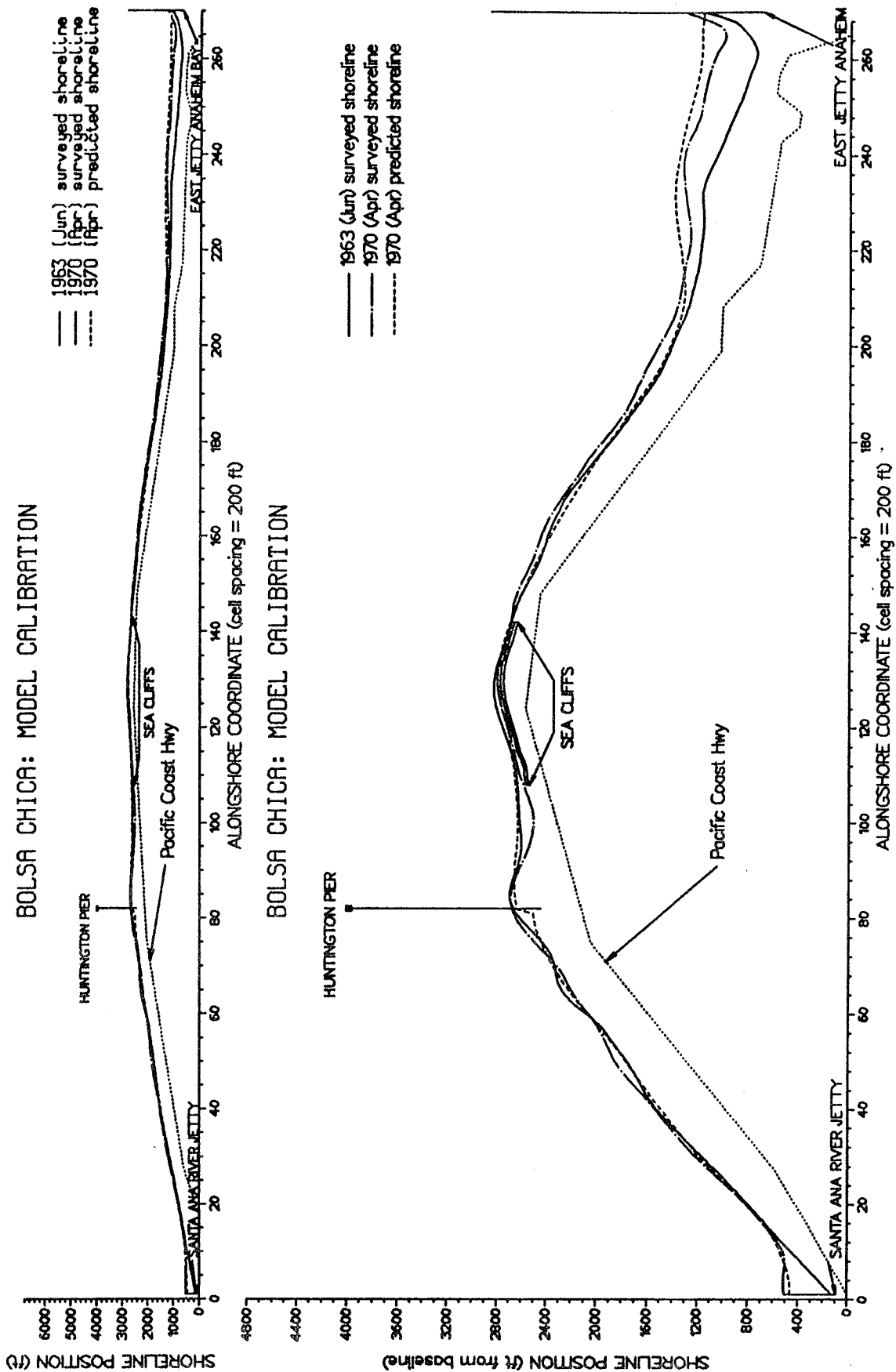


Figure 25. Model calibration results

modeled reach, including the beach fill and boundary structures, are simulated well in the model. An alternative and perhaps more informative presentation of the calibration results is obtained by plotting the calculated and surveyed shoreline change from the June 1963 shoreline, as shown in Figure 26.

97. The results given in Figure 26 show that the numerical model slightly overpredicts the transport of sand away from the feeder beach area (between alongshore coordinates 230 and 270) at Surfside. Presumably this disagreement between calculated and surveyed shoreline positions results from absence of a representation of reflected waves from Anaheim Bay jetty. At the proposed ocean entrance channel site, shown in Figure 26, the model predicts an accretive beach as indicated in the surveyed data.

98. The average annual net longshore sand transport rates for the calibration period vary from 0 at the Anaheim Bay jetty to a maximum of 140,000 cu yd/year (to the north) at alongshore coordinate 180 to about 75,000 cu yd/year (to the south) between alongshore coordinates 1 and 90. Plots of the average annual gross (dashed line) and net (solid line) longshore sand transport rates obtained from the model calibration are shown in Figure 27 together with the net rates for the one year with the greatest northerly net rate and the one year with the greatest southerly net rate. This figure indicates that the net longshore sand transport rate varies significantly from year to year and depends on the actual wave conditions which occur during the year.

99. The effect of the boundary condition imposed at the Huntington Beach Pier was investigated and the results are shown in Figure 28. The chain-dash line depicts the 10-year predicted shoreline position for the case where the pier was simulated as an impermeable groin, and the dash line depicts the 10-year predicted shoreline position for the case where the pier was simulated as a completely permeable groin (i.e., no constraints were placed on the longshore transport rates at the pier). As seen in Figure 28, shoreline change near the proposed entrance system is identical in both cases. Therefore, it may be concluded that the boundary condition imposed at the pier has no effect on the predicted shoreline change in the vicinity of the proposed entrance system for the simulation interval.

100. The next step was to verify the model by performing a simulation using the same calibration parameters for a different time period. The

BOLSA CHICA: CALIBRATION

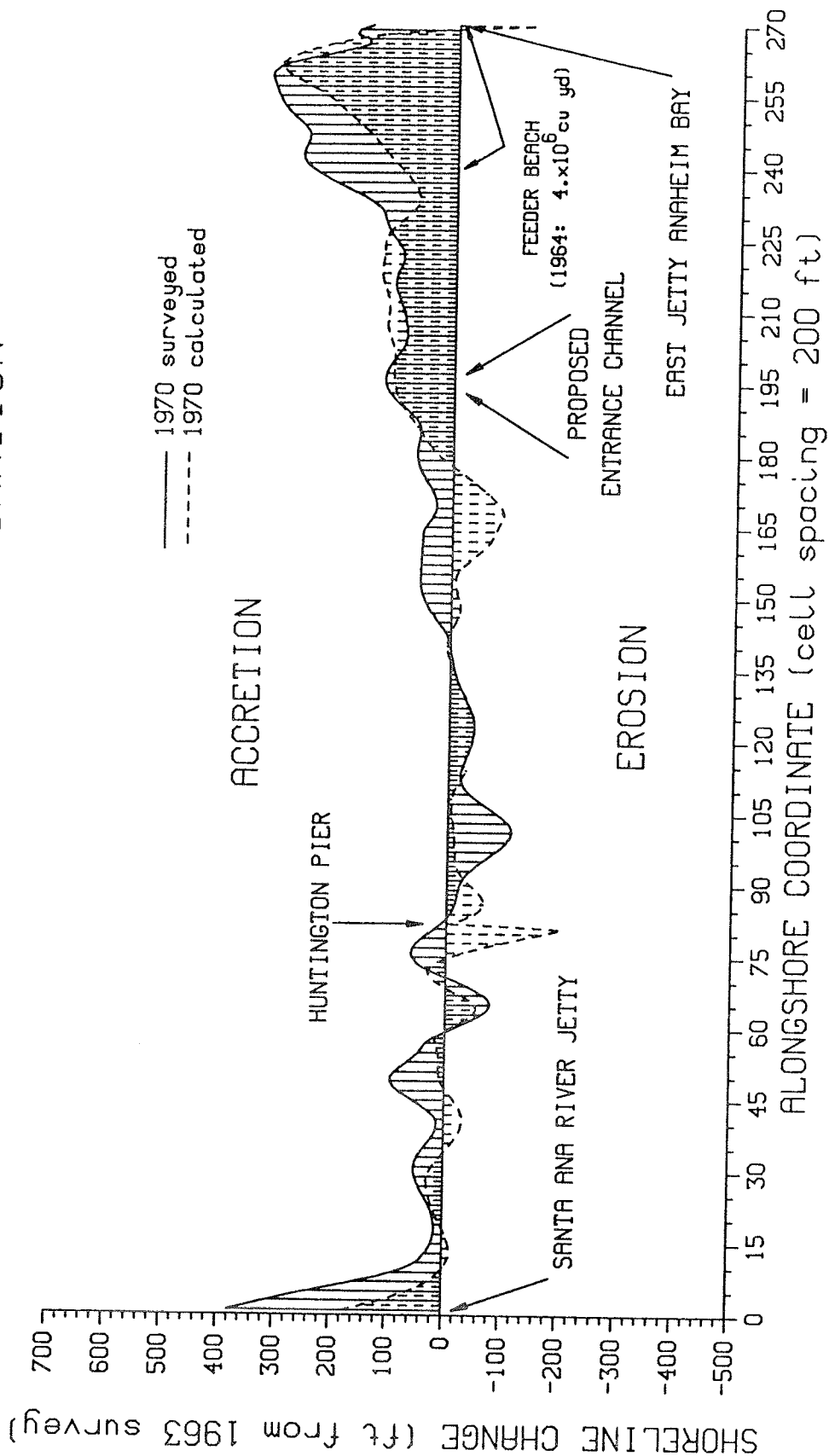


Figure 26. Model calibration: surveyed vs. calculated shoreline change

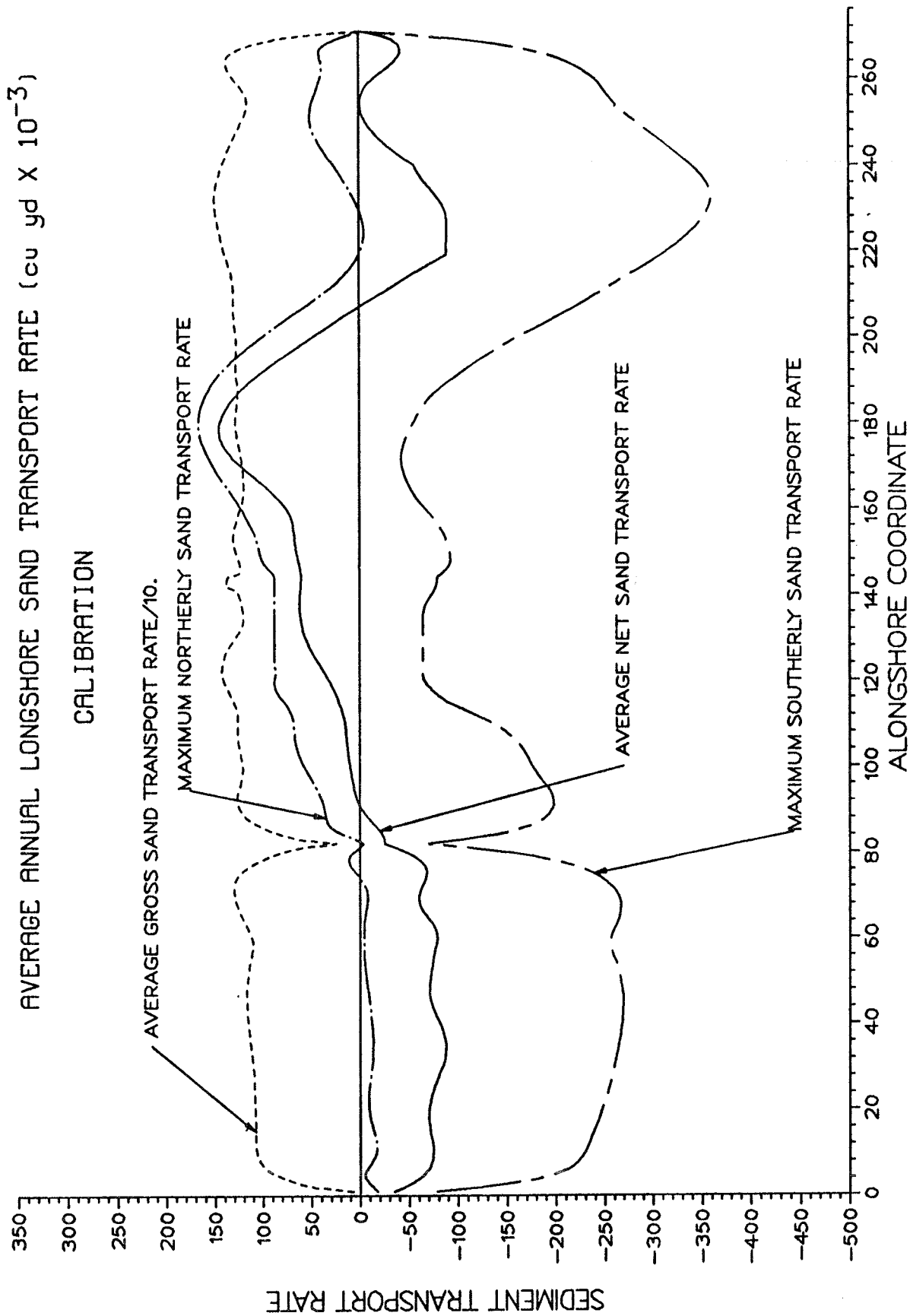


Figure 27. Average annual longshore sand transport rates for the calibration period (1963 -1970)

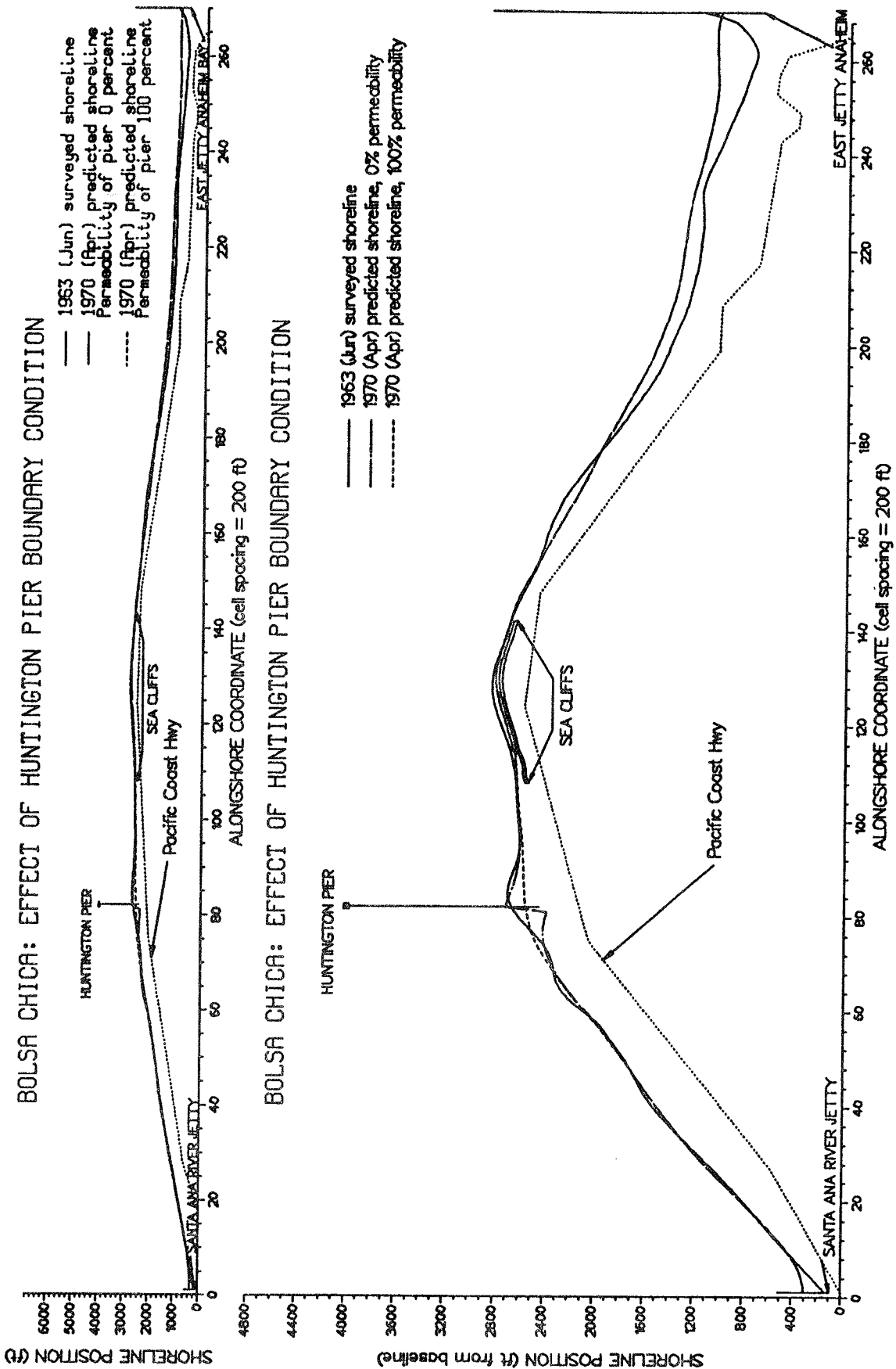


Figure 28. Effect of the Huntington Pier boundary condition

verification period was the 13-year period from April 1970 to January 1983. This period included two beach fill projects, one performed in March 1971 and one in April 1979. Both beach fills renourished the feeder beach at Surfside-Sunset. The 1971 beach fill consisted of the placement of 2.3 million cu yd of dredged material from the US Naval Weapons Station Harbor on the Surfside-Sunset feeder beach (from the Anaheim bay jetty to approximately 6000 ft down coast). The 1979 beach fill consisted of the placement of 1.66 million cu yd of fill on the same stretch of coast. The results of the model verification simulation are shown in Figure 29. As before, the solid line is the initial shoreline position (the April 1970 surveyed shoreline position), the chain-dot line is the January 1983 surveyed shoreline position, and the dash line represents the calculated January 1983 shoreline position. Although the agreement between the calculated and surveyed shoreline positions is not as close for the verification as for the calibration, the overall measured change in shoreline position is reproduced and considered acceptable. The largest discrepancies between the calculated and surveyed shoreline positions occur adjacent to the Anaheim bay jetty at the location of the Surfside-Sunset feeder beach. It is believed that the differences are due to initial losses of fine-grained material in the beach fills to offshore regions and to the fact that estimates of incident wave conditions between January 1976 and January 1983 were not available and arbitrarily selected from the available 20-year hindcast. Figure 30 shows the surveyed versus calculated shoreline change from the April 1970 shoreline position. The trends noted for the calibration period are also indicated for the verification period. Plots of the gross and net longshore sand transport rates for the verification period are given in Figure 31 together with maximum annual net northerly and the maximum annual net southerly longshore sand transport rates.

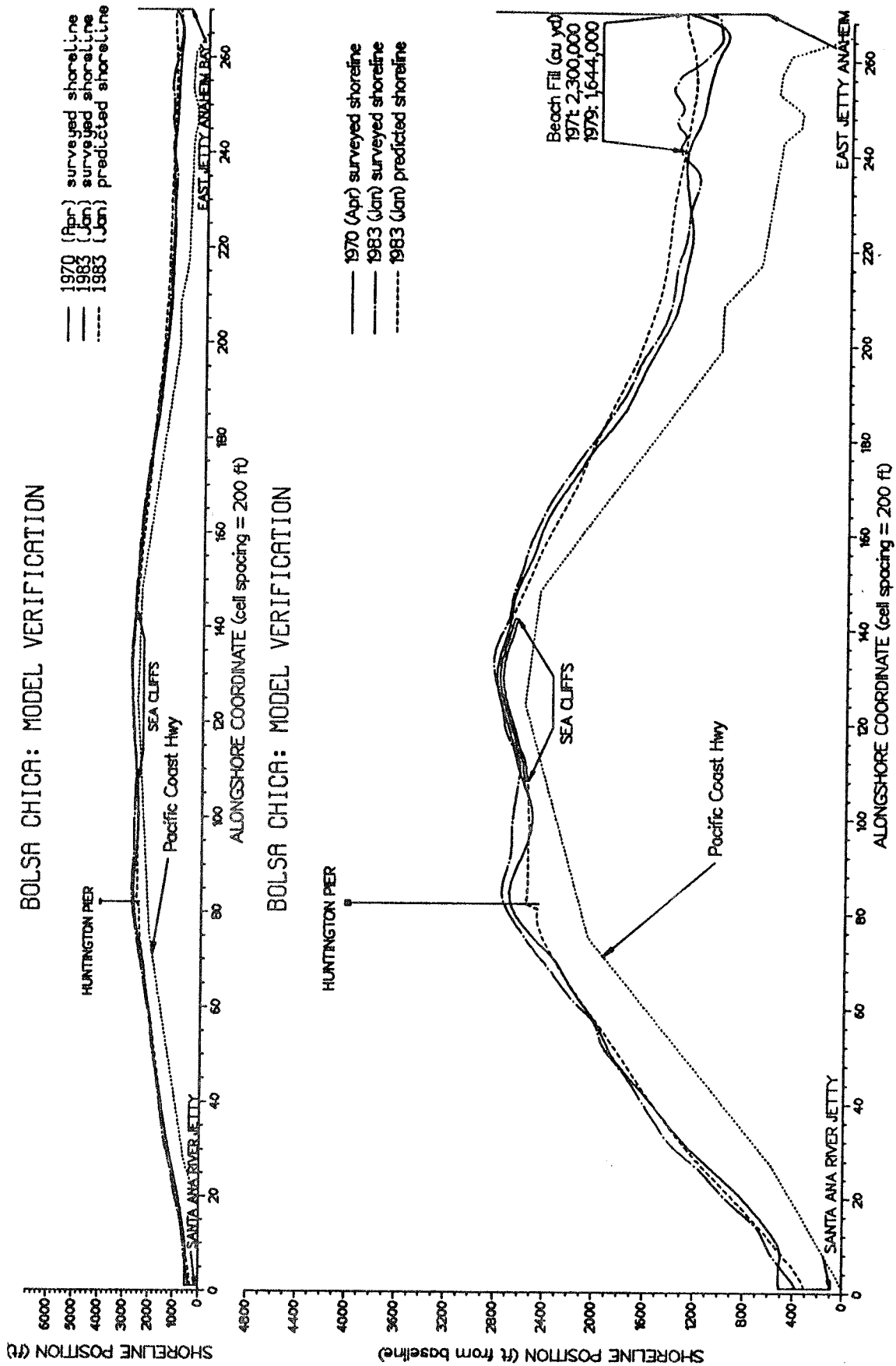


Figure 29. Model verification results

BOLSA CHICA: VERIFICATION

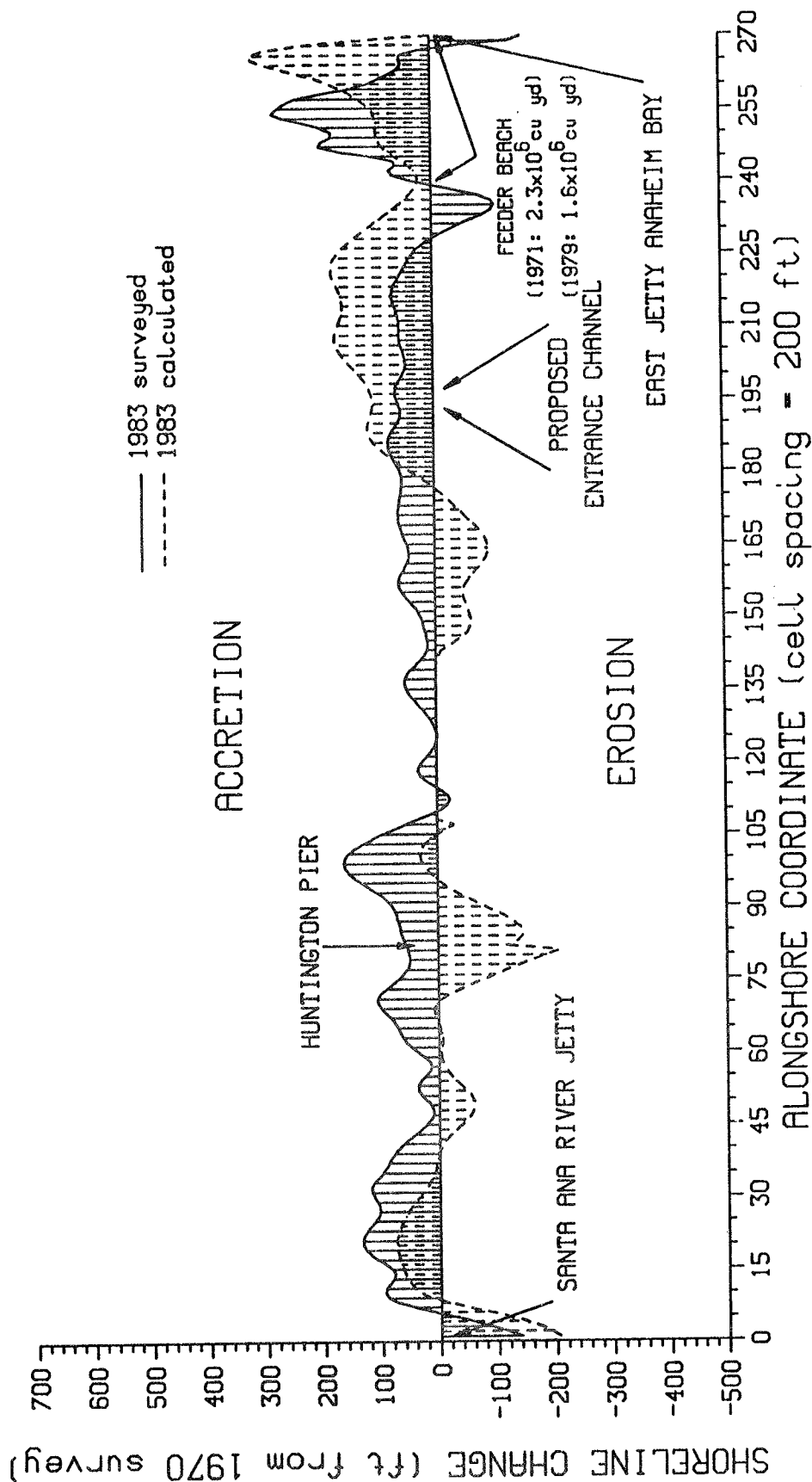


Figure 30. Model verification: surveyed vs. calculated shoreline change

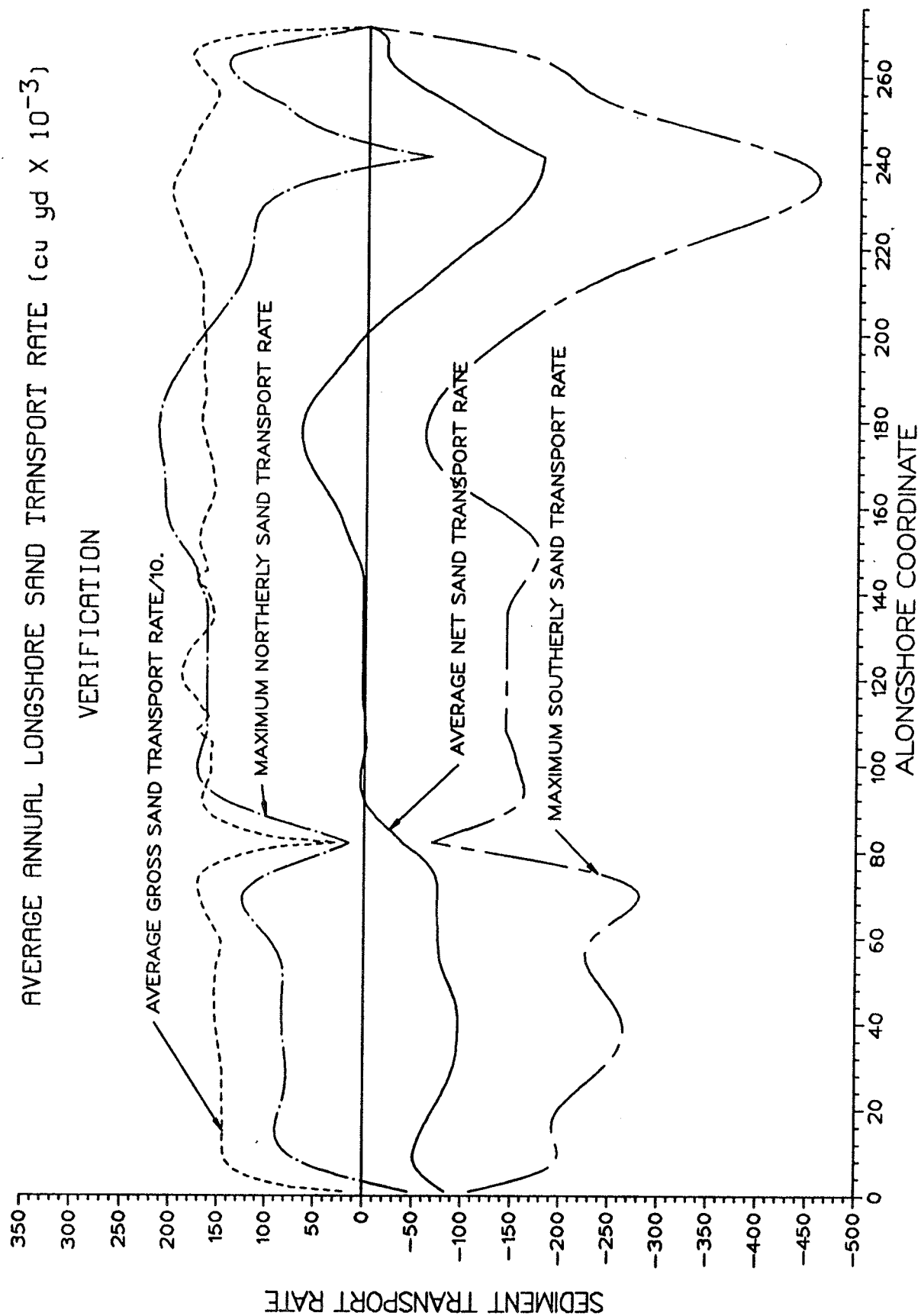


Figure 31. Average annual longshore sand transport rates for the verification period (1970 - 1983)

PART V: SHORELINE CHANGE MODEL TESTS: PROPOSED NAVIGABLE ENTRANCE

Model Tests

101. Eight design alternatives described below were modeled using the verified shoreline change model GENESIS. Several variations were simulated for each of the alternatives. The intent of the simulations was to quantify the shoreline impacts of the proposed Bolsa Chica navigable ocean entrance system. In the simulation of Alternatives 1 and 3, no sand management activities were specified; in other words, there were no inputs of beach nourishment material along the modeled reach. In the simulation of Alternatives 2, 4, 5, 6, and 8, renourishment of the Surfside-Sunset feeder beach was specified at 1 million cu yd every 5 years. In the simulation of Alternatives 7 and 8, sand management techniques for mitigating impacts were modeled. A summary of the eight design alternatives is given in Table 8.

Table 8
Summary of Modeled Design Alternatives*

<u>Design Alternative No. & Simulation Code</u>	<u>Entrance Channel Location and Width</u>	<u>Surfside-Sunset Feeder Beach</u>	<u>Impact Mitigation Sand Management</u>
1 WP1A,WP1B,WP1C	Without Project	No	No
2 WP2A,WP2B,WP2C	Without Project	Yes	No
3 PRO1A,PRO1B,PRO1C	Proposed Site, 800 ft	No	No
4 PRO2A,PRO2B,PRO2C	Proposed Site, 800 ft	Yes	No
5 PUC2A,PUC2B,PUC2C	Warner Avenue, 800 ft	Yes	No
6 PDC2A,PDC2B,PDC2C	South of Site, 800 ft	Yes	No
7 SM1A,SM1B,SM1C	Proposed Site, 800 ft	No	Yes
8 SM2A,SM2B,SM2C	Proposed Site, 800 ft	Yes	Yes

- * Design Alternatives 1 through 8 were simulated three times to investigate the effect of potential variabilities in the incident wave climate as follows:
- a. Alternating available southern swell wave conditions (years 1 and 2).
 - b. Low-intensity southern swell wave conditions (year 1).
 - c. High-intensity southern swell wave conditions (year 2).

102. In the model tests, the 1983 surveyed shoreline position was used as the initial shoreline. All tests were performed for 5- and 10-year simulation (prediction) periods using the same randomly selected 10-year time history of northern hemisphere sea and swell wave conditions. The southern

hemisphere swell component of the incident wave climate was varied depending on the particular model simulation, as shown in Table 8. The model simulations were performed assuming that the proposed entrance channel and detached breakwater were constructed in 1983. Hence, the predicted 1988 and 1993 shoreline positions represent the expected shoreline positions after 5- and 10-years. In the simulations, sand transport into the proposed ocean entrance channel (between entrance jetties) was permitted, but transport out of the ocean entrance channel was not. Thus, the ocean entrance channel was modeled as a sand sink.

Results

Alternative 1 (WP1)

103. The purpose of these simulations was to evaluate the expected shoreline change for the without-project alternative, in the absence of continued renourishment of the Surfside-Sunset feeder beach. These simulations also provide a baseline for evaluating the impacts directly resulting from the structured ocean entrance system. In Alternative WP1A, the available 2-year-long hindcast of southern swell wave conditions were input to the model. Because all the available wave data are utilized in this simulation, it is assumed to represent the most likely case. However, because only 2 years of southern swell wave conditions are available and because they differ significantly in their potential for producing longshore sand transport, two additional simulations were performed, one using the low-energy year (year 1) of southern swell wave conditions (Alternative WP1B) and one using the high-energy year (year 2) of southern swell wave conditions (Alternative WP1C). The simulation of Alternatives WP1B and WP1C provide a reasonable range of shoreline change and longshore sand transport rates that could be expected in the baseline case (Alternative WP1A), and should allow planners and engineers to develop contingency plans for addressing the great variability in the incident wave climate along the project coast. The results of the simulations of design Alternative 1 are summarized in Figures 32 through 37 and are the basis of comparison for the remaining alternatives.

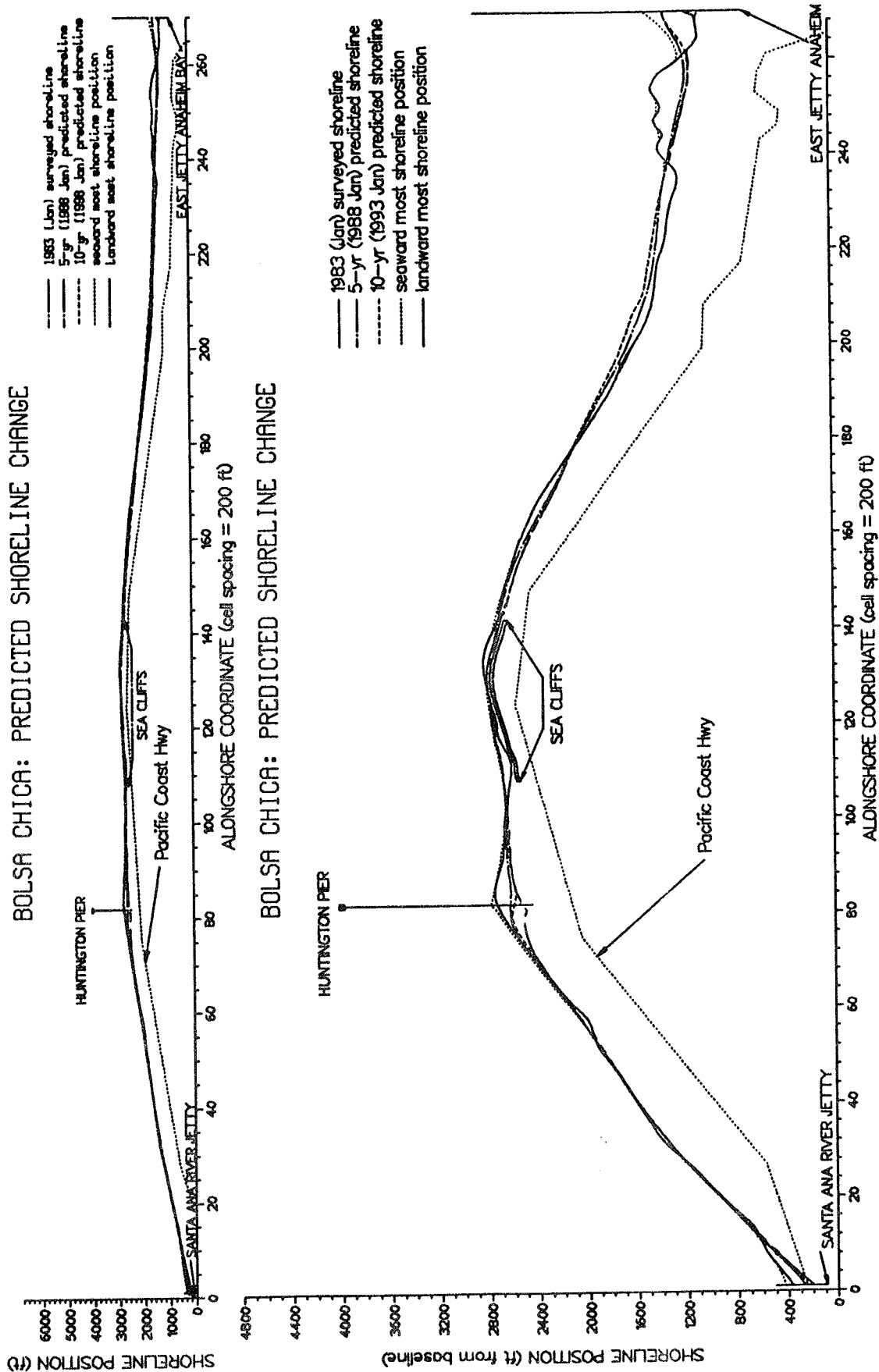


Figure 32. Alternative WPLA: without-project, without feeder beach

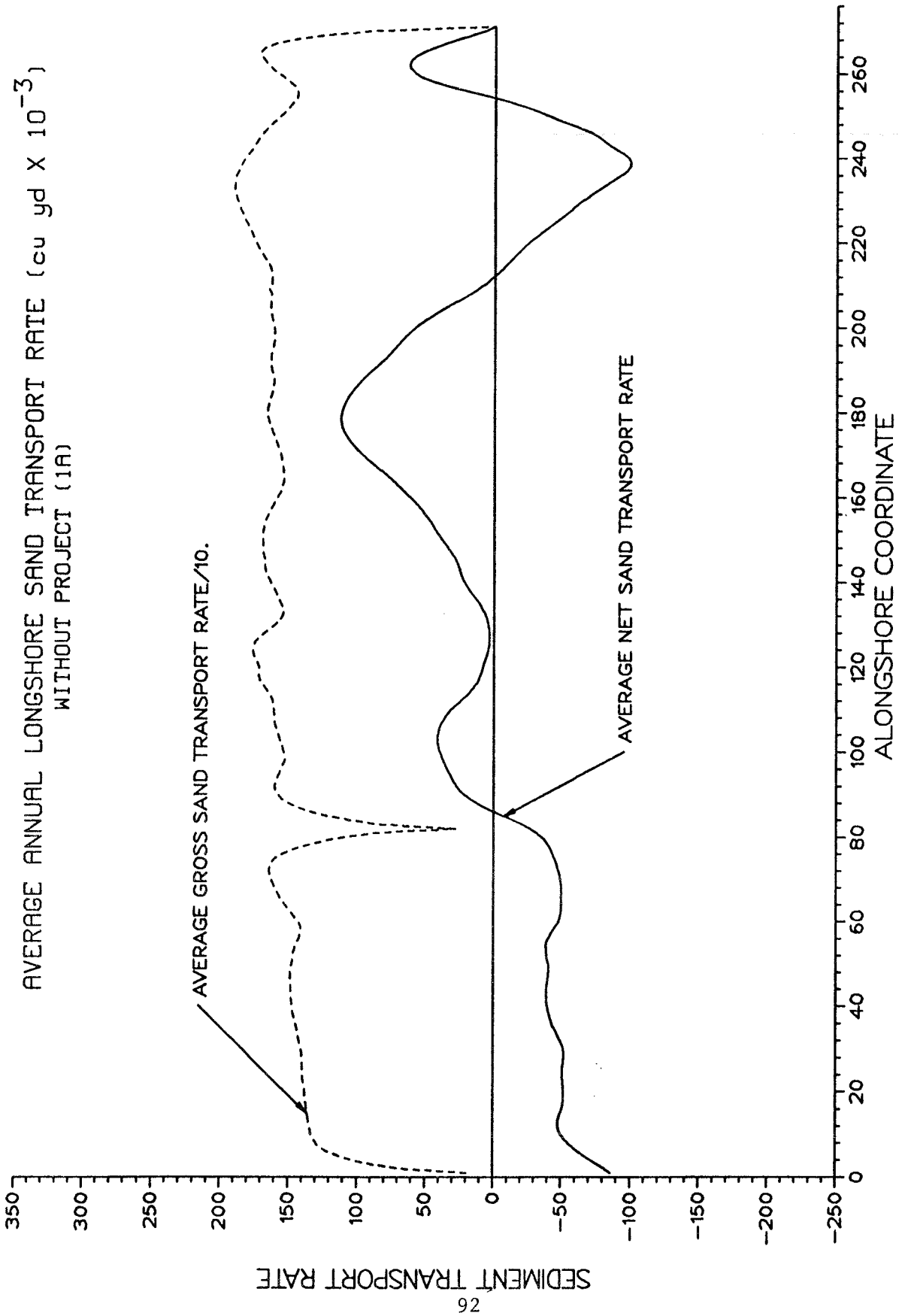


Figure 33. Alternative WPlA: average annual longshore sand transport rates

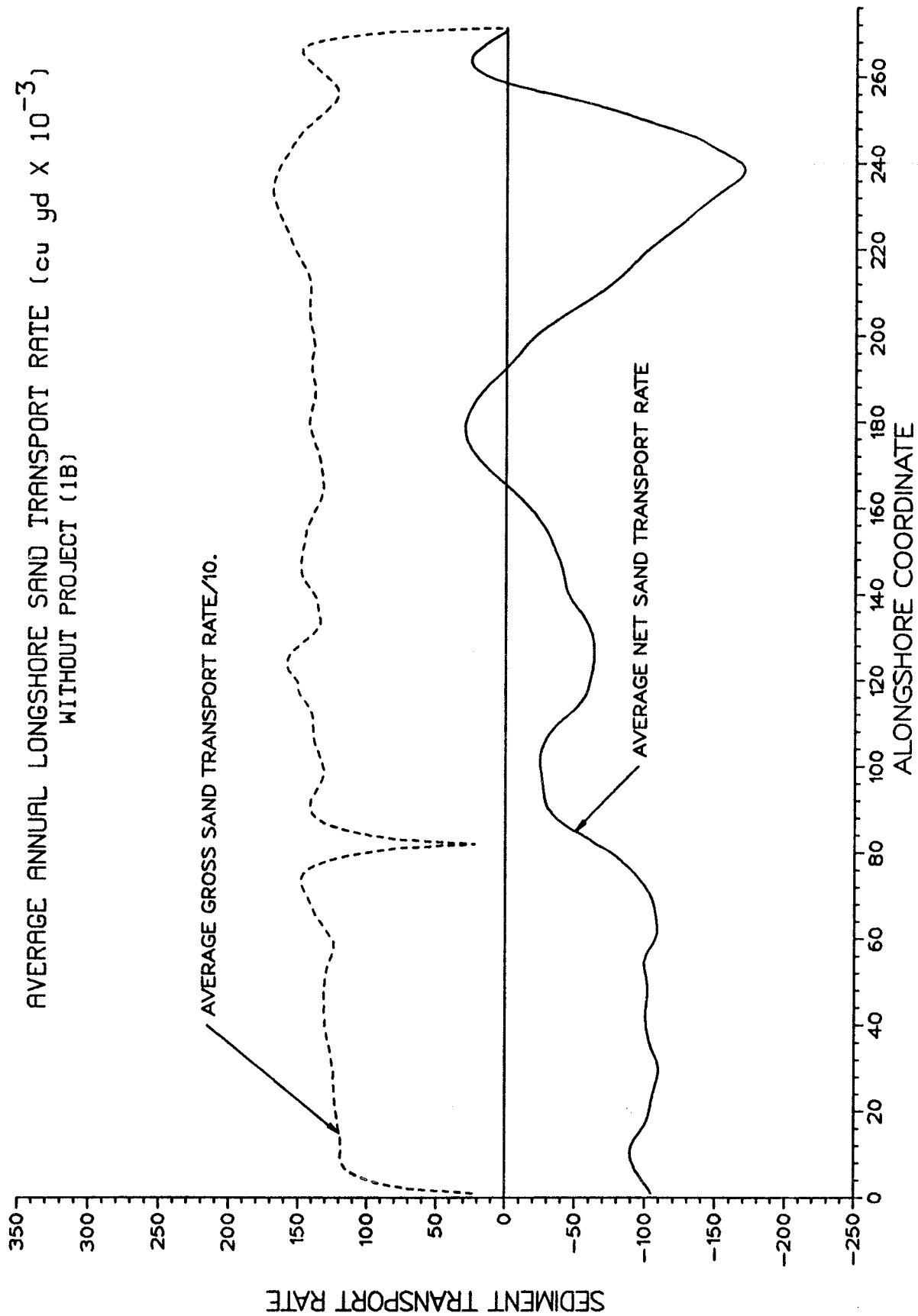


Figure 35. Alternative WPlB: average annual longshore sand transport rates

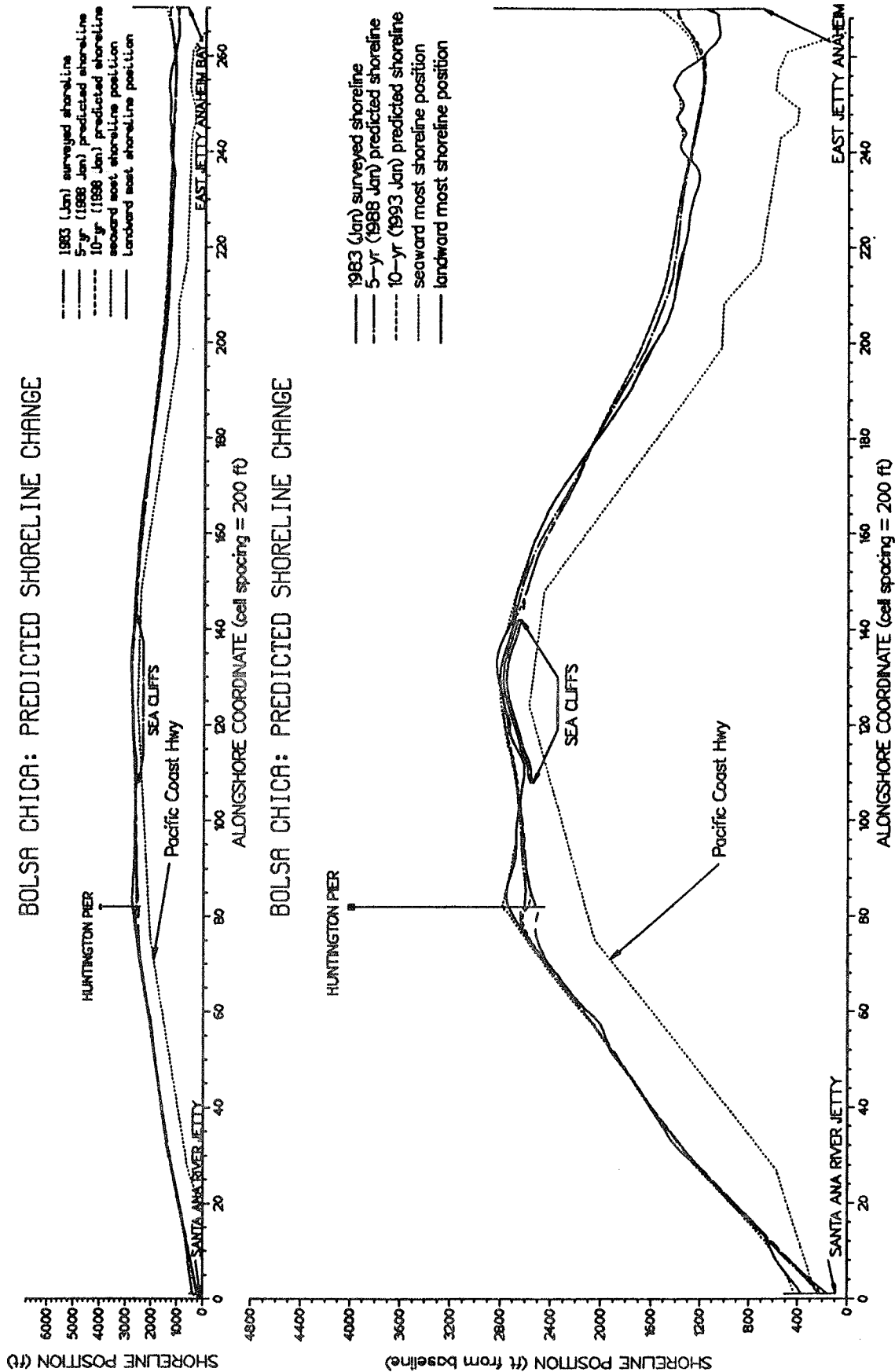


Figure 36. Alternative WPlC: without-project, without feeder beach, year 2 southern swell wave conditions

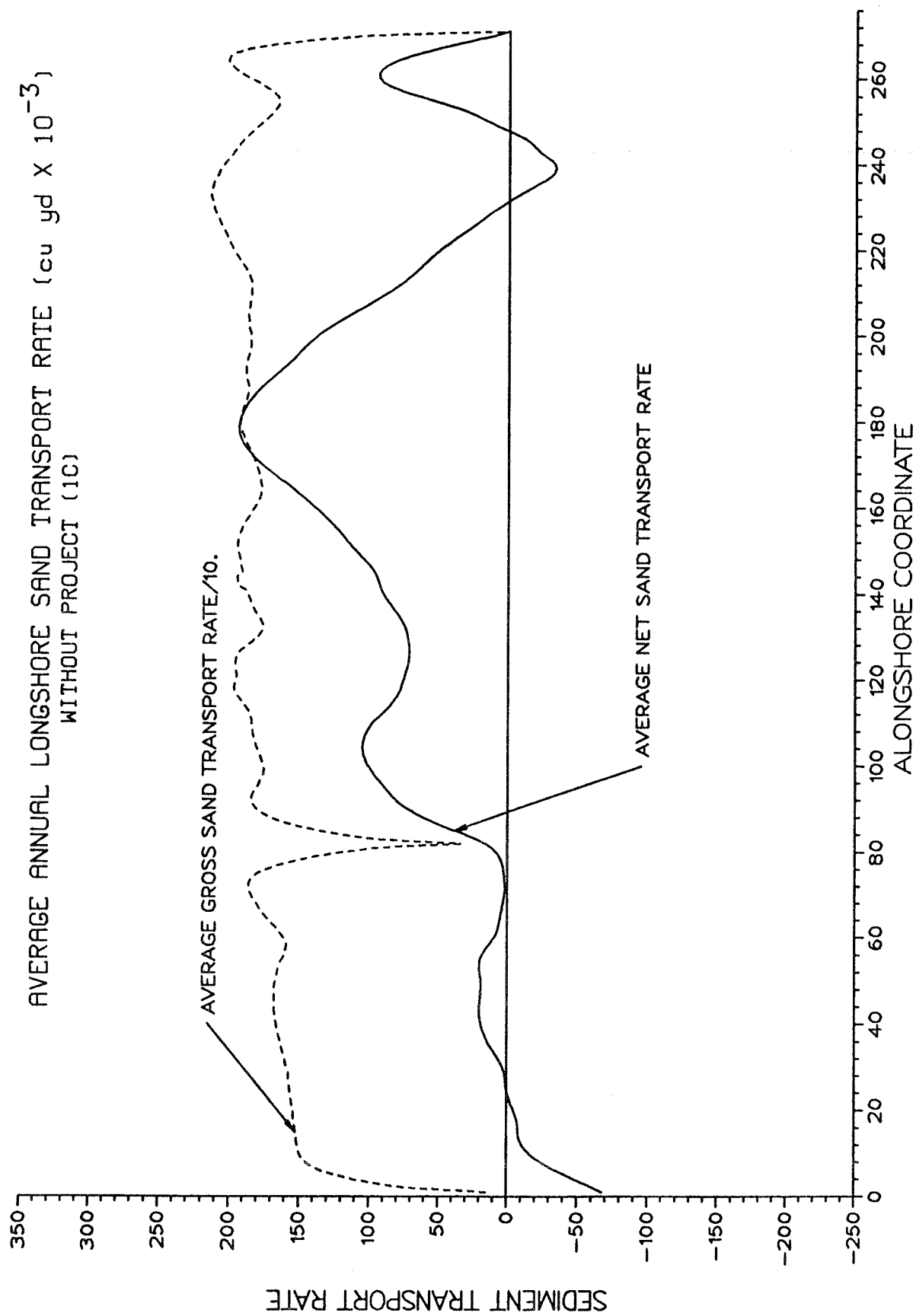


Figure 37. Alternative WPIC: average annual longshore sand transport rates

Alternative 2 (WP2)

104. The simulation of this design alternative was performed to investigate the expected shoreline change for the without-project assuming the continuation of the Surfside-Sunset feeder beach nourishment program. In these simulations, a 1-million cu yd beach fill was implemented in 1983 and 1988. The shorelines plotted in the figures are the pre-nourishment shoreline positions. As before, Alternative WP2A represents the baseline case (all available southern swell wave information was used and repeated as necessary); in Alternative WP2B, year 1 of southern swell wave conditions was used; and in Alternative WP2C, year 2 of southern swell wave conditions was used. The results of the Alternative 2 simulations are given in Figures 38 through 43.

105. The calculated average annual net longshore sand transport rates for the without-project design alternatives (Figures 33, 35, 37, 39, 41 and 43) all have the same form but are shifted upward (indicating more northwesterly sand transport) or downward (indicating more southeasterly sand transport) depending on the southern swell wave conditions used as input to the shoreline change model. Note also that a reversal in the average net sand transport direction occurs between alongshore coordinates 190 and 230 in all of the without project design alternatives. This general characteristic of the local longshore sand transport regime will become important when the model is used to predict shoreline changes in the vicinity of a structured ocean entrance system located in this region.

106. Comparing Figures 32, 34, and 36 with Figures 38, 40, and 42, it is noted that the effect of the Surfside-Sunset feeder beach on the predicted shoreline position extends approximately 2 miles downcoast (to alongshore coordinate 210). This is about twice the alongshore length of the placed feeder beach nourishment area.

Alternative 3 (PRO1)

107. The purpose of these model simulations was to evaluate the potential shoreline impacts of the proposed Bolsa Chica navigable ocean entrance channel and detached breakwater in the absence of continued renourishment of the Surfside-Sunset feeder beach.

108. The various coastal structures considered in the proposed navigable ocean entrance channel design included:

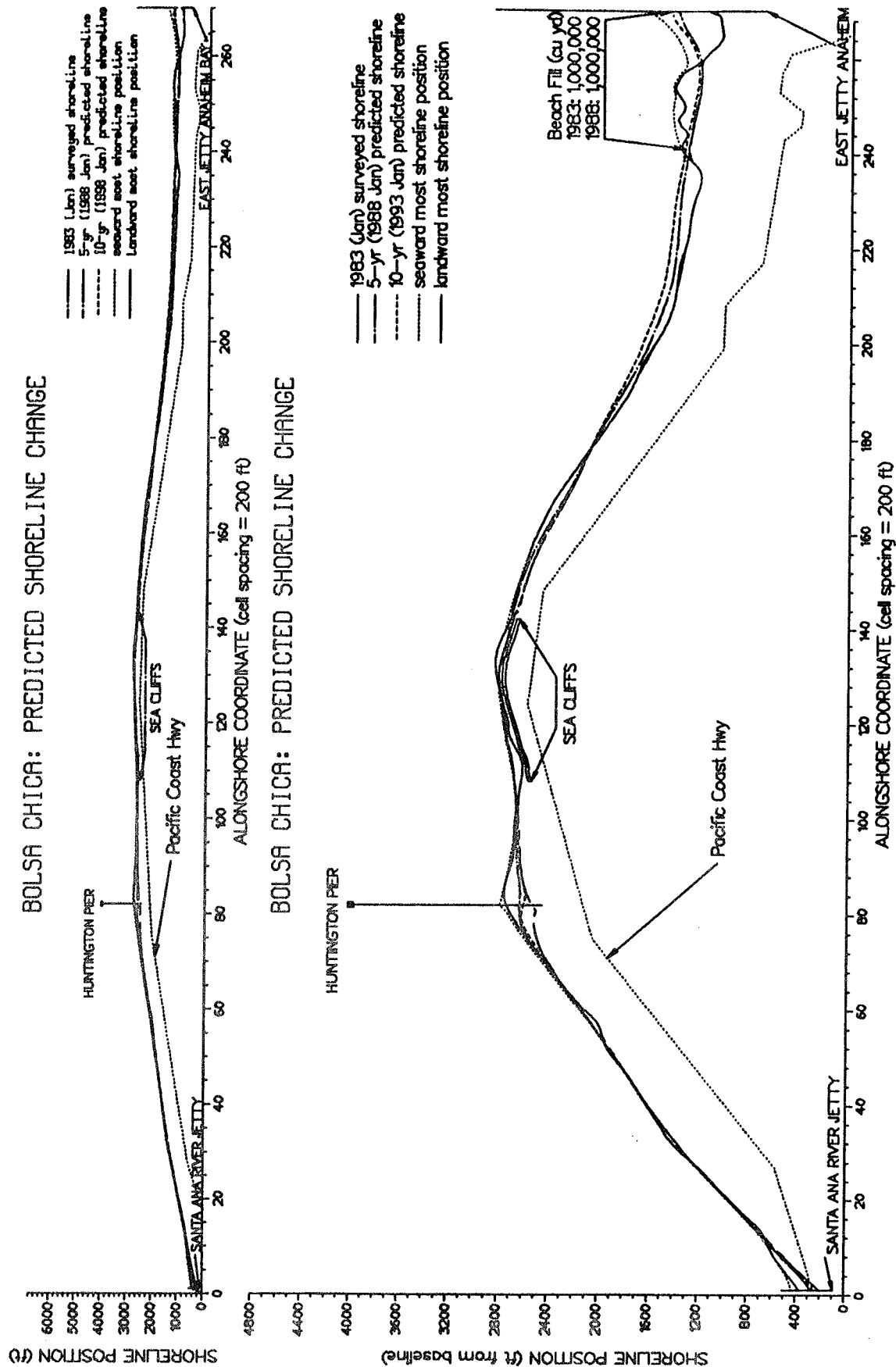


Figure 38. Alternative WP2A: without-project, with feeder beach

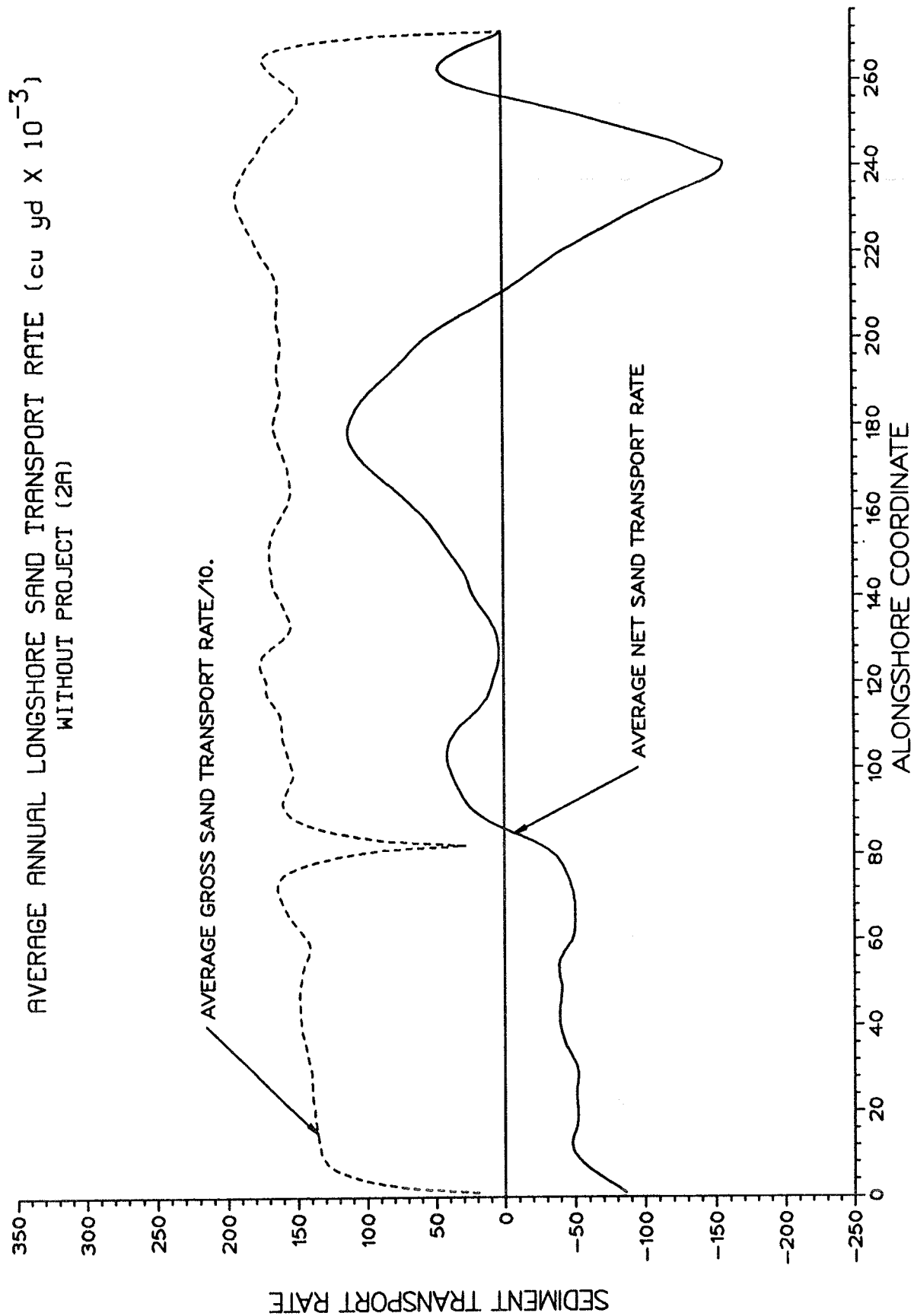


Figure 39. Alternative WP2A: average annual longshore sand transport rates

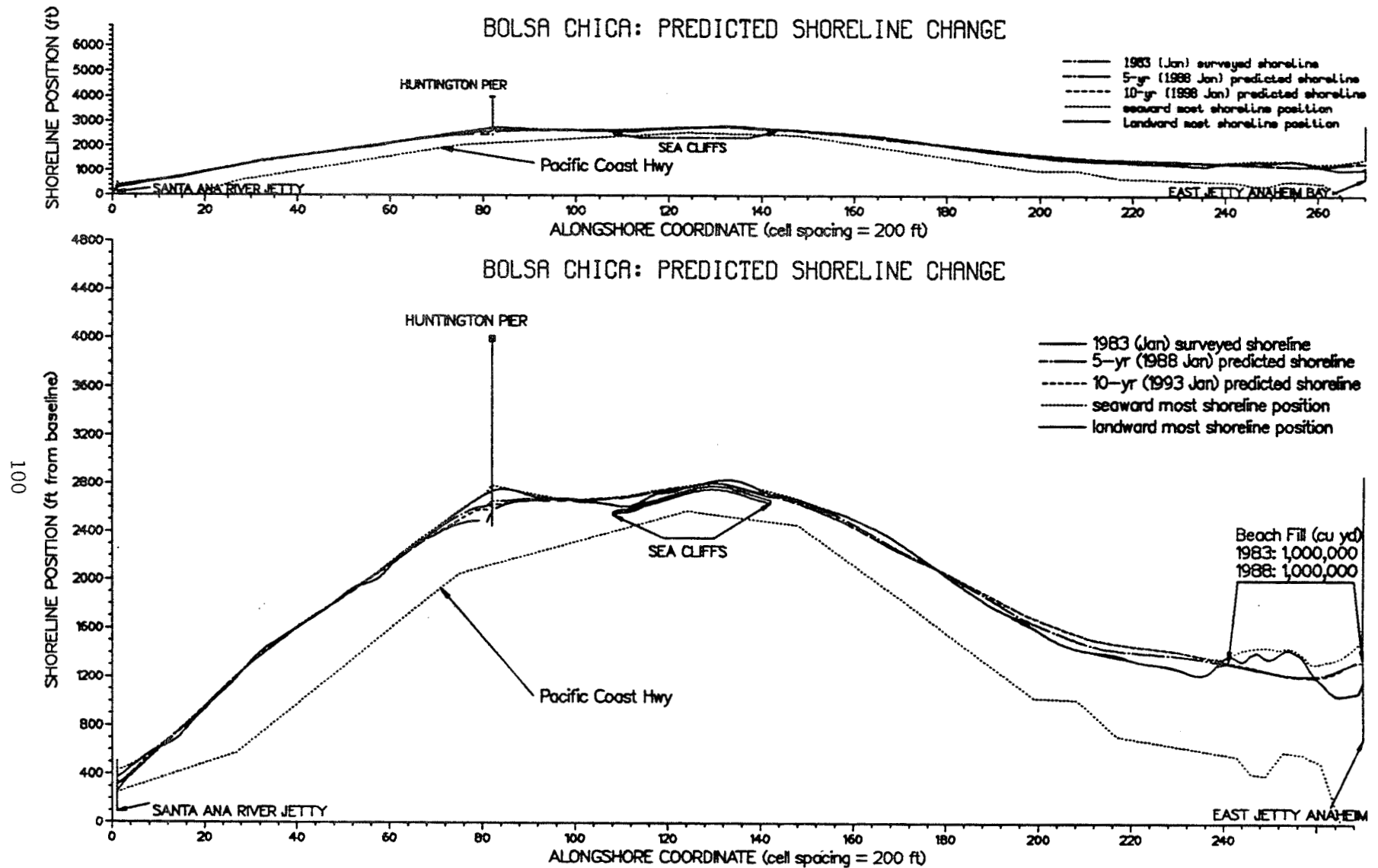


Figure 40. Alternative WP2B: without-project, with feeder beach, year 1 southern swell wave conditions

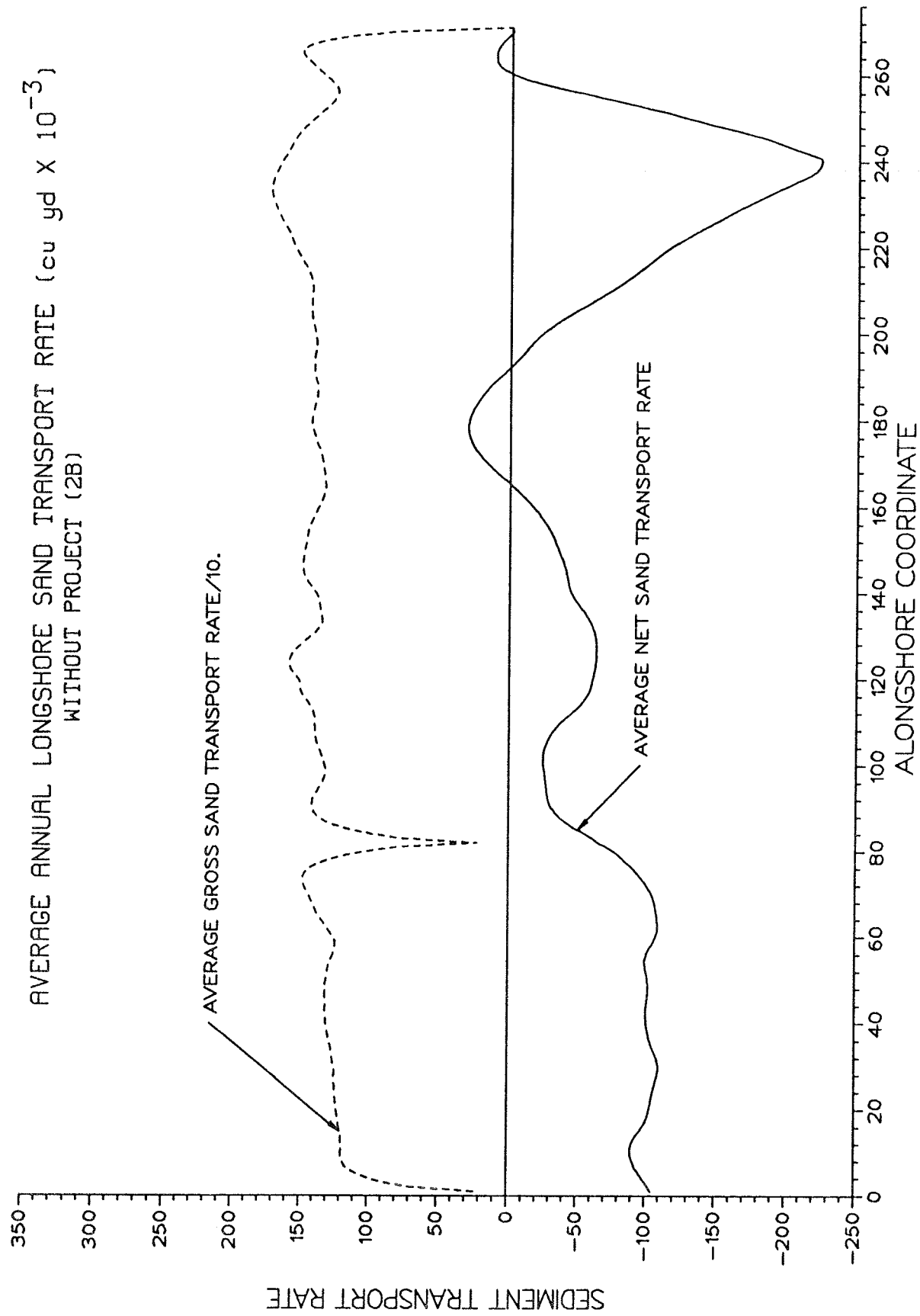


Figure 41. Alternative WP2B: average annual longshore sand transport rates

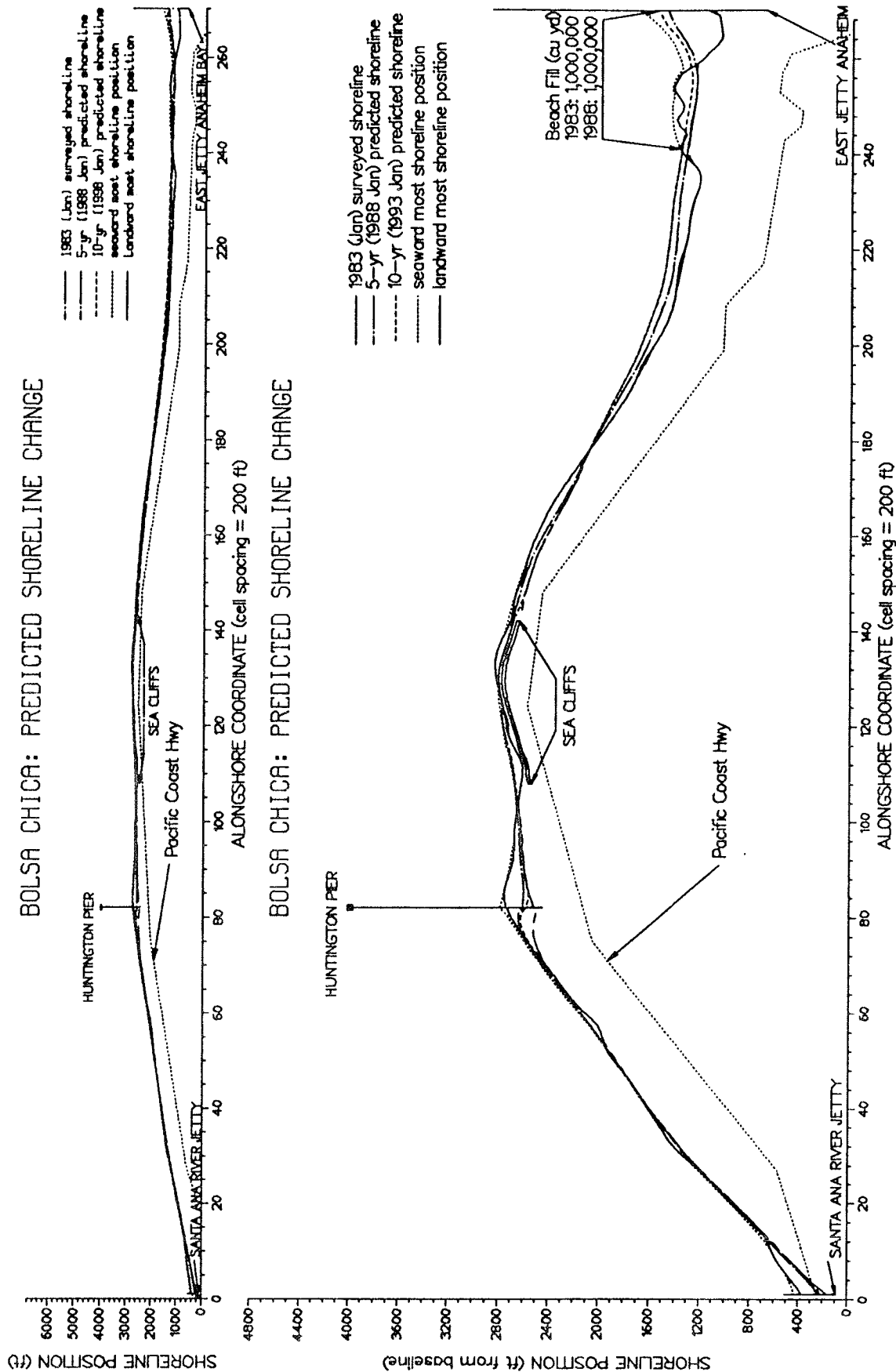


Figure 42. Alternative WP2C: without-project, with feeder beach, year 2 southern swell wave conditions

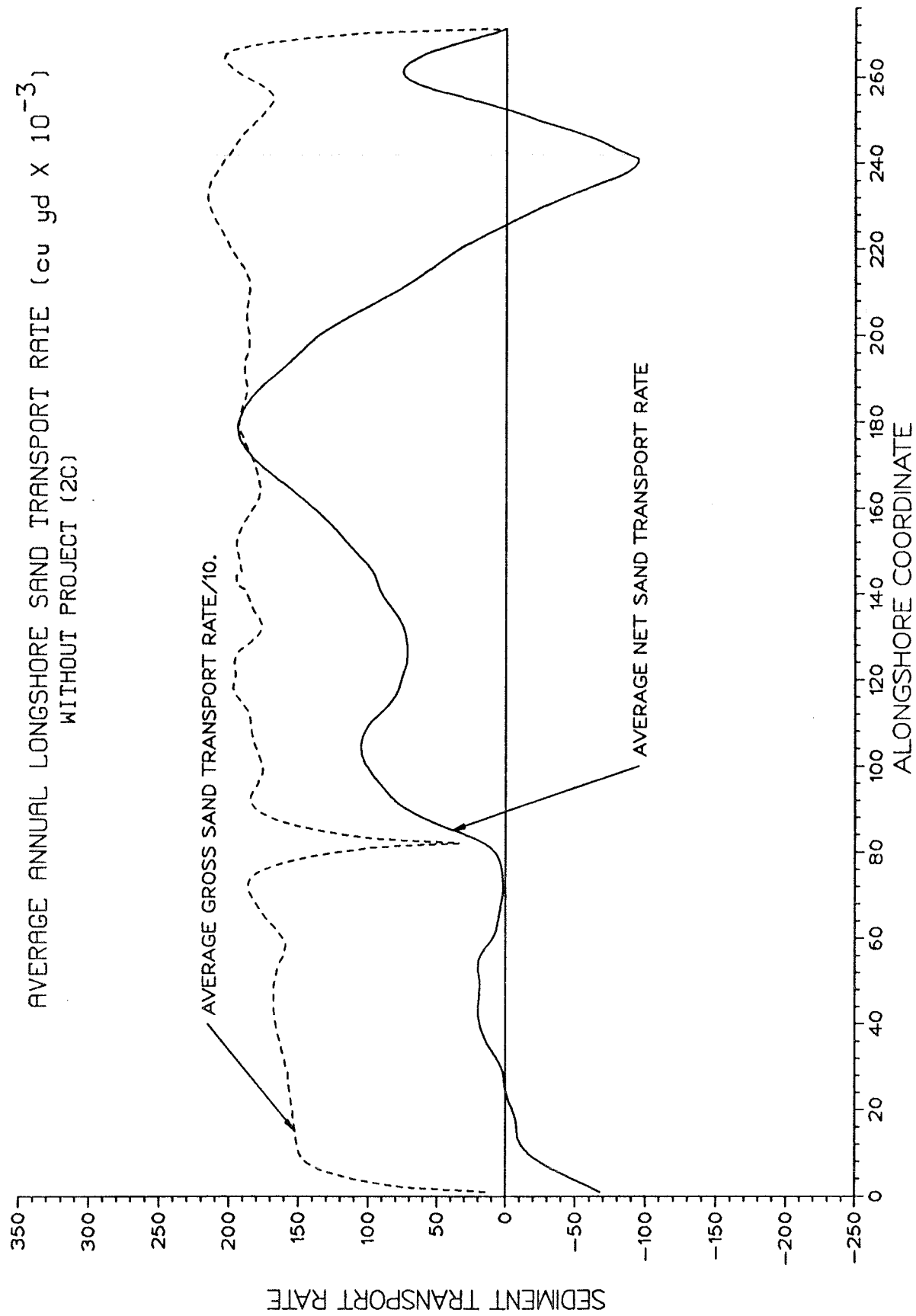


Figure 43. Alternative WP2C: average annual longshore sand transport rates

- a. Two shore-perpendicular jetties spaced 800 ft apart and extending to the 20-ft MLLW depth contour, approximately 1400 ft offshore of the 1983 MHW shoreline position.
- b. A detached breakwater composed of three sections as follows; a 900-ft long shore-parallel section centered about the entrance channel at a depth of approximately 22.5 ft MLLW, a 1500-ft long section extending to the north and terminating at a depth of approximately 22 ft MLLW, and a 750-ft long section extending to the south and terminating at a depth of approximately 24 ft MLLW.

All of the following model tests (design Alternatives 3 through 8) were conducted with the above-described structural constraints in addition to the previously mentioned existing structures in the modeled reach, i.e., the Anaheim Bay east jetty, Huntington sea cliffs, Huntington Pier, and the Santa Ana River jetty.

109. Alternative PRO1A was conducted using all the available southern swell wave conditions and the results represent the most likely shoreline response to the construction and stabilization of the proposed navigable ocean entrance channel at Bolsa Chica. Likewise, Alternative PRO1B models shoreline response assuming a low-energy (year 1) southern swell wave climate, and Alternative PRO1C models the response assuming a high-energy (year 2) southern swell wave climate. The results of these model simulations are depicted in Figures 44 through 49. As shown in Figures 44, 46, and 48 there is significant shoreline accretion on both sides of the proposed entrance system. This is a unique result and it arises from the local longshore sand transport regime in which sand is transported southeast (downcoast) towards the entrance system from the northwest and northwest (upcoast) towards the entrance system from the southeast as shown in Figures 45, 47, and 49. In other words the proposed entrance system is located in a region of converging longshore sand transport. This result, although not intuitively apparent at first, can be reasoned out by considering the shoreline orientation on either side of the proposed entrance system. On the northwest side of the entrance the shoreline is oriented nearly parallel to the model baseline (45 deg from north measured counter-clockwise). In contrast, on the southeast side of the entrance the shoreline is oriented approximately 50 deg from north measured counter-clockwise. This difference in shoreline orientation is enough to result in a reversal in the net longshore sand transport direction under the given wave

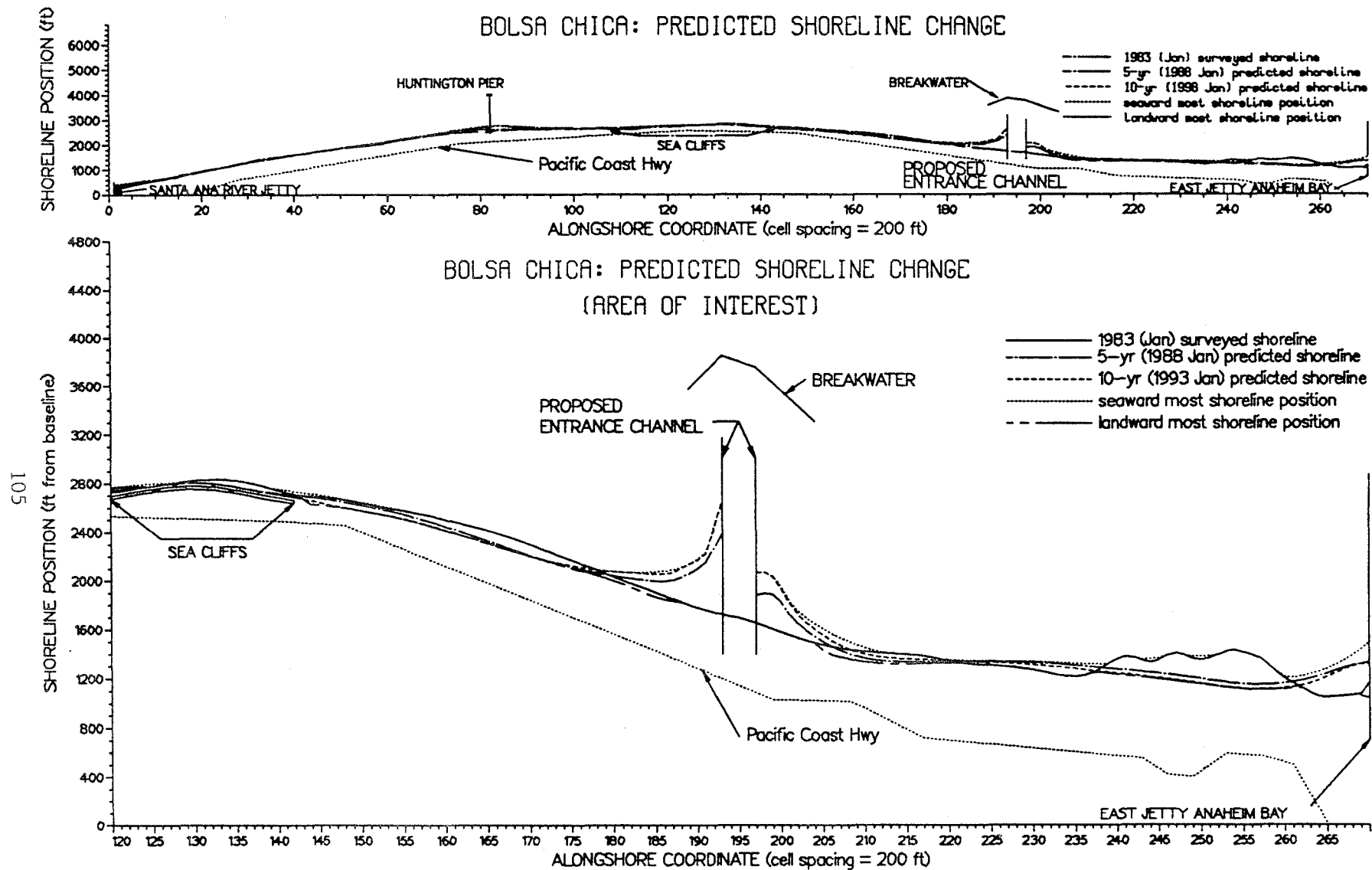


Figure 44. Alternative PRO1A: preferred alternative, without feeder beach

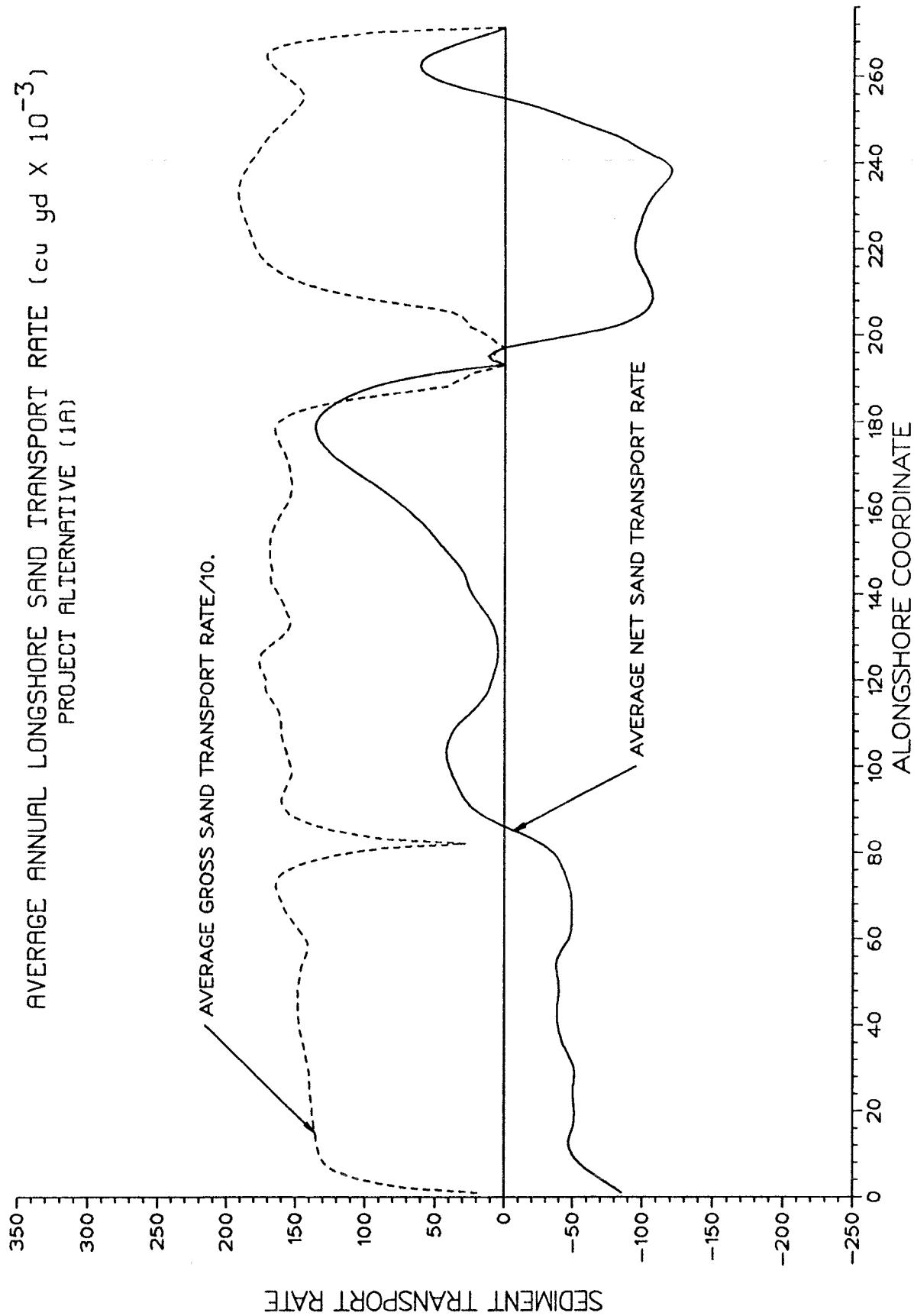


Figure 45. Alternative PRO1A: average annual longshore sand transport rates

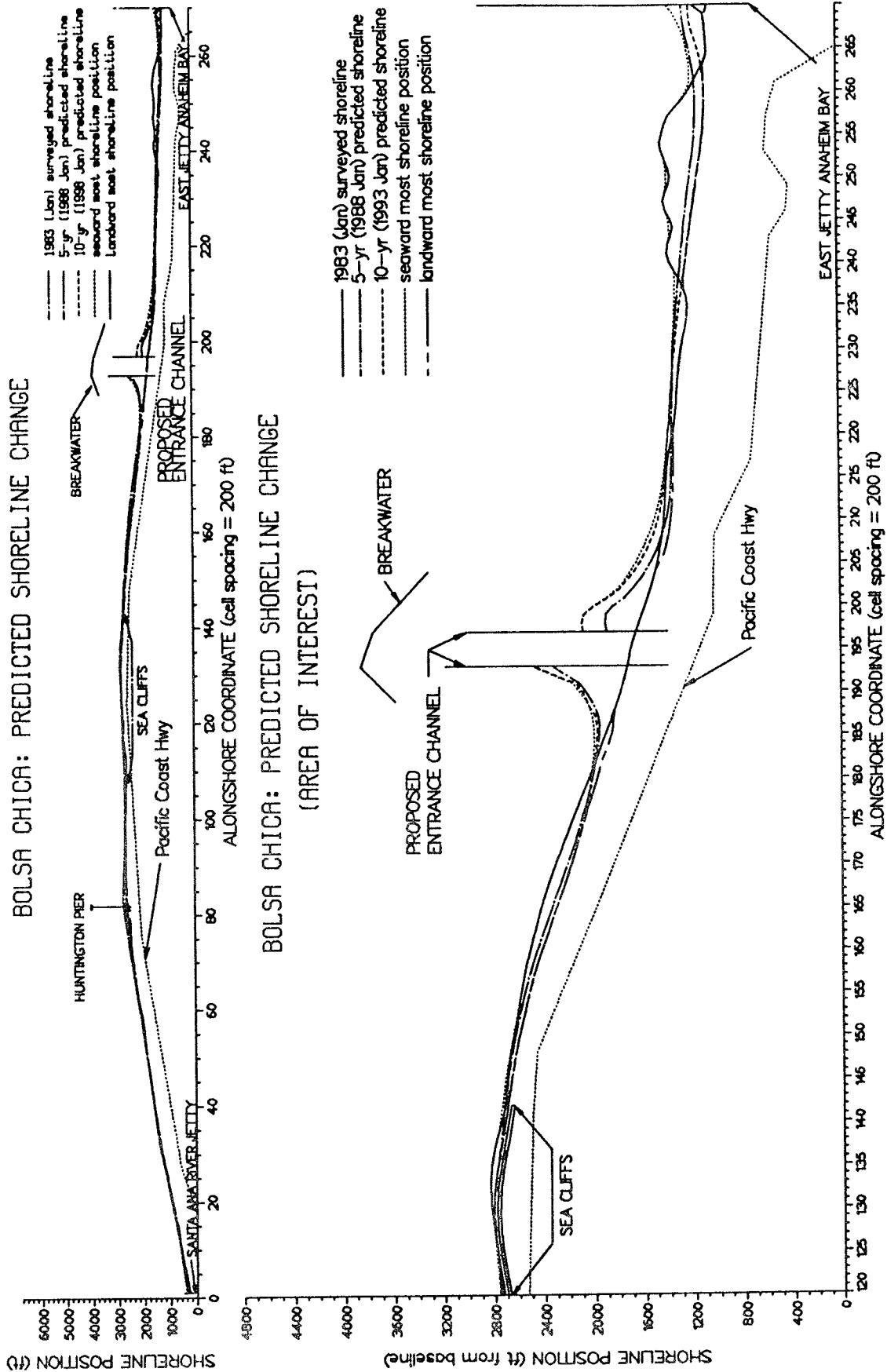


Figure 46. Alternative PROLB: preferred alternative, without feeder beach, year 1 southern swell wave conditions

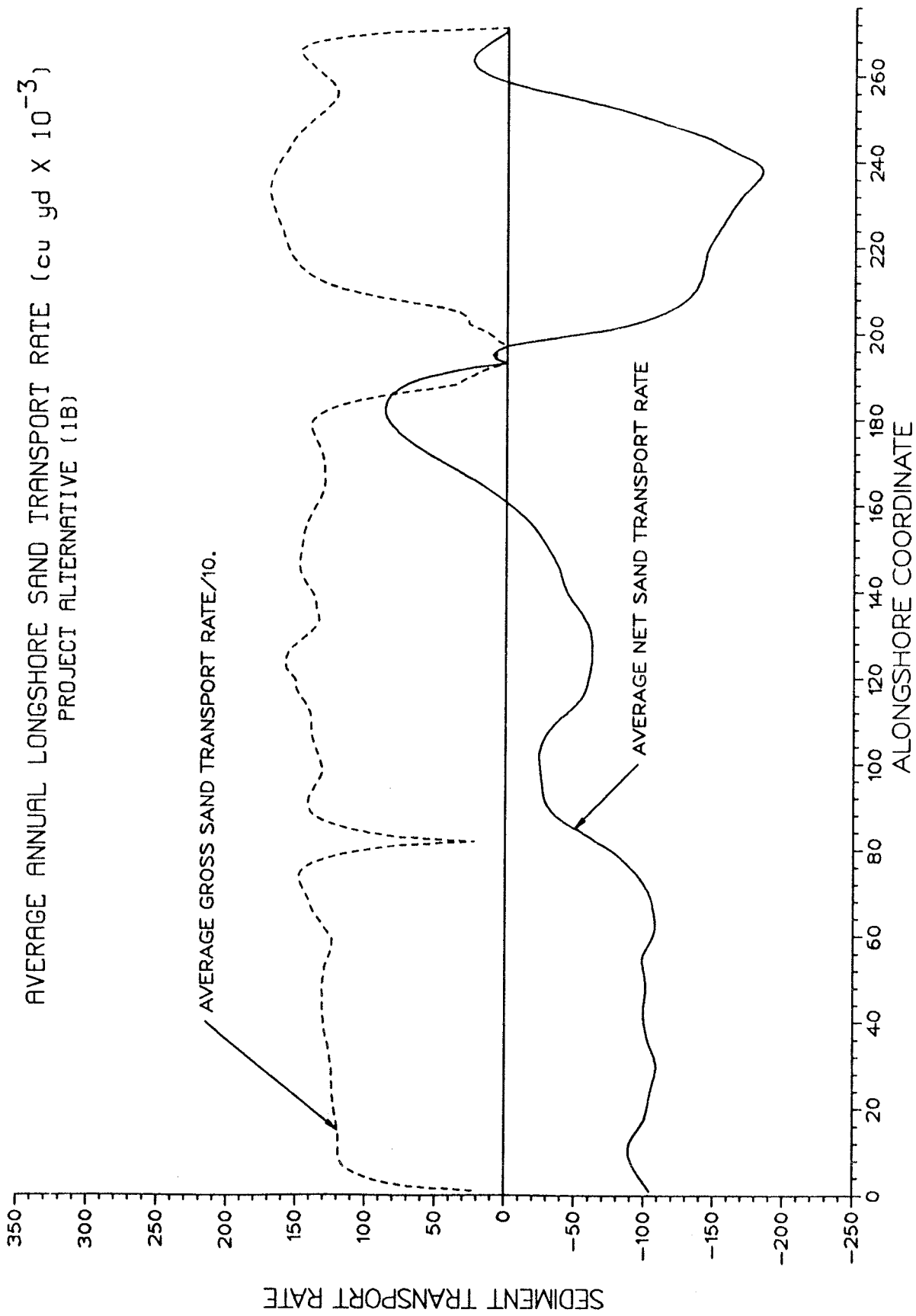


Figure 47. Alternative PRO1B: average annual longshore sand transport rates

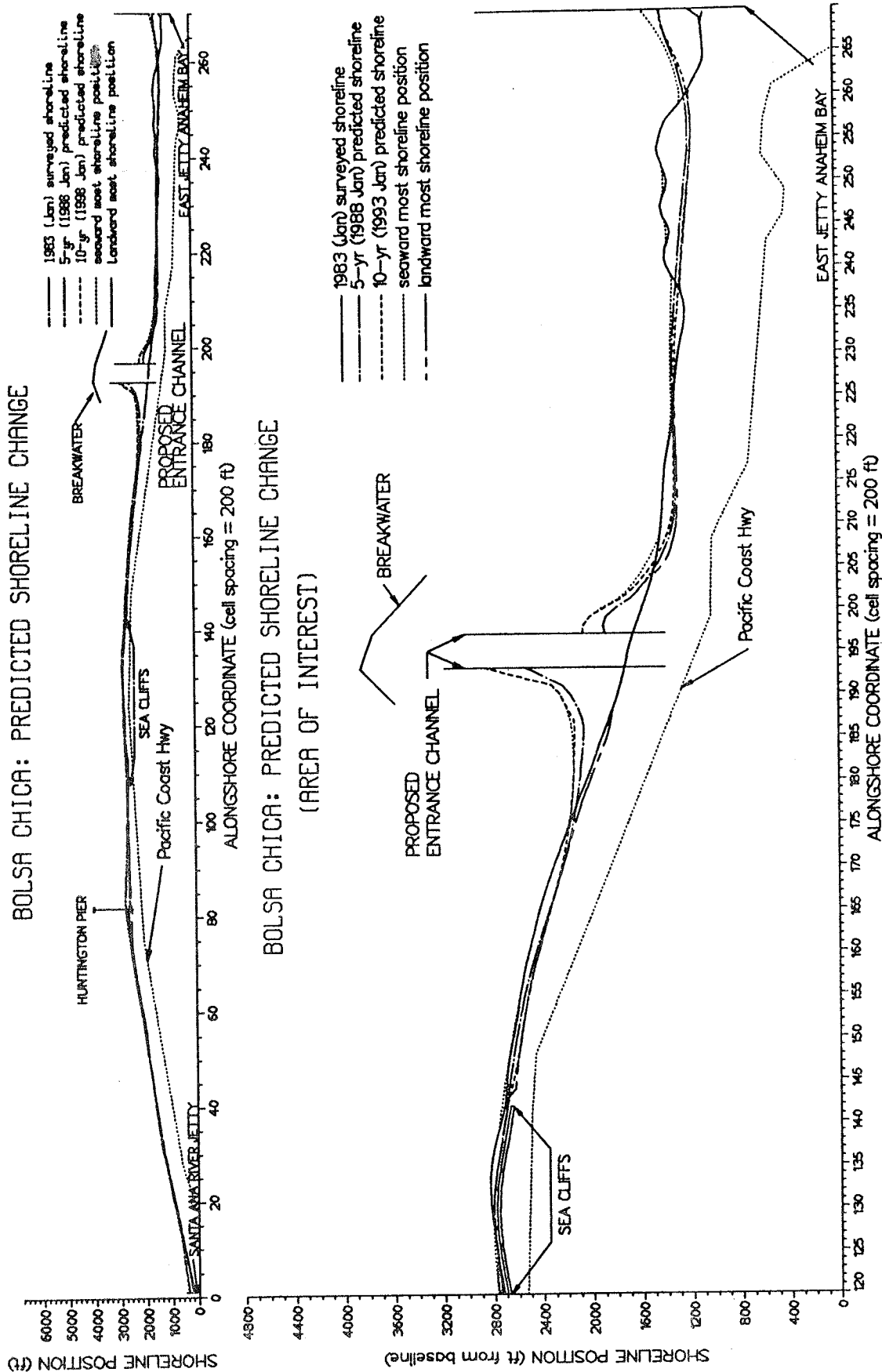


Figure 48. Alternative PRO1C: preferred alternative, without feeder beach, year 2 southern swell wave conditions

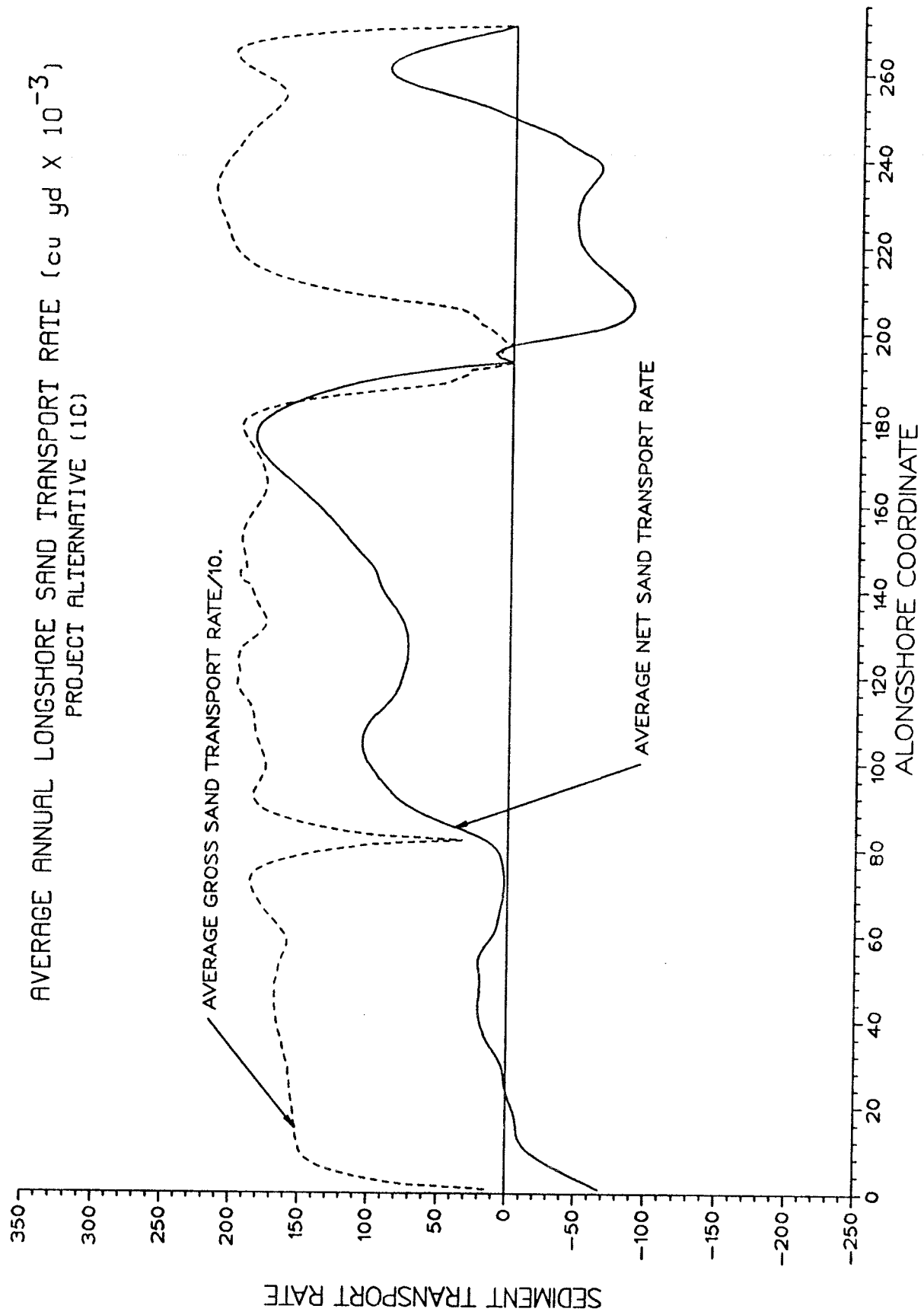


Figure 49. Alternative PRO1C: average annual longshore sand transport rates

conditions. This is substantiated by the total littoral drift plots given in Part IV (Figures 23 and 24).

Alternative 4 (PRO2)

110. This set of model simulations is identical to that of design Alternative 3 except that the Surfside-Sunset feeder beach was renourished with 1 million cu yd of sand in 1983 and in 1988. Plots of the model results are given in Figures 50 through 55. Again, shoreline accretion on both sides of the proposed entrance system is indicated. The Surfside-Sunset feeder beach does not, however, significantly increase or decrease the magnitude of the accretion adjacent to the entrance system. It therefore appears that the Surfside-Sunset feeder beach serves primarily to maintain the shoreline adjacent to the Anaheim Bay entrance and does not significantly increase in the width of the beach more than approximately 2 miles southeast of Anaheim Bay.

Alternative 5 (PUC2)

111. The entrance channel and structures specified for Alternative 4 (the proposed navigable ocean entrance system) was moved approximately 0.8 miles northwest (upcoast) of the proposed site in this simulation. This corresponds to locating the entrance channel at the intersection of Warner Avenue and the Pacific Coast Highway. The assumed nourishment program at the Surfside-Sunset feeder beach was specified in all of the Alternative 5 model simulations. The results are presented in Figures 56 through 61.

112. At this location, shoreline progradation on the northwest side of the entrance system is greater and the accretion on the southeast side is less than at the proposed project site. Otherwise, the trends in the predicted shoreline change and the longshore transport regime are very similar.

Alternative 6 (PDC2)

113. In this set of model simulations the entrance channel and structures specified for Alternative 4 were placed approximately 0.8 miles southeast (downcoast) of the proposed site. The results are given in Figures 62 through 67. Again, there is accretion indicated on both sides of the entrance system. However, the magnitude of the accretion is less than that predicted for the proposed site. Also, for Alternative PDC2C (Figure 66) there is a area of shoreline erosion located approximately 3000 ft northwest of the entrance. This area of erosion results from a divergence in the net

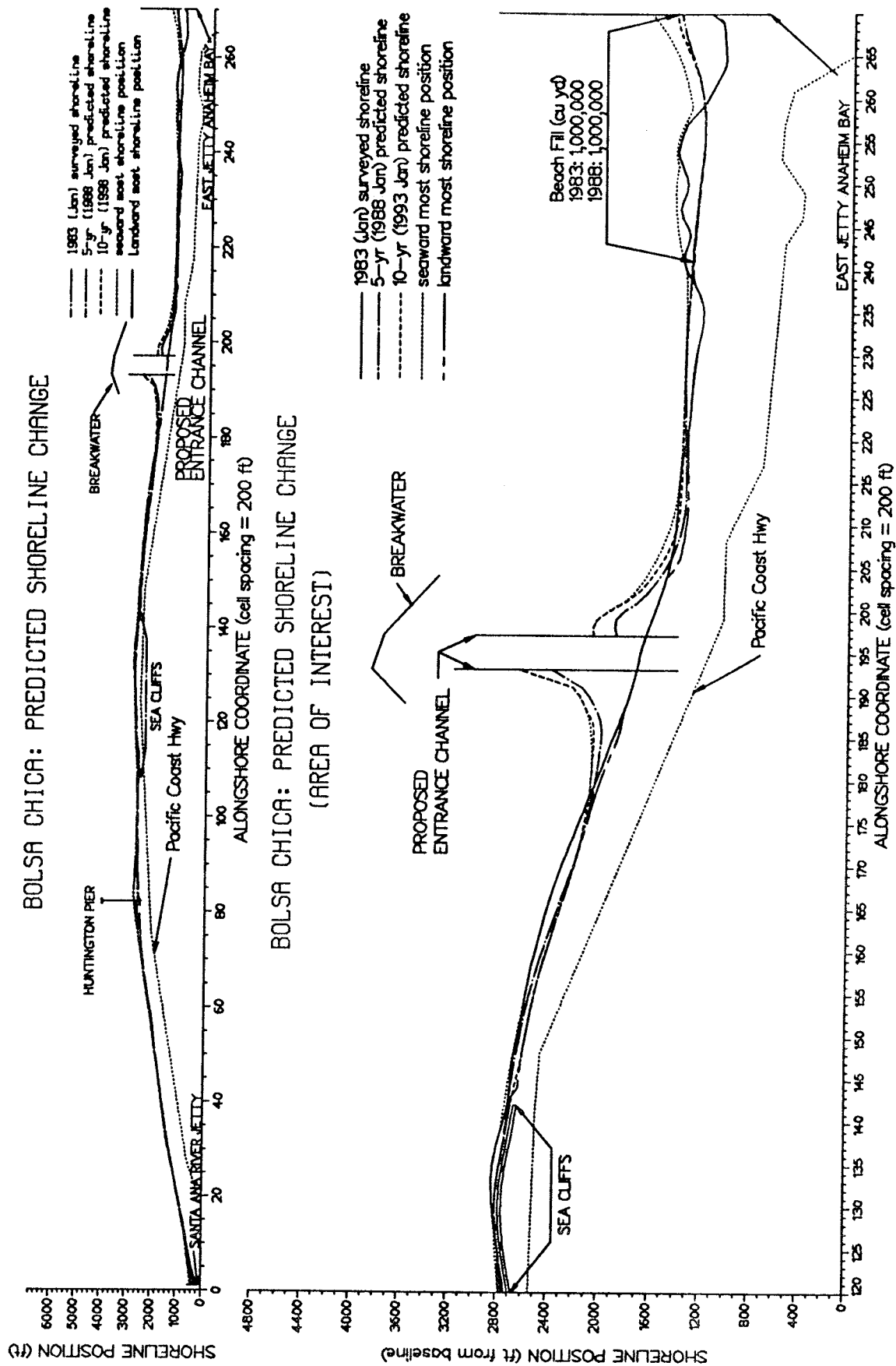


Figure 50. Alternative PRO2A: preferred alternative, with feeder beach

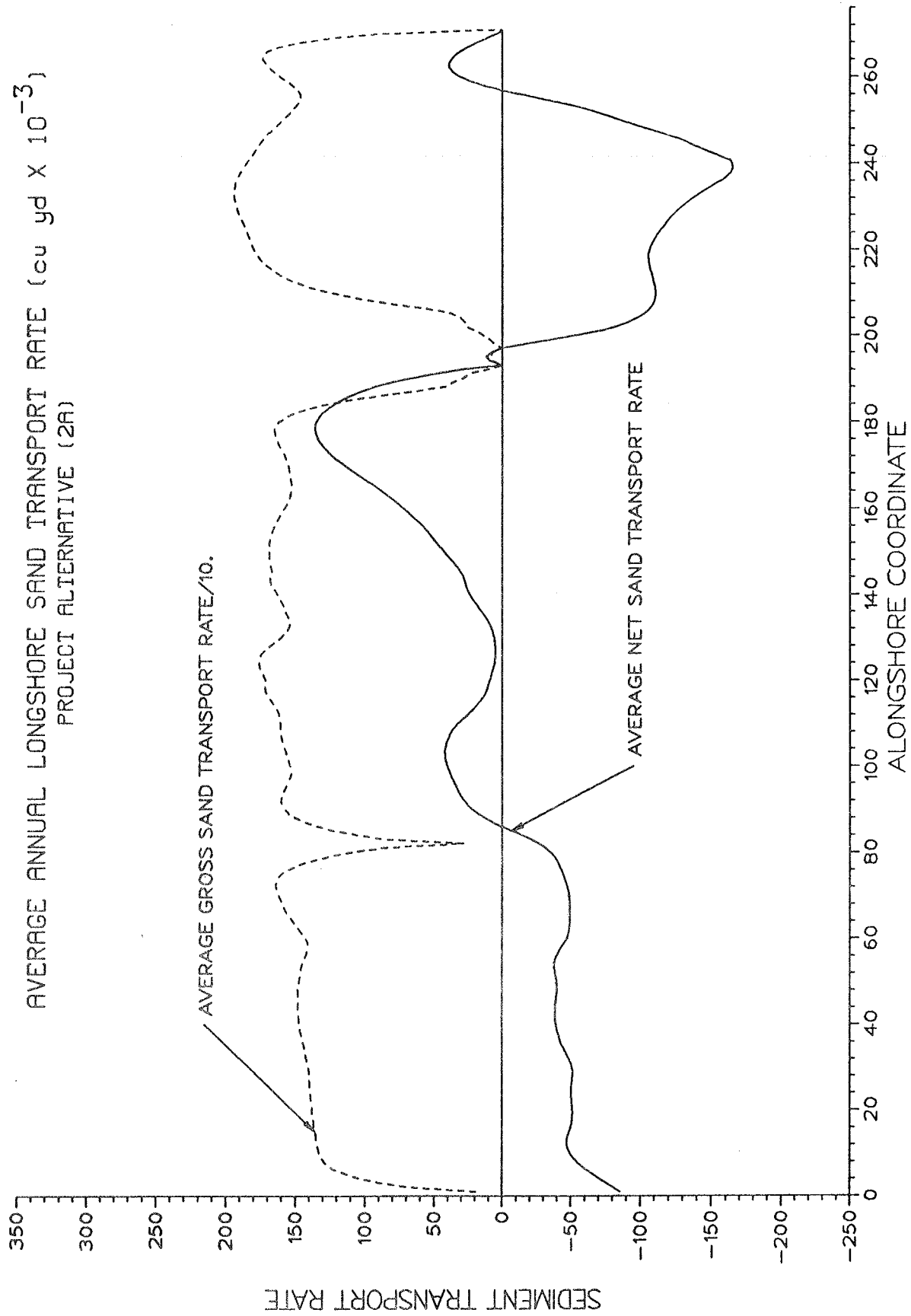


Figure 51. Alternative PRO2A: average annual longshore sand transport rates

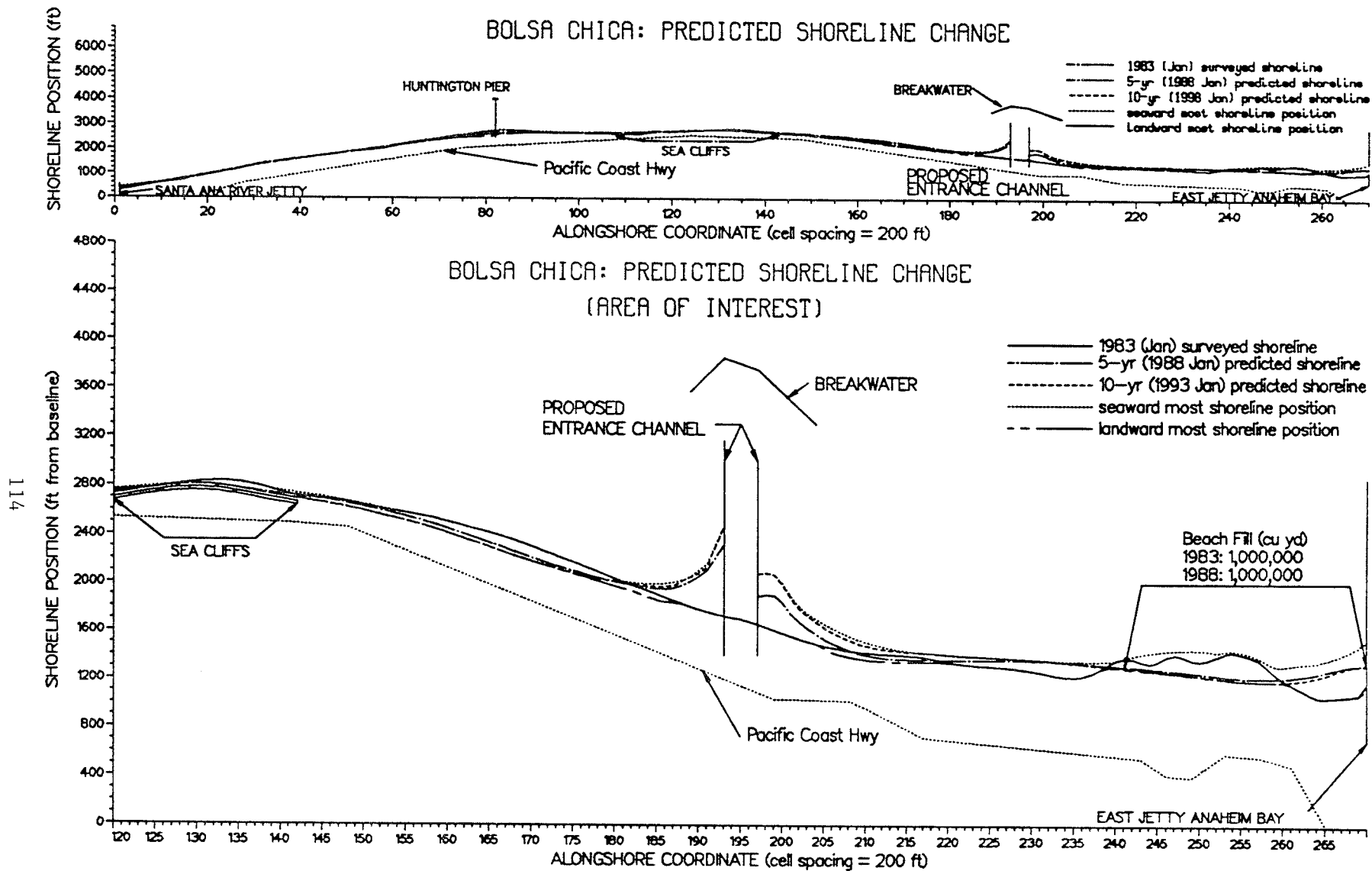


Figure 52. Alternative PR02B: preferred alternative, with feeder beach, year 1 southern swell wave conditions

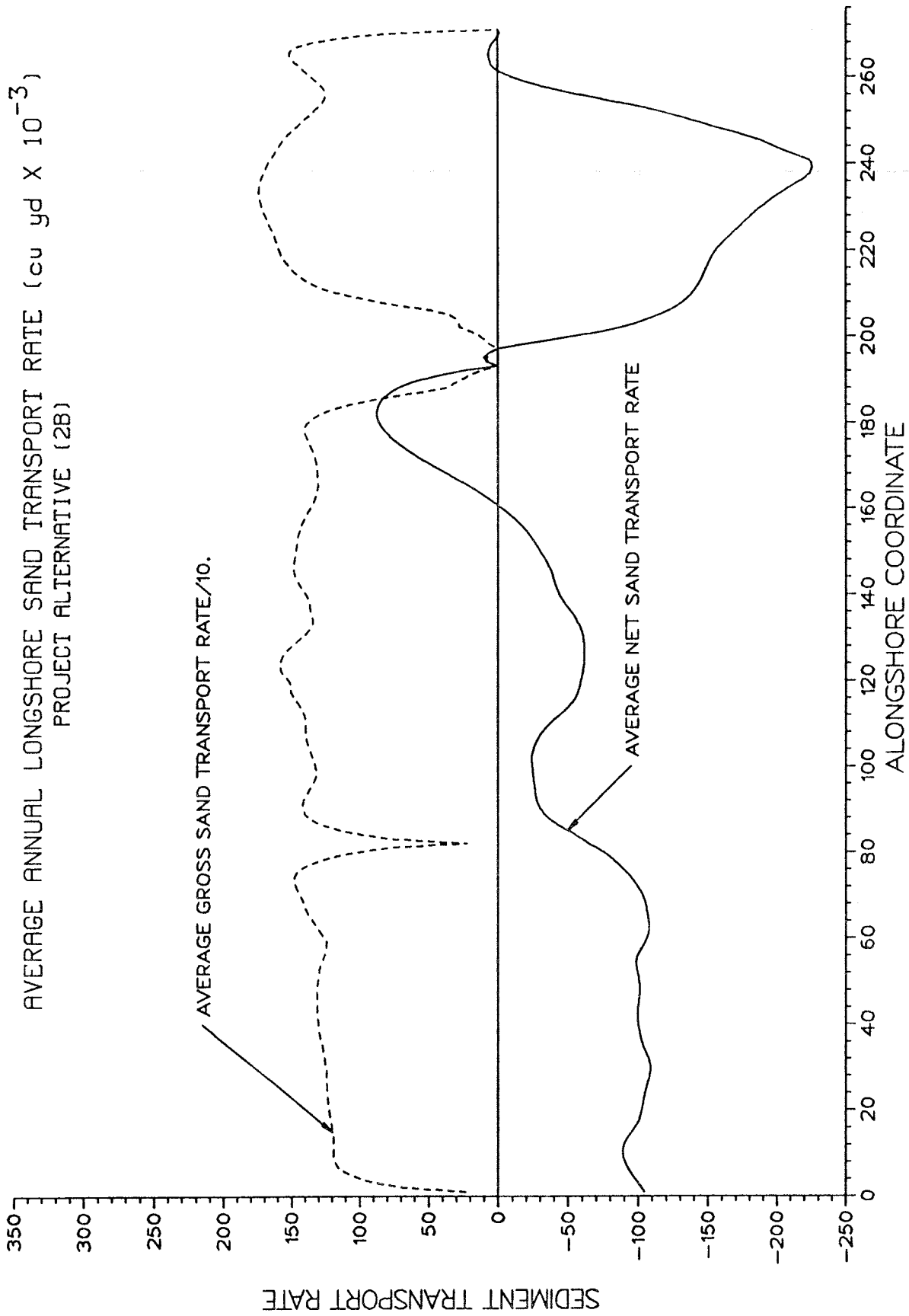


Figure 53. Alternative PRO2B: average annual longshore sand transport rates

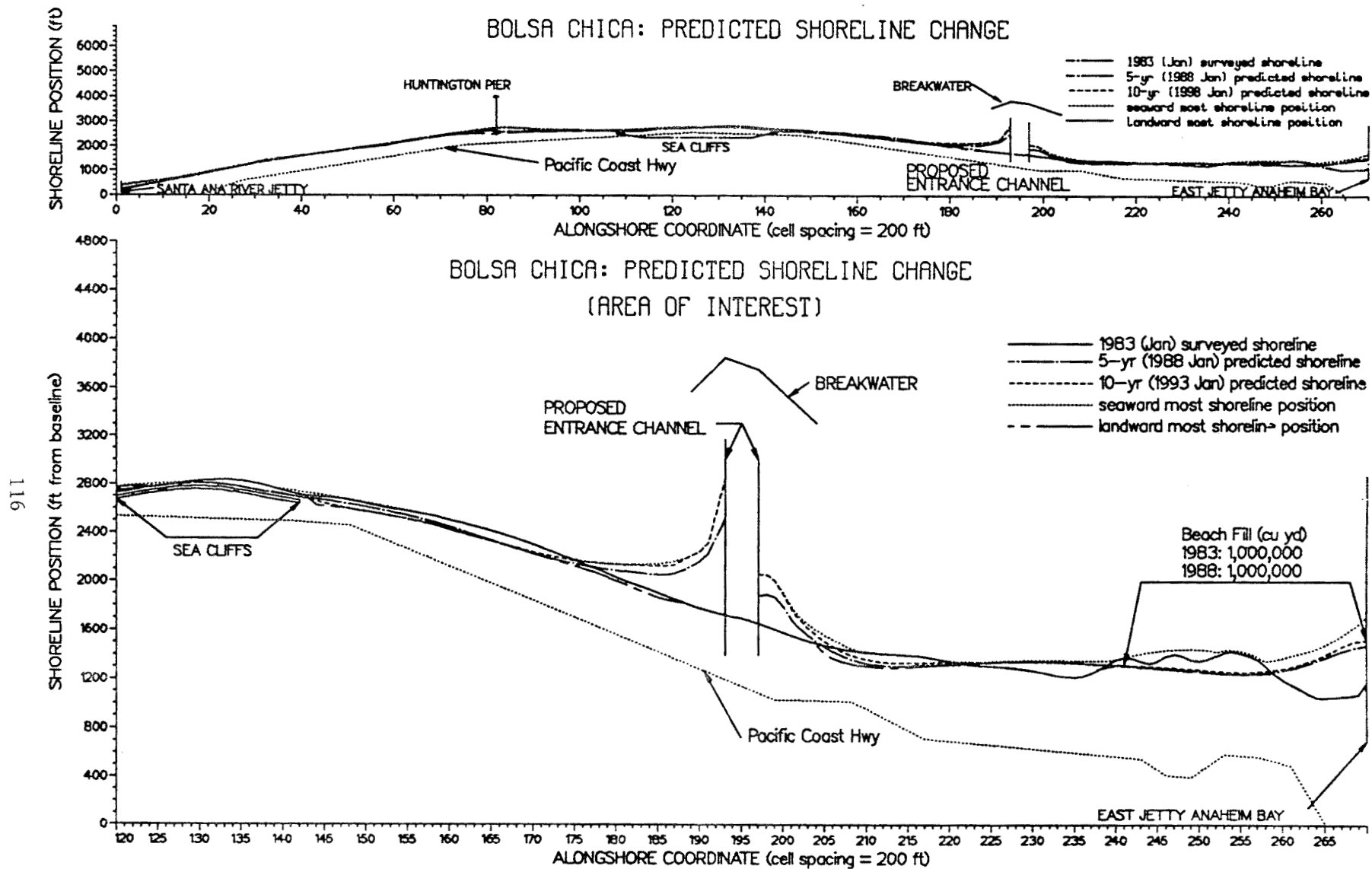


Figure 54. Alternative PR02C: preferred alternative, with feeder beach, year 2 southern swell wave conditions

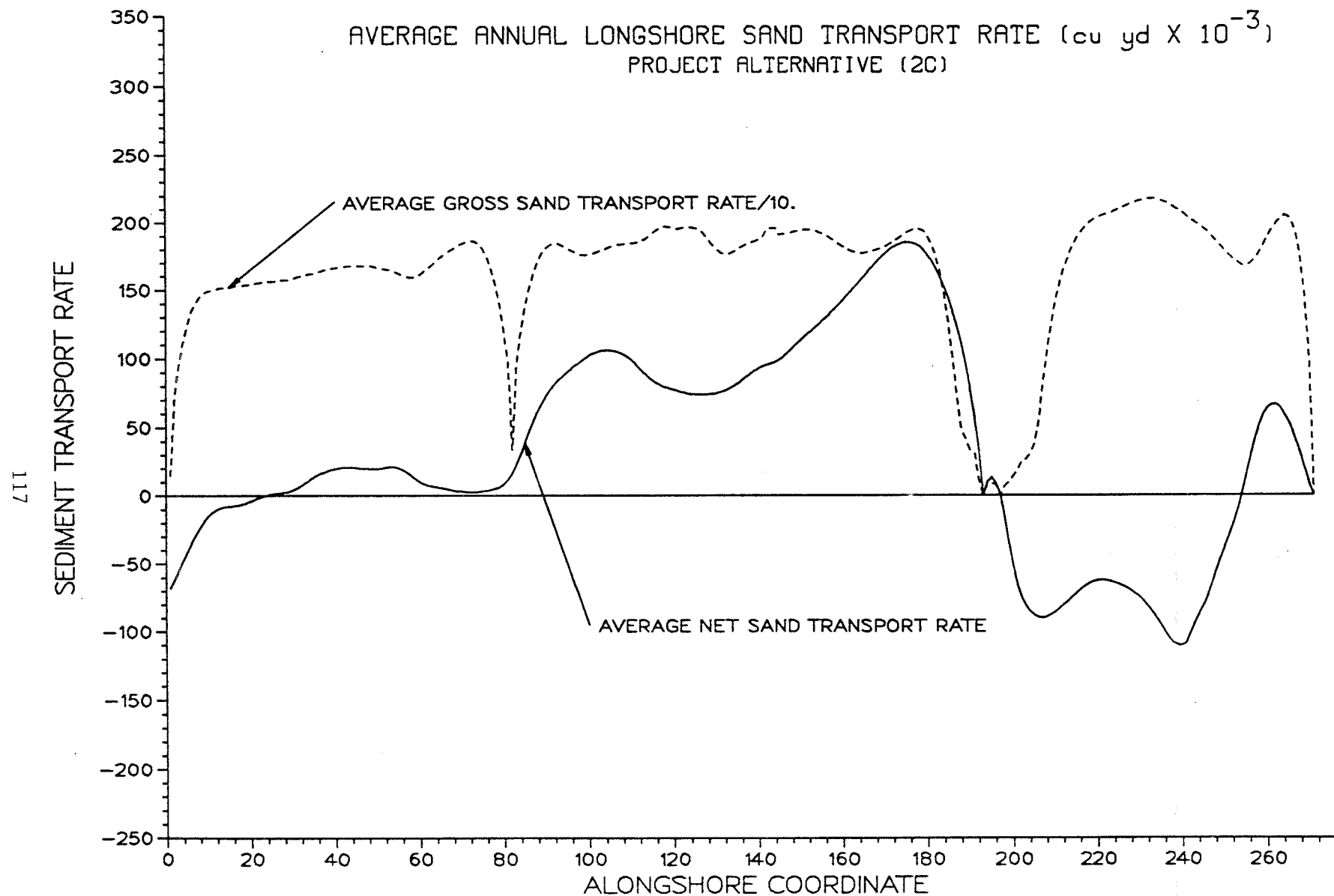


Figure 55. Alternative PR02C: average annual longshore sand transport rates

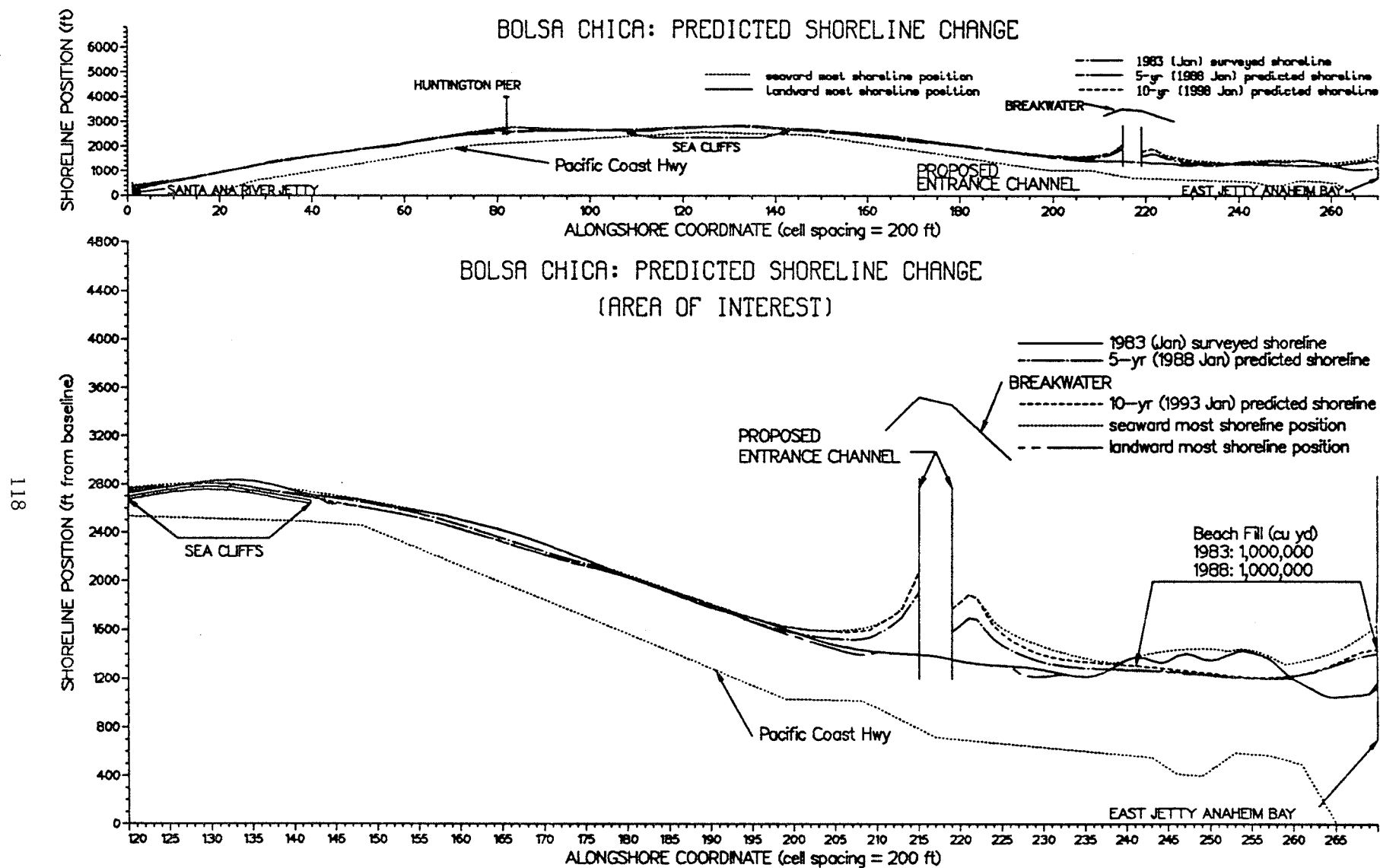


Figure 56. Alternative PUC2A: upcoast site, with feeder beach

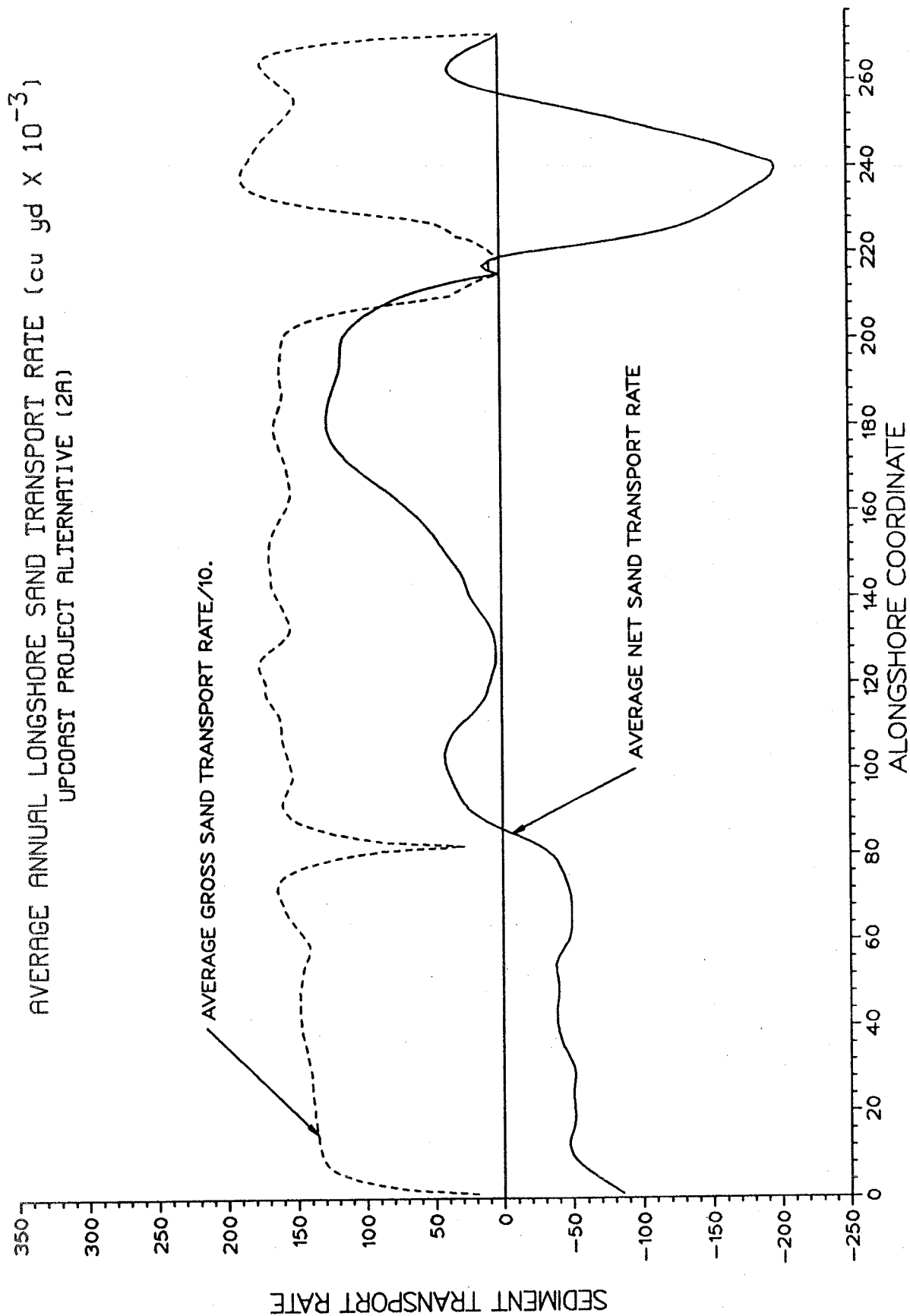


Figure 57. Alternative PUC2A: average annual longshore sand transport rates

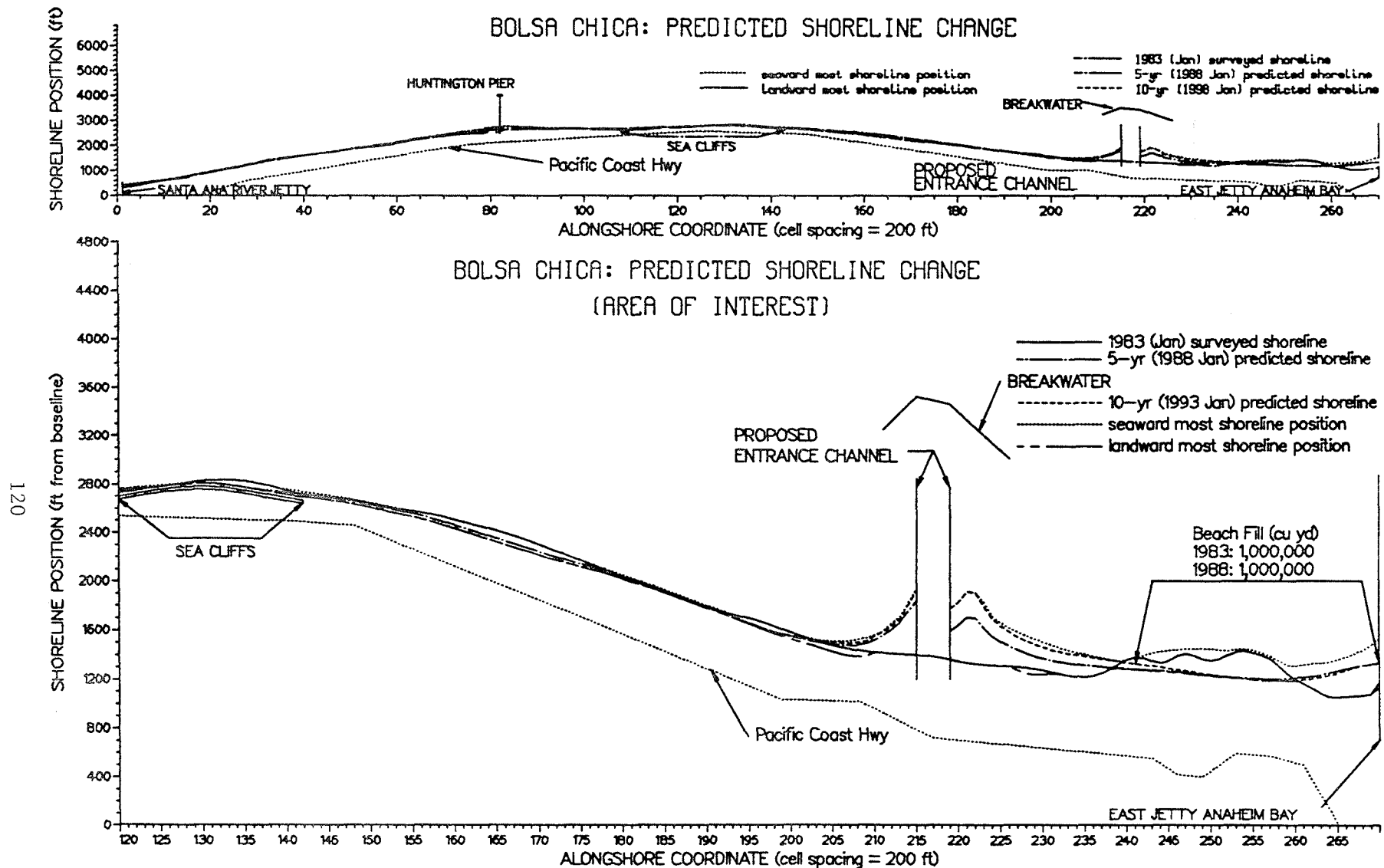


Figure 58. Alternative PUC2B: upcoast site, with feeder beach, year 1 southern swell wave conditions

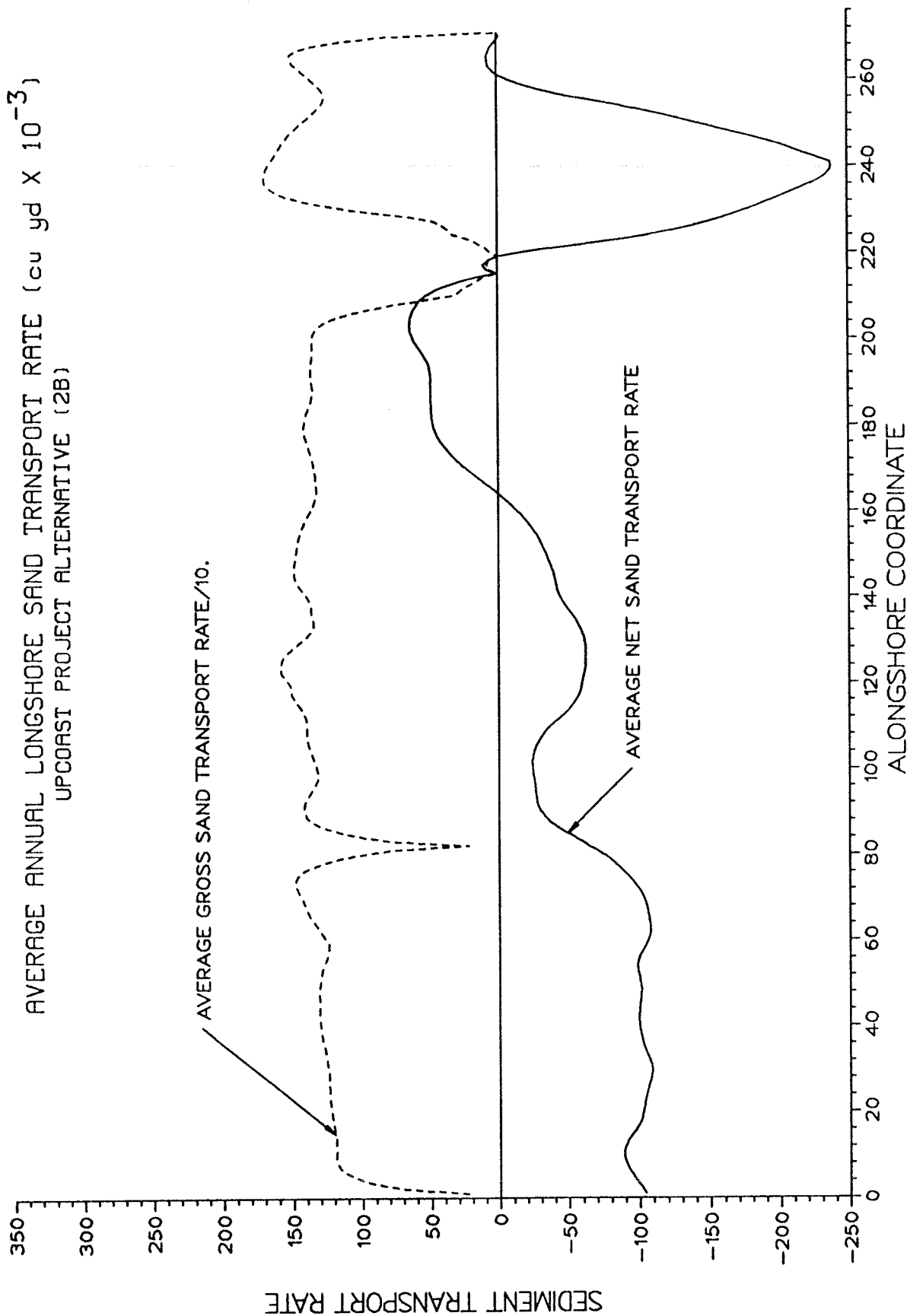


Figure 59. Alternative PUC2B: average annual longshore sand transport rates

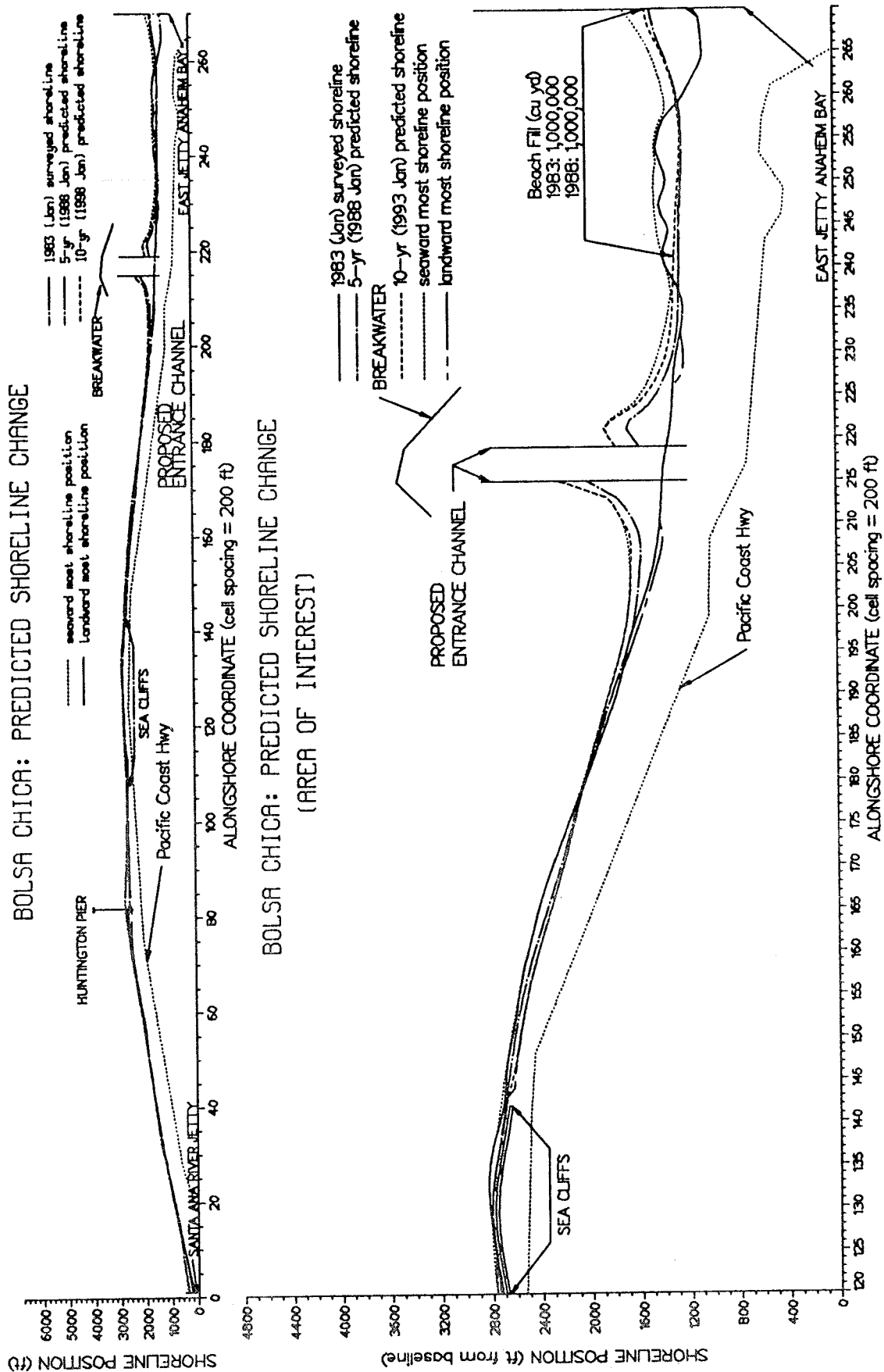


Figure 60. Alternative PUC2C: upcoast site, with feeder beach, year 2 southern swell wave conditions

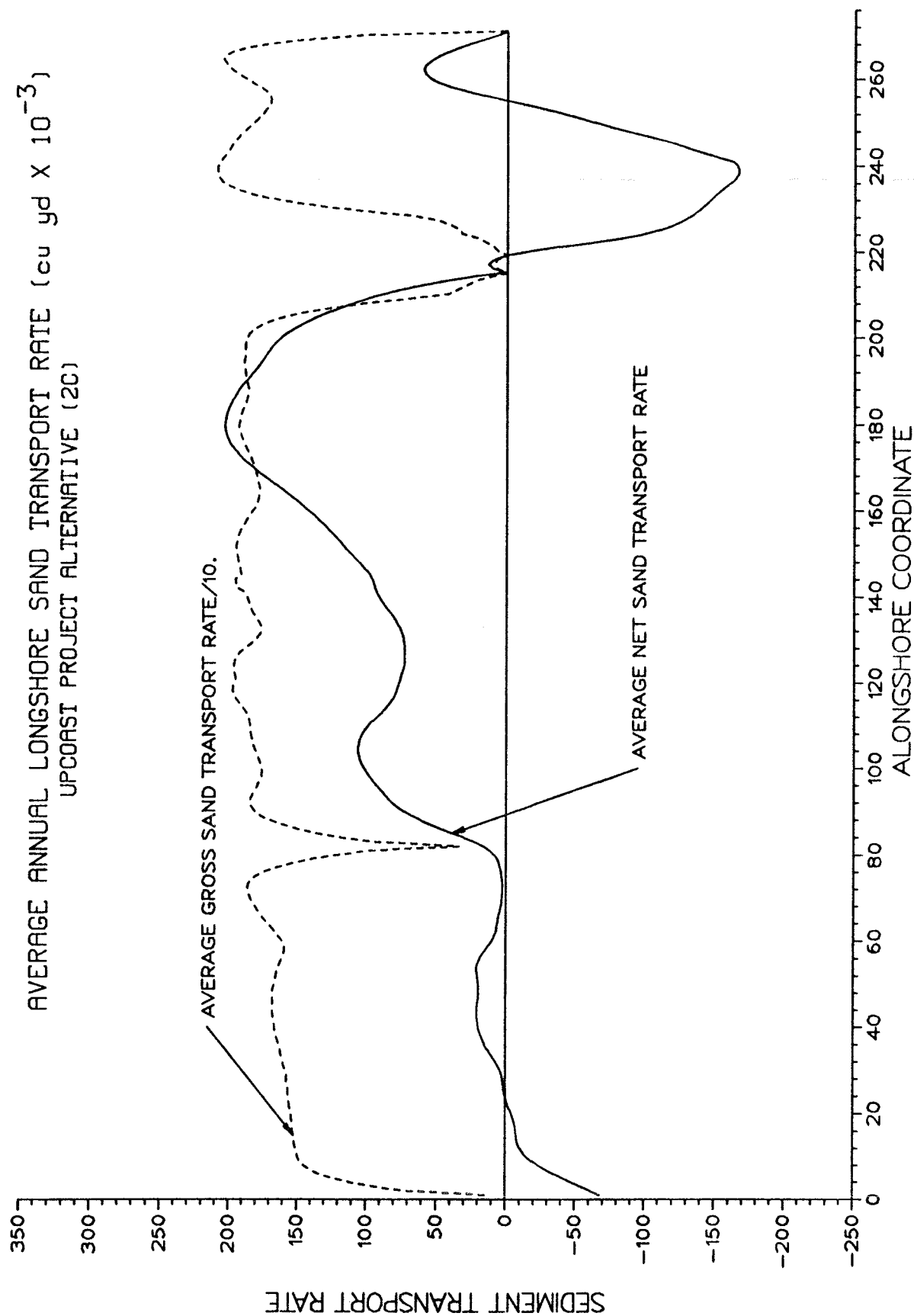


Figure 61. Alternative PUC2C: average annual longshore sand transport rates

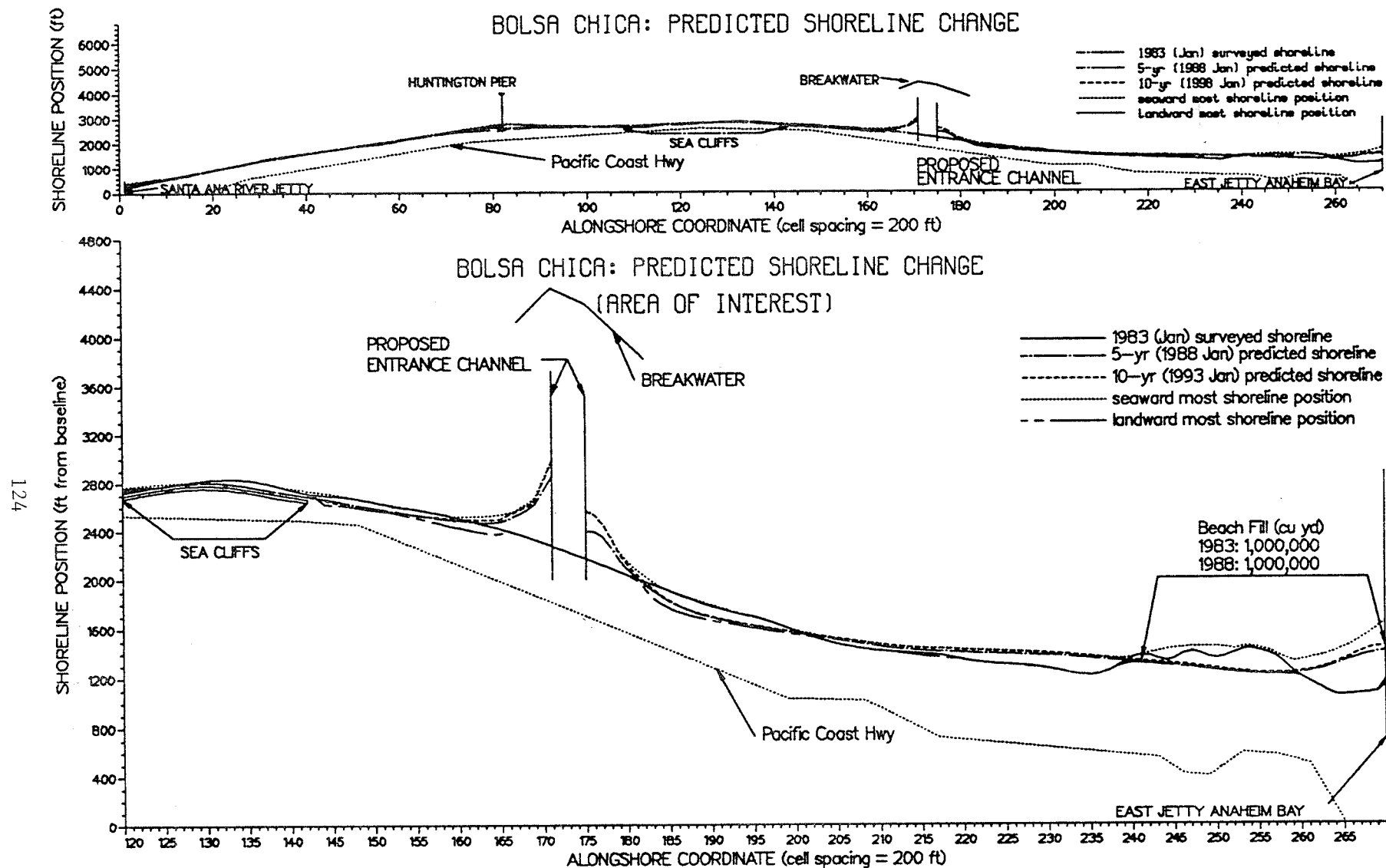


Figure 62. Alternative PDC2A: downcoast site, with feeder beach

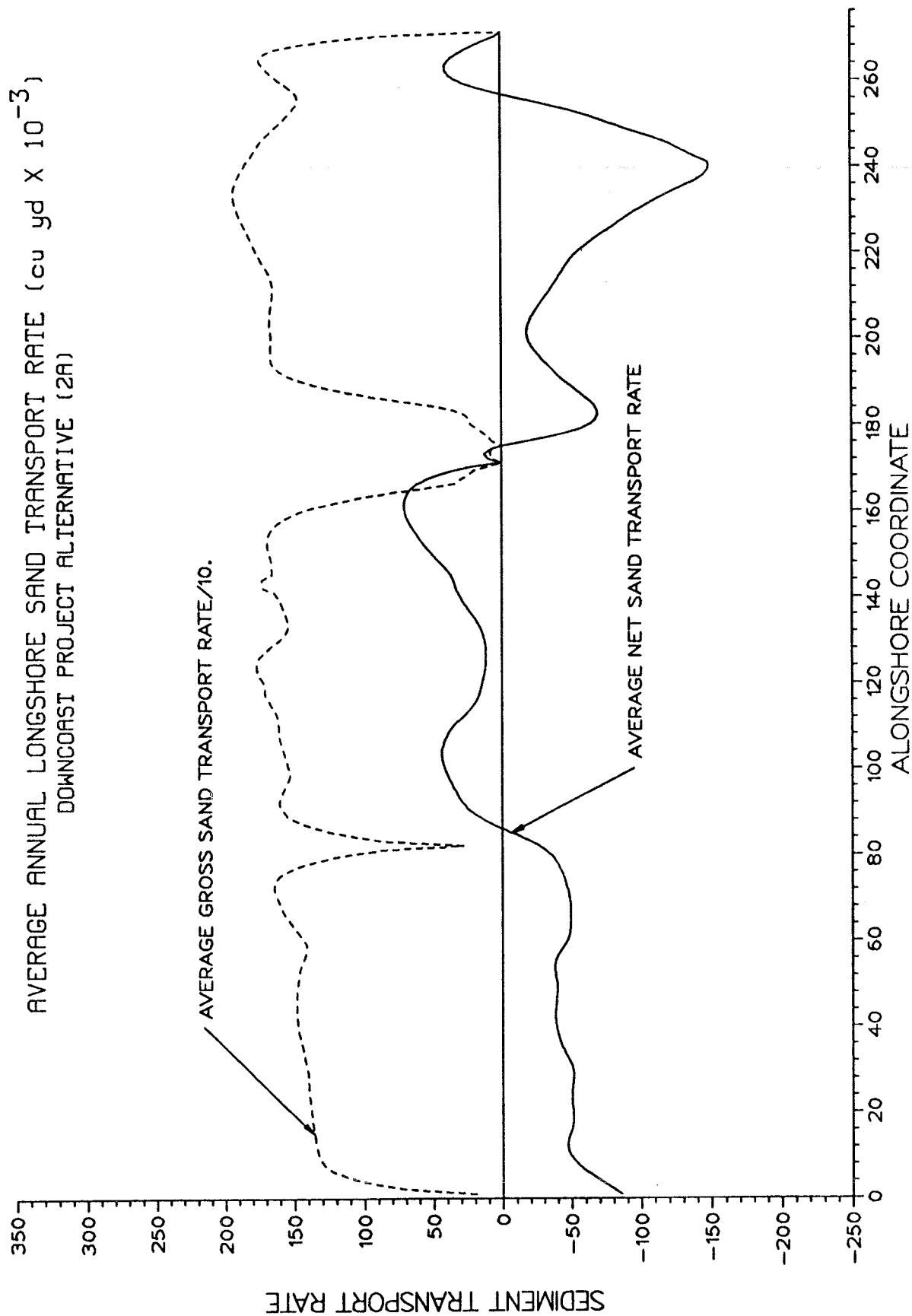


Figure 63. Alternative PDC2A: average annual longshore sand transport rates

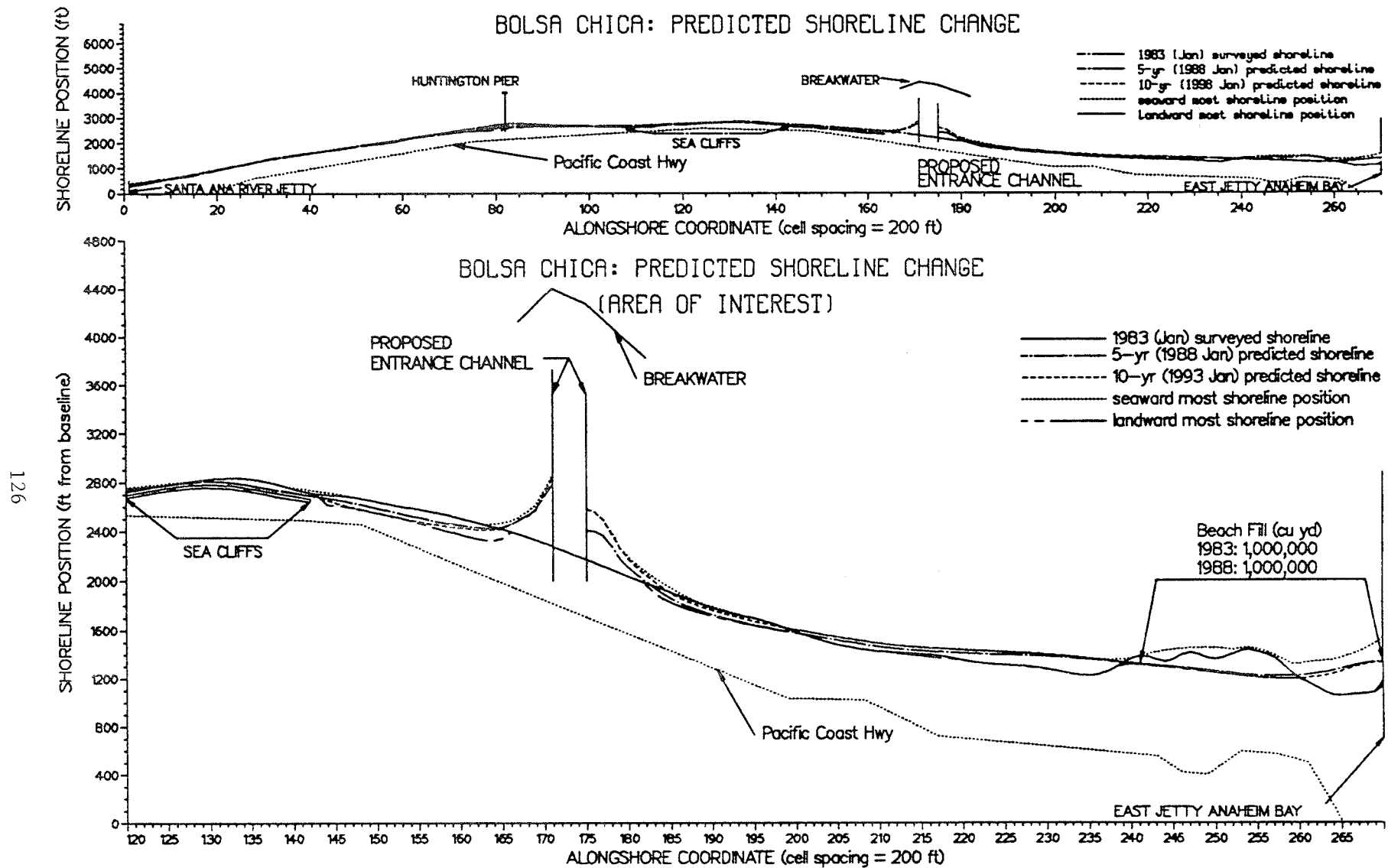


Figure 64. Alternative PDC2B: downcoast site, with feeder beach, year 1 southern swell wave conditions

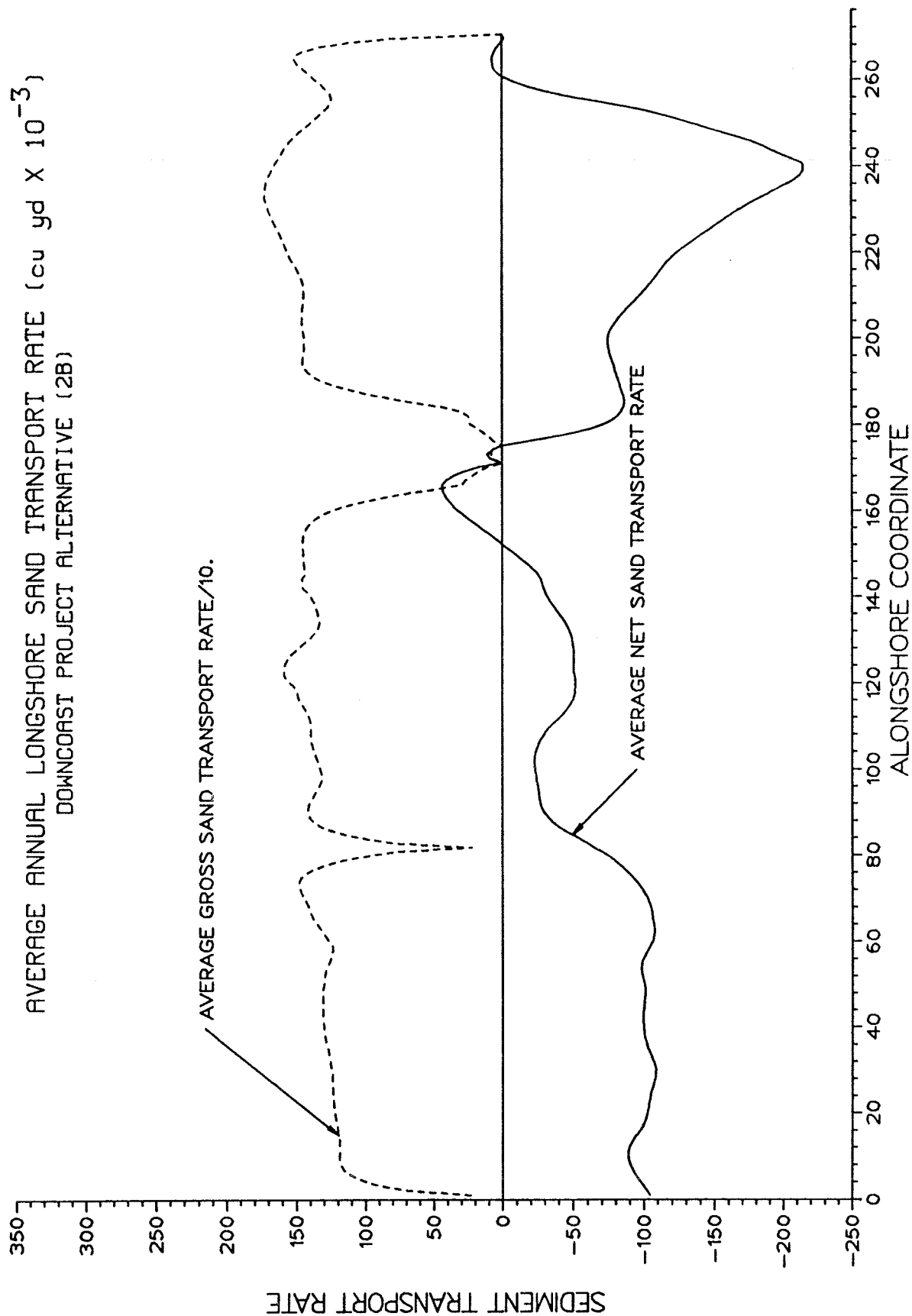


Figure 65. Alternative PDC2B: average annual longshore sand transport rates

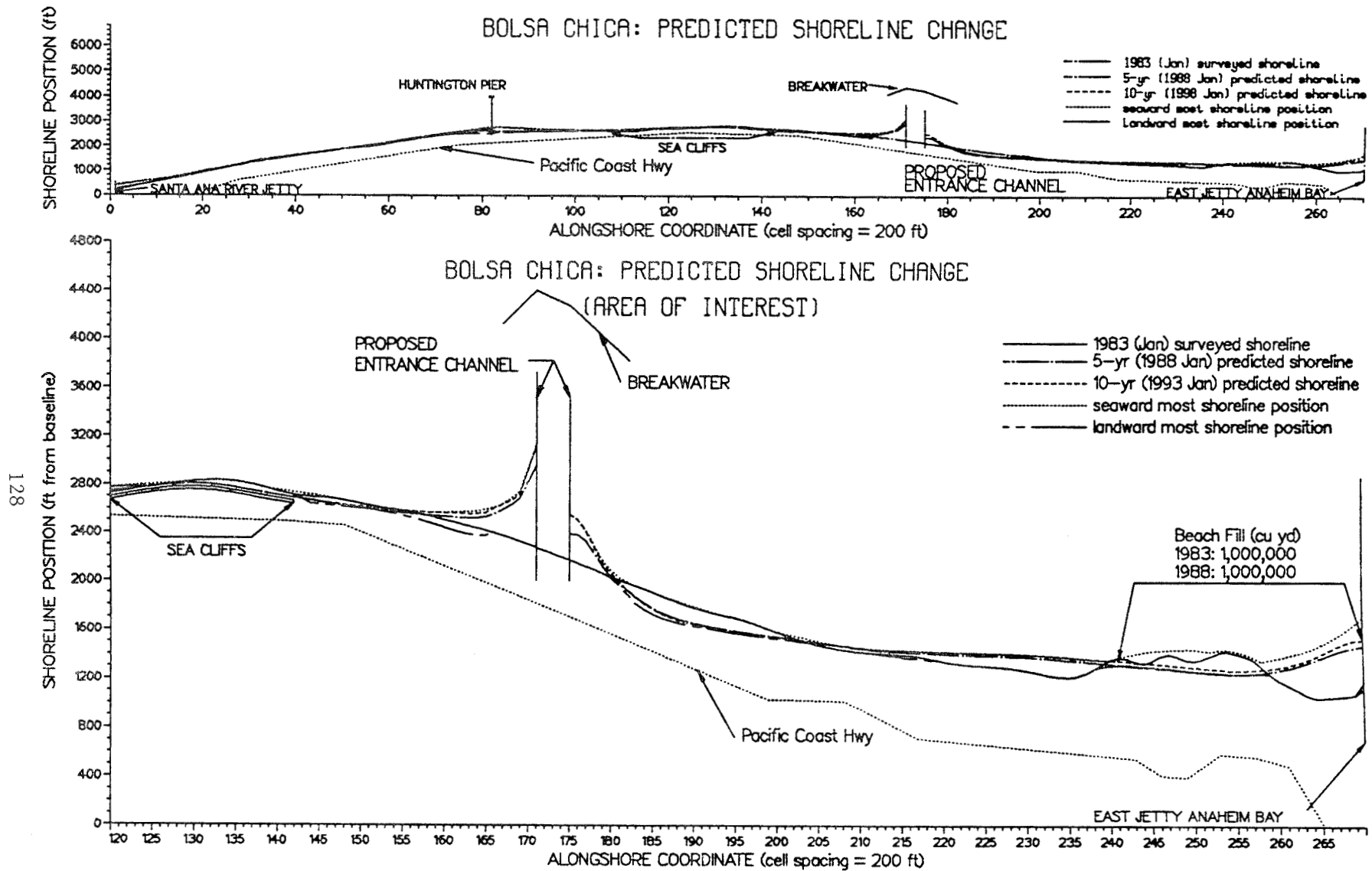


Figure 66. Alternative PDC2C: downcoast site, with feeder beach, year 2 southern swell wave conditions

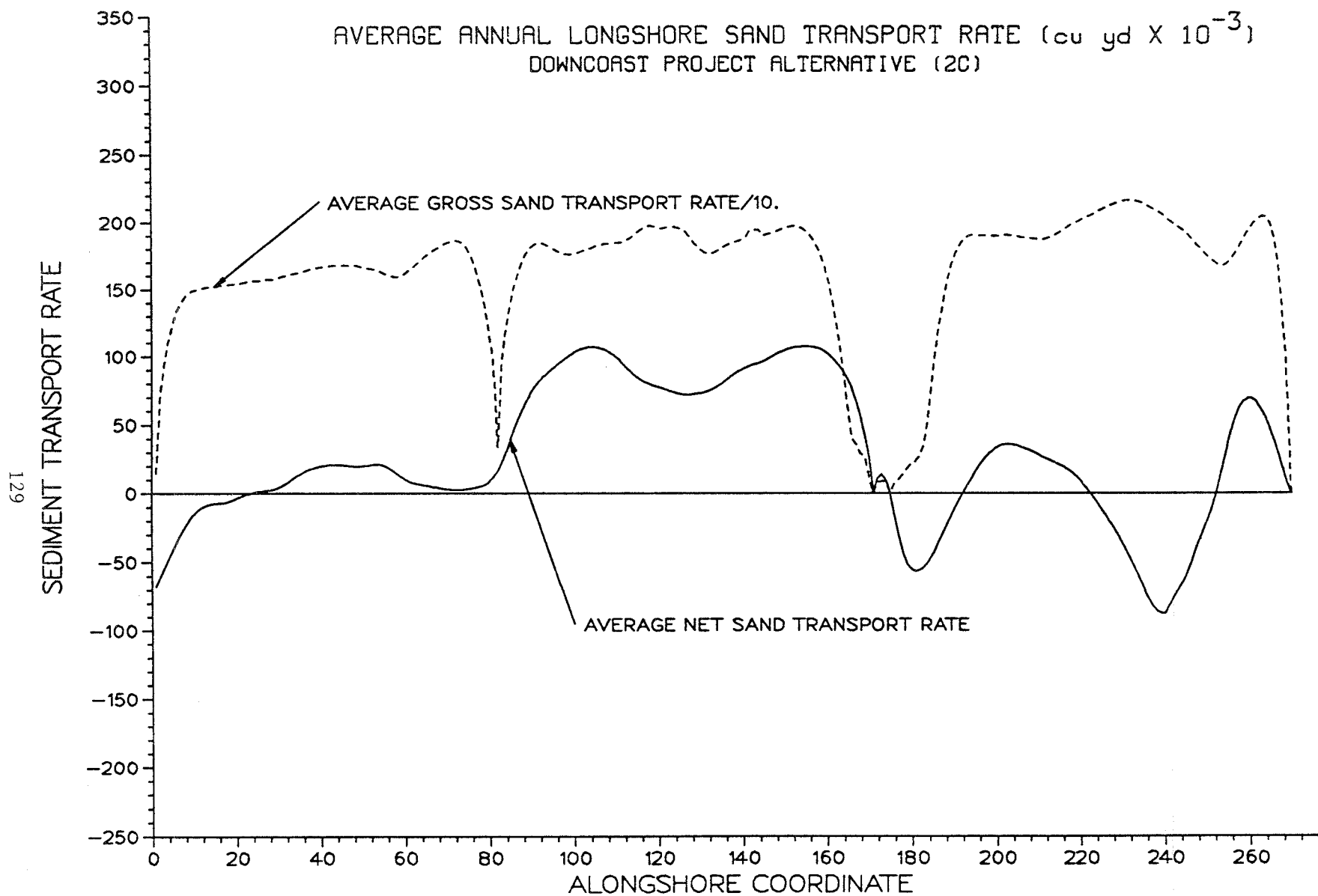


Figure 67. Alternative PDC2C: average annual longshore sand transport rates

longshore sand transport located at alongshore coordinate 190 (see Figure 67). By comparing Figure 67 with Figure 55 (Alternative PRO2C), it is seen that this divergence was created by location of the entrance in this alternative and the input wave characteristics.

Shoreline Impact Mitigation: Requirements, Criteria, and Plans

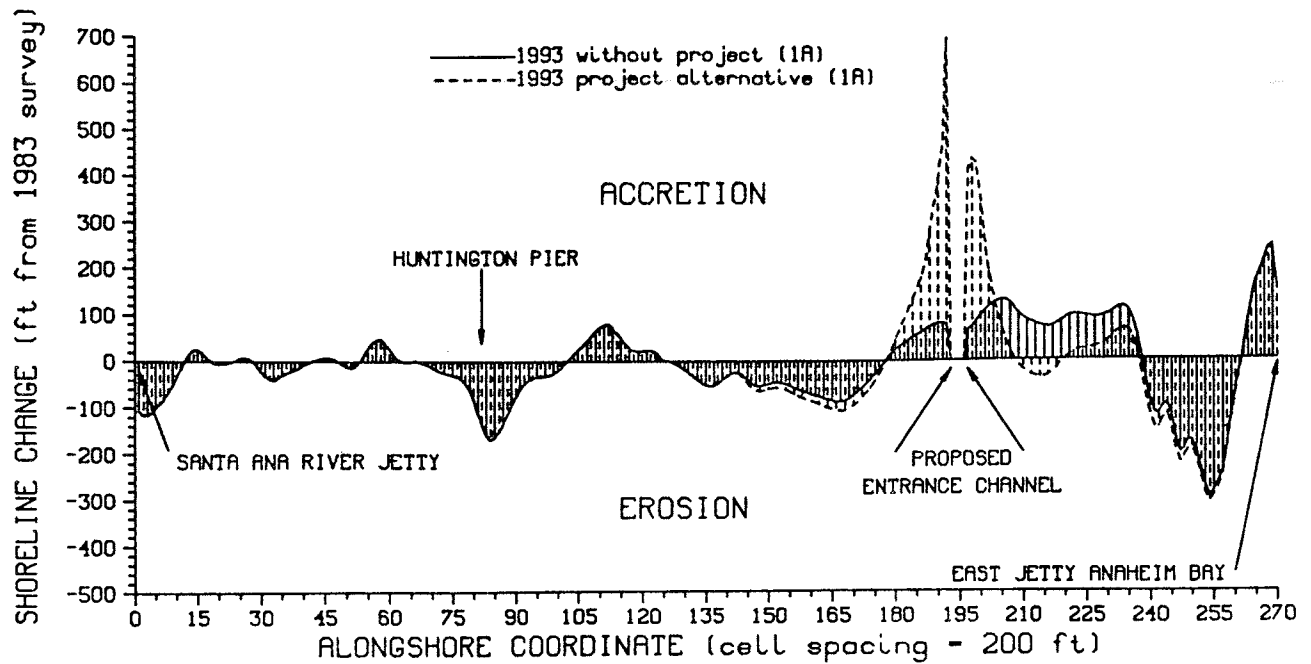
Sand management requirements

114. At this point in the shoreline response study an analysis was performed to assess the magnitude of the shoreline impacts resulting from the construction of a navigable ocean entrance system proposed for Bolsa Chica Bay. In the model simulations discussed above no special impact mitigation or sand management activities were implemented as part of the overall project design other than the continuation of the already established Surfside-Sunset feeder beach nourishment program in some of the alternative simulations (denoted as the type "2" simulations in the simulation code), as indicated in Table 8.

115. In order to isolate the shoreline impacts directly attributable the proposed navigable ocean entrance system, the results of the without-project simulations (Alternatives 1 and 2) were compared to the results of the preferred alternative simulations (Alternatives 3 and 4). The comparisons were made based on shoreline change from the 1983 surveyed shoreline positions. Figures 68 through 70 show the shoreline change from the initial (January 1983) shoreline position to the predicted 10-year (January 1993) shoreline position.

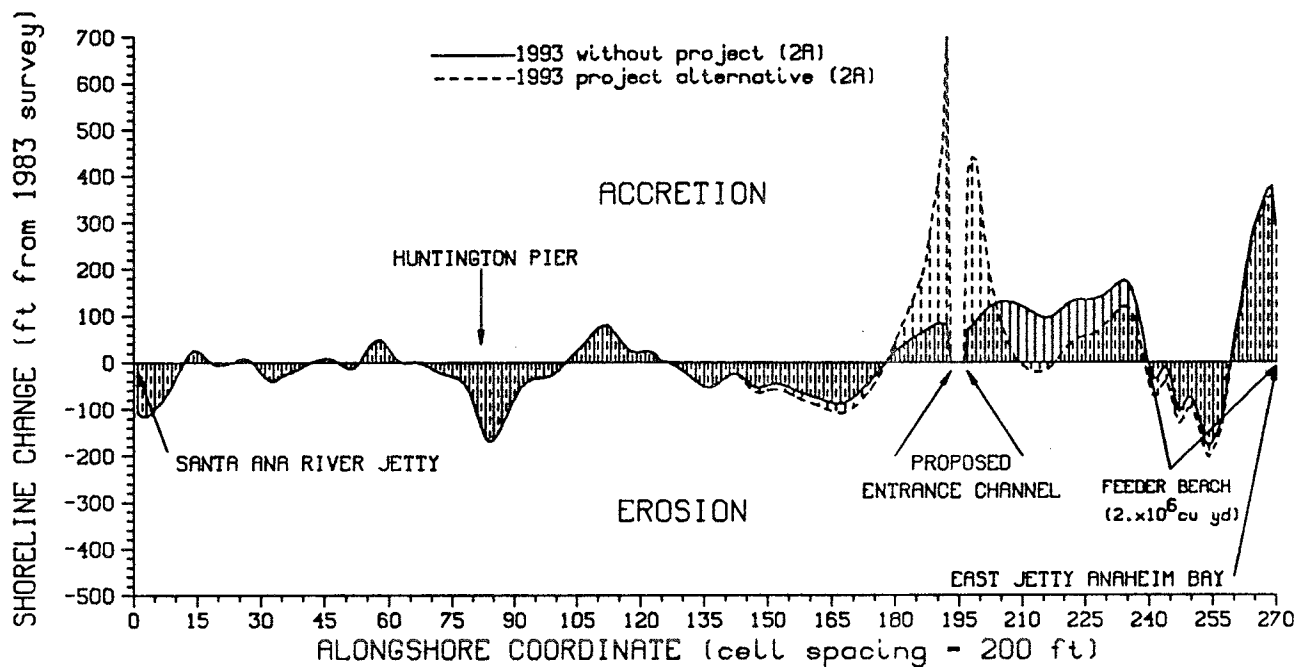
116. In all of the preferred alternative simulations, there is a narrow region of shoreline accretion adjacent the entrance jetties on both sides of the proposed channel. This region of accretion is followed by a wider zone of shoreline erosion further away from the entrance system. On the southeast side of the proposed entrance system, the alongshore width of the accretive beach varies from 1400 ft (Figure 69) to 2800 ft (Figure 70). The maximum berm width of the accretive beach occurs immediately adjacent to the jetty and varies from between 460 ft (Figure 69) and 700 ft (Figure 70). On the northwest side of the entrance system, the width of the accretive beach

BOLSA CHICA: SHORELINE IMPACTS



(a)

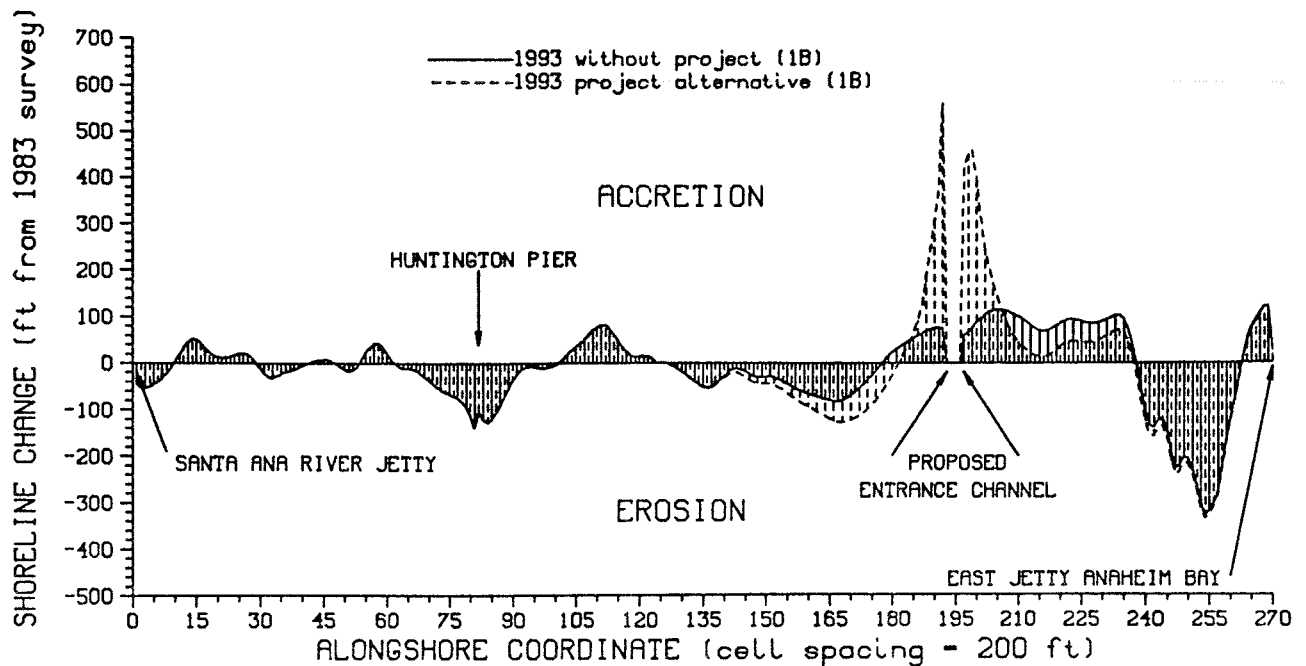
BOLSA CHICA: SHORELINE IMPACTS



(b)

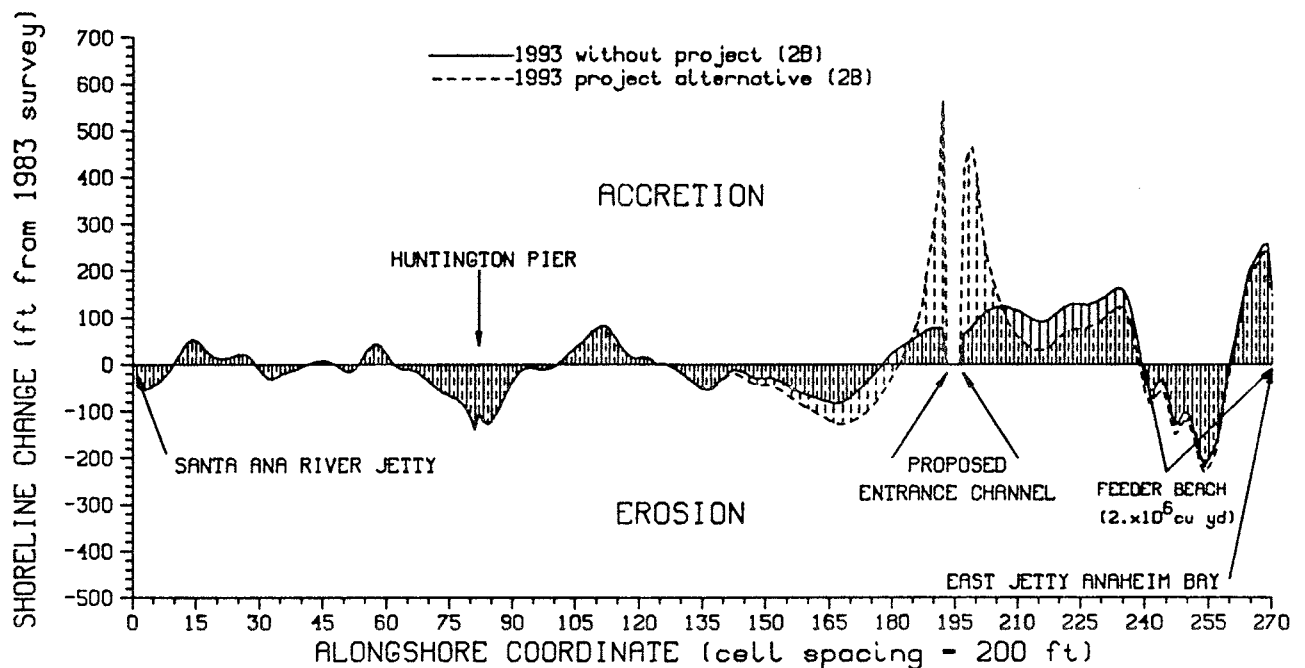
Figure 68. Predicted shoreline change from 1983 shoreline position
 (a) Alternative WP1A vs. Alternative PRO1A
 (b) Alternative WP2A vs. Alternative PRO2A

BOLSA CHICA: SHORELINE IMPACTS



(a)

BOLSA CHICA: SHORELINE IMPACTS



(b)

Figure 69. Predicted shoreline change from 1983 shoreline position
 (a) Alternative WP1B vs. Alternative PRO1B
 (b) Alternative WP2B vs. Alternative PRO2B

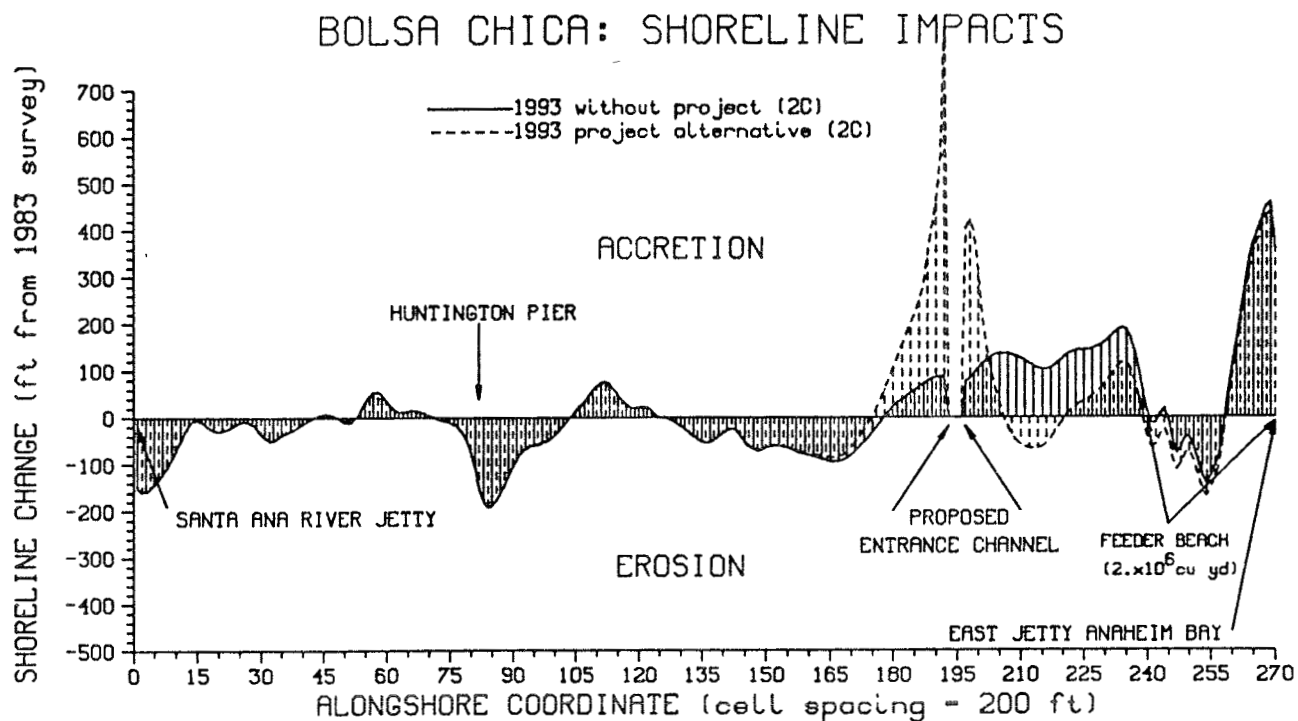
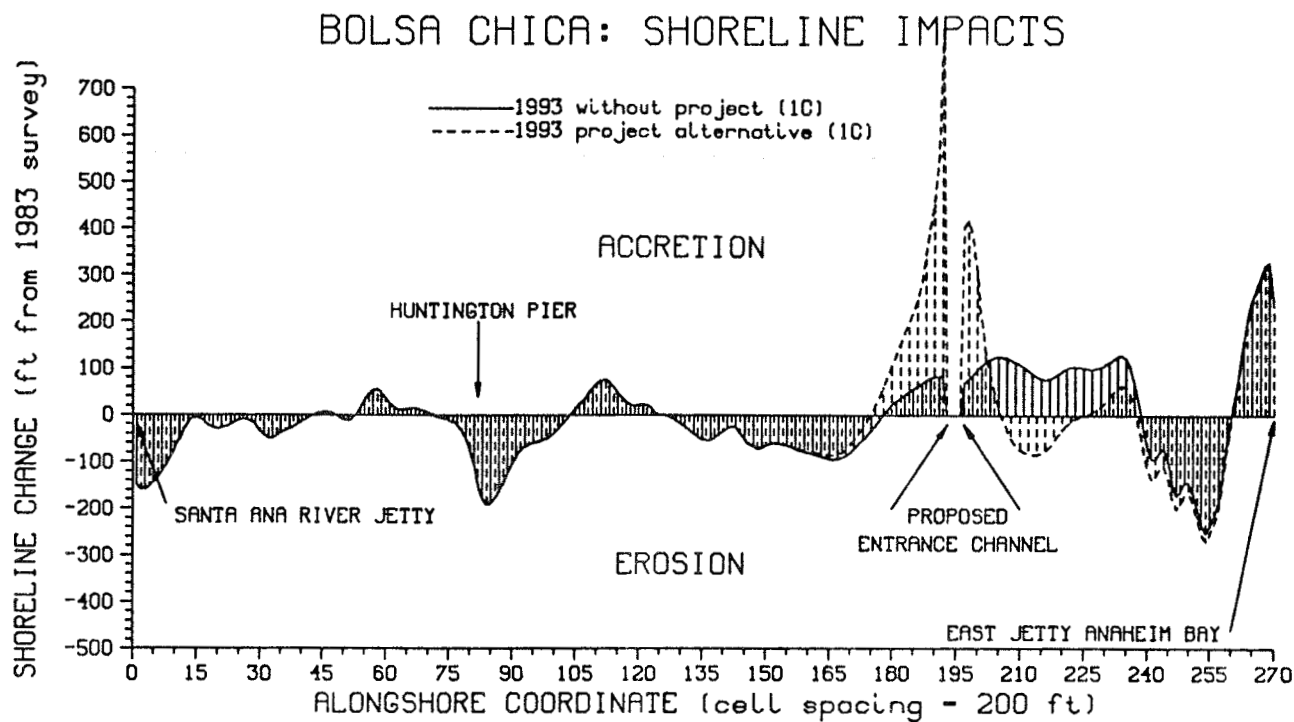


Figure 70. Predicted shoreline change from 1983 shoreline position
 (a) Alternative WP1C vs. Alternative PRO1C
 (b) Alternative WP2C vs. Alternative PRO2C

varies from 1200 ft to 2000 ft. The maximum berm width on the northwest side again occurs immediately adjacent to the jetty and varies from 330 ft to 380 ft.

117. In the simulations in which year 1 of the southern swell wave conditions were used (Alternatives PRO1B, and PRO2B) as input to the shoreline change model, the longest region of shoreline erosion on the southeast side of the entrance system was predicted. In these simulations, the alongshore width of the erosion zone is on the order of 8400 ft and within this region the shoreline is displaced about 60 ft landward (Figure 69).

118. The simulations in which year 2 of the southern swell wave conditions were used (Alternatives PRO1C, and PRO2C) resulted in the longest region of shoreline erosion on the northwest side of the entrance system. The predicted length of the erosion zone is on the order of 11,000 ft, and shoreline erosion was about 180 ft at its maximum.

119. The simulations in which all of the available southern swell wave conditions (year 1 and year 2) were used (shown in Figure 68) resulted in less overall shoreline erosion. The results of these simulations represent our best estimate of the expected shoreline evolution resulting from the construction of the proposed ocean entrance system at Bolsa Chica Bay. The results of the other simulations shown in Figures 69 and 70, represent possible extremes in variation from the best estimate, shown in Figure 68. This variation will require the impact mitigation plans (sand bypassing and/or backpassing at the entrance) to be flexible as will be discussed in the following paragraphs.

Impact mitigation criteria

120. The previous model results and analysis were presented to the SLC, which established the following criteria for the impact mitigation simulations:

- a. Only that sand which accumulates within 1500 ft of the entrance jetties maybe utilized for sand bypassing and/or sand backpassing. The utilization of new sand sources was not investigated as part of these impact mitigation plans.
- b. A successful sand management plan will be one in which shoreline change from the 1983 surveyed shoreline position is accretive, or if the without-project alternative indicates erosion, the sand management plan must indicate equal or less erosion.

Sand management plans

121. Three different sand management plans were developed for the three different input wave data sets (the "A", "B", and "C" simulations as indicated in the simulation code, see Table 8). The designation of the various sand bypassing and backpassing borrow and fill sites are as follows:

a. Plan "A."

Southeast side: Annually (on 1 January) shoreline accretion between alongshore coordinates 186 and 192 is limited to +50 ft from the January 1983 surveyed shoreline position. The excess sand accumulated in this region is backpassed to a fill area located between alongshore coordinates 160 and 185.

Northwest side: Annually (on 1 January) shoreline accretion between alongshore coordinates 197 and 203 is limited to +50 ft from the January 1983 surveyed shoreline position. The excess sand accumulated in this region is backpassed to a fill area located between alongshore coordinates 205 and 230.

b. Plan "B."

Southeast side: Annually (on 1 January) shoreline accretion between alongshore coordinates 186 and 192 is limited to +50 ft from the January 1983 surveyed shoreline position. The excess sand accumulated in this region is backpassed to a fill area located between alongshore coordinates 165 and 185.

Northwest side: Annually (on 1 January) shoreline accretion between alongshore coordinates 197 and 206 is limited to +50 ft from the January 1983 surveyed shoreline position. The excess sand accumulated between coordinates 197 and 200 is backpassed to a fill area located between alongshore coordinates 207 and 217. The excess sand accumulated between alongshore coordinates 201 and 206 is bypassed to a fill area located between coordinates 175 and 185.

c. Plan "C."

Southeast side: Annually (on 1 January) shoreline accretion between alongshore coordinates 187 and 192 is at first limited to +180 ft from the January 1983 surveyed shoreline position. The excess sand accumulated in this region is bypassed to a fill area located between alongshore coordinates 208 and 250. Then the shoreline accretion is limited to +100 ft from the January 1983 surveyed shoreline position. The excess sand in this region is backpassed to a fill area located between alongshore coordinates 165 and 186.

Northwest side: Annually (on 1 January) shoreline accretion between alongshore coordinates 197 and 204 is limited to +100 ft from the January 1983 surveyed shoreline position. The excess sand accumulated in this region is backpassed to a fill area located between alongshore coordinates 207 and 216.

Sand management simulations: Alternatives 7 & 8

122. The purpose of this set of model simulations was to estimate the nourishment volumes required to mitigate potential shoreline erosion resulting from the construction of the proposed navigable ocean entrance channel and detached breakwater. The results of the plan A sand management simulations (Alternatives SM1A and SM2A) are shown in Figures 71 through 74, and are compared (based on shoreline change from the January 1983 surveyed shoreline position) to the A type without-project simulations in Figure 75. The calculated volumetric sand management requirements resulting from the implementation of sand management plan A are as follows:

a.	Southeast side:	<u>cu yd/year</u>
	Average annual backpassing volume	210×10^3
	Maximum backpassing volume (year 6)	277×10^3
	Minimum backpassing volume (year 9)	165×10^3
b.	Northwest side:	<u>cu yd/year</u>
	Average annual backpassing volume	155×10^3
	Maximum backpassing volume (year 6)	271×10^3
	Minimum backpassing volume (year 9)	50×10^3

123. The results of the plan B sand management simulations (Alternatives SM1B and SM2B) are given in Figures 76 through 79, and are compared (based on shoreline change from the January 1983 surveyed shoreline position) to the B type without-project simulations in Figure 80. The calculated volumetric sand management requirements of sand management plan B are:

a.	Southeast side:	<u>cu yd/year</u>
	Average annual backpassing volume	161×10^3
	Maximum backpassing volume (year 4)	183×10^3
	Minimum backpassing volume (year 1)	120×10^3
b.	Northwest side:	<u>cu yd/year</u>
	Average annual backpassing volume	117×10^3
	Maximum backpassing volume (year 8)	198×10^3
	Minimum backpassing volume (year 1)	41×10^3
c.	Northwest side:	<u>cu yd/year</u>
	Average annual bypassing volume	57×10^3
	Maximum bypassing volume (year 9)	148×10^3
	Minimum bypassing volume (year 1)	6×10^3

124. The results of the plan C sand management simulations (Alternatives SM1C and SM2C) are given in Figures 81 through 84, and are compared

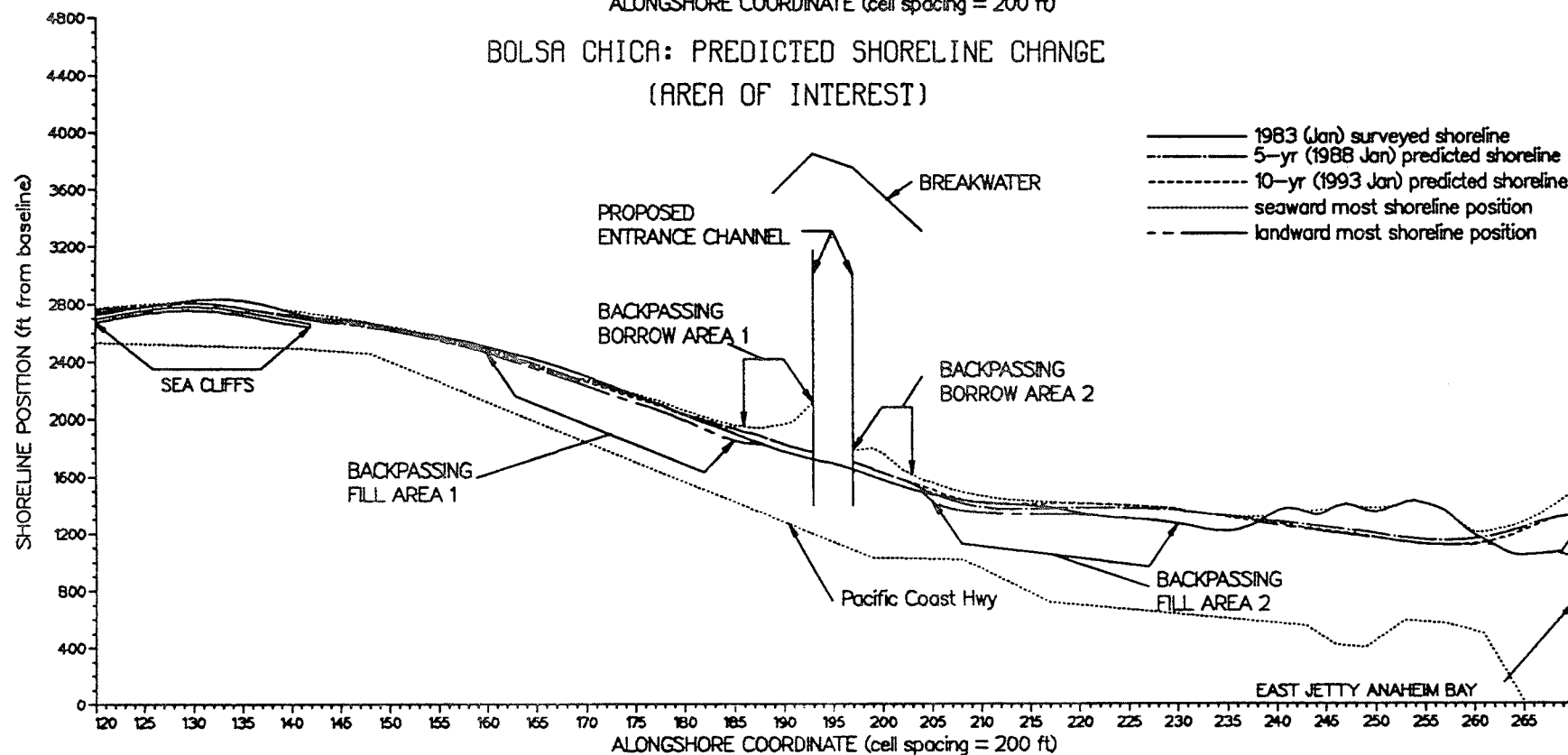
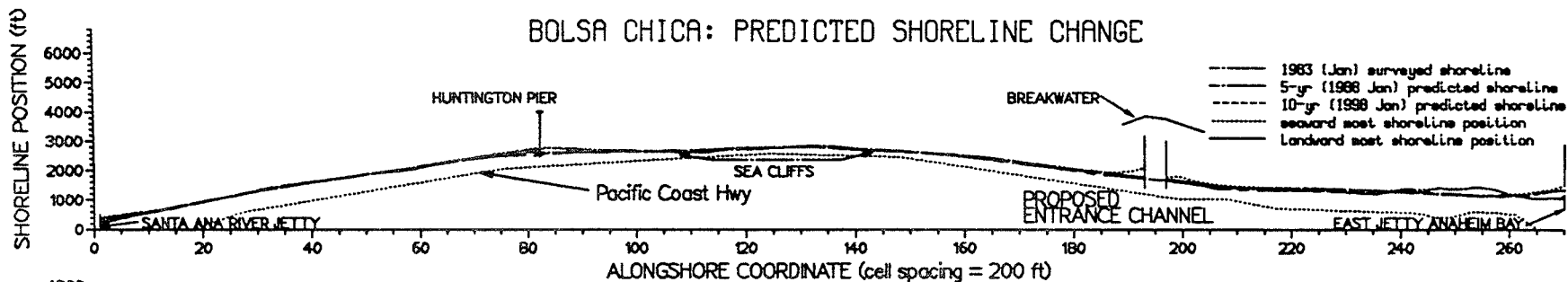


Figure 71. Alternative SM1A: sand management, without feeder beach

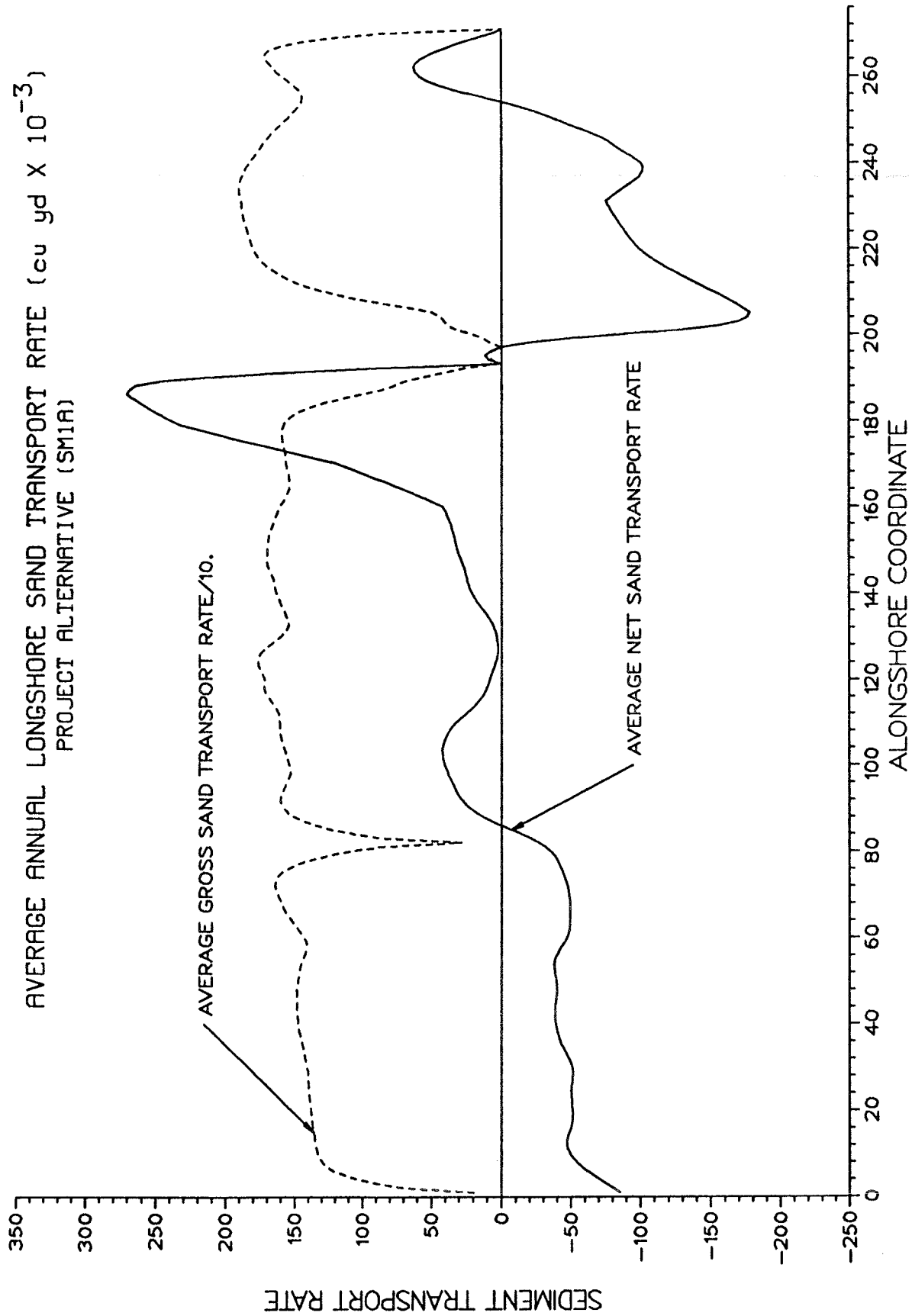


Figure 72. Alternative SM1A: average annual longshore sand transport rates

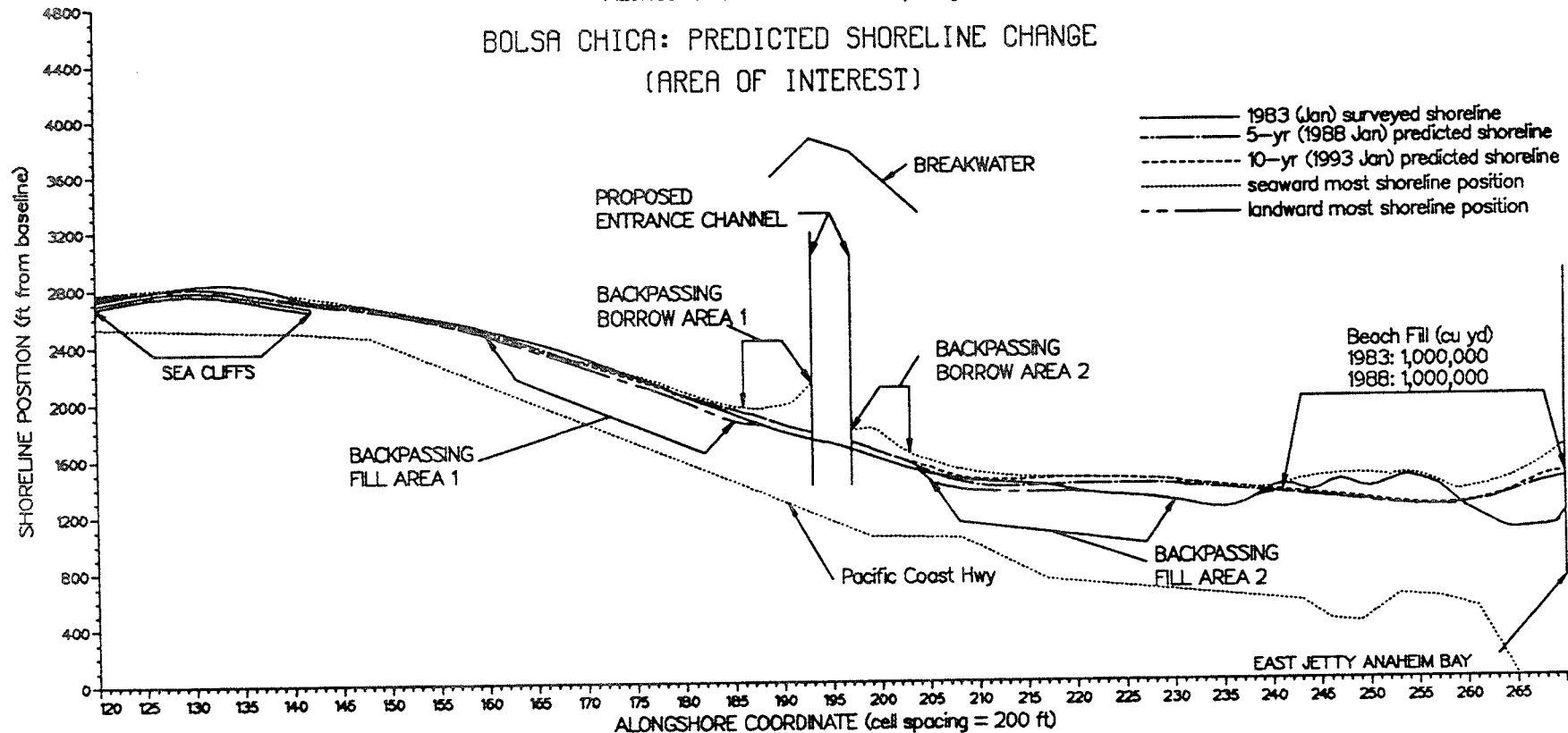
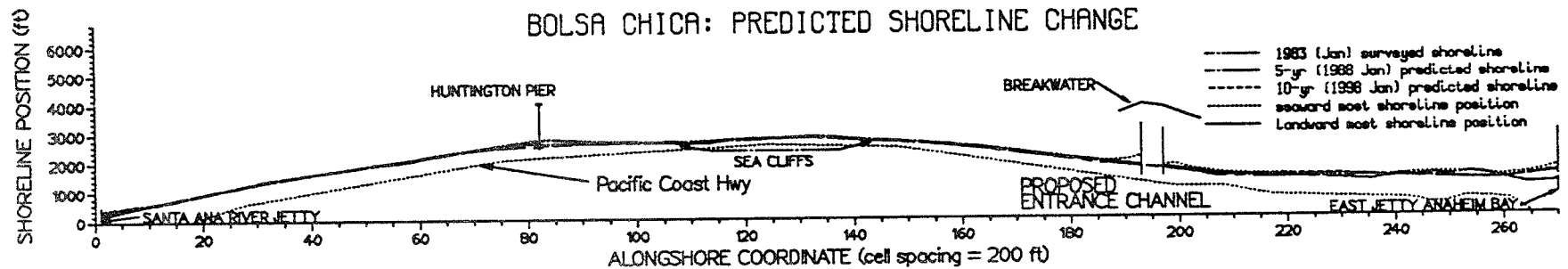


Figure 73. Alternative SM2A: sand management, with feeder beach

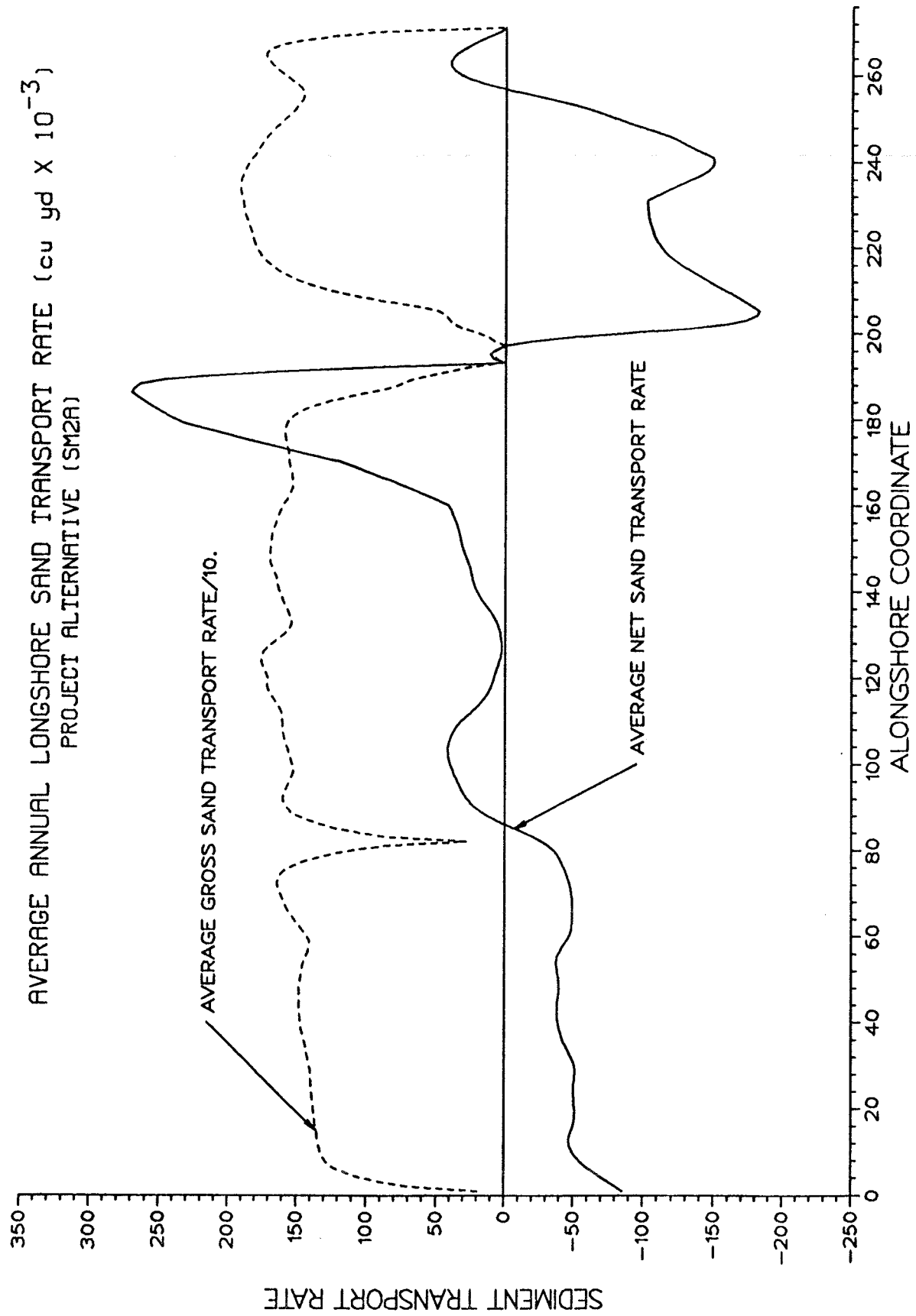
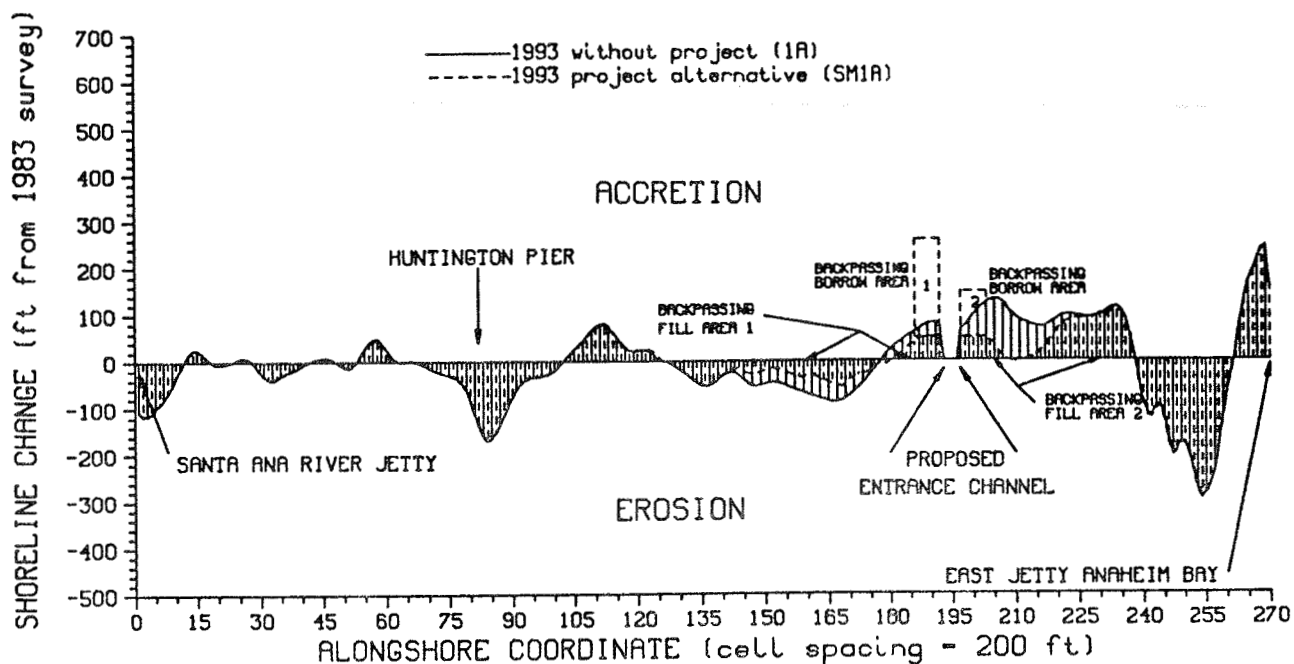


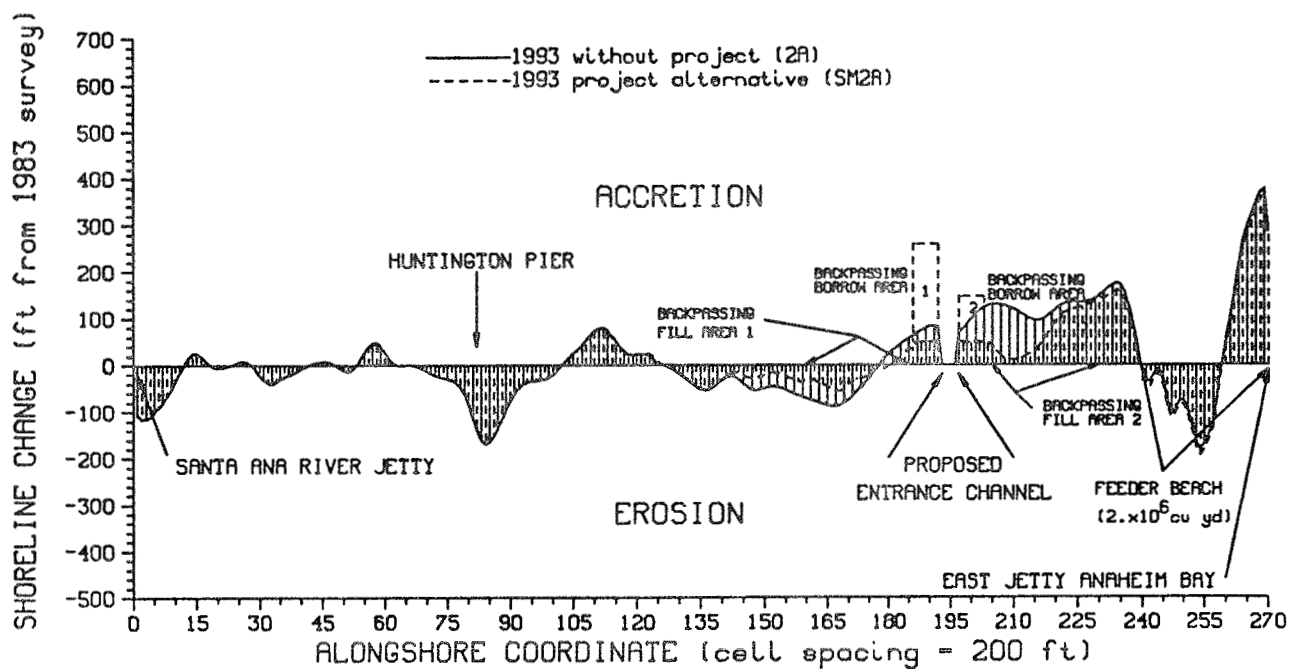
Figure 74. Alternative SM2A: average annual longshore sand transport rates

BOLSA CHICA: SHORELINE IMPACTS



(a)

BOLSA CHICA: SHORELINE IMPACTS



(b)

Figure 75. Predicted shoreline change from 1983 shoreline position
 (a) Alternative WP1A vs. Alternative SM1A
 (b) Alternative WP2A vs. Alternative SM2A

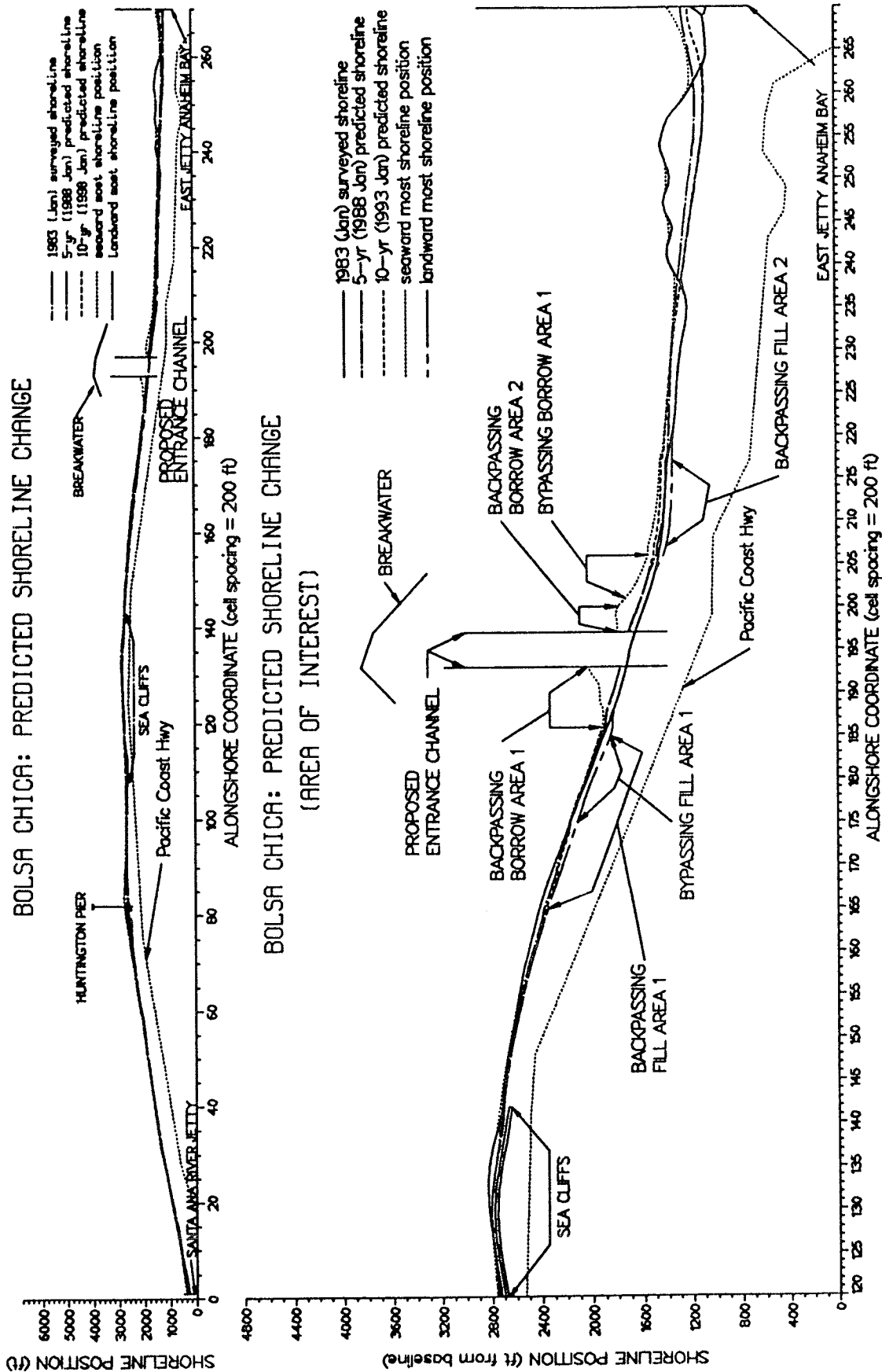


Figure 76. Alternative SM1B: sand management, without feeder beach

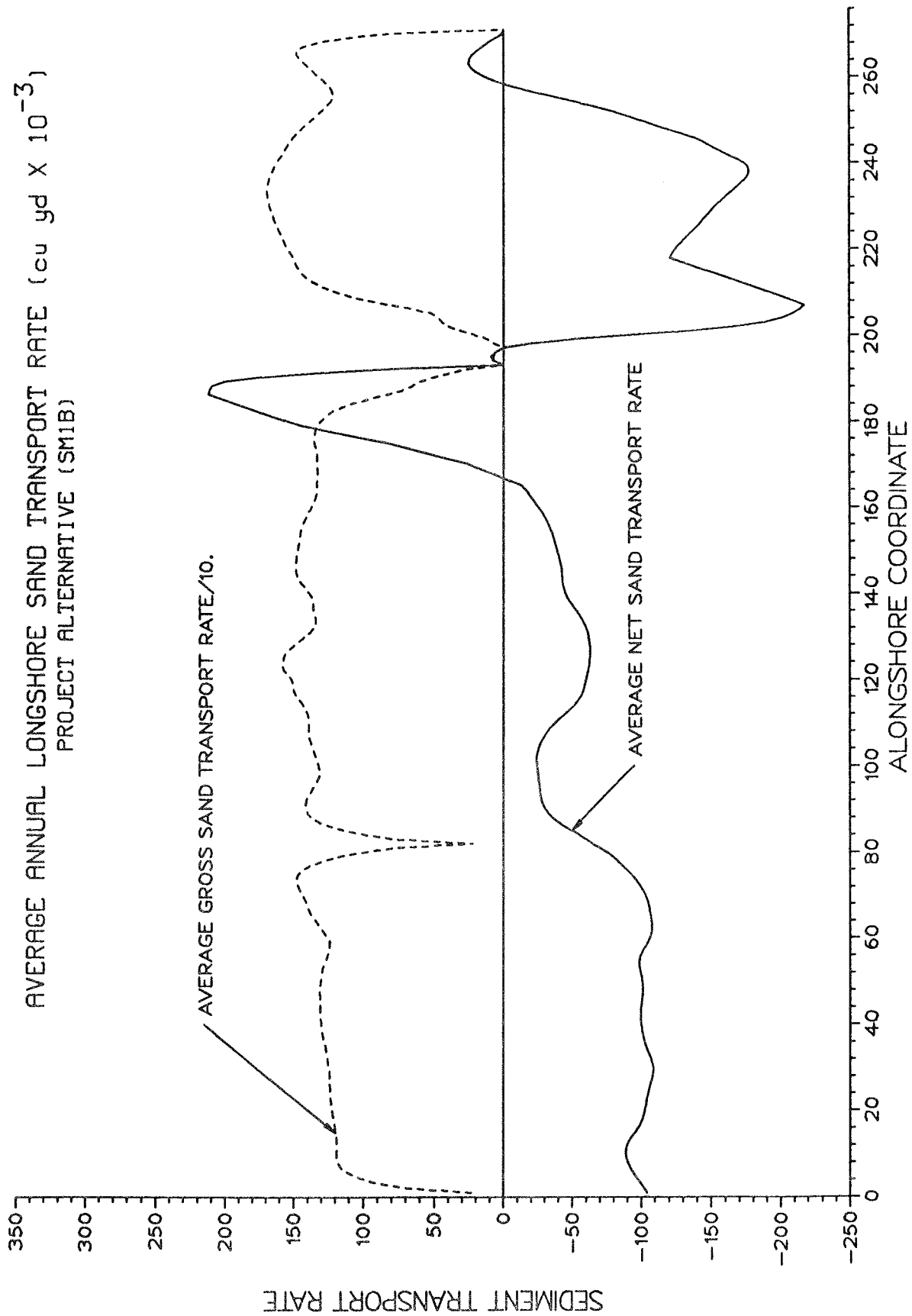


Figure 77. Alternative SM1B: average annual longshore sand transport rates

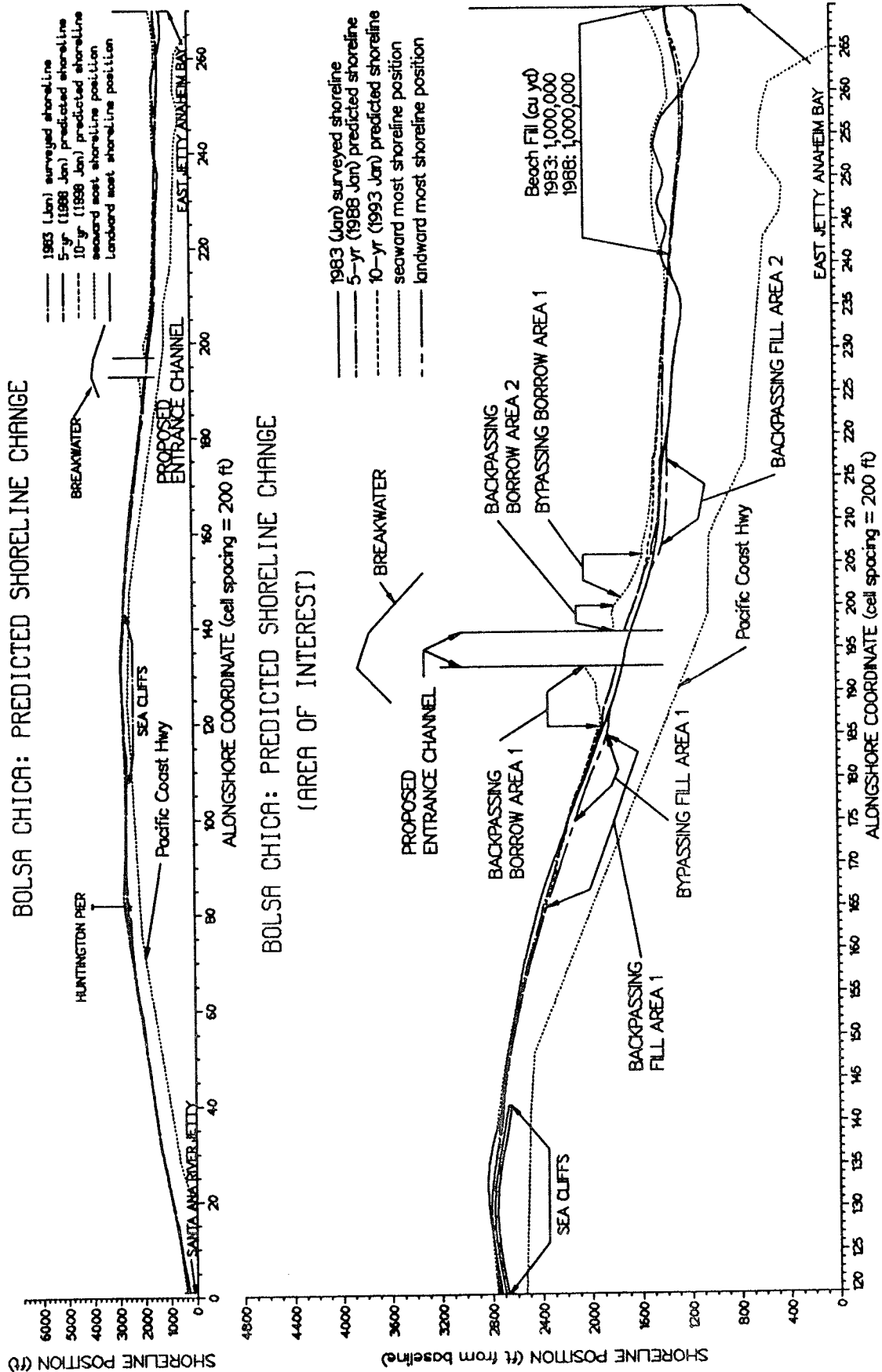


Figure 78. Alternative SM2B: sand management, with feeder beach

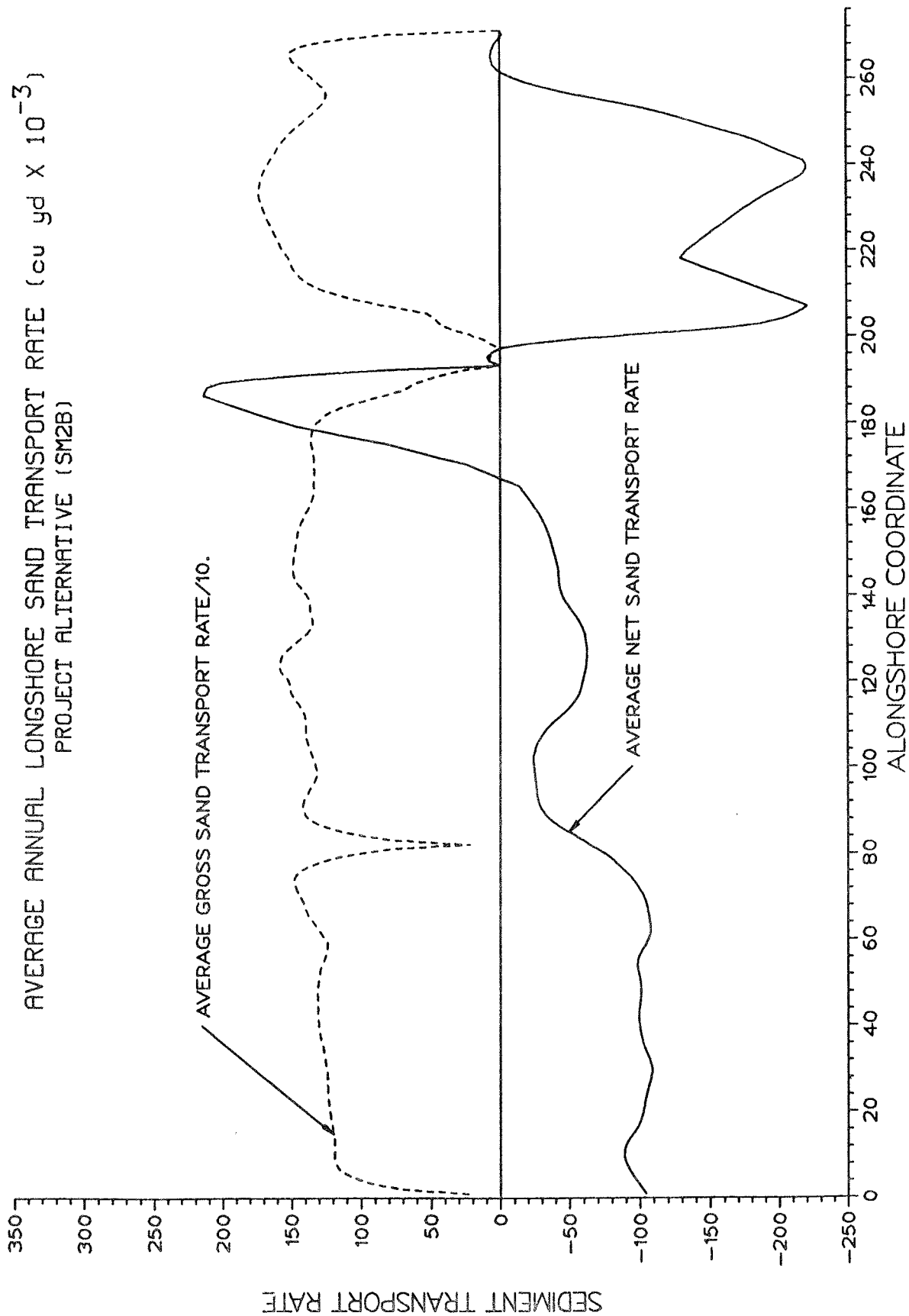
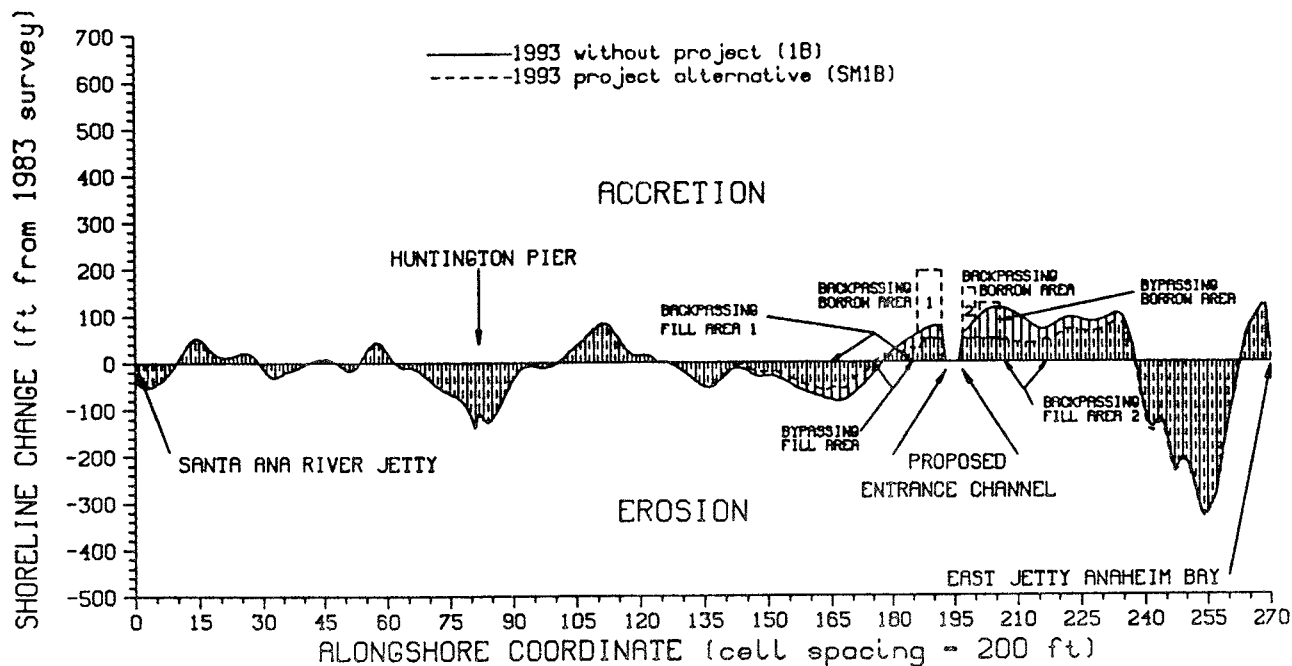


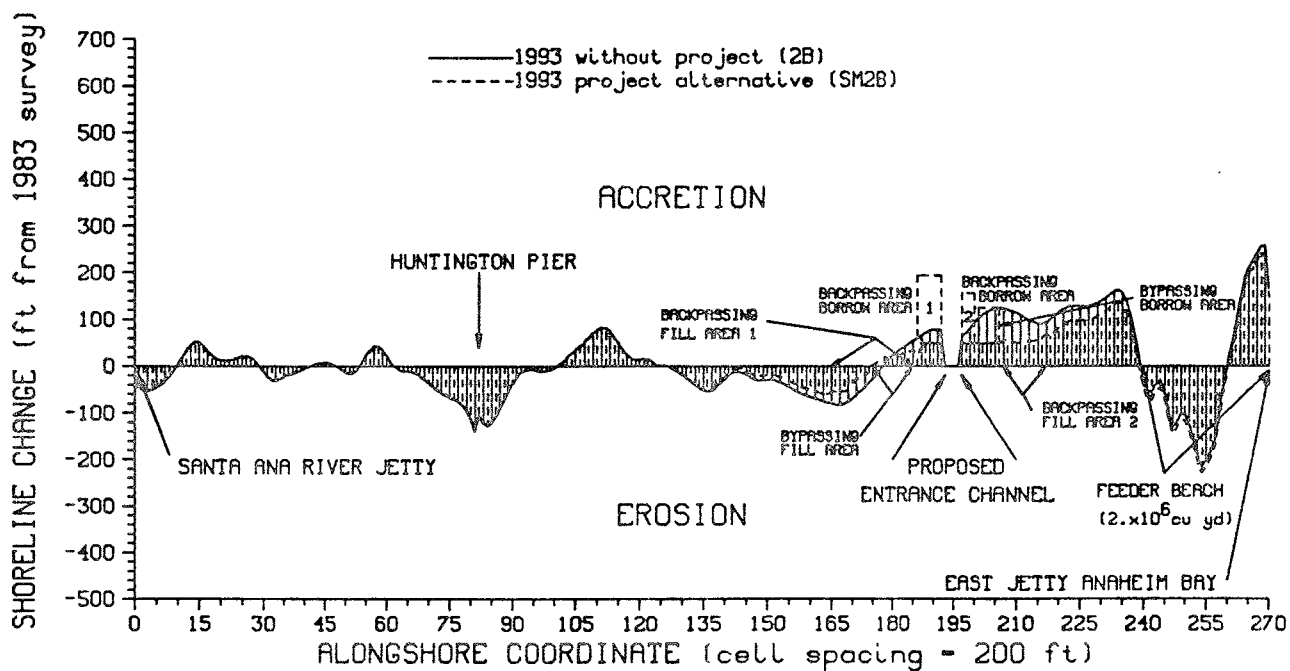
Figure 79. Alternative SM2B: average annual longshore sand transport rates

BOLSA CHICA: SHORELINE IMPACTS



(a)

BOLSA CHICA: SHORELINE IMPACTS



(b)

Figure 80. Predicted shoreline change from 1983 shoreline position
 (a) Alternative WP1B vs. Alternative SM1B
 (b) Alternative WP2B vs. Alternative SM2B

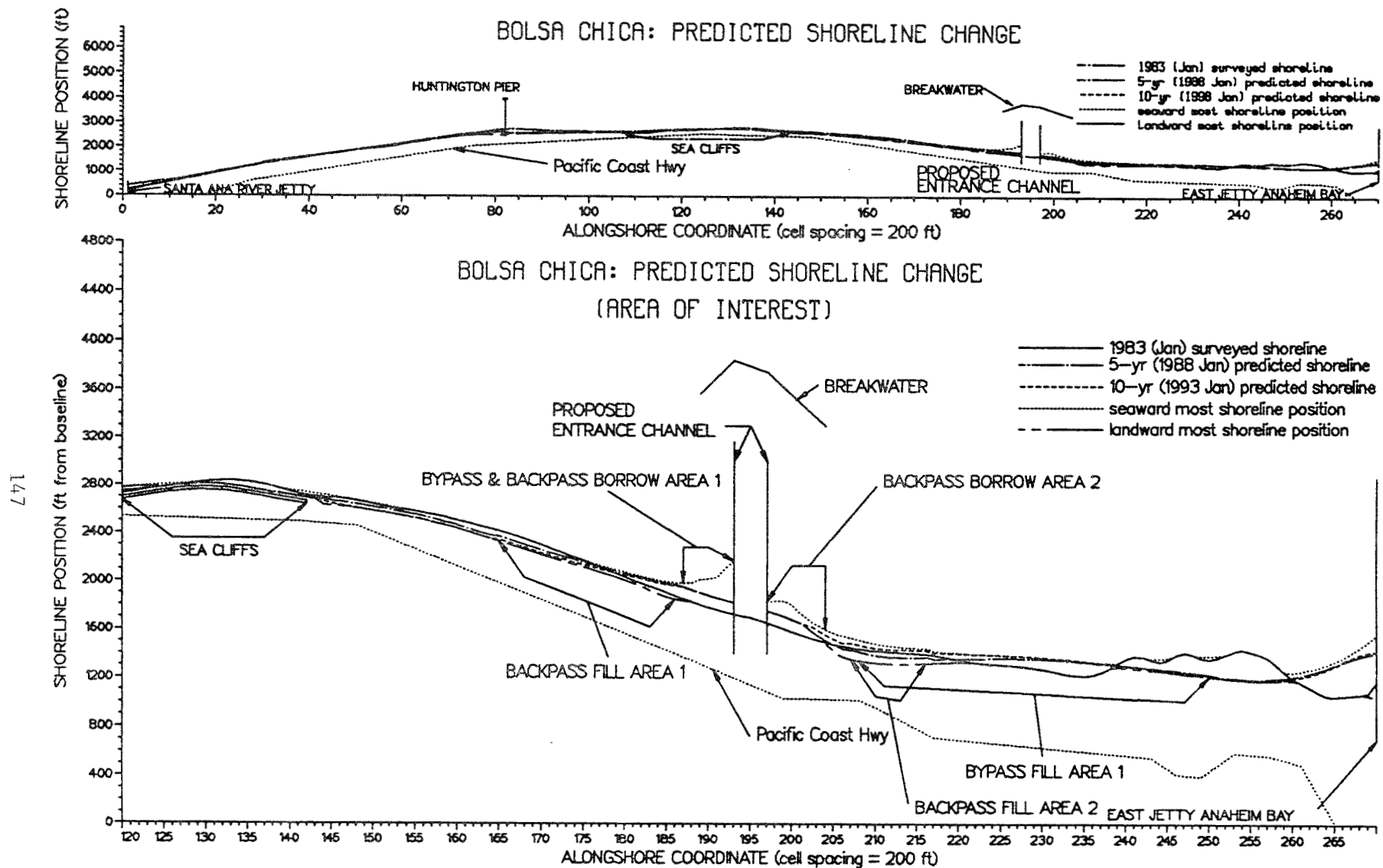


Figure 81. Alternative SM1C: sand management, without feeder beach

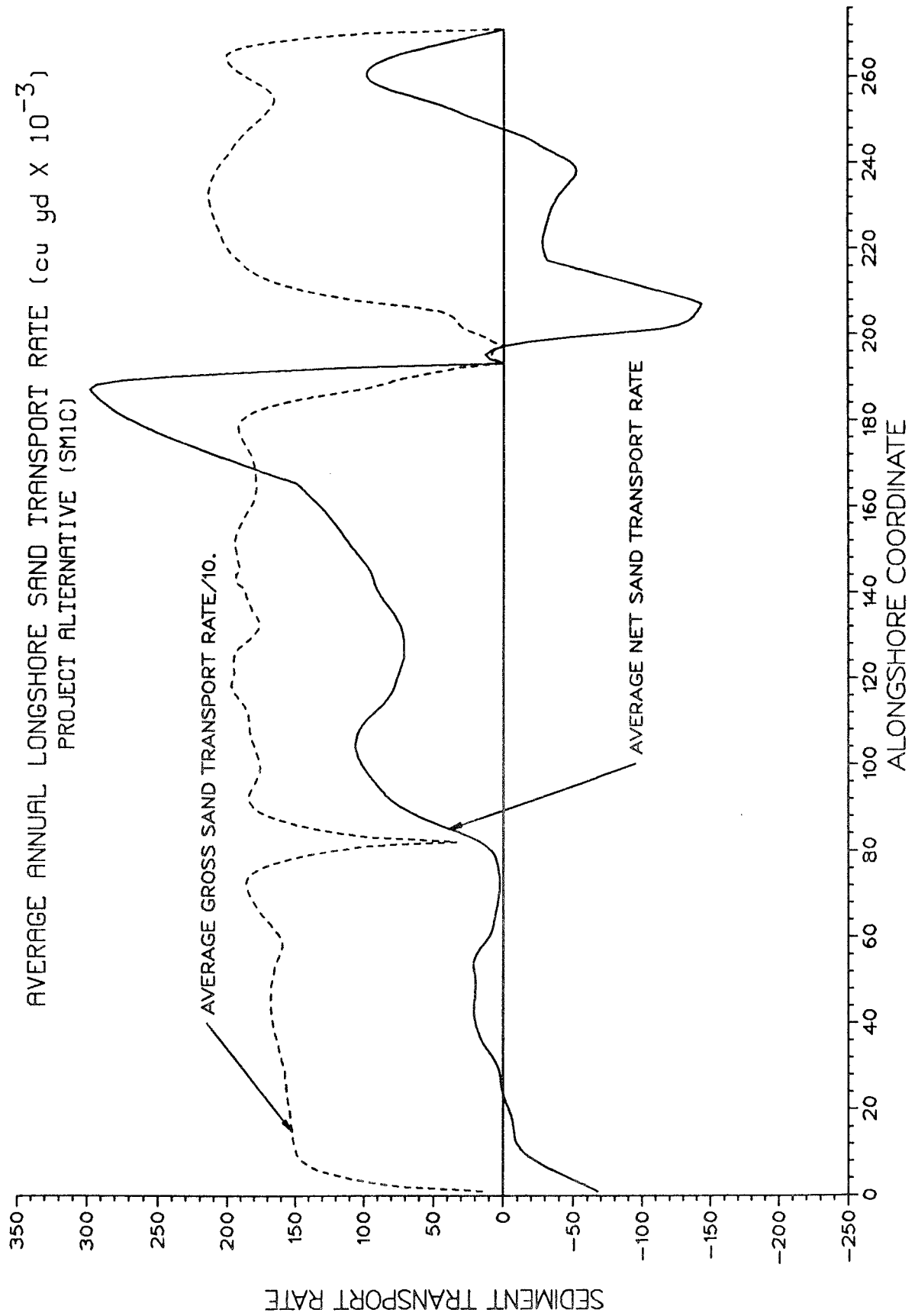


Figure 82. Alternative SM1C: average annual longshore sand transport rates

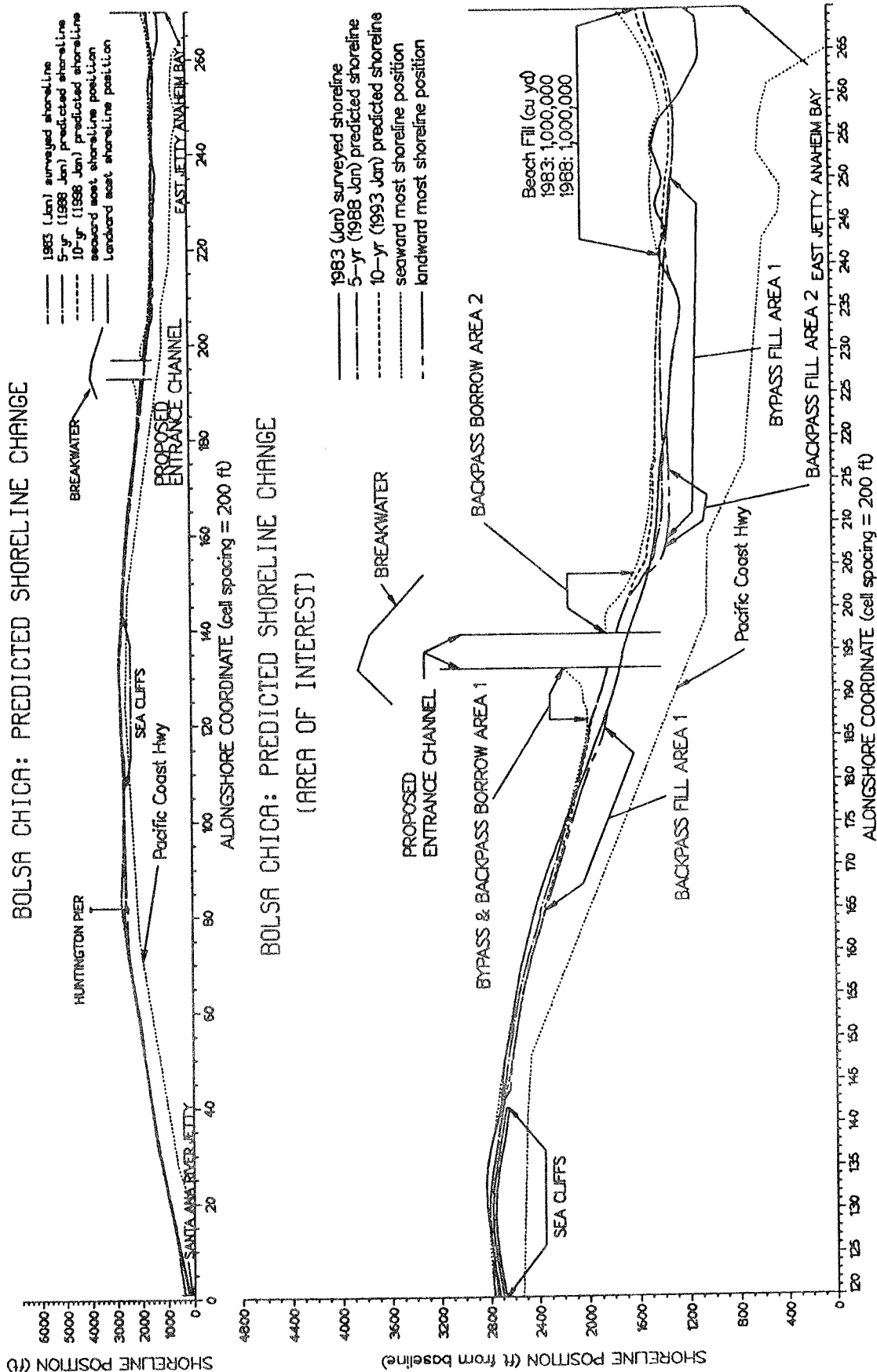


Figure 83. Alternative SM2C: sand management, with feeder beach

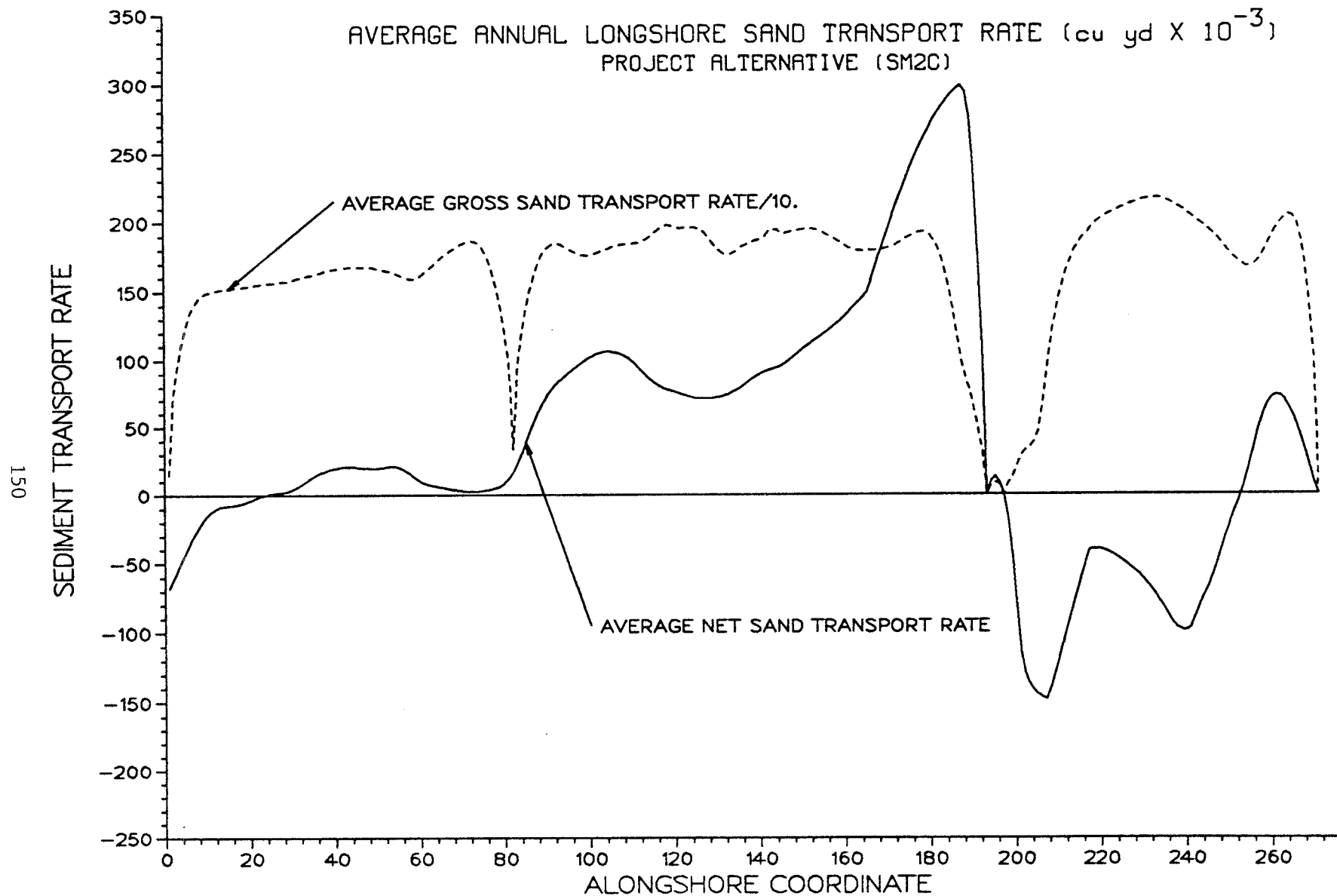
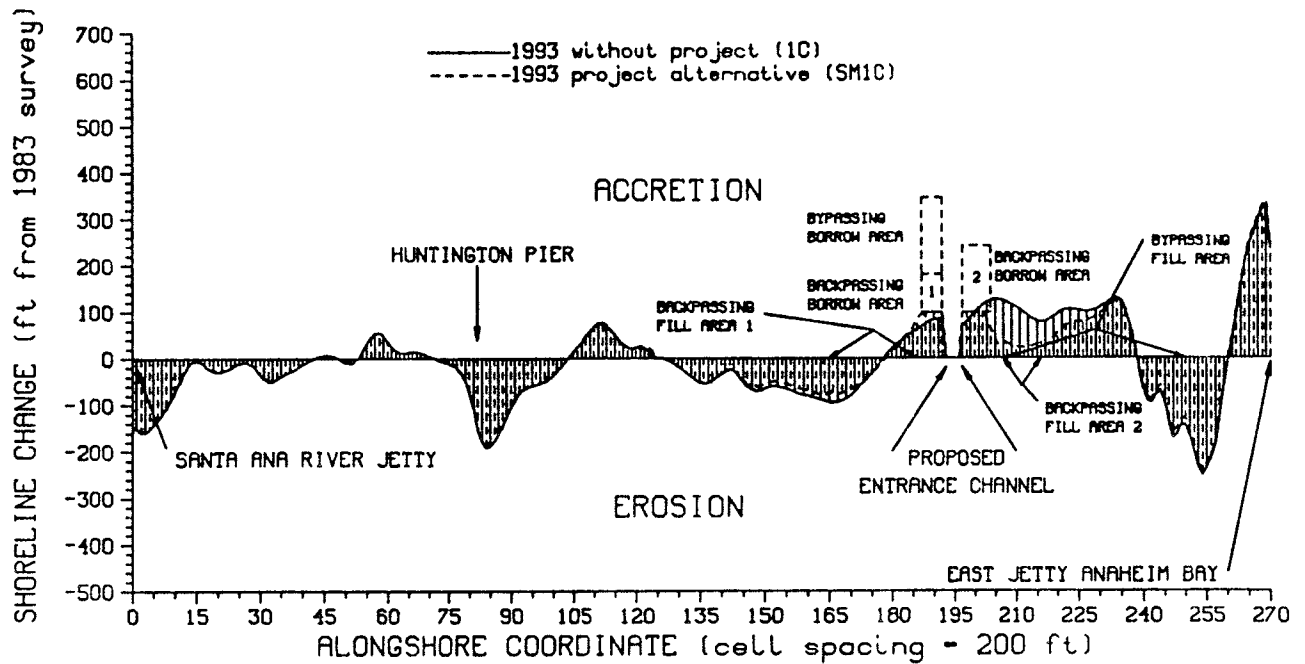


Figure 84. Alternative SM2C: average annual longshore sand transport rates

(based on shoreline change from the January 1983 surveyed shoreline position) to the C type without-project simulations in Figure 85. The calculated volumetric sand management requirements resulting from the implementation of sand management plan C are as follows:

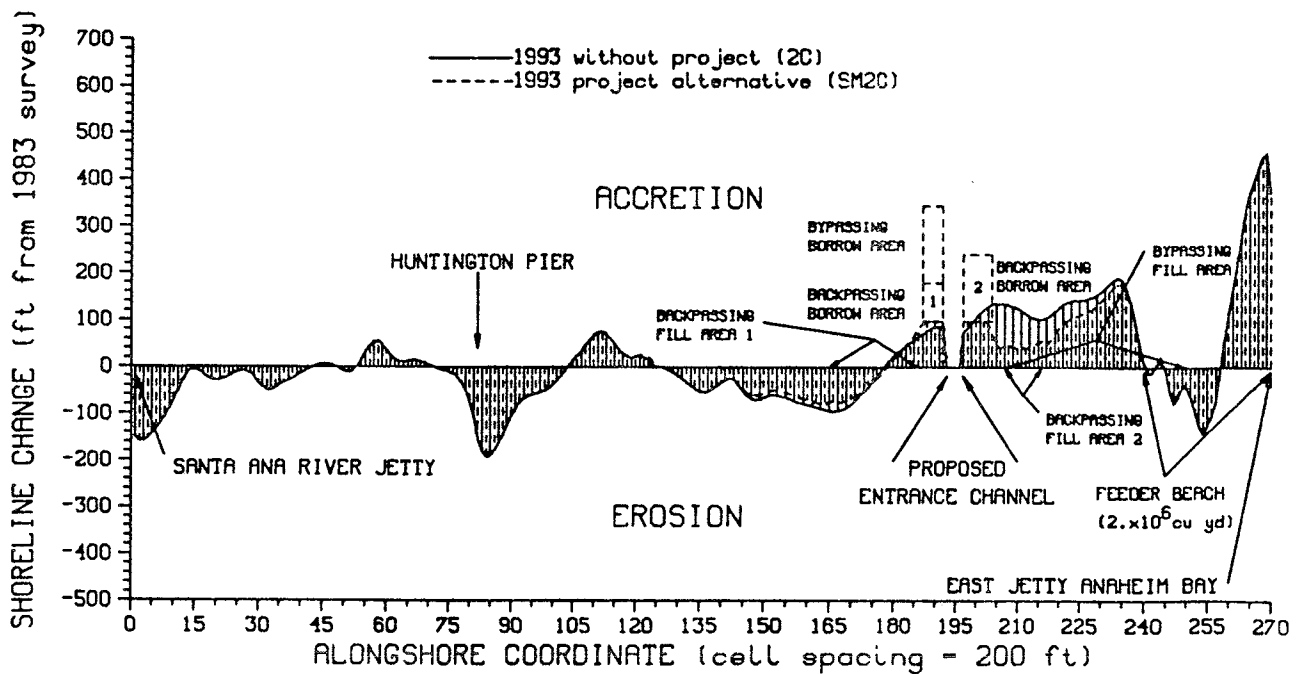
<u>a.</u> Southeast side:		<u>cu yd/year</u>
Average annual backpassing volume		134×10^3
Maximum backpassing volume (year 6)		149×10^3
Minimum backpassing volume (year 1)		93×10^3
<u>b.</u> Southeast side:		<u>cu yd/year</u>
Average annual bypassing volume		88×10^3
Maximum bypassing volume (year 4)		110×10^3
Minimum bypassing volume (year 1)		31×10^3
<u>c.</u> Northwest side:		<u>cu yd/year</u>
Average annual backpassing volume		105×10^3
Maximum backpassing volume (year 9)		213×10^3
Minimum backpassing volume (year 1)		0×10^3

BOLSA CHICA: SHORELINE IMPACTS



(a)

BOLSA CHICA: SHORELINE IMPACTS



(b)

Figure 85. Predicted shoreline change from 1983 shoreline position
 (a) Alternative WP1C vs. Alternative SM1C
 (b) Alternative WP2C vs. Alternative SM2C

PART VI: DISCUSSION OF RESULTS AND CONCLUSIONS

Summary of Model Results

125. The shoreline evolution model GENESIS was calibrated and verified for the project reach between Anaheim Bay and the Santa Ana River. The model was calibrated for the six-year period between July, 1964 and April, 1970. During the calibration phase of the study the model parameters were adjusted to achieve the appropriate shoreline change, then without modification of the calibration parameters the model was verified for the 13-year period between April 1970 and January 1983. General trends in shoreline evolution along the project reach were quantitatively reproduced through this procedure.

126. The calibration and verification results demonstrate the predictive ability of model. These results can also be used as an indicator of the expected accuracy of the model's predictions at various points along the project reach. As discussed in Part IV, the boundary condition imposed at the Huntington Pier does not appropriately simulate model the local physical processes occurring at the pier. However, it was demonstrated through Figure 28 that this boundary condition does not affect model results northwest of the sea cliffs. Along the proposed project site (between alongshore coordinates 140 and 220) the model performed well in both the calibration and verification. The 2-mile-long reach immediately adjacent to Anaheim Bay is affected by wave reflection from the east Anaheim Bay entrance jetty and nourishment projects in both the calibration and verification periods. Model results in this localized area must be viewed with caution because wave reflection from the jetty was not simulated.

127. The model was utilized to calculate expected shoreline change for several project design alternatives including a without-project alternative (Part V). The final simulations (Figures 71 through 85) indicate that potentially adverse shoreline impacts could be mitigated with a flexible sand management program and infrastructure capable of:

- a. Annually backpassing on the order of 300,000 cu yd of sand adjacent to the southeast jetty to a fill area between 1/2- and 1- mile southeast of the entrance.

- b. Annually backpassing on the order of 300,000 cu yd of sand adjacent to the northwest jetty to a fill area between 1/2- and 1- mile northwest of the entrance.
- c. Annually bypassing on the order of 150,000 cu yd of sand adjacent to both the northwest and southeast sides of the entrance and depositing it in the fill areas between 1/2- and 1- mile away from the entrance system.

Conclusions

128. This study of longshore sand transport processes and shoreline response resulting from the construction of the proposed ocean entrance system at Bolsa Chica has shown that mitigation of adverse impacts on the adjacent shorelines is feasible. The results presented herein supersede those in the previous study (Gravens 1988) "Preliminary Shoreline Response Computer Simulation, Report 1: Bolsa Bay, California, Proposed Ocean Entrance System Study". Appendix A provides a discussion of the relationship between the Preliminary and Comprehensive shoreline response studies.

129. Based on the results of the model simulations presented above the following conclusions are made:

- a. The proposed site of the new entrance system is located in a region of converging longshore sand transport, i.e., sand is transported toward the location of the proposed entrance system from both upcoast and downcoast.
- b. Locating the entrance system approximately 1-mile upcoast or downcoast from the proposed site does not significantly change the estimated shoreline response. The calculated magnitude of the accretion and erosion are not exceedingly different and are limited to within 2 miles either side of the entrance.
- c. Implementation of a sand management plan and infrastructure capable of the minimum requirements listed above will allow for the mitigation of potentially adverse shoreline impacts.
- d. The Surfside-Sunset feeder beach nourishment program must be continued in order to maintain the shoreline within 2-miles of the Anaheim Bay entrance. However, the proposed entrance system at Bolsa Chica is not anticipated to aggravate or lessen the requirement for periodic beach nourishment there.

130. If the proposed navigable ocean entrance system at Bolsa Chica Bay is constructed, a monitoring program should be established in order to create a data base of process information which may be used to refine and modify the sand management program as well as to evaluate the performance of the entrance system.

REFERENCES

- Bakker, W. T. 1968. "The Dynamics of a Coast with a Groyne System," Proceedings 11th Coastal Engineering Conference, American Society of Civil Engineers, pp 492-517.
- Caldwell, J. M. 1956. "Wave Action and Sand Movement Near Anaheim Bay, California," Technical Memorandum No. 68, Beach Erosion Board, US Army Corps of Engineers, Washington, DC.
- California Division of Oil and Gas. 1973. "Summary of Operations," Oil, Gas, and Geothermal Statistics, Vol 59, No. 2, Sacramento, CA.
- Chu, Y., Gravens, M. B., Smith, J. M., Gorman, L. T., and Chen, H. S. 1987. "Beach Erosion Control Study, Homer Spit, Alaska," Miscellaneous Paper CERC-87-15, US Army Engineer Waterways Experiment Station, Coastal Engineering Research Center, Vicksburg, MS.
- Dean, R. G. 1986. "The Ultimate High Tide," Civil Engineering, Vol 56, No. 9, pp 64-66.
- Ebersole, B., Cialone, M., and Prater, M. 1986. "Regional Coastal Processes Numerical Modeling System; Report 1, RCPWAVE - A Linear Wave Propagation Model for Field Use," Technical Report CERC-86-4, US Army Engineer Waterways Experiment Station, Coastal Engineering Research Center, Vicksburg, MS.
- Gravens, M. B. 1988. "Preliminary Shoreline Response Computer Simulation, Report 1: Bolsa Bay, California, Proposed Ocean Entrance System Study," unpublished draft report, US Army Engineer Waterways Experiment Station, Coastal Engineering Research Center, Vicksburg, MS.
- Gravens, M. B., Scheffner, N. W., and Hubertz, J. M. 1989. "Coastal Processes from Asbury Park to Manasquan, New Jersey," Miscellaneous Paper CERC-89-11, US Army Engineer Waterways Experiment Station, Coastal Engineering Research Center, Vicksburg, MS.
- Hales, L. Z. 1984. "Potential Effects of New Entrance Channel to Bolsa Chica Bay, California, on Unstabilized Adjacent Shorelines," Miscellaneous Paper CERC-84-10, US Army Engineer Waterways Experiment Station, Coastal Engineering Research Center, Vicksburg, MS.
- Hanson, H. 1987. "GENESIS, A Generalized Shoreline Change Numerical Model for Engineering Use," Report No 1007, Dept. of Water Resources Engineering, Lund Institute of Science and Technology, University of Lund, Lund, Sweden.
- Hanson, H., and Kraus, N. C. 1989. "GENESIS: Generalized Model for Simulating Shoreline Change," Technical Report CERC-89-19, US Army Engineer Waterways Experiment Station, Coastal Engineering Research Center, Vicksburg, MS.

Hanson, H., Gravens, M. B., and Kraus, N. C. 1988. "Prototype Applications of a Generalized Shoreline Change Numerical Model," Proceedings 21st Coastal Engineering Conference, American Society of Civil Engineers, pp 1265-1279.

Hanson, H., Kraus, N. C., and Nakashima, L. D. 1989. "Shoreline Change Behind Transmissive Detached Breakwaters," Proceedings Coastal Zone '89, American Society of Civil Engineers, pp 568-582.

Hoffman, J. S. 1983. "Projecting Sea Level Rise to Year 2100," Proceedings Coastal Zone '83, American Society of Civil Engineers, pp 2784-2795.

Hoffman, J. S., Keyes, D., and Evans, J. R. 1983. "Projecting Future Sea Level Rise, Methodology, Estimates to Year 2100, and Research Needs," US Environmental Protection Agency, Report No. EPA-230-09-007, Washington, DC.

Kraus, N. C. 1983. "Applications of a Shoreline Prediction Model," Proceedings of Coastal Structures '83, American Society of Civil Engineers, pp 632-645.

Kraus, N. C. 1989. "Beach Change Modeling and the Coastal Planning Process," Proceedings Coastal Zone '89, American Society of Civil Engineers, pp 553-567.

Kraus, N. C., and Harikai, S. 1983. "Numerical Model of the Shoreline Change at Oarai Beach," Coastal Engineering, Vol 7, No. 1, pp 1-28.

Kraus, N. C., Scheffner, N. W., and Hanson, H., Chou, L. W., Cialone, M. A., Smith, J. M., and Hardy, T. A. 1988. 2 Vols, "Coastal Processes at Sea Bright to Ocean Township, New Jersey," Miscellaneous Paper CERC-88-12, US Army Engineer Waterways Experiment Station, Coastal Engineering Research Center, Vicksburg, MS.

Larson, M., Hanson, H., and Kraus, N. C. 1987. "Analytical Solutions on the One-Line Model of Shoreline Change," Technical Report CERC-87-15, US Army Waterways Experiment Station, Coastal Engineering Research Center, Vicksburg, MS.

Marine Advisors. 1961. "A Statistical Survey of Ocean Wave Characteristics in Southern California Waters," La Jolla, CA.

Marine Board. 1987. "Responding to Changes in Sea Level: Engineering Implications," National Research Council, Washington, DC.

Moffatt & Nichol, Engineers. 1987. "Hydraulic Design Approach for Muted-Tide Wetlands," Moffatt & Nichol, Engineers, Long Beach, CA, Prepared for Signal Landmark, Irvine, CA.

National Marine Consultants. 1960. "Wave Statistics for Seven Deep Water Stations Along the California Coast," Santa Barbara, CA.

Orange County Environmental Management Agency. 1985. "Bolsa Chica Land Use Plan," Local Coastal Program, North Coast Planning Unit, Orange County Board of Supervisors, County of Orange, Huntington Beach, CA.

Ozasa, H., and Brampton, A. H. 1980. "Mathematical Modeling of Beaches Backed by Seawalls," Coastal Engineering, Vol 4, No. 1, pp 47-64.

Pelnard-Considere, R. 1956. "Essai de Th'eorie de l'Evolution des Forms de Rivages en Plage de Sable et de Galets," 4th Journees de l'Hydraulique, les Energies de la Mer, Question III, Rapport No. 1, pp 289-298.

Perlin, M., and Dean, R. G. 1983. "A Numerical Model to Simulate Sediment Transport in the Vicinity of Coastal Structures," Miscellaneous Report 83-10, US Army Engineer Waterways Experiment Station, Coastal Engineering Research Center, Vicksburg, MS.

Revelle, R. R. 1983. "Probable Future Changes in Sea Level Resulting from Increased Atmospheric Carbon Dioxide," Changing Climate: Report of the Carbon Dioxide Assessment Committee, National Research Council, Washington, DC, pp 433-448.

Scheffner, N. W., and Rosati, J. D. 1987. "A User's Guide to the N-line Model: A Numerical Model to Simulate Sediment Transport in the Vicinity of Coastal Structures," Instruction Report CERC-87-4, US Army Engineer Waterways Experiment Station, Coastal Engineering Research Center, Vicksburg, MS.

Seidel, S., and Keyes, D. 1983. "Can We Delay a Greenhouse Warming?, The Effectiveness and Feasibility of Options to Slow a Build-up of Carbon Dioxide in the Atmosphere," US Environmental Protection Agency, Washington, DC.

Sherlock, A. R. and Szuwalski, A. 1987. "A User's Guide to the Littoral Environment Observation Retrieval System," Instruction Report CERC-87-3, US Army Engineer Waterways Experiment Station, Coastal Engineering Research Center, Vicksburg, MS.

Shore Protection Manual. 1984. 4th ed., 2 vols, US Army Engineer Waterways Experiment Station, Coastal Engineering Research Center, US Government Printing Office, Washington, DC.

Signal Landmark, Inc. 1988. "Historical shoreline Changes Anaheim Bay to Huntington Beach," unpublished report, prepared by Moffatt & Nichol, Engineers for Signal Landmark, Inc., Irvine, CA.

State of California. 1974. "Bolsa Chica Marsh Re-Establishment Project: Environmental Impact Report," Vol 2, Department of Fish and Game, CA.

US Army Engineer District, Los Angeles. 1978. "Monitoring Program for Stage 7 Construction, Surfside-Sunset Beach, California," US Army Engineer District, Los Angeles, Los Angeles, CA.

US Army Engineer District, Los Angeles. 1987. "Draft Plan of Study for the Bolsa Chica/Sunset Bay Area, Orange County, California, Feasibility Study," US Army Engineer District, Los Angeles, Los Angeles, CA.

US Army Engineer Waterways Experiment Station. 1981. "Preliminary Numerical Tidal Circulation Results for the Bolsa Chica Study," unpublished Memorandum for Record, US Army Engineer Waterways Experiment Station, Coastal Engineering Research Center, Vicksburg, MS.

US Congress. 1954. "Anaheim Bay Harbor, California," House Document 349, 83rd Congress, 2nd Session, Washington, DC.

Walton, T. L., and Dean, R. G. 1973. "Application of Littoral Drift Roses to Coastal Engineering Problems," Proceedings First Australian Conference on Coastal Engineering, National Committee on Coastal and Ocean Engineering of Institution of Engineers, Australia.

Williams, P. B. 1984. "An Evaluation of the Feasibility of a Self-Maintained Ocean Entrance at Bolsa Chica," Philip Williams & Associates, San Francisco, CA.

Woodward-Clyde Consultants. 1984. "Preliminary Evaluation of Ground Subsidence, Bolsa Chica Local Coastal Program, Bolsa Chica Planning Unit, Orange County, California," Santa Ana, CA, prepared for Signal Landmark, Inc., Irvine, CA.

Woodward-Clyde Consultants. 1986. "Subsidence in the Bolsa Chica Project Area," Santa Ana, CA, prepared for Signal Landmark, Inc., Irvine, CA.

APPENDIX A: PRELIMINARY STUDY

Introduction

131. Prior to making the Comprehensive Shoreline Response Computer Simulation (the subject of this report), a preliminary study called the Preliminary Shoreline Response Computer Simulation was performed (Gravens 1988). This appendix discusses the relation between the Preliminary and Comprehensive shoreline response studies.

132. The Preliminary modeling study was conducted to provide information for a special Coastal Commission "Confirmation Review" hearing on the Bolsa Chica LUP. Therefore, the Preliminary Study had to be performed in advance of detailed wave hindcasts that were to be utilized in the Comprehensive Study. The Preliminary Study was termed preliminary because its purpose was to estimate the range of potential impacts of a new entrance on adjacent beaches using the best wave data available at the time (2 July 1987 through 30 April 1988).

Differences in Wave Data

133. The major difference between the Preliminary and Comprehensive shoreline response studies is the wave data set used to drive the shoreline change model GENESIS. In the Preliminary Study, a comparison and analysis of several existing wave data sets was performed to determine the most appropriate available wave data set for use with the shoreline change model. At the time of the analysis it was determined that the SIO gage data were best suited for use.

134. During conduct of the Comprehensive Study significant differences in the longshore sand transport rate became apparent as compared to the Preliminary Study. These differences were significant enough to prompt a re-evaluation of the Preliminary Study model setup and model inputs. Inspection of the Preliminary Study data inputs revealed an error in the procedure used to prepare the input wave conditions. Specifically, the height component of the nearshore waves (RCPWAVE results) read from an intermediate data base were not correctly related to the offshore wave height for the particular time

step. This error resulted in wave heights approximately one third of the correct value. As a result of applying the smaller wave heights, offshore wave angles had to be rotated 20 deg clockwise (such that waves propagate from a more northerly direction) in order to calibrate the model. This procedure is described in detail in Gravens (1988).

135. The error in the treatment of the wave data was corrected and the Preliminary Study model calibration simulation was rerun without rotating the offshore wave angles. The calculated net longshore sand transport rates for this simulation are shown in Figure A1. The important point of this simulation is the shape of the longshore sand transport rate distribution shown in Figure A1. From this figure it is seen that the shape for the "revised" Preliminary Study is very similar to the one calculated in the Comprehensive study (see Figure 27 of the main text).

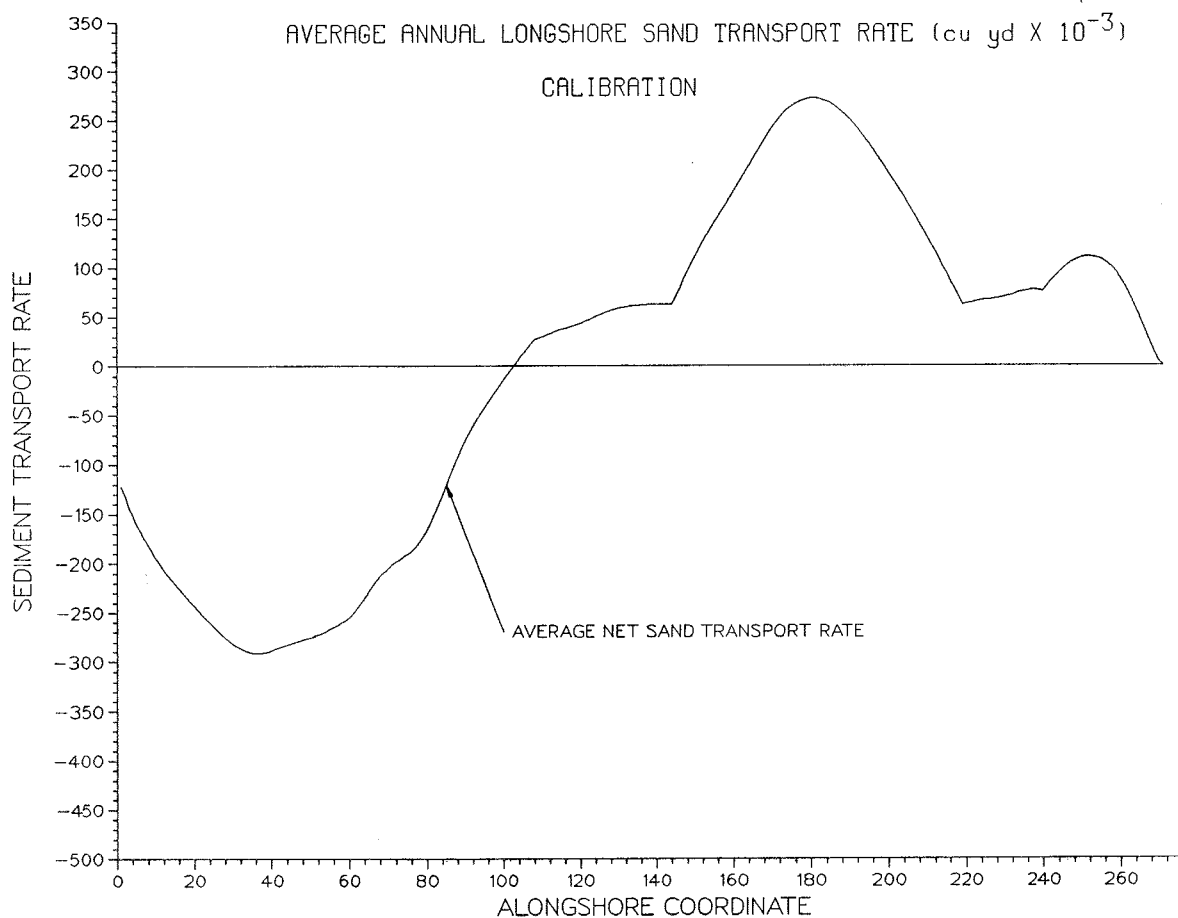


Figure A1. Average annual longshore sand transport rate (Preliminary model with corrected input wave conditions)

Conclusions

136. The input wave conditions used in the Preliminary Study were incorrect due to an error made in pre-processing of the nearshore wave conditions. Rotation of the input offshore wave conditions by 20 deg for the Preliminary Study would not have been necessary if this error had not been made. After correction of the nearshore wave conditions, net longshore transport rates calculated using the SIO gage data have the same qualitative form as calculated using the transform WIS hindcast wave estimates.

APPENDIX B: SOUTHERN CALIFORNIA HINDCAST*

A MULTI-FACETED WIND-WAVE HINDCAST METHOD TO DESCRIBE A SOUTHERN CALIFORNIA WAVE CLIMATE

R.E. Jensen, C.L. Vincent, and R.H. Reinhard

Introduction

1. A 20-year wind-wave hindcast was performed for the Southern California Bight of the Pacific Coast from Point Conception, California to the U.S.-Mexican border. This study must resolve a highly complex system of forcing functions and local effects that control the wave climate. Such mechanisms include: large scale forcing by northern Pacific swell; synoptic East Pacific wind fields southern hemisphere swell; and localized effects such as island sheltering and diffraction, as well as meso-scale meteorological systems such as land-sea breezes.

2. The purpose of this paper is to describe the methodology developed to hindcast wind-waves in Southern California. The hindcast is broken into three parts, wind field generation (synoptic scale and meso-scale), Northern Pacific wave generation, and localized Southern California Bight wave generation.

Wind Field Generation

3. One of the most important factors governing the estimation of a wave climate is the critical assessment of the winds in the study area. Both the synoptic-scale, and meso-scale effects contribute to the generation of the wave field. This leads to a twofold solution method. Synoptic scale winds were generated from gridded surface pressure fields, Holl and Mendenhall (1971). Calculations of surface wind fields were made in a coordinate system that consisted of great circle paths that included much of the Northern

* This Appendix provides a discussion of the methods used in the generation of the southern California WIS Hindcast. This material was presented at the 2nd International Workshop on Wave Hindcasting and Forecasting, sponsored by the Federal Panel on Energy R&D, April 25-28, 1989, Vancouver, B.C. Canada.

Pacific Ocean Basin, (Figure B1). Geostrophic to gradient to near surface wind conditions were computed from techniques described in Resio, et al. (1982).

4. The coastal wind pattern along the Southern California Bight is affected by a land-sea breeze pattern. A variation in flow is caused by the heating of the land surface during the day, and cooling during the evening. Historical evidence has suggested that the land breeze (blowing from land to sea) is strongest in the winter months and the sea breeze is strongest in the summer. Eight land based meteorological stations along the Southern California Bight were used to evaluate the land-sea breeze effect, (Figure B2). The data sets spanned the period from 1956-1975, (hourly observations from 1956-1965, and 3-hour observations from 1965-1975). Although gaps in the records appeared with a certain amount of regularity, they were not detrimental to the analysis outlined later. The land-based meteorological data showed that the synoptic-scale winds were not the only factor governing local wind fields. Synoptic-scale wind variations normally occur over days, whereas the land based station data indicated significant variation over several hours. These variations were assumed to be a result of the land-sea breeze effect.

5. A procedure was sought to incorporate the land-based winds into the synoptic-scale winds to account for the land-sea breeze. The requirements were that the solution be time dependent and statistically representative of the physical phenomena.

6. The spatial and temporal variation (on a daily, monthly and yearly basis), the intensity, the lateral extent, the triggering mechanisms, and the overall contribution of the land-sea breeze effect to the synoptic-scale winds had to be considered.

7. A simple approach decoupling the winds into X and Y components (independent of all other physical properties), was used as a first attempt to describe the land-sea breeze pattern. The months of February, May, August and November were selected as the baseline for the analysis, two months in an intense land-sea breeze regime (February and August) and two months during a non-land-sea breeze time period. Time histories for each station were resolved into X and Y components. The components were scaled according to the maximum displacement (ranging from 10 to 40 m/s) occurring in any given 24-hour period (Figure B3).

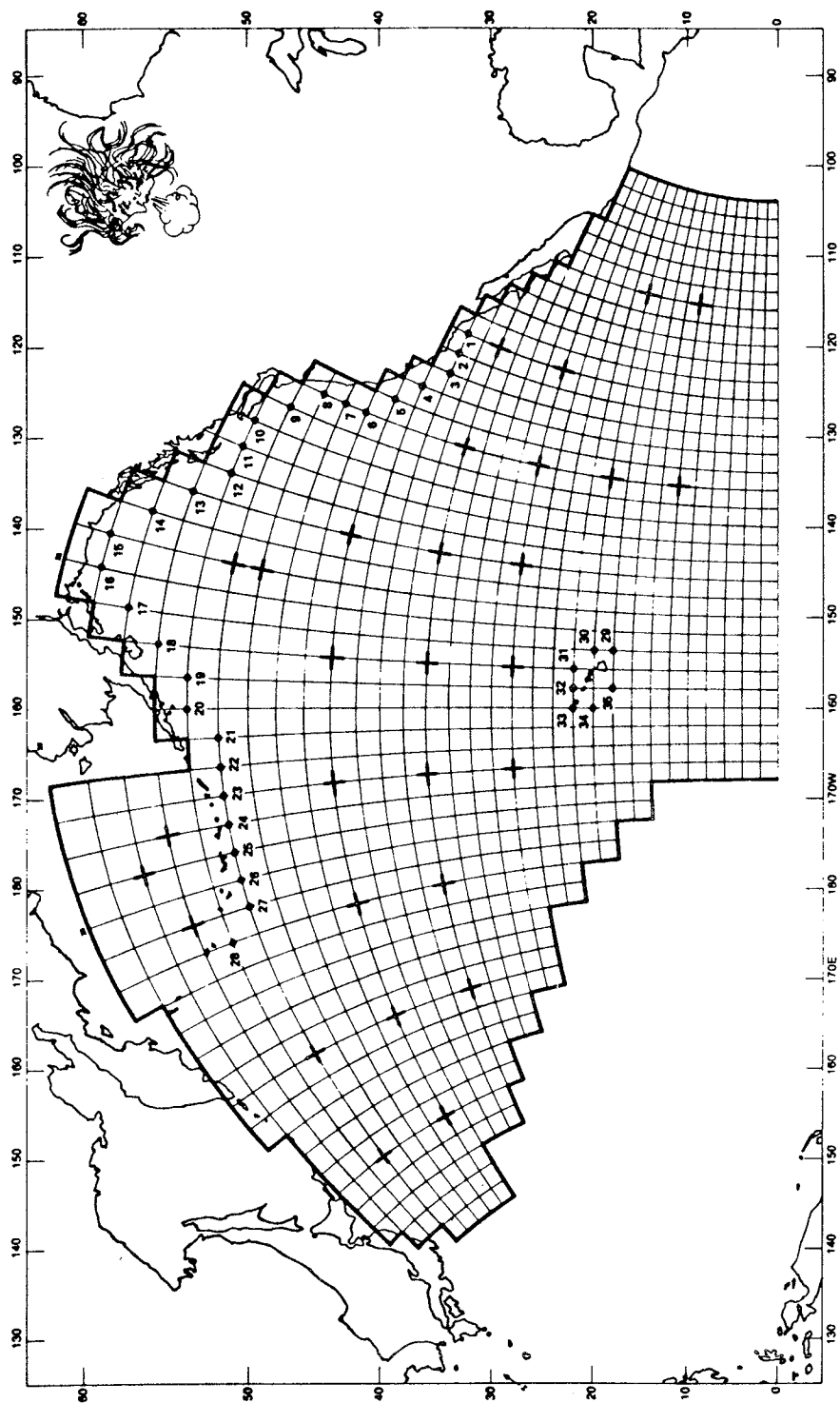


Figure B1. Wave Information Study (WIS) Phase I grid for the North Pacific
(2 deg, Mercator projection)

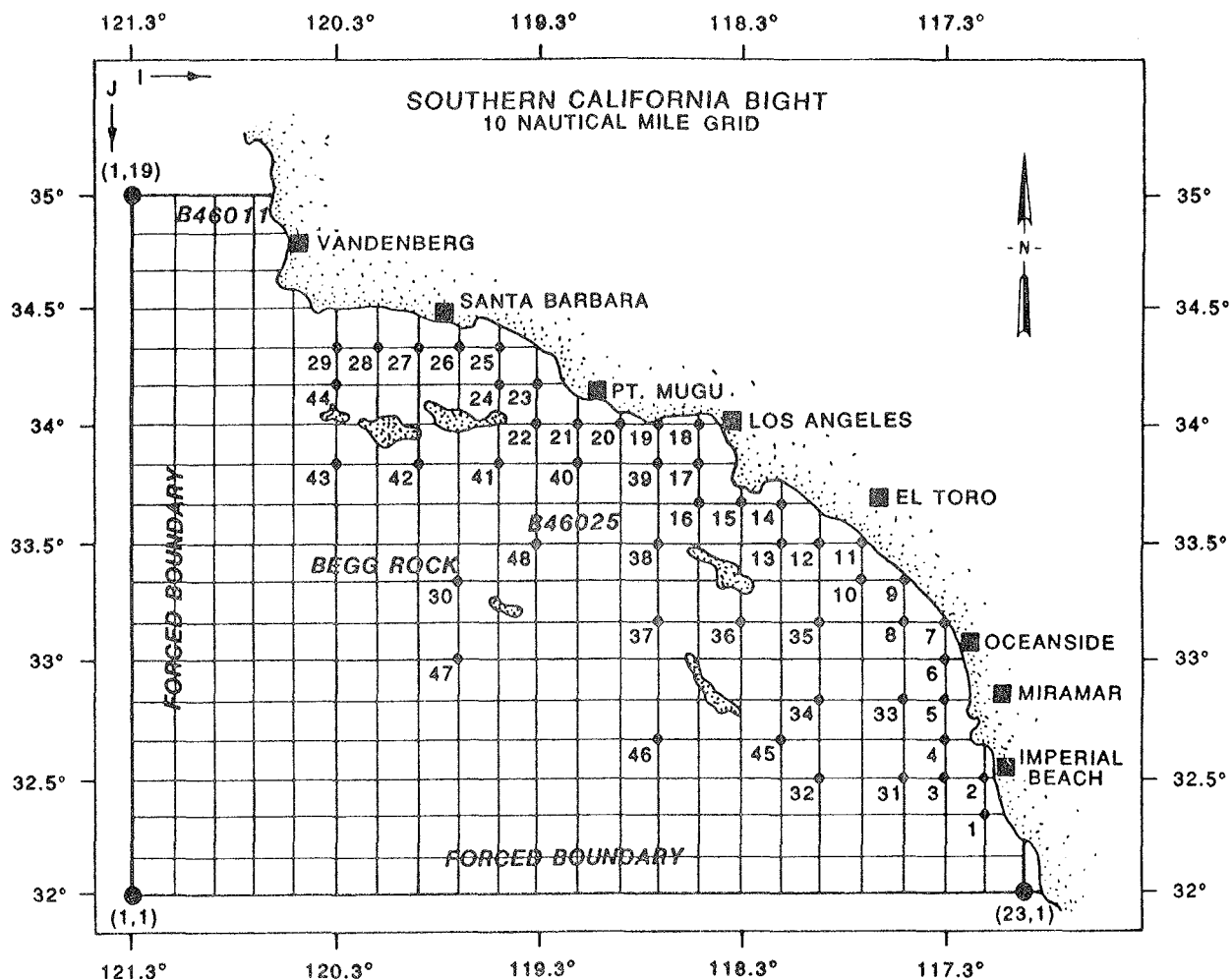


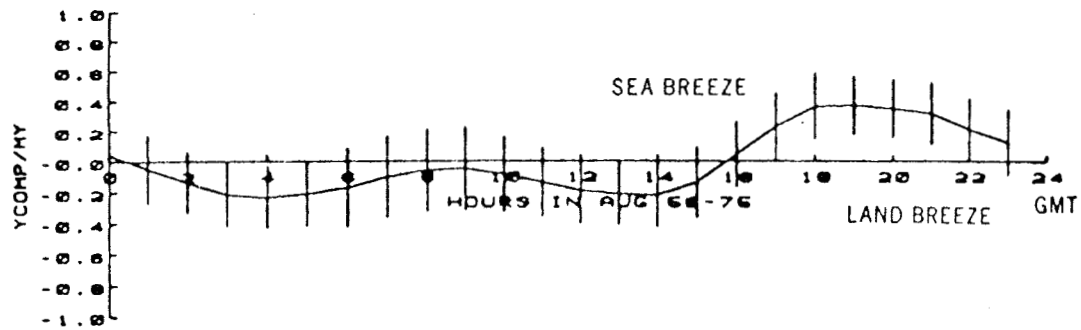
Figure B2. Southern California Bight study area, (10-nm grid)
Meteorological stations

$$X'(t) = [WS(t) \cdot \cos (WD(t) - X)]/M_x \quad (1)$$

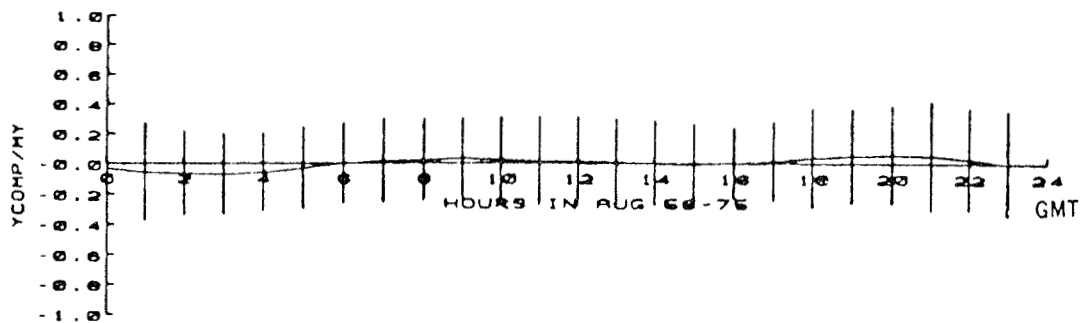
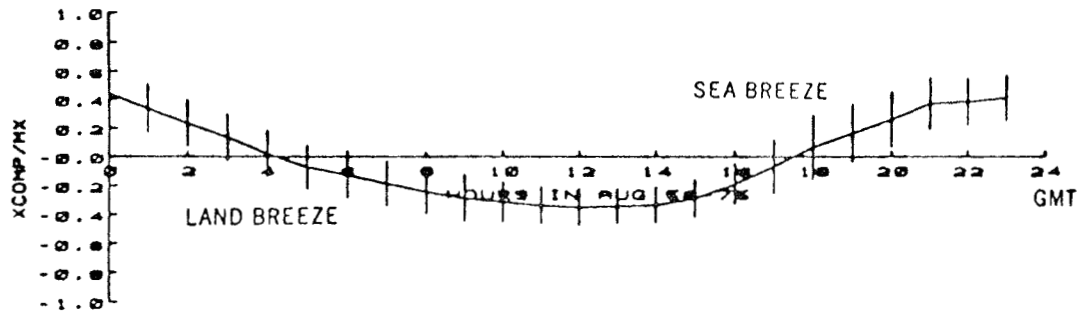
$$Y'(t) = [WS(t) \cdot \sin (WD(t) - Y)]/M_y \quad (2)$$

Where:

$WS(t)$ = hourly or 3-hour wind speed at the 10-m elevation
 $WD(t)$ = wind direction (mathematical coordinate system)
 X = mean X component signal for all 24-hour periods in a month
 Y = mean Y component signal for all 24-hour periods in a month
 M_x = maximum X displacement in the 24-hour period
 M_y = maximum Y displacement in the 24-hour period
 $X'(t)$ = response function for the X component of the wind
 $Y'(t)$ = response function for the Y component of the wind



- POINT MUGU AUG 68-75



- IMPERIAL BEACH AUG 68-75

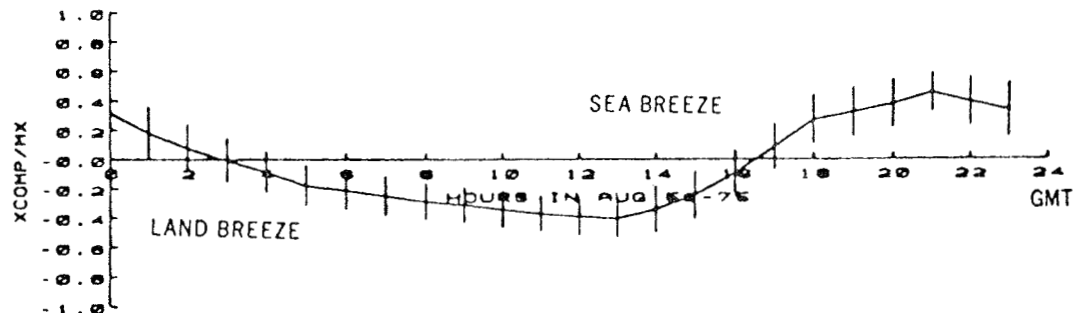


Figure B3. $X'(t)$ and $Y'(t)$ average response function for land station wind information mean conditions for all Januarys 1956-1975 (vertical lines represent one standard deviation)

8. Although the variance about the hourly mean signal was large in magnitude, magnified by the formulations used, the trends in the mean response function for all stations were well established. This was further verified through an analysis of the actual deviations from the mean response. The deviations closely approximated a normal distribution. It was concluded that the variations from the mean response could be accounted by simple random noise that was amplified by the nondimensional scaling. This procedure was followed for all 8 stations, and similar trends were displayed indicating that land-sea breeze effects are evident over the entire Southern California Bight. Changes in angles from one site to the next are primarily caused by changes in the shoreline orientation. For example, Imperial Beach displayed a periodic displacement in the East-West direction, winds from Los Angeles varied more Northeast-Southwest, and at Point Mugu, a well defined Southwesterly component was observed. The additional physical parameters governing the land-sea breeze effect such as, wind speed, wind direction, cloudiness, and air-sea temperature differences were assumed to be of lower order and thus neglected. The remaining 8 months were similarly analyzed and response functions (dimensionless hourly average $X'(t)$ and $Y'(t)$ components) defining the land-sea breeze at the 8 station locations were developed.

9. From the above analysis, the land-sea breeze effect was directly related to the shoreline orientation, so rather than work on the cartesian coordinate system (Figure B2) a new orthogonal coordinate system was created, based on a logarithmic fit to the shoreline. This made the alongshore interpolation between the 8 locations less cumbersome, and also simplified the calculations of the land-sea breeze extent in the offshore direction. It was assumed that the maximum offshore extent of the land-sea breeze was 20-nm. Weighting functions were generated for spatial interpolation and also for temporal interpolation relating phase differences between the stations. A mapping routine was generated to relate the Shoreline-Normal grid to the original (X,Y) grid (or I,J grid) shown in Figure B2.

10. The procedures thus far have dealt with the generation of a statistically sound model that reproduces the land-sea breeze along the entire Southern California Bight. We have established average response functions ($X'(t)$ and $Y'(t)$) for each station for each month. A 20-year time history (1956-1975) at the 8 locations were used to evaluate the daily X and Y

maximum displacements (M_x and M_y) and the values were tabulated. Also, a correlation coefficient was computed relating the daily response functions (in X and Y) to the mean functions. This correlation coefficient was used to determine if that particular day represented a land-sea breeze day.

11. The procedure to combine the synoptic-scale winds with the land-based meteorological data worked quite simply. It followed:

$$W(I,J) = \lambda \cdot W_{\text{syn}}(I,J) + (1 - \lambda) \cdot W_{\text{land}}(I,J) + \epsilon \cdot W_{\text{land}}(I,J) \quad (3)$$

where:

- $W(I,J)$ = blended wind condition at point (I,J),
- $W_{\text{syn}}(I,J)$ = synoptic scale wind at (I,J),
- $W_{\text{land}}(I,J)$ = land based wind condition at (I,J),
- λ = Weighting function relating the spatial variation between the land and synoptic scale wind for non-land-sea breeze days,
- ϵ = Weighting function for the land-sea breeze effect, related to the correlation coefficient for the day, and to the temporal variation in offshore extent..

12. Two important factors are evident in Equation (3), the land-sea breeze effect is an additive effect superimposed on the synoptic-scale wind conditions, and 2) this equation retains the characteristics of the land station information. The triggering of the land-sea breeze effect was based on the precomputed daily correlation coefficient at each station location. From the analysis, a correlation coefficient of 0.6 (or greater) was selected to identify a land-sea breeze day.

13. Synoptic scale wind fields derived from the WIS Phase I deepwater wind hindcast are input every 3 hours on a 2-deg spherical orthogonal grid. That information is spatially interpolated to a 10-nm grid (Figure B2), and linearly interpolated to a one hour time step. Measured wind conditions from the 8 land based stations are accessed as well as all pre-computed statistical quantities. For each day the correlation coefficient was checked to determine, if at that particular location a land-sea breeze day was in effect. If so, λ was set to 1.0, and the land-sea breeze was generated based on the synthesis of the daily observations and the mean response function. The temporal interpolation weights were systematically used, covering the 24-hour period. If the meteorological station data indicated that the land-sea breeze effect was not in effect, then the wind speeds were simply blended, ($\epsilon = 0.$) and based only on spatial parameters.

14. Unfortunately, few data exist to verify the methods employed in this study. Ship observation information was available, but was limited by the accuracy of the location. Hence, synthetic tests were used to validate the procedures. It was found in all cases that the procedure performed adequately. One source of error was uncovered during this process, the Vandenberg site consistently represented the land-sea breeze effect for a shoreline orientation in a North-South direction, rather than an East-West direction. That meant the site was located closer to the Northern Pacific Basin, and was not indicative of conditions present in the Southern California Bight. Because of this, the Vandenberg information was deleted from the procedure.

Forced Two-Dimensional Spectral Boundary Condition

15. The contribution of Northern Pacific storm systems to the wave climate in the Southern California Bight can be included by two methods. The first method is to hindcast the entire Pacific Ocean Basin using the same grid spacing employed in the study area (10-nm). This method becomes computationally and cost prohibitive realizing the geographic extent and the duration of the hindcast. The second method employs successively nesting smaller scale grids until the study area is quantified. This method optimizes computational time in-lieu of resolving details not required in each gridded area. The nested-grid method was adopted in this study.

16. The Pacific Coast Wave Information Study (PCWIS) generated a 20-year wind-wave hindcast derived from historical surface pressure and measured wind data for the North Pacific Ocean basin (Figure B1). A discrete spectral wave model was used to generate the wave condition, Resio (1981). Output information consisted of two-dimensional (frequency/direction) spectral estimates every three hours for the period 1956-1975, Corson, et al. (1986). Twenty frequencies (from 0.03 to 0.22 Hz), and 16 direction bands (at 22.5 deg intervals) were used to approximate the frequency/direction spectra. Energy derived from wind-seas under active growth were estimated via parametric relationships. Two-dimensional spectra from PCWIS Stations 1-4 (Figure B1) were used to drive the open boundary in the Southern California Bight hindcast study, (Figure B2). Additional spectral estimates from the Phase II PCWIS

study (based on a 0.5-deg grid) supplemented areas between the original 2-deg information, Corson, et al. (1987).

Southern California Bight Hindcast

17. An arbitrary water depth, pseudo-discrete, spectral wave model, SHALWV Hughes and Jensen (1986) was employed in the 20-year hindcast study, using the aforementioned wind fields and spectral boundary conditions as input. The theoretical framework relies on four fundamental assumptions. One, the total momentum flux from the atmosphere to the water surface is approximately constant and independent of the water depth. Two, the partitioning of this momentum into the current field and wave field is approximately constant and independent of the water depth. Three, the spectral shape of the waves being generated is approximately constant in wave number space and is independent of the water depth. And four, wave-wave interactions are the primary mechanism by which wave energy transformed to the forward face of the spectrum. Spectral energy is stored in a discrete matrix of frequency and direction bands for each computation point, but the sources and sinks in the energy balance equation associated with energy input, transfer and dissipation are parameterized.

18. The homogeneous portion of the energy balance equation is solved first. All steady-state mechanisms and associated parameters (such as the ray trajectory equation for refraction and shoaling mechanisms) are precomputed and stored for later use, hence reducing the numerical calculation to a single propagation step in time. Wave energy in each discrete frequency-direction band is propagated independently using a first-order upstream differencing scheme. This is a step-wise solution that estimates the change in energy level and direction along the wave ray that is capable of propagating into the grid point in one time step. During this process, the effects of island sheltering and diffraction were estimated.

19. In the 10-nm grid portions of the offshore islands were resolved and defined as land points. No energy is allowed to propagate through these land points. Since many islands are irregular in shape or relatively small compared to the 10-nm grid spacing, a method was developed to include spectral energy sheltering. The method of solution is sub-scale modeling of these

features, embedded in the 10-nm grid. A series of coefficients were generated that represent the percentage of energy in an angle band allowed to reach a grid point. The coefficients were determined via graphical means. Only points surrounding island locations were considered.

20. Energy propagating toward a point directly behind an island may be geometrically sheltered by an island, but some of the energy will reach the shadow region by diffraction. Island diffraction is also included in SHALWV, based on original work by Penny and Price (1944). This method applies Sommerfield's solution for diffraction of light waves at the edge of a semi-infinite screen to water wave diffraction at the edge of a semi-infinite breakwater or in this case, an island. The method is based on: a) linear wave theory (and the principle of linear superposition in the spectral version), b) uniform water depth, c) semi-infinite breakwater, and d) complete reflection off the breakwater. Only the effects of diffraction in the lee of the island are considered in this application. Diffractive effects are applied only to energy that has been sheltered. Thus, it adds back a percentage of the energy that was initially lost due to sheltering.

21. After the propagation sequence, energy is added to or removed from each discrete energy band by the source terms. These source/sink mechanisms consist of wind-wave growth, nonlinear wave-wave interactions, high frequency dissipation, and surfzone breaking Jensen (1987). At the end of each time step (600 seconds for this study), the directional spectrum at each grid point is calculated as the sum of the independently propagated spectral elements and the changes in energy caused by the source/sink mechanisms. This sequence was followed for the Southern California Bight hindcast study for the 20-year period of record, (1956-1975) at two-month intervals, with provisions for a restart mechanism. This insured continuous simulation of the wave environment without loss in energy levels from one run to the next. Actual run time for a two-month simulation was approximately 50 minutes on a CRAY 2 computer.

12-19 January 1988 Storm Simulation

22. An intense storm, accompanied by high winds and damaging surf, struck the southern California coast on 17-18 January 1988. The storm was associated with an intense extratropical cyclone which formed about 500-nm

west of the California coast on 16 January. Three reasons for its damaging effect were the minimum pressure of 990.5 mb (the lowest level measured in over 100 years), the initial generation area location, and eventual storm track relative to the southern California coastline. Measurements of significant wave heights in the area ranged from 6.0 to 10.0 m.

23. Dr. V.J. Cardone, Oceanweather, Inc., was contracted to develop a description of the surface wind fields (on a 2-deg spherical orthogonal grid, Figure B1) for this storm. The wind fields were produced with the best effort consistent with the meteorological data available at the time Cardone (1988). These data consisted of basic weather maps and surface weather observations available in real time. The wind field estimates are being improved at this time, (based on additional data) and the wave conditions will be re-hindcast based on those improvements. Hence, the results shown in Figures B4 through B7 are preliminary.

24. The wave hindcast was performed on three spatial scales, a 2-deg grid covering the Northern Pacific Ocean basin, a 0.5-deg grid covering a subscale region from 29 to 41 deg N latitude and 118 to 134 deg W longitude. The final region was the 10-nm grid system shown in Figure B2. All subscale wind fields (the 0.5-deg and 10-nm gridded systems) were generated directly by vectorially averaging the original 2-deg winds. Hence, they are a gross approximation of what occurred during the storm, and are not a direct outcome of Dr. Cardone's original analysis. Comparisons were made to offshore buoy data. Cardone's 2-deg grid wind speeds and directions compared favorably to the buoy data. Comparisons between measured conditions and interpolated winds clearly showed a disparity, principally caused by the interpolation. This will be resolved during the re-analysis process.

25. Energy-based wave heights and peak spectral wave periods are compared in Figures B4 through B7 for various locations in the 0.5-deg grid and the 10-nm grid. Agreement between wave estimates and measured buoy data is good with the exception of Buoy 46011 (Figure B6). This buoy is located slightly west of Point Conception. The primary discrepancy between the estimated and measured conditions is caused by the lack of energy in the initial portion of the estimated storm sequence. At the beginning of the storm simulation the buoy measured 3.0 m waves generated by a cyclonic disturbance located in the northern region of the Pacific Ocean basin which

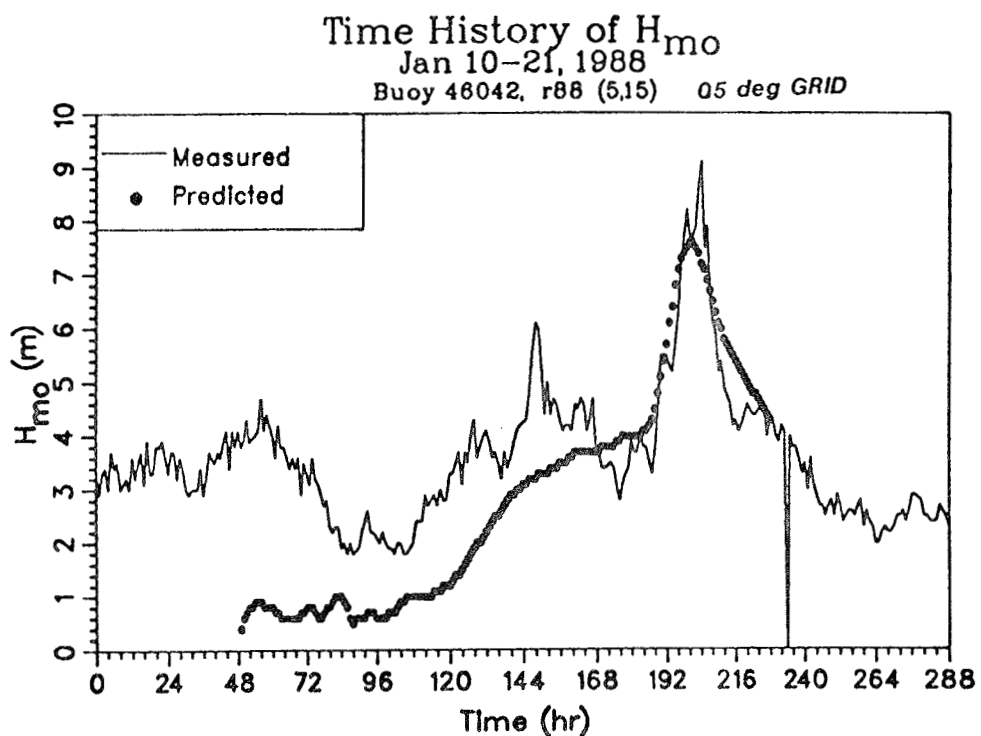
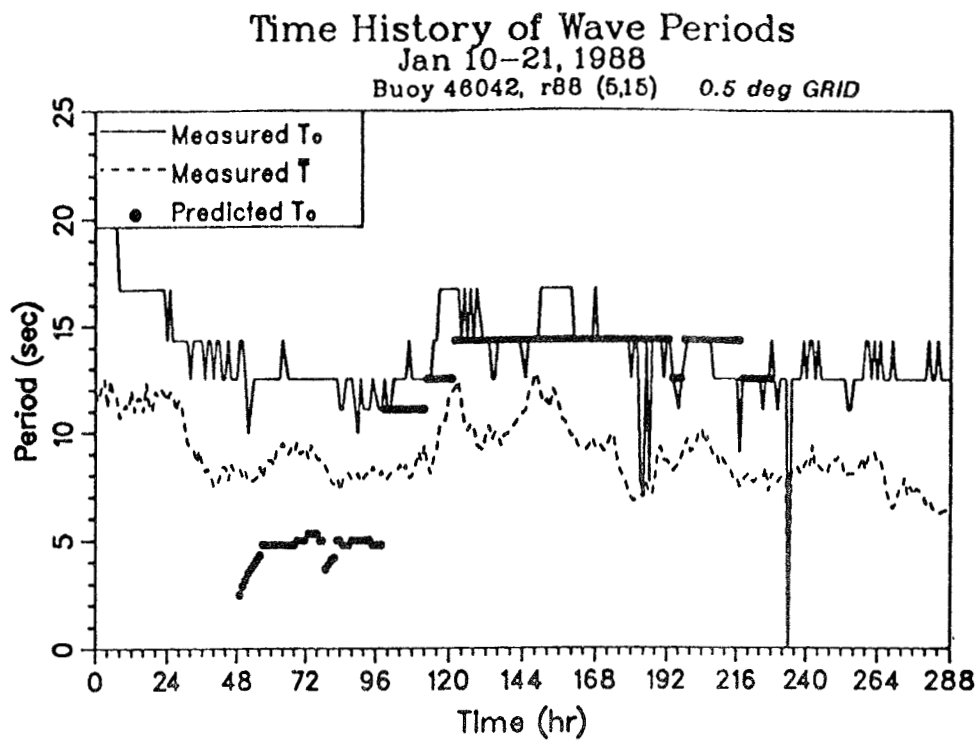


Figure B4. Comparison between hindcast and measured energy based wave heights and peak spectral wave periods
 (NDBC 46042 located 36.8N, 122.4W)

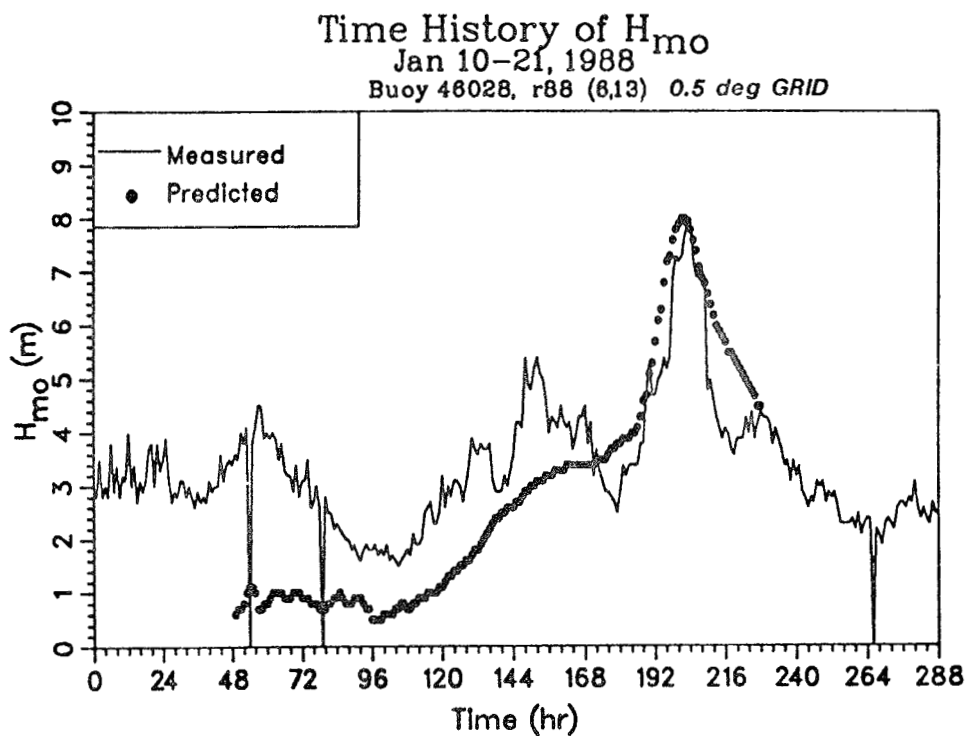
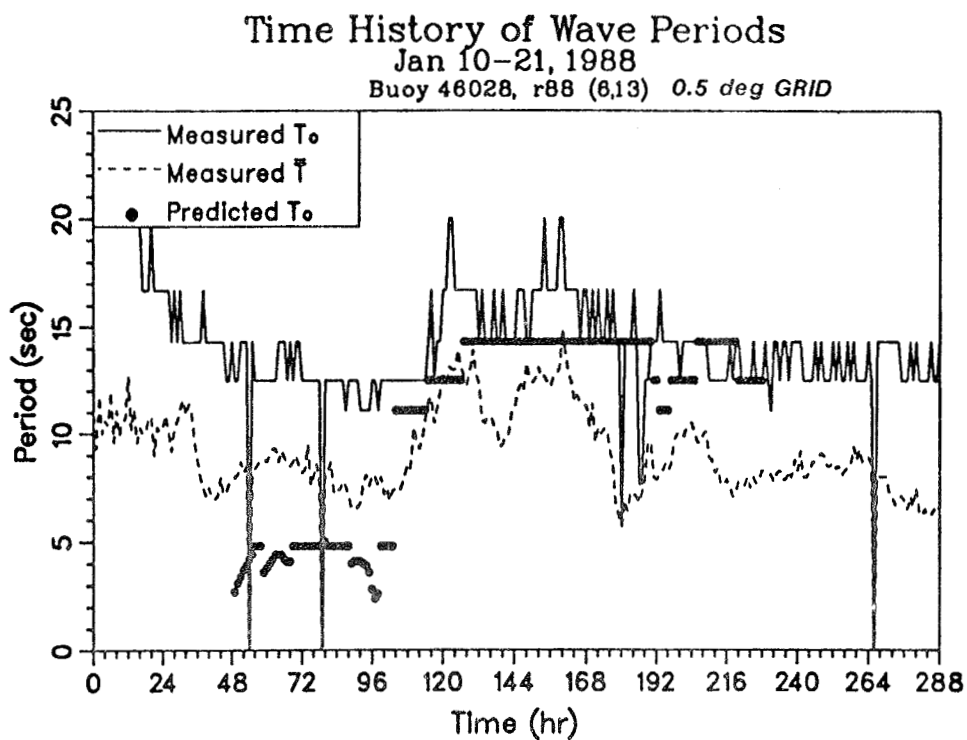


Figure B5. Comparison between hindcast and measured energy based wave heights and peak spectral wave periods
 (NDBC 46028 located 35.8N, 121.9W)

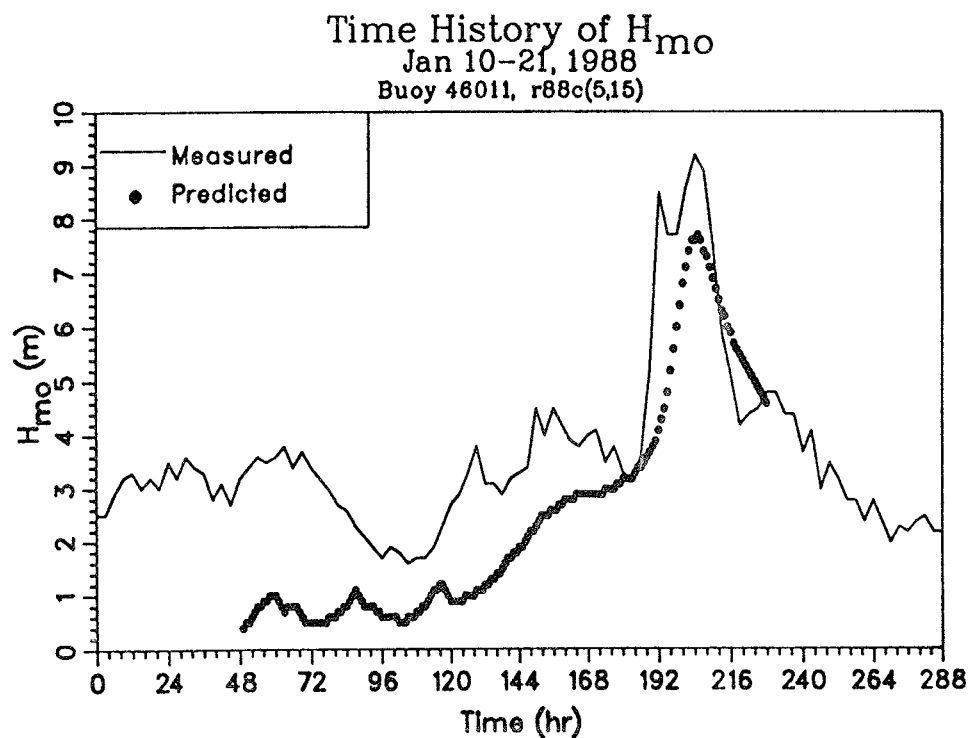
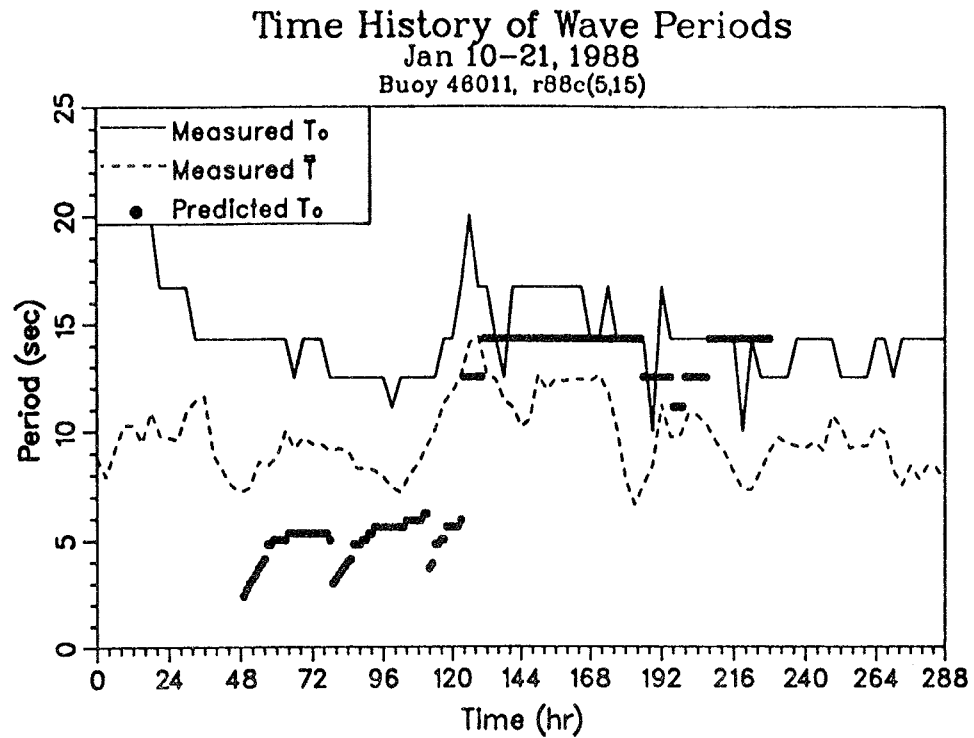


Figure B6. Comparison between hindcast and measured energy based wave heights and peak spectral wave periods
(NDBC 46011 located 34.9N, 120.9W)

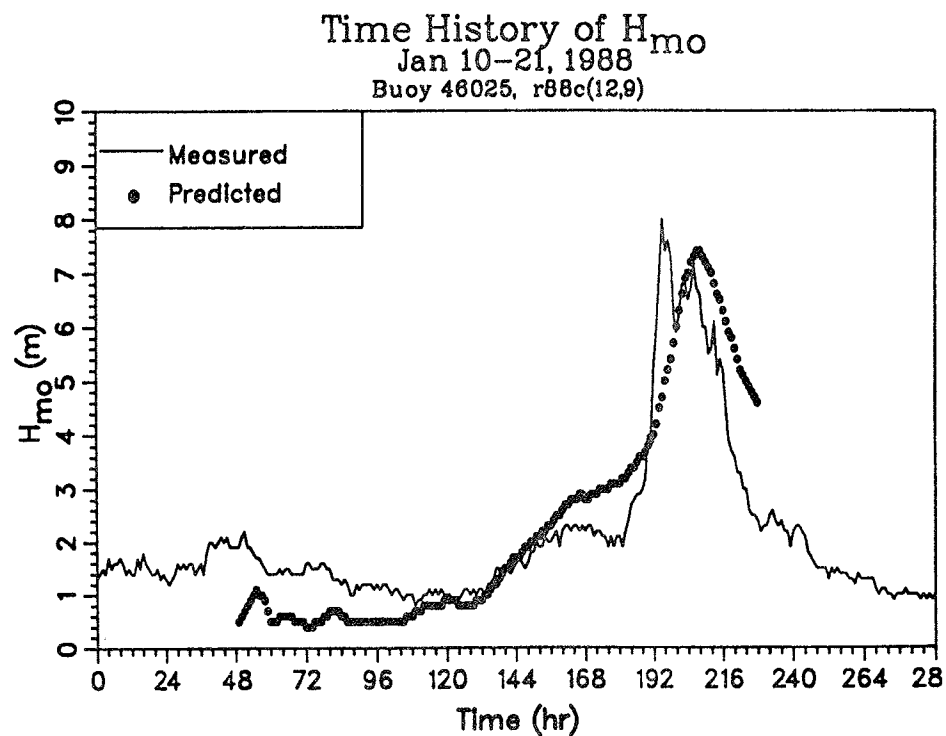
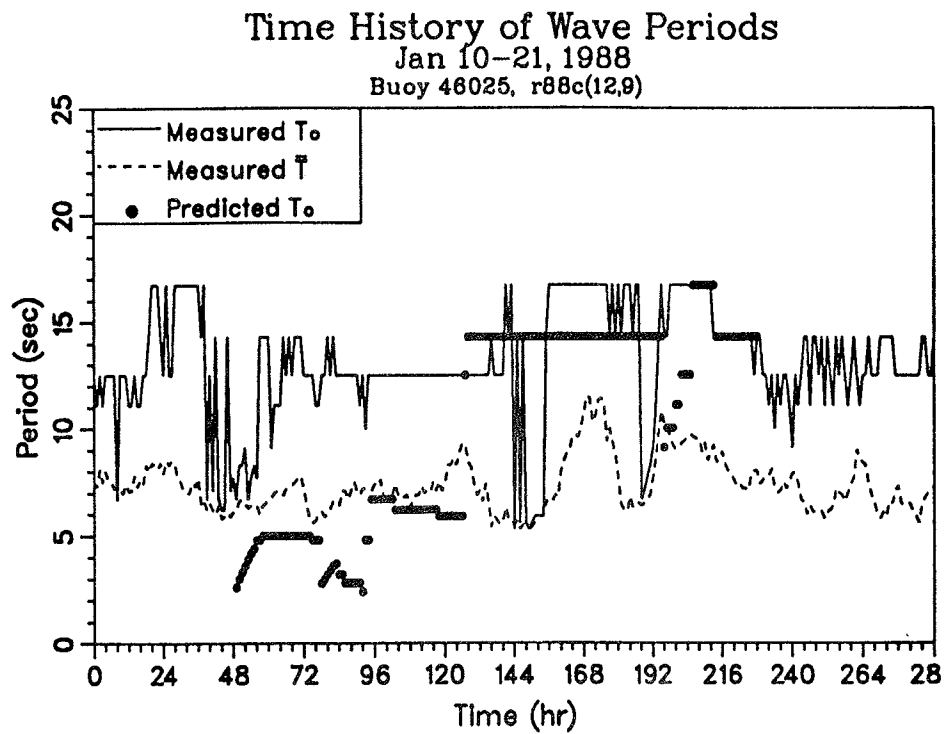


Figure B7. Comparison between hindcast and measured energy based wave heights and peak spectral wave periods
(NDBC 46025 located 33.7N, 119.1W)

was not part of the kinematic analysis procedures used in the estimation of the southern storm system. This energy propagated along the Oregon-California coastline in a south-easterly direction. Wave measurements at Begg Rock (near location I=9, J=9 in Figure B2) exceeded 10 m whereas the model simulation maximum was at 8.5 m. Approximately 20-nm east of this location (Buoy 46025), the wave conditions peaked at 8.0 m, indicating that additional energy producing storm near the Oregon coast influenced selected regions in the Southern California Bight.

Summary

26. A 20-year, wind-wave hindcast for the Southern California Bight was performed. Numerous site-specific techniques were used to resolve the land-sea breeze effect, include wave attenuation from island sheltering and diffraction, and represent multiple wave populations in a complex coastal regime. Results of the study will be presented in a Wave Information Study (WIS) report, documenting the methods and procedures in greater detail.

Acknowledgments

27. I would like to acknowledge Dr. D. T. Resio, OCTI, Inc. for his efforts in the generation of the land-sea breeze methodology, Ms. Jane M. Smith, CERC, for her assistance in the island sheltering and diffraction portion of this work, Dr. V. J. Cardone, Oceanweather, Inc., for providing the wind fields for the 12-19 January 1988 storm sequence, and Mr. Jack E. Davis, CERC, for generating the final graphics. This research was conducted at the Coastal Engineering Research Center, Waterways Experiment Station, as part of the work unit "Wave Estimation for Design" of the Coastal Flooding and Storm Protection Program of the United States Army Corps of Engineers. Permission was granted by the Chief of Engineers to publish these results.

References

Cardone, V. J. 1988. "Surface Wind Fields in North Pacific Storm of January 12 - 19, 1988, Oceanweather," Inc., Informal Report submitted to Coastal Engineering Research Center, US Army Engineer Waterways Experiment Station, Vicksburg, MS.

Corson, W. D., and Co-Authors, 1986. "Pacific Coast Hindcast Deepwater Wave Information," WIS Report 14, US Army Engineer Waterways Experiment Station, Vicksburg, MS.

_____, and Co-Authors, 1987. "Pacific Coast Hindcast Phase II Wave Information," WIS Report 16, US Army Engineer Waterways Experiment Station, Vicksburg, MS.

Holl, M. M., and Mendenhall, B. R. 1971. The FIB Methodology and Applications, Meteorology International, Inc., Monterey, CA.

Hughes, S. A. and Jensen, R. E. 1986. "A USERS Guide to SHALWV, Numerical Model for Simulation of Shallow-Water Wave Growth, Propagation and Decay," Instruction Report CERC-86-2, US Army Engineer Waterways Experiment Station, Vicksburg, MS.

Jensen, R. E. 1987. "Modeling Spectral Wave Conditions," Proceedings Coastal Hydrodynamics, American Society of Civil Engineers, Newark, DE., 28 June-1 July, pp 603-617.

Penny, W. G., and Price, A.T. 1944. "Diffraction of Sea Waves by a Breakwater," Artificial Harbors, Technical History No. 26, Sec. 3-D, Directorate of Miscellaneous Weapons Development.

Resio, D. T. 1981. "The Estimation of a Wind Wave Spectrum in a Discrete Spectral Model," J. Phys. Oceanogr., No. 11, pp 510-525.

_____, Vincent, C. L., and Corson, W. D. 1982 "Objective Specification of Atlantic Ocean Wind Fields from Historical Data," WIS Report 4, US Army Engineer Waterways Experiment Station, Vicksburg, MS.

APPENDIX C: STABILITY ANALYSIS OF PROPOSED OCEAN
ENTRANCE CHANNELS, BOLSA CHICA, CALIFORNIA

Dr. Steven A Hughes

Abstract

1. An analysis is presented on the stability of the non-navigable and navigable ocean entrance channel alternatives proposed for Bolsa Chica. Tidal prisms calculated from numerical modeling simulations of tidal circulation for both alternatives are used to apply O'Brien's (1931, 1969) criteria for equilibrium cross-sectional channel area. Interpretation of the results is included, and the performance of two existing entrances similar in size to the proposed non-navigable entrance is examined.

Background

2. The original Scope of Work for the Bolsa Chica Studies included provision for numerically simulating the effects of a proposed non-navigable ocean entrance channel at Bolsa Chica. The details of this entrance channel had not been specified at the time the Scope of Work was prepared. Subsequently, preliminary design of the proposed non-navigable entrance was completed, and the designed channel was different than the original concept because it featured channel training structures that terminated on the beach at the high water line. The shoreline response simulation model used in the studies could not successfully simulate responses of coastal structures that do not penetrate into the surf zone. For this reason WES was unable to provide computer simulations of possible shoreline change resulting from construction of the currently proposed non-navigable entrance.

3. Bolsa Chica study sponsor, California State Lands Commission (SLC), requested that WES substitute a stability analysis of the proposed non-navigable ocean entrance channel in lieu of providing the computer shoreline response modeling of the non-navigable entrance as specified in the Scope of Work. WES agreed to this amendment to the Scope of Work.

4. The inlet stability analysis for the proposed ocean entrance systems at Bolsa Chica is contained in this Appendix. Included is a discus-

sion of methodology, an analysis of the non-navigable entrance alternative, an analysis of the navigable entrance alternative, a summary, and a list of cited references.

Methodology

Introduction

5. Estimating stability characteristics of ocean entrance channels that connect lagoonal waters directly with the tidal sea is one of the most difficult coastal problems to approach deterministically. The stable tidal inlet represents a natural balance between wave-driven longshore and onshore currents that tend to deposit sediment in the entrance throat and tidally-driven (as well as freshwater) flow in the channel throat that tends to scour the channel bottom. A tidal inlet that achieves such a balance is not guaranteed future stability because conditions may change, causing a once stable inlet to close.

6. Because of the complexities involved in the various processes at work in the vicinity of a tidal entrance, engineers have relied heavily on observation and on empirical relationships in attempting to understand and predict inlet stability. Hence, tidal inlet stability analysis concerns, for the most part, determining several important parameters for the entrance system in question, using these parameters in empirical relationships developed from field observations of stable inlets, and finally making qualitative comparisons with existing entrances having similar characteristics.

O'Brien's Relationships

7. In 1930 Dean M. P. O'Brien made a reconnaissance survey of beaches and harbors on the Pacific Coast. The obvious fact that large bays had large entrances to the ocean and small bays had small entrances suggested to O'Brien that a relationship must exist between the entrance cross-sectional area and the volume of water flowing through the entrance over a half-tidal cycle. Using data from the west coast entrances, O'Brien established the relationship given by Eq. C1 (O'Brien 1931).

$$A = 4.69 \times 10^{-4} p^{0.85} \quad (C1)$$

where

- A = minimum throat cross-sectional area measured at mean sea level (expressed in sq ft), and
P = tidal prism defined as the volume of water stored in the bay between high and low waters corresponding to the diurnal or the spring range of tide (expressed in cu ft).

8. O'Brien felt that the close agreement between his simple relationship and the available data was fortuitous because of the inaccuracies inherent in the calculation of parameters, the apparent lack of grain-size effect on the entrance throat cross-sectional area, and the fact that jettied and unjettied entrances followed the same relationship. He stated that precise and extensive data would demonstrate the influence of these additional factors.

9. Thirty-five years after his original publication, O'Brien revisited his relationship by including additional data that had become available in the interim (O'Brien 1969). This review included 9 Atlantic Coast inlets, 18 Pacific Coast inlets, and 1 entrance on the Gulf Coast. O'Brien concluded that his original formulation agreed closely with the new data for inlets with two jetties, but a linear relationship more closely approximated inlets without jetties. Although the data seem to support O'Brien's original relationship, O'Brien himself views his tidal inlet stability guidance with more pessimism than most practicing coastal engineers (O'Brien 1976). Among his concerns is that the gross and net littoral transport rates do not seem to effect the relationships.

Jarrett's Analysis

10. Jarrett (1976) extended the data set used by O'Brien to include a total of 162 inlets. Jarrett then reanalyzed the tidal prism cross-sectional area relationships of O'Brien to determine if differences arose between the Atlantic, gulf, and Pacific coast inlets. He concluded that there were differences between regions for unjettied entrances and single-jetty entrances; however, the available data indicated that O'Brien's relationship was still valid for entrances stabilized with two jetties. Jarrett presented the data on a series of plots specific to certain categories of entrance (eg., all Atlantic coast inlets, or Pacific coast inlets with two jetties) along with regression lines representing best-fit relationships between tidal prism and cross-sectional area.

11. Jarrett's refinement of O'Brien's relationships is generally accepted as a sound engineering approach for examining tidal inlet stability, and this is the methodology that is applied in the present analysis of the proposed ocean entrance systems at Bolsa Chica.

12. Other methods exist for examining tidal inlet stability that typically plot the maximum tidal flow velocity versus the cross-sectional throat area giving that velocity. O'Brien's relationship is then superimposed onto this curve so that an optimal throat area for equilibrium can be selected. These types of analysis are suited for more detailed design phases when optimization of the entire bay and entrance configuration is desirable, but they were considered unnecessary for this preliminary analysis on whether the specified entrance channel channels would maintain a stable configuration.

Non-Navigable Entrance

Entrance Channel

13. Figure C1 shows the conceptual layout of the non-navigable ocean entrance alternative for the development of Bolsa Chica and enhancement of the wetlands. Further hydraulic and geometric details were provided to WES as part of the Tidal Circulation and Water Quality Task of the Bolsa Chica studies, and details are given in Hales, et al. (1989).

14. The proposed non-navigable entrance channel cross-section was specified as shown on Figure C2, with a depth of 5 ft at Mean Sea Level (MSL), yielding a minimum cross-sectional area of 850 sq ft at MSL. Variation of cross-sectional area as a function of tidal fluctuations about MSL is given by Eq. C2.

$$\text{Area} = 850 + 180 e + 2 e^2 \quad (C2)$$

where area is given in sq ft, and e is the water elevation in ft above or below MSL.

Tidal Prism

15. Calculation of tidal prism for the non-navigable entrance utilized results from the numerical tidal circulation simulation of the non-navigable entrance system conducted as part of the WES studies (Hales, et al. 1989).

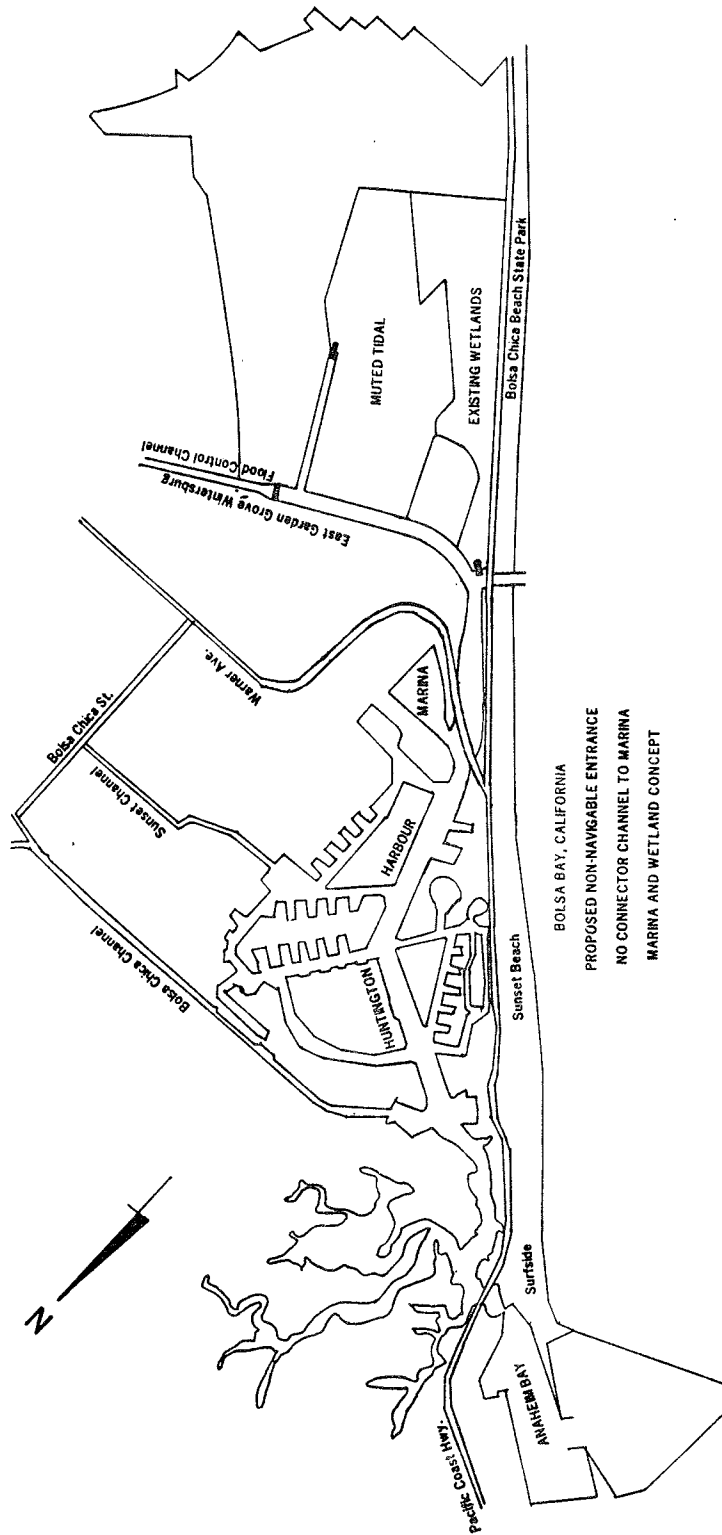


Figure C1. Non-navigable entrance channel alternative - conceptual layout

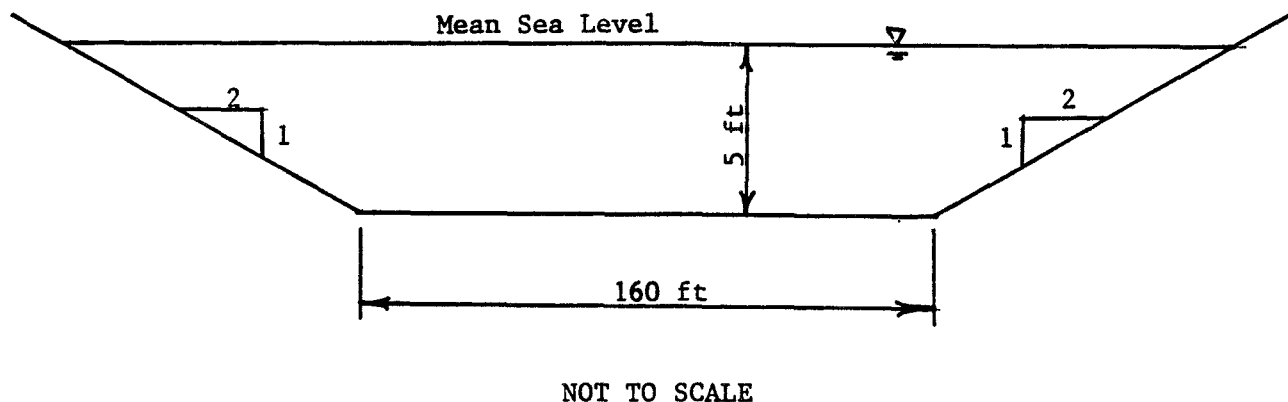


Figure C2. Non-navigable ocean entrance channel cross-section

This simulation employed a calibrated link/node computer model to reproduce surface elevations (at the nodes) and water velocities (between nodes) at 15-minute intervals over approximately an 11-day period spanning a spring tide episode. The numerical model was started using a simple sine wave; then after approximately 24 hours, input was switched to a tidal signal generated by tidal constituents at the ocean boundary. Results produced during the startup phase were not included in the determination of tidal prism. Complete details of channel geometry and water connections are given in Hales, et al. 1989).

16. The surface elevation time history at the channel entrance is given in Figure C3, and the corresponding mean water velocity in the throat of the entrance channel is given in Figure C4. In Figure C4, positive velocities indicate ebb flows. The link/node model assumes uniform discharge between nodes, hence the calculated velocities are assumed to be uniform over the entire cross-section of the channel.

17. Volumetric water discharge through the entrance channel was calculated at 15-minute intervals using the time-history surface elevation and velocity data obtained from the numerical model. At each time step discharge was determined as the product of the velocity times the cross-sectional area calculated by Eq. C2 for the tide elevation at that time step. A time history of the discharge in cubic feet per second (cfs) is shown on Figure C5.

BOLSA BAY, CALIFORNIA
WATER SURFACE TIME HISTORY
NNECC1 NODE 78

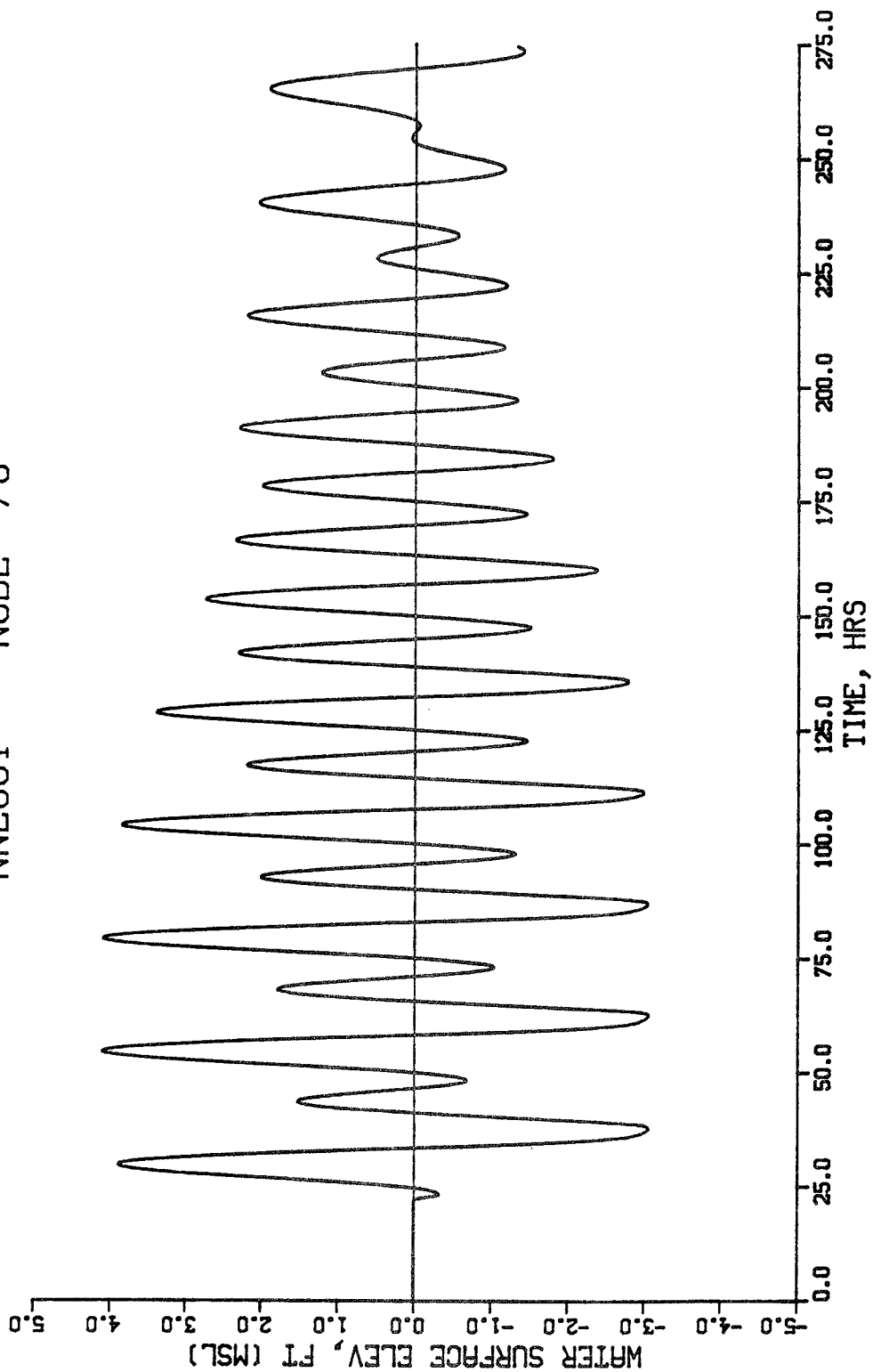


Figure C3. Non-navigable entrance channel - water surface elevations

BOLSA BAY, CALIFORNIA
VELOCITY TIME HISTORY
NNECC1 LINK 90

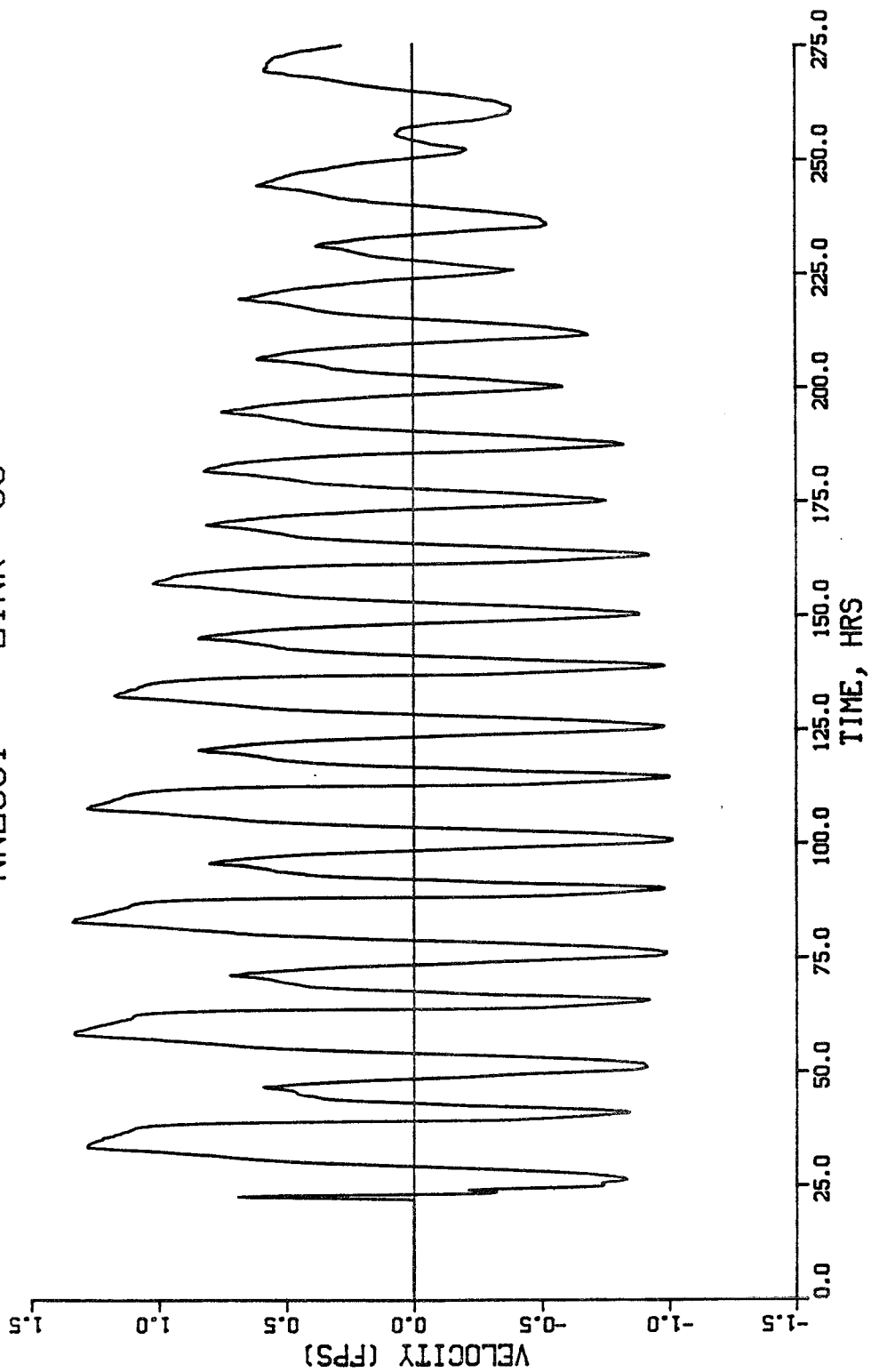


Figure C4. Non-navigable entrance channel - water velocities

BOLSA BAY, CALIFORNIA
ENTRANCE DISCHARGE TIME HISTORY
(Ebb Flow - Positive)

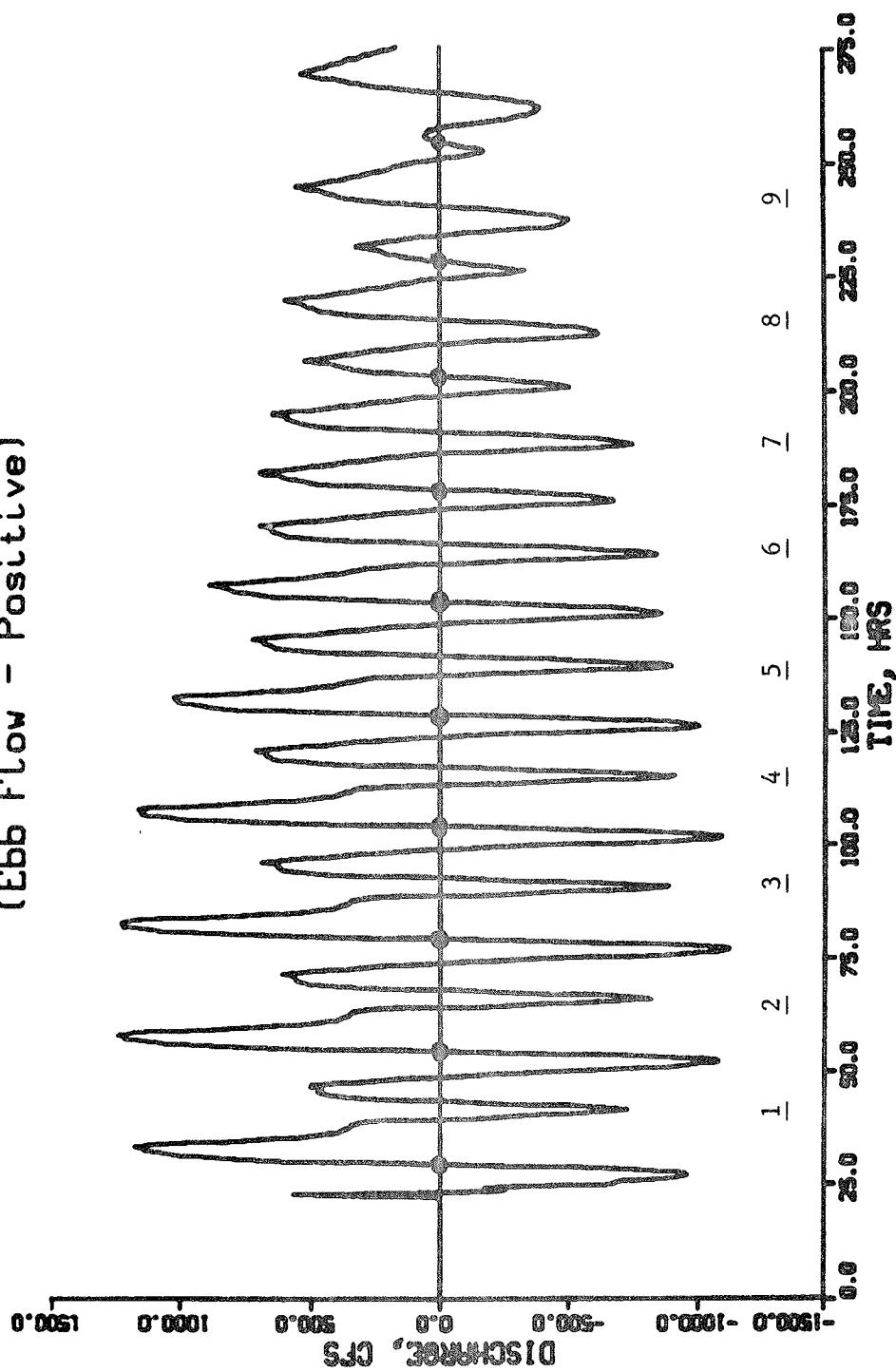


Figure C5. Non-navigable entrance channel - flow discharge

18. The discharges for ebb and flood flows were numerically integrated separately and then averaged over the diurnal tidal cycle to arrive at values of the tidal prism (Jarrett 1976). Table C1 presents tidal prism values for the tidal cycles delineated by the zero-upcrossing dots on Figure C5.

19. The maximum tidal prism value in Table C1 has been plotted versus the minimum channel cross-sectional area at MSL (850 sq ft) in Figures C6 and C7. Figure C6 is Jarrett's (1976) regression for all Pacific coast inlets for which data were available, whereas Figure C7 is the regression for Pacific coast inlets with one or no jetties.

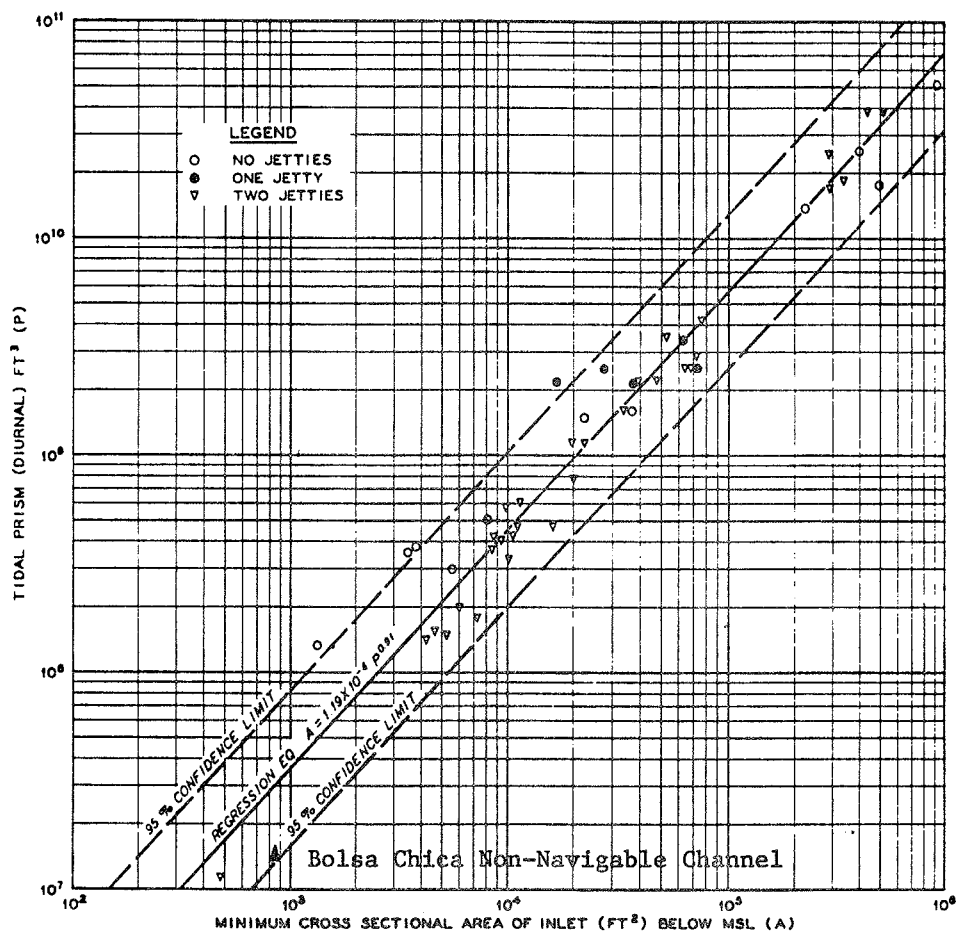
Table C1
Non-Navigable Entrance Tidal Prism Values

<u>Tidal Cycle</u>	<u>Tidal Prism (cu ft)</u>
1	12.46 (10) ⁶
2	13.31 (10) ⁶
3	13.54 (10) ⁶
4	13.17 (10) ⁶
5	12.19 (10) ⁶
6	10.73 (10) ⁶
7	9.00 (10) ⁶
8	7.27 (10) ⁶
9	5.99 (10) ⁶

Discussion

20. The analysis for the proposed non-navigable ocean entrance channel at Bolsa Chica indicates that the present design cross-sectional area is greater than the equilibrium cross-sectional area that might be expected using Jarrett's (1976) curves. This is particularly indicated by Figure C7, which shows the regression for Pacific coast inlets with one or no jetties. Because the non-navigable entrance channel training structures terminate at the high water line, they provide no barrier to longshore moving sediment that will enter the channel. Hence, this entrance should be considered an entrance with no jetties, making Figure C7 the more appropriate choice for comparison.

21. If the ocean entrance system and accompanying bay development as proposed for the non-navigable alternative were to be constructed as presently configured, it should be expected that the entrance channel would immediately



(from Jarrett 1976)

NOTE: REGRESSION CURVE WITH 95 PERCENT
CONFIDENCE LIMITS.

TIDAL PRISM VS
CROSS-SECTIONAL AREA
ALL INLETS ON PACIFIC COAST

Figure C6. Non-navigable entrance channel tidal prism vs. throat area,
all inlets on Pacific coast

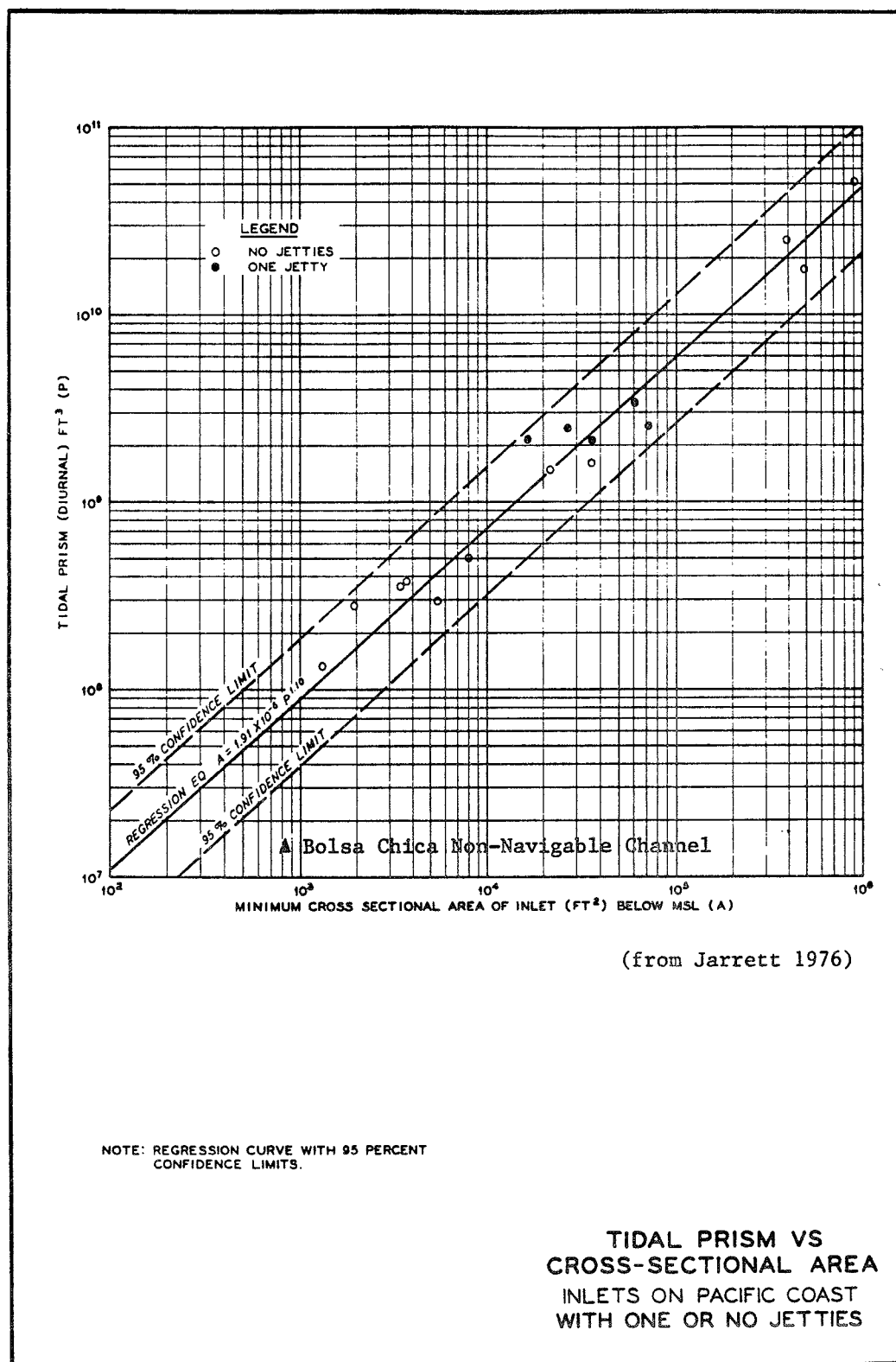


Figure C7. Non-navigable entrance channel tidal prism vs. throat area, inlets on Pacific coast with one or no jetties

shoal by deposition of littoral sediment until a somewhat smaller equilibrium area is reached. A first estimate of the new equilibrium area could be obtained from Figure C7 by assuming the tidal prism remains constant. However, the total tidal prism stored in the lagoonal area is apportioned between two entrances, Anaheim and Bolsa Chica. Reducing the area of one entrance may significantly alter the system's flow characteristics, and thus, change that portion of the tidal prism that is served by the non-navigable entrance. During any final design phase, it is recommended that tidal circulation numerical modeling be performed using different inlet cross-sectional areas to obtain reasonable estimates of the tidal prism expected at the non-navigable entrance.

22. It is difficult to state whether the proposed non-navigable entrance would continue to shoal to the point of closure after reaching an equilibrium area compatible with the regressed curve given on Figure C7. The lower portion of the curve in Figure C7 has been extrapolated from data obtained for larger entrances, therefore caution must be used in drawing conclusions about entrances the size as examined here. O'Brien (1969) in his conclusions regarding the equilibrium area relationships states, "Very small inlets can be kept open by tidal currents, if they are protected against strong surf and littoral drift." He also states that jetties not only stabilize inlet position, they protect the inlet against closure under wave action. From O'Brien's conclusions it can be inferred that the unprotected non-navigable entrance proposed for Bolsa Chica would be susceptible to closure because of its size and its direct exposure to an active surf zone and littoral transport regime.

23. Some of the littoral sediment swept into the lagoon by tidal currents will be deposited in the form of interior shoals. No estimate is given of the quantity of material that may potentially be removed from the littoral system, but maintenance dredging operations may be required to return trapped material to the beaches.

24. Finally, it is instructive to compare the proposed non-navigable entrance with other Pacific coast inlets, structured and unstructured, of similar size because this is often an indicator of the proposed inlet's future functionality.

25. Camp Pendleton. This is a small entrance that most closely matches the tidal prism cross-sectional area relationship determined for the proposed non-navigable entrance. It is plotted on Figure C6 immediately to the left of, and slightly lower than, the Bolsa Chica data point. This small boat harbor was built by the Marine Corps at the start of the Second World War. According to Peel (U. S. Army Engineer District, Los Angeles 1986), this entrance immediately underwent sedimentation and closed. After construction of the Oceanside entrance jetties, the Camp Pendleton entrance remained open and stable. This is certainly due in part to the fact that this channel is an entrance within an entrance, and protected from strong littoral action by the Oceanside structures. O'Brien (1969) states that the Camp Pendleton entrance is "subjected to the mild but continuous action of long, low waves diffracted and refracted inside the jetties." Because of its unique positioning, the stability of Camp Pendleton entrance channel does not support the hypothesis that the proposed non-navigable channel on the open coast at Bolsa Chica could maintain a stable cross-sectional throat area.

26. Agua Hedionda Lagoon. This lagoon is located in the city of Carlsbad, and it serves as a cooling water source for a power generating station. Its tidal prism has been given as $49.0(10)^6$ cu ft (Johnson 1973). In its undeveloped state the inlet channel to the lagoon apparently was closed for months at a time (U. S. Army Engineer District, Los Angeles 1986). The entrance was stabilized by construction of surf-zone-penetrating twin jetties that provided a cross-sectional throat area as dictated by O'Brien's relationship, but reduced slightly to assure high flow velocities for channel scouring capability. Still, littoral sediment is transported into the lagoon and deposited, requiring systematic dredging of the lagoon (every couple of years) and placement of the material back into the littoral system (U. S. Army Engineer District, Los Angeles 1986; Jenkins, et al. 1980).

27. The success of the inlet channel at Agua Hedionda indicates that a stable non-navigable entrance at Bolsa Chica could be feasible provided a dual jetty system similar to Agua Hedionda is incorporated into the design. However, structures that penetrate into the active surf zone are expected to impact littoral processes and adjacent shoreline to some extent, and these impacts must be evaluated within the context of the project.

Navigable Entrance

Entrance Channel

28. Although stability analysis of the navigable entrance was not specified in the revised Scope of Work, calculations were made for comparative purposes since the necessary data were at hand. Figure C8 shows the conceptual layout of the navigable ocean entrance alternative for the development of Bolsa Chica and enhancement of the wetlands. Further hydraulic and geometric details were provided to WES as part of the Tidal Circulation and Water Quality Task of the Bolsa Chica studies (Hales, et al. 1989).

29. The proposed non-navigable entrance channel cross-section was specified as shown on Figure C9, with a depth of 23 ft at Mean Sea Level (MSL), yielding a minimum cross-sectional area of 19,458 sq ft at MSL. Variation of cross-sectional area as a function of tidal fluctuations about MSL is given by Eq. C3.

$$\text{Area} = 19,458 + 892 e + 2 e^2 \quad (\text{C3})$$

where area is given in sq ft, and e is the water elevation in ft above or below MSL.

Tidal Prism

30. Calculation of tidal prism for the navigable entrance was performed in the same manner as described above for the non-navigable entrance. Results from numerical tidal circulation simulation of the navigable entrance system were utilized. Complete details of channel geometry and water connections are given in Hales, et al. (1989).

31. The surface elevation time history at the channel entrance is given in Figure C10, and the corresponding mean water velocity in the throat of the entrance channel is given in Figure C11. In Figure C11, positive velocities indicate ebb flows.

32. Volumetric water discharge through the entrance channel was calculated at 15-minute intervals using the time-history surface elevation and velocity data obtained from the numerical model. At each time step discharge was determined as the product of the velocity times the cross-sectional area calculated by Eq. C3 for the tide elevation at that time. A time history of the discharge in cfs is shown on Figure C12.

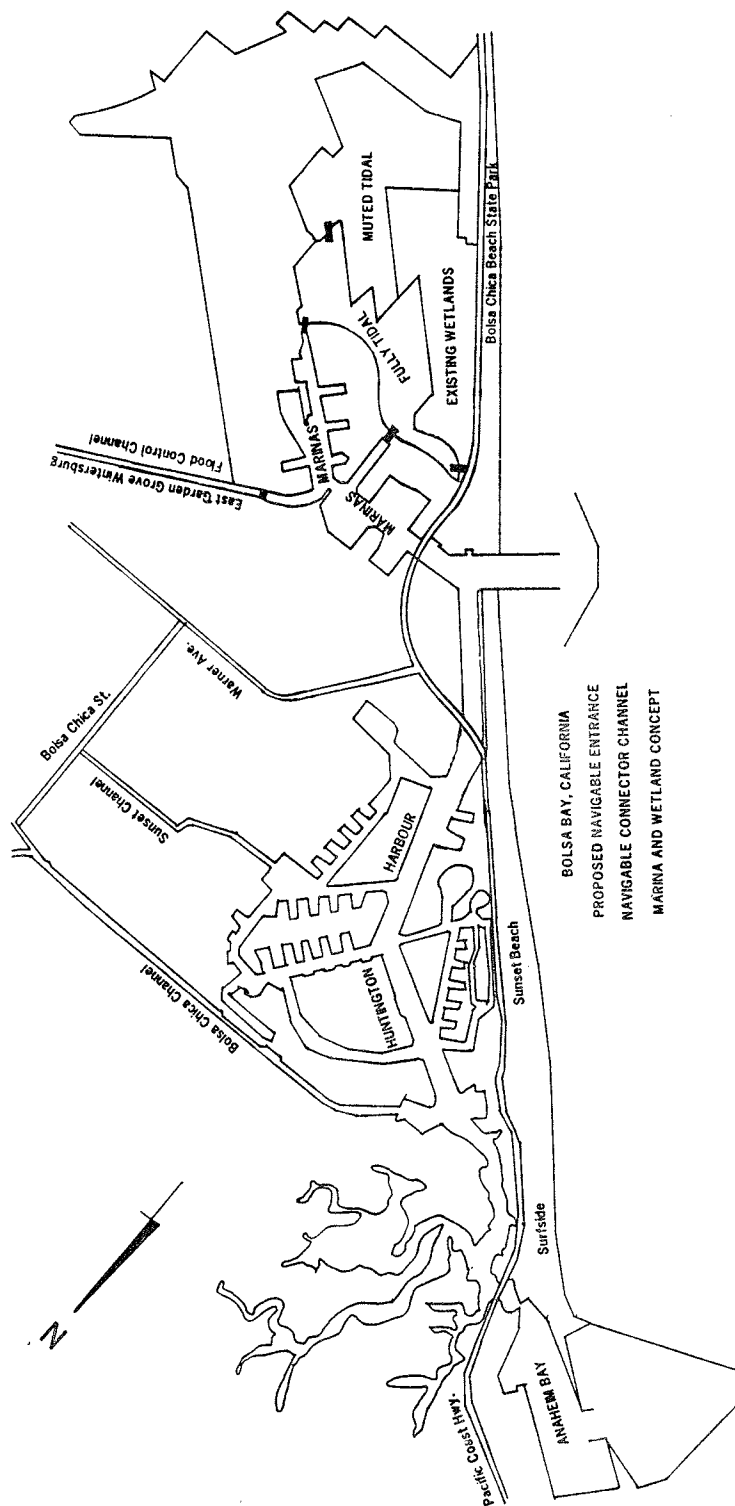
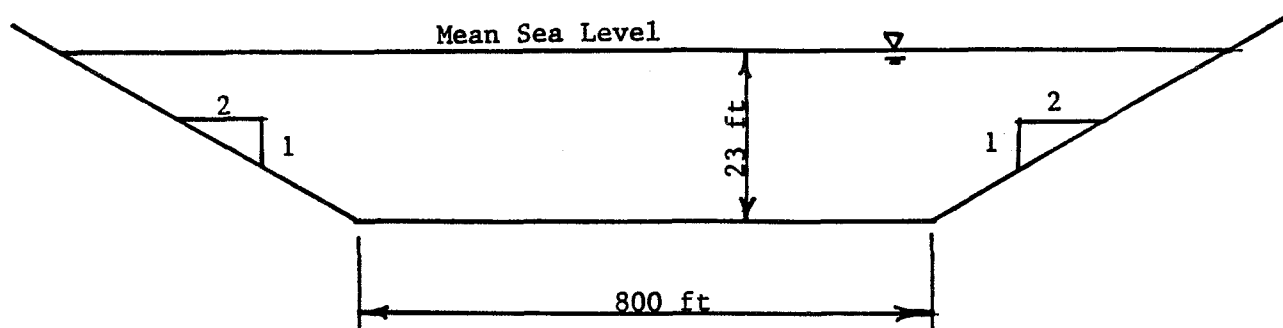


Figure C8. Navigable entrance channel alternative - conceptual layout



NOT TO SCALE

Figure C9. Navigable ocean entrance channel cross-section

33. Table C2 presents tidal prism values for the tidal cycles delineated by the zero-upcrossing dots on Figure C12. Calculations were made as described above for the non-navigable entrance.

Table C2
Navigable Entrance Tidal Prism Values

<u>Tidal Cycle</u>	<u>Tidal Prism (cu ft)</u>
1	82.1 (10) ⁶
2	88.0 (10) ⁶
3	89.7 (10) ⁶
4	87.1 (10) ⁶
5	80.7 (10) ⁶
6	71.5 (10) ⁶
7	60.1 (10) ⁶
8	37.3 (10) ⁶
9	37.7 (10) ⁶

34. The maximum tidal prism value in Table C2 has been plotted versus the minimum channel cross-sectional area at MSL (19,458 sq ft) on Figure C13, which is Jarrett's (1976) regression for all two-jettied Pacific coast inlets for which data were available.

BOLSA BAY, CALIFORNIA
WATER SURFACE TIME HISTORY
NENC1 NODE 76

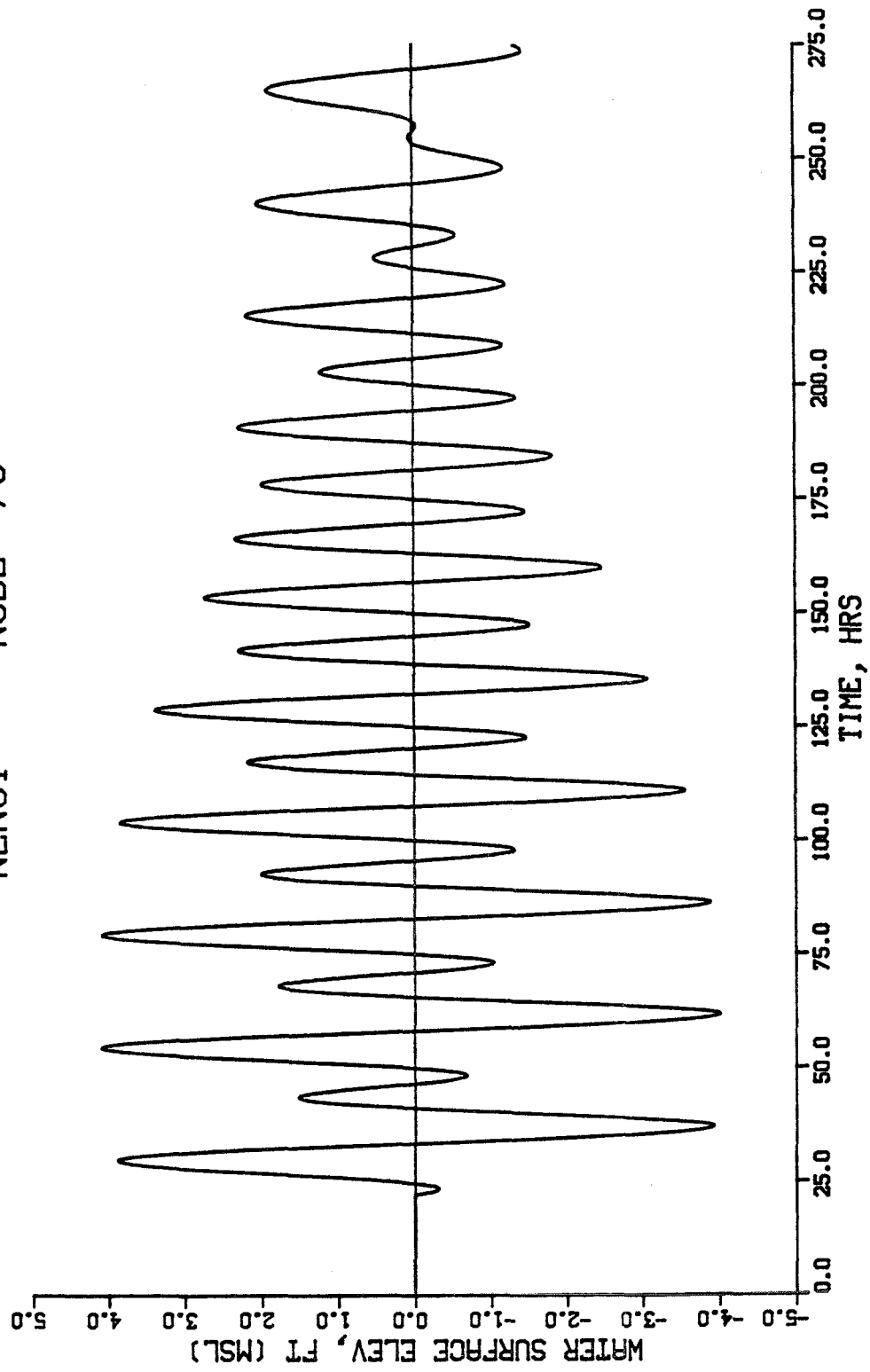


Figure C10. Navigable entrance channel - water surface elevations

BOLSA BAY, CALIFORNIA
VELOCITY TIME HISTORY
NENC1 LINK 109

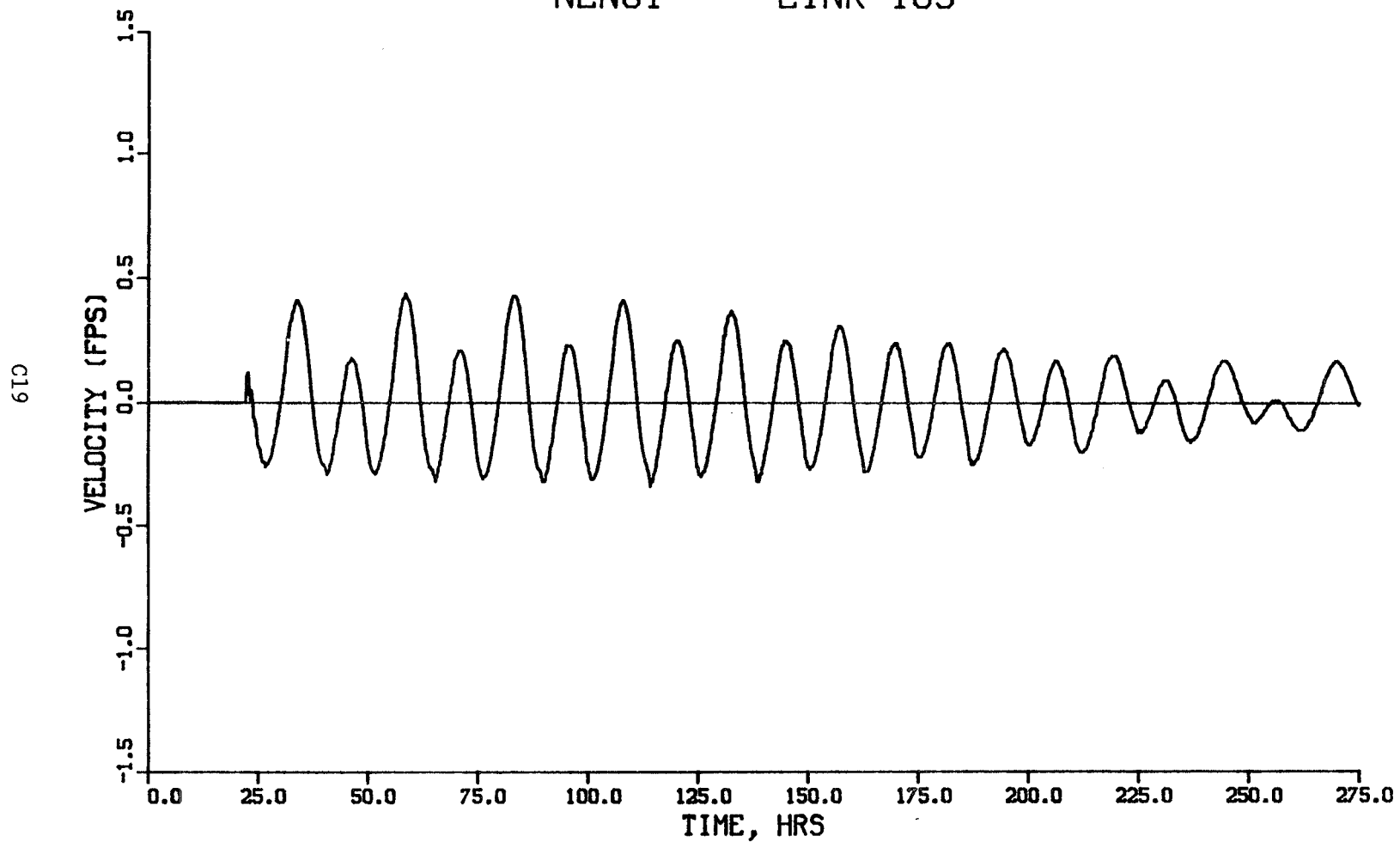


Figure C11. Navigable entrance channel - water velocities

BOLSA BAY, CALIFORNIA
ENTRANCE DISCHARGE TIME HISTORY
(Ebb Flow - Positive)

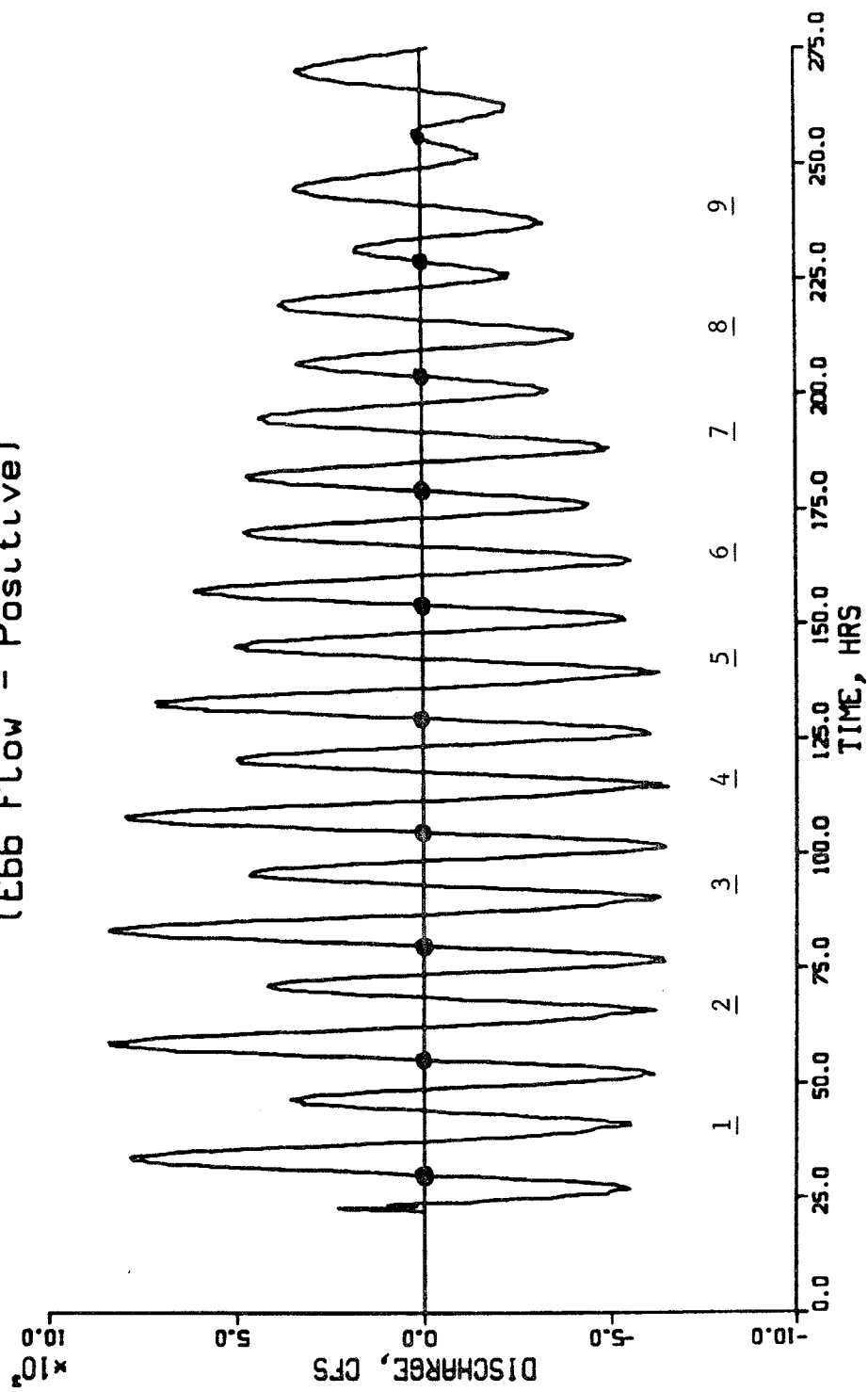
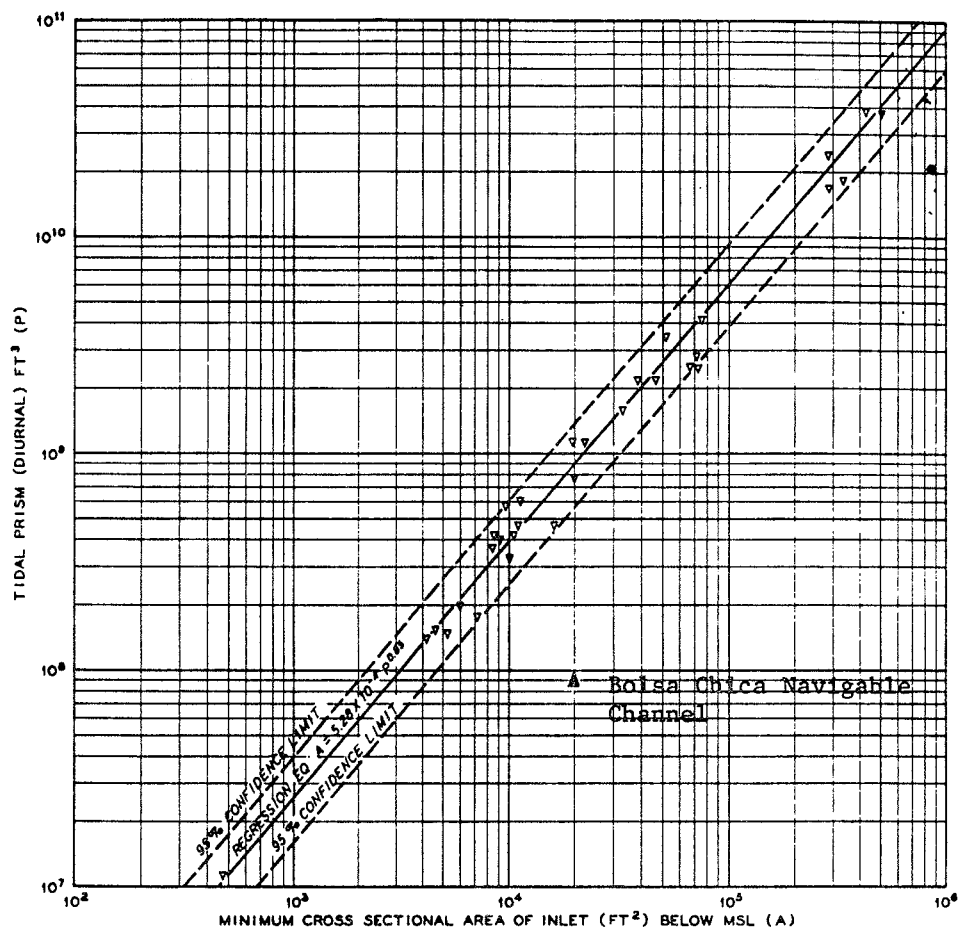


Figure C12. Navigable entrance channel - flow discharge



(from Jarrett 1976)

NOTE: REGRESSION CURVE WITH 95 PERCENT
CONFIDENCE LIMITS.

TIDAL PRISM VS
CROSS-SECTIONAL AREA
INLETS ON PACIFIC COAST
WITH TWO JETTIES

Figure C13. Navigable entrance channel tidal prism vs. throat area,
Inlets on Pacific coast with one or no jetties

Discussion

35. The inlet stability calculation for the proposed navigable ocean entrance at Bolsa Chica indicates the throat cross-sectional area is much larger than necessary to maintain a stable tidal entrance channel. If this entrance were to be constructed with only a short jetty system and without the benefit of the offshore breakwater, the channel would be expected to shoal until an equilibrium area is reached, or perhaps until the entrance closed. An estimate could be made of an equilibrium area using Figure C13, however, the same caveats as stated in the non-navigable analysis apply here.

36. Other design considerations for the navigable entrance channel, such as maintaining lower water velocities in the navigation channel for safety and boating reasons, dictate the need for a channel with cross-sectional area greater than required for equilibrium as a tidal inlet. Provided this increased area can be maintained, the channel will still function as a conduit for water exchange between the ocean and the bay system.

37. The low channel velocities (see Figure C11) will not effectively scour sediment that enters the channel, and the entrance system design needs to consider methods of preventing sedimentation by littoral materials. Jetties extending to the 20-ft depth contour, combined with the offshore breakwater that reduces waves and littoral currents in the entrance vicinity will help in this regard. Such a system can be regarded as a fairly effective barrier to the longshore movement of material, however, it may still be possible for sediment to enter the entrance channel where it will be deposited, and periodic maintenance dredging may be required.

38. Possibly the best indicator of the future response of the designed navigable entrance would be to compare it to the functionality and maintenance requirements of similar projects; however, such a comparison is beyond the scope of the present stability analysis of the non-navigable entrance alternative.

Summary

39. Application of accepted criteria for determining the equilibrium cross-sectional throat area that will be maintained by a given tidal prism has been performed for both the non-navigable and the navigable alternatives

proposed for Bolsa Chica. Tidal prism was calculated from numerical simulation results of the tidal circulation within the proposed configurations for the bay area.

40. The non-navigable entrance channel, as presently designed, appears to be larger than what would be maintained by the calculated tidal prism. However, this doesn't represent a problem unless subsequent analysis of the tidal circulation in the bay indicates a reduced entrance throat area somehow degrades the circulation within the bay and the water exchange between the bay and ocean. Greater concern is expressed about the ability of the channel to remain open under the action of littoral processes without the protection of a dual jetty system extending into the surf zone at least beyond the mean lower low water line. Two examples of similar-sized projects were discussed. The possibility that the presently designed non-navigable entrance may close periodically or may require routine maintenance dredging should be a consideration in evaluation of this alternative.

41. The proposed navigable ocean entrance system, as designed, cannot be classed as a tidal inlet in equilibrium because the design is not based on the entrance being maintained by scouring water velocities. The entrance instead is designed to prevent sediment from entering the inlet channel, thus making the entrance system a barrier to the majority of longshore-moving sediment. Material that does enter the channel will deposit, and periodic dredging may be required to maintain the entrance channel at its design dimensions.

References

Hales, L. Z., Bird, S. L., Walton, R., and Ebersole, B. A. 1989. "Tidal Circulation and Transport Computer Simulation, and Water Quality Assessment, Report 3: Bolsa Bay, California, Proposed Ocean Entrance System Study," Miscellaneous Paper CERC-, US Army Engineer Waterways Experiment Station, Coastal Engineering Research Center, Vicksburg, MS.

Jarrett, J. T. 1976. "Tidal Prism - Inlet Area Relationships," GITI Report 3, US Army Engineer Waterways Experiment Station, Coastal Engineering Research Center, Vicksburg, MS.

Jenkins, S. A., Inman, D. L., and Bailard, J. A. 1980. "Opening and Maintaining Tidal Lagoons & Estuaries," Proceedings of the 17th Conference on Coastal Engineering, ASCE, Vol 2, pp 1528-1547.

Johnson, J. W. 1973. "Characteristics and Behavior of Pacific Coast (sic) Tidal Inlets," Journal of the Waterways, Harbors, and Coastal Engineering Division, ASCE, Vol 99, No. WW3, pp 325-339.

O'Brien, M. P. 1931. "Estuary Tidal Prisms Related to Entrance Areas," Civil Engineer, Vol 1, No. 8, pp 738-739.

O'Brien, M. P. 1969. "Equilibrium Flow Areas of Tidal Inlets on Sandy Coasts," Journal of Waterways and Harbors Division, ASCE, Vol 95, No. WW1, pp 43-45.

O'Brien, M. P. 1976. "Notes on Tidal Inlets on Sandy Shores," GITI Report 5, US Army Engineer Waterways Experiment Station, Coastal Engineering Research Center, Vicksburg, MS.

US Army Engineer District, Los Angeles. 1986. "Oral History of Coastal Engineering Activities in Southern California," US Army Engineer District, Los Angeles, Los Angeles, CA.

APPENDIX D: BOLSA CHICA SURF CLIMATE STUDIES

Dr. William R. Dally

Background

1. Before describing existing surfing conditions at Bolsa Chica, and identifying potential impacts of the proposed navigation project on the local wave climate and the subsequent effects on recreational surfing, some background on the criterion for a good surfbreak will be useful. In general the suitability of a particular wave for surfing is determined by the comparison of two speeds: 1) the speed that can be maintained by the surfer as he travels along the face of the wave (called the "board speed"), and 2) the speed at which the point at incipient breaking moves along the wave crest (called the "peel rate"). For a wave to be rideable, the surfer must be able to travel with a mean speed sufficient to stay ahead of the translating break point; otherwise, the wave is said to "close out." The board speed that can be attained is determined by the size and shape of the face of the breaking wave, board characteristics, and the weight of the surfer. The peel rate is for the most part governed by the local gradient in wave height along the wave crest, and the wave celerity. The board speed and peel rate can be quantified to some degree using commonly measured wave parameters.

Board Speed

2. Quantitative prediction of board speed relative to the wave face for given board and wave characteristics is beyond present capabilities, and would require a comprehensive program of basic research. Although direct measurements of the speeds attainable by surfers have (to the author's knowledge) never been attempted, estimates of mean board speed have been made by Walker (1974) based on aerial photographs and a calculated wave celerity. Of the 16 rides examined by Walker, the largest sustained speed was approximately 38 ft/s, which provides some indication of the upper limit that can be associated with prime surfing conditions. To move beyond a solely descriptive treatment of attainable board speed, several engineering parameters are available which provide a qualitative model.

3. For a given surfboard and surfer weight, the physical parameters that govern the mean board speed that can be sustained during the ride are the size of the breaker, denoted by the wave height at breaking, H_b , and the steepness of the face of the wave in the region ahead of the white water. General observations indicate that the minimum breaker height required for enjoyable surfing is approximately 2 ft. As wave height increases beyond this base criterion, the shape of the wave face plays the premier role in determining board speed. Because greater board speeds can be attained on a plunging breaker than a spilling breaker, with plunging conditions clearly preferred by surfers, breaker type can be utilized to characterize wave face shape. The parameters which most directly affect breaker type and thereby the steepness of the face of a wave at its break point are:

- a. Wave period T or deepwater wave length, $L_0 = gT^2/2\pi$.
- b. Wave height in deep water H_0 .
- c. Local bottom slope m .
- d. Local wind speed and direction.

4. Although it is common knowledge that gentle offshore winds tend to enhance the shape of the wave face, and onshore winds are detrimental, the effects of wind on the surfbreak have not been quantified to any degree. If winds are neglected, generally the wave face at breaking becomes steeper as period increases, wave height decreases, or bottom slope increases. The combined effects of these parameters can be expressed in terms of the non-dimensional Irribarren Number I_b given by

$$I_b = \frac{m}{(H_b/L_0)^{1/2}} \quad (D1)$$

5. Battjes (1974) utilizes this "surf similarity" parameter and the laboratory results of Galvin (1968) to loosely classify breaker types. Spilling breakers result from low Irribarren Numbers, generally less than approximately 0.4. These breaking conditions typically do not produce a wave face steep enough to ride, and are termed "mushy" by surfers. Values of I_b between 0.4 and about 2.0 indicate the plunging breaker conditions which provide the best surfing, and are referred to as "hollow" or a "tube". An Irribarren Number greater than 2.0 will usually result in a surging or collapsing breaker, which is unsurfable. The Irribarren Number can therefore be

utilized as a quantitative indicator of attainable board speed. These classifications are summarized in Table D1.

Table D1
Surf Climate Classifications

<u>Irribarren Number</u>	<u>Breaker Type</u>	<u>Surfing Terminology</u>
$I_b < 0.4$	Spilling	"mushy"
$0.4 < I_b < 2.0$	Plunging	"tube", "hollow"
$2.0 < I_b$	Surging	[unsurfable]

Peel Rate

6. Even if wave conditions and bottom slope fall within the best range, and a hollow plunging breaker forms; the wave will not be rideable if it closes out, i.e., if the wave breaks simultaneously, or nearly so, everywhere along its crest. Therefore, the incipient break point must translate at a rate less than the speed attainable by the surfer. As mentioned previously, this peel rate is determined by the local gradient in wave height along the crest. The larger the gradient, the slower the peel rate and the more surfable the wave becomes. If the gradient is only slight and the peel rate large, the surfer must choose a path along a straight line in the region of the wave where the slope of the face is approximately 45° in order to maximize board speed along the wave. As the peel rate decreases, the surfer has time to move up and down the face of the wave and extract a more acrobatic ride.

7. Several mechanisms which cause a gradient in wave height along the crest of the wave are commonly observed at work during good surfing conditions. The simplest case to examine is when the wave crest is continuous and the wave height is nearly uniform in the direction parallel to the bottom contours, i.e., the waves are long-crested. Incipient breaking is attained at the particular location where the wave crest intersects a certain depth contour, and if the waves are obliquely incident, as shown in Figure D1, the break point will translate at a finite speed. In this case the peel rate V_p is given simply by

$$V_p = \frac{C_b}{\sin \alpha} \quad (D2)$$

OBLIQUELY INCIDENT WAVES

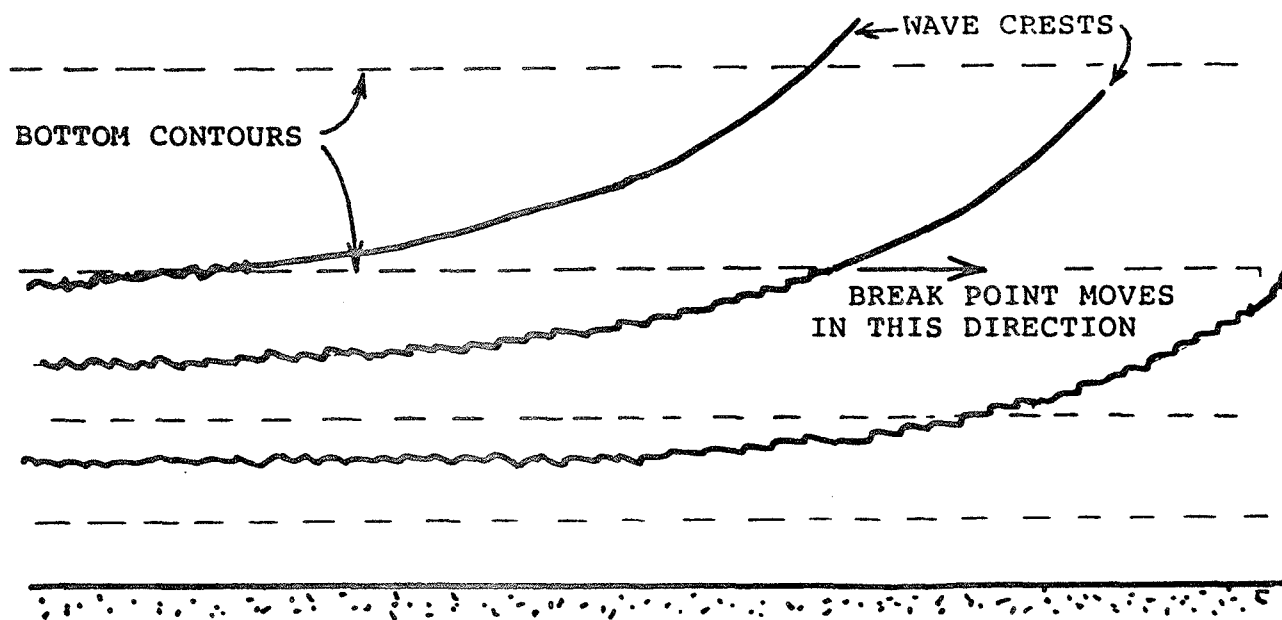


Figure D1. Schematic diagram of obliquely incident waves arriving at the surf zone. Due to angle between wave crests and bottom contours, break point translates along the beach at a finite speed.

where C_b is the wave celerity at the break point and α is the angle between the wave crest and bottom contours. As this angle decreases, the speed of the break point increases. A wave that approaches directly onshore will have a break point that translates at an infinite speed. By adopting linear wave theory to predict shoaling, it can be shown that $\sin \alpha$ can be expressed in terms of the longcrest gradient in wave height, dH/ds , and water depth, h :

$$\sin \alpha = \frac{4 h^{1/4}}{m H_b} \frac{dH}{ds} \quad (D3)$$

8. Wave obliqueness also occurs when waves (even waves approaching directly onshore) encounter irregular bottom features such as crescentic bars, as shown in Figure D2. In this situation, the angle between the wave crest and bottom contours produces two breakpoints that move at finite speeds but in opposite directions. Another bottom feature that often produces a translating breakpoint is a trough that runs perpendicular to shore, as often observed at a pier due to scouring effects.

9. Even when the waves are normally incident to straight and parallel bottom contours, if the wave height is not uniform along the crest, as it peels along the incipient break point will translate from deeper to shallower water due to the local gradient in height. The resulting peel rate is often slow enough for the wave to be surfable. Waves that approach almost directly onshore but initiate breaking at distinct peaks are perhaps the most commonly found surfing condition, often referred to as "beach break." By again invoking linear wave theory, it can be shown that the peel rate in this case is given by

$$V_{bp} = \frac{(gh)^{1/2}}{\sin\{\tan^{-1}[-(4/5) |dH/ds|/(K^{6/5}m)]\}} \quad (D4)$$

where g is gravity, h is the local depth, and K is the ratio of wave height to water depth at incipient breaking. This expression demonstrates that as the magnitude of the gradient increases the peel rate decreases, and the wave becomes more surfable. However, there is a trade-off in that the gradient in height also controls the length of the ride. If dH/ds is too great, the waves become very short-crested and the rides are short in duration. A model for peel rate produced by the combination of short-crested waves and oblique

IRREGULAR BOTTOM TOPOGRAPHY

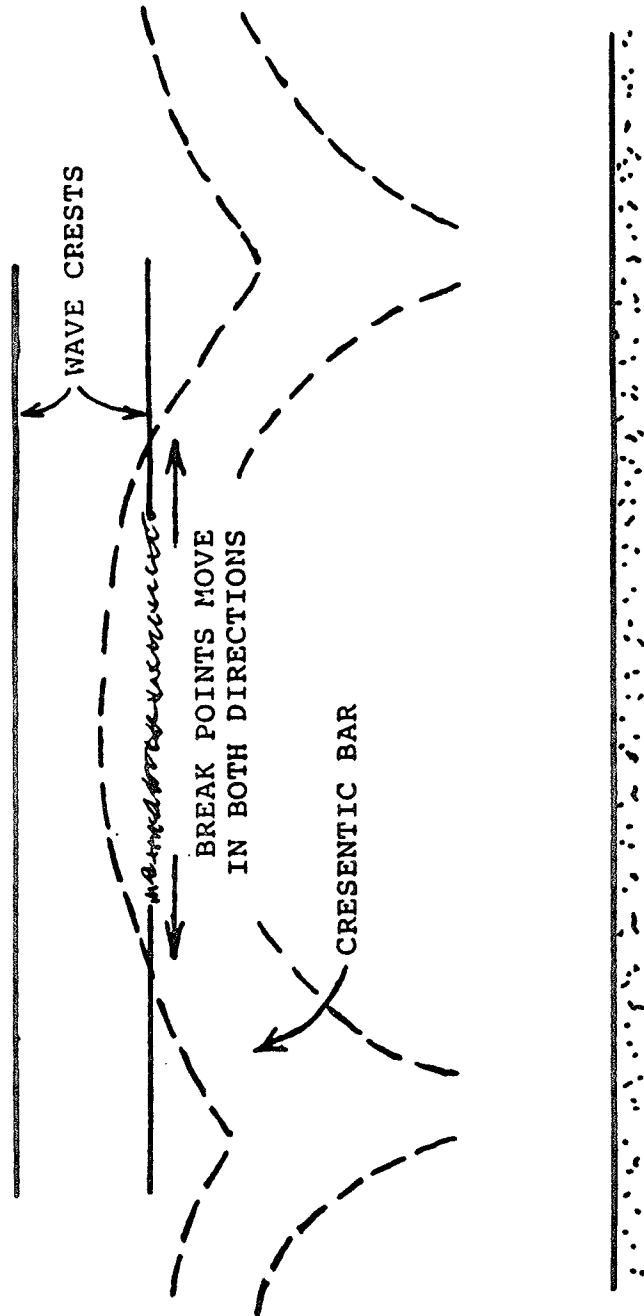


Figure D2. Schematic diagram of normally incident waves breaking over irregular topography (crescentic bar). Two break points form and translate in opposite directions.

incidence over straight and parallel bottom contours would provide a more complete description of beach break. This could be developed in a manner similar to Eqs. (D2), (D3), and (D4), if a typical value for the longshore slope of the wave crest was known.

10. Other common sources of two-dimensionality and the resulting long-crest gradient in height arise from 1) the existence of two different sources of waves, and 2) reflection of waves that are obliquely incident to coastal structures. In these instances, a "bowl" forms at the spot where the wave crests of the two trains superimpose. Here the wave height is increased, a longcrest gradient in height is formed, and the resulting wave face is often steep enough to ride. Because the breakpoint moves as the two waves pass through each other, a rideable surf is often produced. Figure D3 displays these features for waves reflecting from a shore-perpendicular structure. The size of the zone of interaction is determined geometrically by the length of the structure and the angle at which the waves strike.

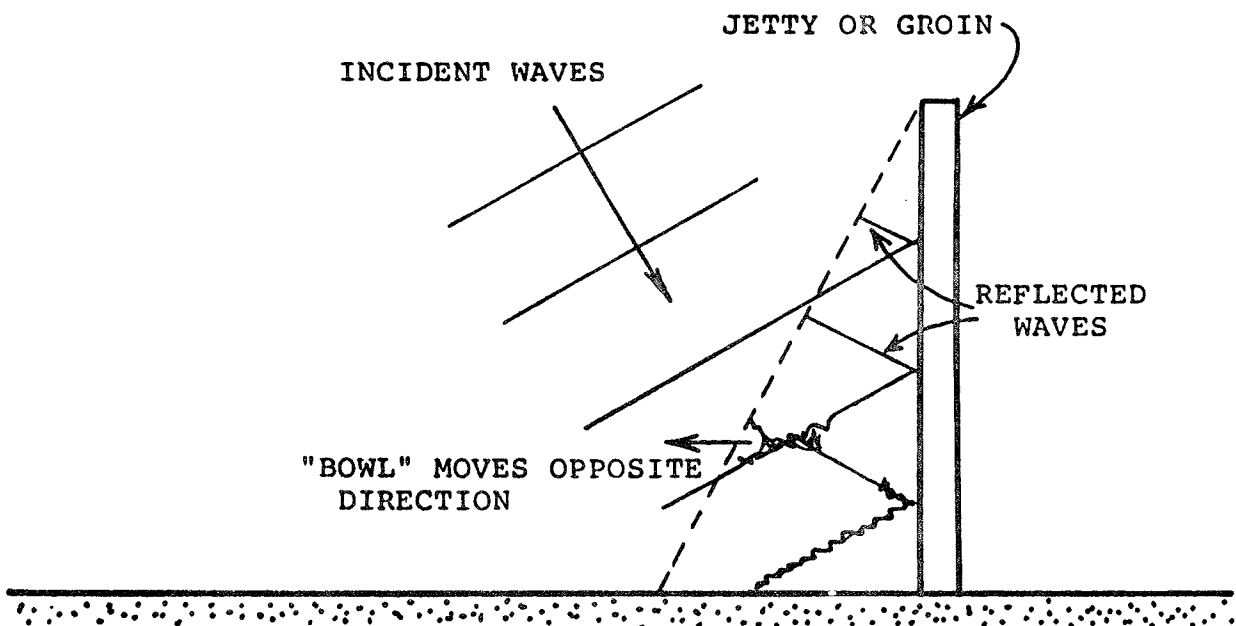


Figure D3. Schematic diagram of obliquely incident waves reflecting from a shore-normal structure. Point where wave crests superimpose steepens to form a "bowl" that translates opposite to the direction of incident waves.

Existing Conditions at Bolsa Chica

11. With some background established on the physical criteria for a good surfbreak, existing surfing conditions at Bolsa Chica can now be examined and discussed. Both qualitative and quantitative information are available for use in this analysis.

Qualitative Description

12. Qualitative information on surfing conditions at Bolsa Chica was obtained during a telephone interview with a local enthusiast who surfs at Bolsa Chica several times per week, and through personal interviews conducted on September 28, 1988, with six different surfers as they exited the water at the project site. The following points comprise a consensus of opinion.

- a. At times when a good (sizeable) swell arrives in the region, there is usually a rideable break at Bolsa Chica. That is, if there is good surf at other surfing spots nearby, such as the pier at Huntington Beach, surfable conditions can be expected at Bolsa Chica.
- b. There is not a particular location in the park where the surf break is best, and the type of break changes frequently.
- c. The break often goes "both right and left", which means that the break point of a single wave translates in both directions and provides the surfer with a greater variety of rides.
- d. The best waves come from the west-north-west during the winter months and from the south in the summer months.
- e. The surfbreak rarely closes out.
- f. Surfing is best in the morning before the sea breeze becomes strong.

13. Based on the discussion in the background section, observations (b), (c), and (e) indicate that the break at Bolsa Chica is a typical beach break, and that the most common surfing conditions are the result of short-crested, two-dimensionality in the wave climate. There is also a possibility that crescentic bars might contribute to the break because both of these conditions promote waves that break right and left, and reduce the tendency to close out. Clearly though, observation (b) indicates that there is not a perennial feature in the nearshore bathymetry on which surfing conditions depend; and if bars do contribute, they are probably of secondary importance. Observation (d) is typical for the region, as winter storms occur in the

northern Pacific while the less frequent summer storms are generated towards the south. These conditions are best because the incoming swell is generally long-crested and therefore promotes long rides, and approaches at angles sufficiently oblique to prevent closing out. The fact that the surf is best in the morning before onshore winds grow is common to most coastlines and is a major factor to consider in surf climate analyses.

Quantitative Description

14. It is noted that the above description of the surfing climate applies only when sizeable waves are present, and provides little quantitative information as to what percent of the time surfable conditions exist at Bolsa Chica. The best available source of quantitative wave climate information for the Bolsa Chica site was provided by the Littoral Environment Observation Program (LEO) operated by the U.S. Army Corps of Engineers. These data were collected visually from the beach by a trained observer as described in Sherlock and Szuwalski (1987). Observations from Bolsa Chica, taken once or twice per day, were available from April, 1968, to December, 1970, and from January, 1980, to May, 1982. These measurements and visual estimates of maximum breaker height, average wave period, wave direction at breaking, breaker type, wind speed, and wind direction were utilized to characterize and quantify the surf climate, as described below. LEO observations are especially appropriate for surfing studies because 1) they focus on the outer surf zone, where surfers prefer to line up to catch waves, and 2) they are taken manually rather than with instruments, and so are more easily understood and interpreted by surfers.

15. To prevent seasonal bias in the results, the available LEO data for Bolsa Chica were edited to include only those time intervals that extended continuously over a whole number of years. Consequently, two years of observations from April 20, 1968, to April 19, 1970, and one year from March 1, 1980, to February 28, 1981, were used in the analysis. The first set contained 880 observations and the second 357. In mid 1970, subsequent to collection of the first set but before collection of the second, the measurement techniques for several of the parameters were improved. The data sets were therefore analyzed separately.

16. Table D2 presents probability of occurrence as a joint function of breaker height and mean wave period for the two data sets. Wave conditions

Table D2
Joint Probability of Wave Height and Period

Periods (s)	Height, ft									
	<1.0	2.0	3.0	4.0	5.0	6.0	7.0	8.0	9.0	10.0
<u>20 April 1968 - 19 April 1970</u>										
<2.0	0.0	0.0	0.1	0.0	0.0	0.0	0.1	0.0	0.0	0.0
3.0	0.0	0.0	0.1	0.2	0.0	0.0	0.0	0.0	0.0	0.0
4.0	0.0	0.0	0.0	0.2	0.0	0.0	0.0	0.0	0.0	0.0
5.0	0.0	0.5	0.6	0.7	0.5	0.0	0.0	0.0	0.0	0.0
6.0	0.0	0.3	0.6	0.6	0.3	0.0	0.0	0.0	0.0	0.0
7.0	0.0	0.1	0.2	0.7	0.0	0.1	0.0	0.0	0.0	0.0
8.0	0.0	1.0	1.0	0.2	0.2	0.2	0.0	0.0	0.0	0.0
9.0	0.0	0.7	1.0	0.7	0.5	0.0	0.2	0.0	0.0	0.0
10.0	0.0	1.3	1.6	1.0	0.3	0.2	0.0	0.0	0.1	0.0
11.0	0.0	2.0	3.4	2.4	0.3	0.1	0.0	0.1	0.0	0.0
12.0	0.0	1.5	3.1	1.9	0.7	0.2	0.0	0.0	0.0	0.0
13.0	0.0	2.6	6.8	3.0	0.7	0.1	0.1	0.0	0.0	0.0
14.0	0.0	3.1	5.7	3.1	0.9	0.1	0.1	0.0	0.0	0.2
15.0	0.0	1.4	3.2	1.6	0.8	0.3	0.1	0.0	0.0	0.0
16.0	0.0	1.0	3.3	1.1	0.3	0.1	0.0	0.0	0.0	0.0
17.0	0.0	1.1	2.4	1.1	0.2	0.0	0.0	0.0	0.0	0.0
18.0	0.0	1.4	2.6	0.8	0.3	0.0	0.0	0.0	0.0	0.0
19.0	0.0	1.0	1.9	1.1	1.0	0.0	0.0	0.0	0.0	0.0
20.0	0.0	1.0	0.5	1.0	0.0	0.0	0.0	0.0	0.0	0.1
21.0	0.0	0.5	1.0	0.3	0.0	0.0	0.1	0.0	0.0	0.0
22.0	0.0	1.8	2.0	1.6	0.3	0.0	0.0	0.0	0.0	0.0
<u>1 March 1980 - 28 February 1981</u>										
<1.0	0.0	0.0	0.0	0.0	0.0	0.0	0.0	0.0	0.0	0.0
2.0	0.0	0.3	0.0	0.0	0.0	0.0	0.0	0.0	0.0	0.0
3.0	0.0	0.0	0.0	0.0	0.0	0.0	0.0	0.0	0.0	0.0
4.0	0.0	0.0	0.0	0.0	0.0	0.0	0.0	0.0	0.0	0.0
5.0	0.0	0.0	0.0	0.0	0.0	0.0	0.0	0.0	0.0	0.0
6.0	0.0	0.0	0.0	0.0	0.0	0.0	0.0	0.0	0.0	0.0
7.0	0.6	0.0	0.6	0.3	0.0	0.0	0.0	0.0	0.0	0.0
8.0	0.3	1.7	0.6	0.0	0.3	0.0	0.0	0.0	0.0	0.0
9.0	0.0	1.1	0.8	0.0	0.0	0.0	0.0	0.0	0.0	0.0
10.0	0.8	1.4	1.4	1.1	0.0	0.0	0.0	0.0	0.0	0.3
11.0	0.3	1.1	2.5	1.4	1.4	0.0	0.3	0.0	0.3	0.0
12.0	0.0	3.1	5.3	2.0	1.4	0.3	0.3	0.3	0.0	0.0
13.0	0.0	9.2	5.6	3.4	0.8	1.1	0.6	0.3	0.3	0.0
14.0	0.6	3.1	4.5	2.5	0.8	0.6	0.6	0.3	0.3	0.0
15.0	0.3	4.8	2.5	2.5	0.8	0.3	0.0	0.0	0.0	0.0
16.0	0.0	2.8	2.5	1.4	0.3	0.0	0.0	0.0	0.0	0.0
17.0	0.3	0.8	2.0	1.7	0.0	0.0	0.0	0.0	0.0	0.0
18.0	0.0	1.4	1.1	0.0	0.3	0.0	0.0	0.0	0.0	0.0
19.0	0.0	0.6	1.4	0.6	0.0	0.0	0.0	0.0	0.0	0.0
20.0	0.0	0.0	0.0	0.0	0.0	0.0	0.0	0.0	0.0	0.0
21.0	0.0	0.3	0.3	0.0	0.0	0.0	0.0	0.0	0.0	0.0
22.0	0.6	2.8	0.3	0.3	0.3	0.0	0.0	0.3	0.0	0.0

were calm ("flat") for 1% of the time in the first set and 2% of the time in the second. In the earlier set, many of the measurements of height were estimated only to the nearest foot. The most commonly occurring conditions are $2.0 < H_b < 2.9$ ft and $12.0 < \bar{T} < 12.9$ s in the first set, and $1.0 < H_b < 1.9$ ft and $12.0 < \bar{T} < 12.9$ s in the second. Figures D4 and D5 display histograms of height and period respectively for the two data sets. The mean values for height and period were 2.2 ft and 13.2 s during the earlier time period, and 2.4 ft and 13.1 s during the latter time period.

17. Table D3 presents histograms of observed breaker angle or direction. In the first set, the direction from which the waves approached was estimated only to the nearest point of an eight point compass (N, NE, E, SE, S, SW, W, and NW), which is somewhat crude and subjective. The breaker angle was measured in the second set in relation to the shoreline orientation (in degrees) using a protractor and line of site, and is judged to be a less subjective and more accurate method. The shoreline orientation at Bolsa Chica is from NW to SE, so the two sets can be compared to each other within reason. The dominant direction is clearly out of the SW ($80^\circ < \theta < 100^\circ$) which is directly onshore. The greater spread present in the earlier set is attributed to the inherent inaccuracies in the estimates, and the second set is in all likelihood more reliable.

Table D3
Probability of Breaker Angle and Direction

a) April 20, 1968 - April 19, 1970				
SE	S	SW	W	NW
3%	22%	41%	23%	3%

b) March 1, 1980 - February 28, 1981								
Angle in degrees (90° = SW)								
<34	34-56	56-80	80-84	84-88	88-92	92-96	96-100	>100
.3%	.3%	8.4%	2.2%	14.0%	30.0%	17.4%	16.2%	10.6%
SE	S	WSW	SW					W

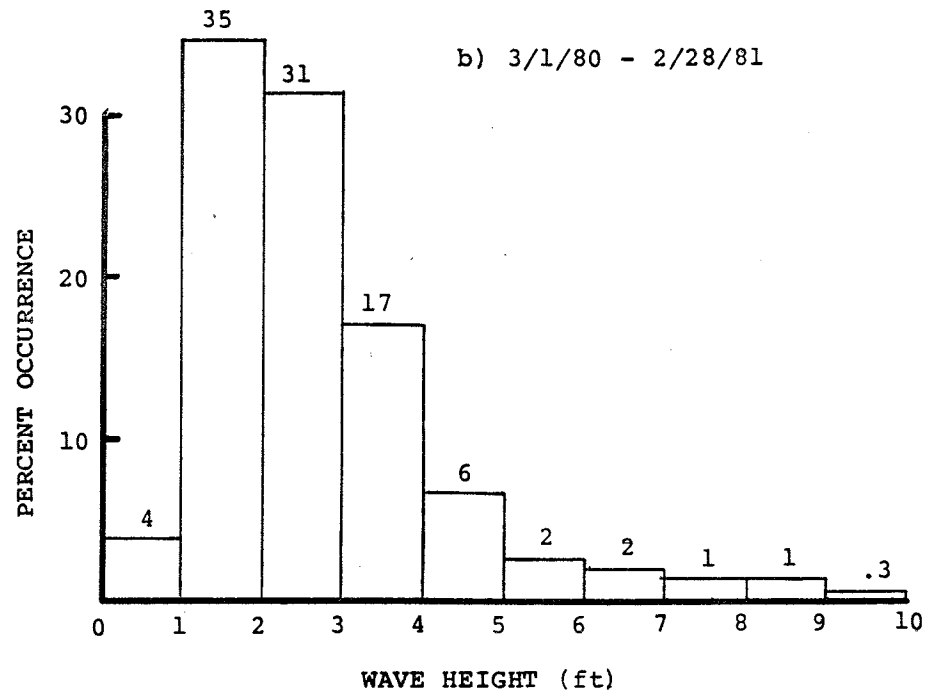
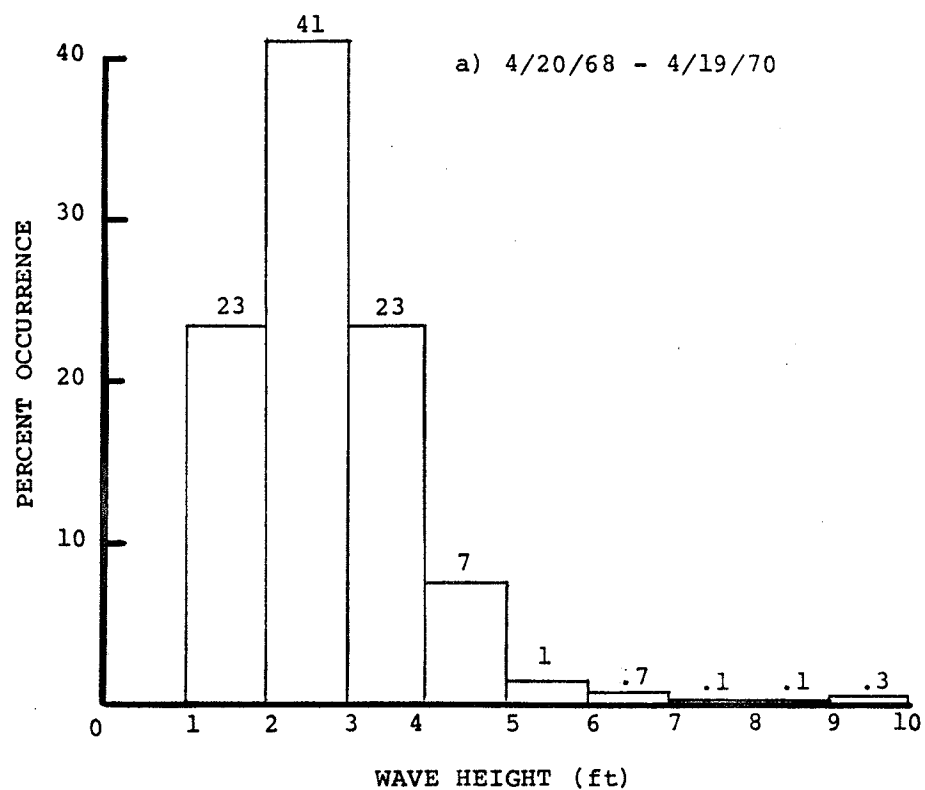


Figure D4. Histograms of maximum breaking wave height for Bolsa Chica generated from LEO data. Mean height is 2.2 ft in (4a) and 2.4 ft in (4b).

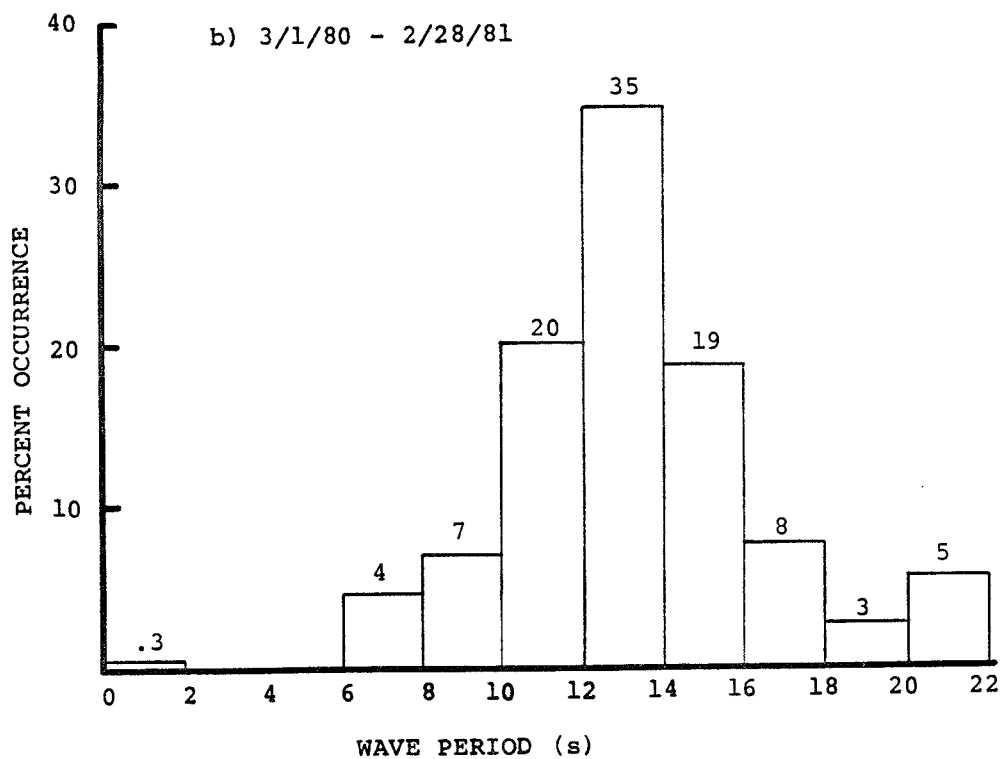
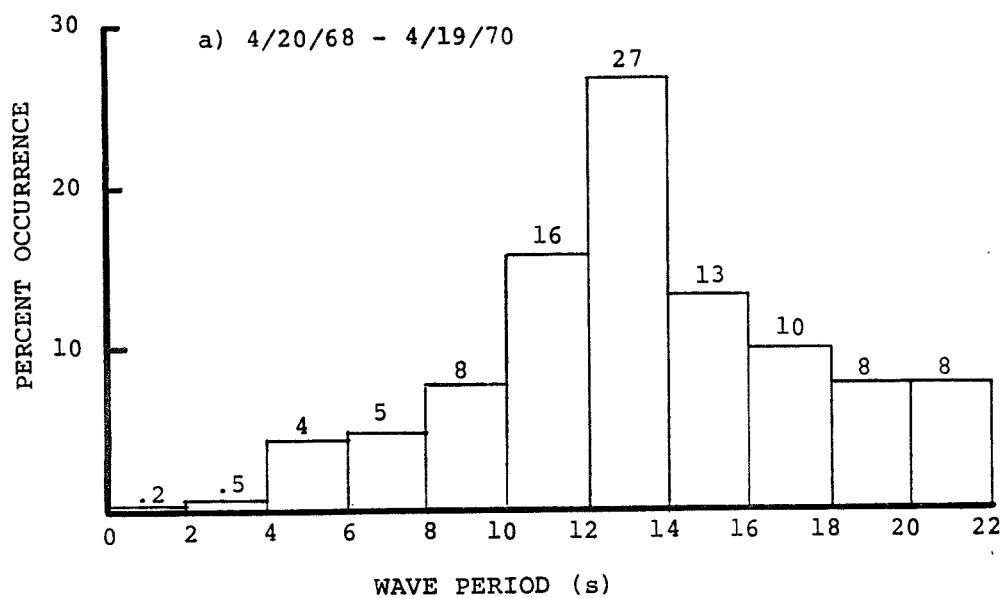


Figure D5. Histograms of mean wave period for Bolsa Chica. Average value in (5a) is 13.2 s and in (5b) 13.1 s.

18. Table D4 presents tabular joint probability of wind speed and direction, and Figures D6 and D7 display histograms of these parameters individually. Winds typically come out of the west and southwest (onshore), and are attributed to the sea breeze that occurs on many days. However, there was a distinct change in average wind speed between the two time periods, where the first set indicates an average of 2-6 mph while the second set shows 8-16 mph. Also, the winds were calm 16.8 and 4.8 percent of the time respectively. It is possible that long term climate cycles are responsible for this consistent increase in wind activity. Unfortunately, local onshore winds are detrimental to surfing conditions because they tend to reduce the steepness of the wave face at breaking, and result in spilling rather than plunging breakers. The data indicate that offshore winds (NE and E), which are favorable for surfing, occur at Bolsa Chica only a few times per year. They were found only 8.6% of the time in the first set and 3.2% in the second. A precise quantitative estimate of the effect of the wind on the shape of an individual breaker is not within present capabilities, so the role played by the wind in determining the surf climate at the park cannot be quantified to a significant degree. However, LEO data can be used to refine the descriptive observation stated previously, i.e., that surfing is best in the morning before the sea breeze becomes strong.

19. The final parameter recorded in the LEO data set that is relevant to surfing is observed breaker type. Table D5a contains the percent occurrence of breaker type from the first data set, in which the categories spilling, plunging, and surging were used. Spilling breakers had a 67% occurrence, plunging 18%, and surging 10%. Conditions were calm 2% of the time, and breaker type was unrecorded 3%. As shown in Table D5b, during collection of the second set the additional category in the transition between spilling and plunging was added. Spilling occurred 60%, spilling-plunging 29%, plunging 8%, surging 2%, and calm 1% of the time. These observations provided a basis for an initial estimate of the percent of time surfable waves can be found at Bolsa Chica. If large enough in height, plunging and spilling-plunging breakers usually provide the best surfing conditions. Although not the most desirable type, some spilling breakers are surfable. The second set indicates that, neglecting restrictions on height for the moment, surfable waves occur at least 37% of the time at Bolsa Chica.

Table D4
Joint Probability of Wind Speed and Direction

Speed (mph)	Direction							
	N	NE	E	SE	S	SW	W	NW
	<u>20 April 1968 - 19 April 1970</u>							
< 2.0	0.0	0.0	0.0	0.3	0.8	0.5	0.9	0.6
4.0	0.7	2.7	1.0	2.4	1.9	4.2	4.4	1.0
6.0	0.5	2.0	0.6	1.3	3.4	4.5	5.5	2.3
8.0	0.1	0.2	0.5	1.3	2.3	2.8	3.4	1.7
10.0	0.0	0.6	0.1	0.3	0.8	0.6	1.8	0.8
12.0	0.0	0.2	0.1	0.3	0.8	0.6	1.7	0.0
14.0	0.0	0.3	0.0	0.5	0.6	2.6	2.3	0.8
16.0	0.0	0.0	0.0	0.1	0.5	0.3	1.7	0.1
18.0	0.0	0.0	0.0	0.0	0.2	0.3	0.7	0.1
20.0	0.0	0.0	0.0	0.3	0.1	0.0	0.3	0.3
22.0	0.1	0.0	0.0	0.0	0.2	0.0	0.5	0.3
24.0	0.0	0.0	0.0	0.1	0.1	0.1	0.2	0.1
26.0	0.0	0.0	0.0	0.0	0.1	0.1	0.3	0.0
28.0	0.0	0.0	0.0	0.0	0.0	0.0	0.0	0.0
30.0	0.0	0.0	0.0	0.0	0.0	0.0	0.0	0.0
32.0	0.1	0.3	0.0	0.0	0.0	0.2	0.3	0.1

Winds calm - 16.8%

	<u>1 March 1980 - 28 February 1981</u>							
< 2.0	0.0	0.0	0.0	0.0	0.0	0.3	0.0	0.0
4.0	0.0	0.3	0.8	0.0	2.0	2.0	1.4	0.0
6.0	0.0	0.6	0.3	0.3	3.9	4.2	5.0	0.0
8.0	0.0	0.3	0.0	0.3	1.7	3.1	3.1	0.6
10.0	0.0	0.0	0.0	0.0	0.8	3.4	7.6	0.0
12.0	0.0	0.0	0.0	0.0	1.7	4.2	8.4	0.0
14.0	0.0	0.0	0.0	0.0	0.3	0.3	7.0	0.6
16.0	0.0	0.3	0.0	0.0	0.8	2.0	7.3	0.3
18.0	0.0	0.0	0.0	0.0	0.0	0.0	1.4	0.0
20.0	0.0	0.0	0.0	0.0	0.0	0.6	3.1	0.0
22.0	0.0	0.3	0.0	0.0	0.0	0.8	5.0	0.3
24.0	0.0	0.0	0.0	0.0	0.0	0.3	1.4	0.0
26.0	0.0	0.0	0.0	0.0	0.6	0.0	3.6	0.0
28.0	0.0	0.0	0.0	0.0	0.0	0.3	0.0	0.3
30.0	0.0	0.0	0.0	0.0	0.0	0.0	0.3	0.0
32.0	0.3	0.3	0.0	0.0	0.0	0.3	1.4	0.0

Winds calm - 4.8%

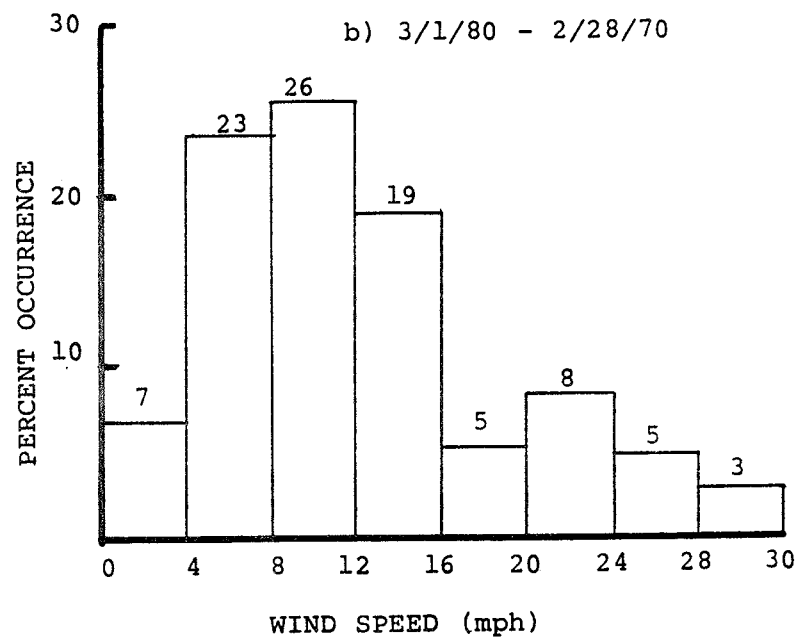
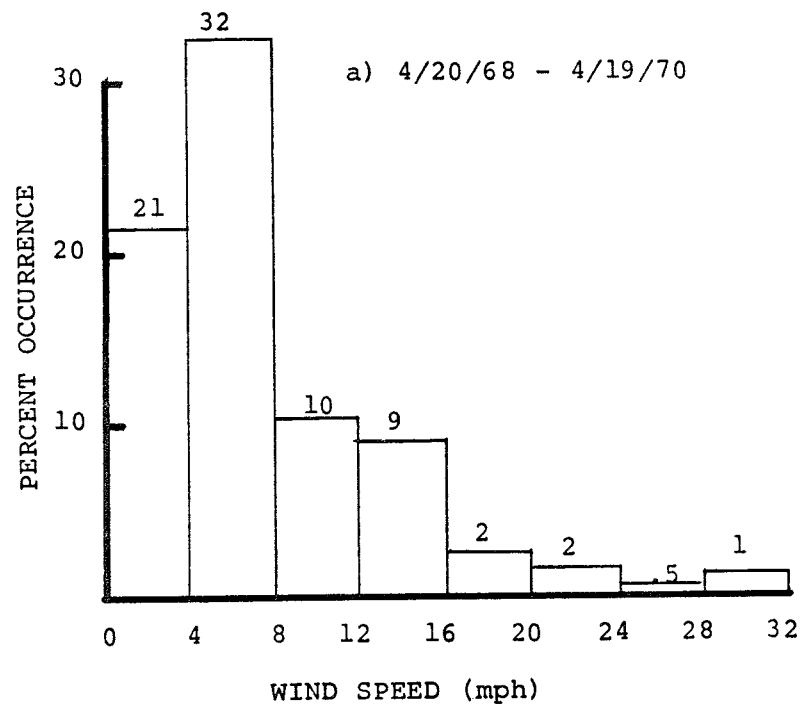


Figure D6. Histograms of wind speed generated from LEO data.

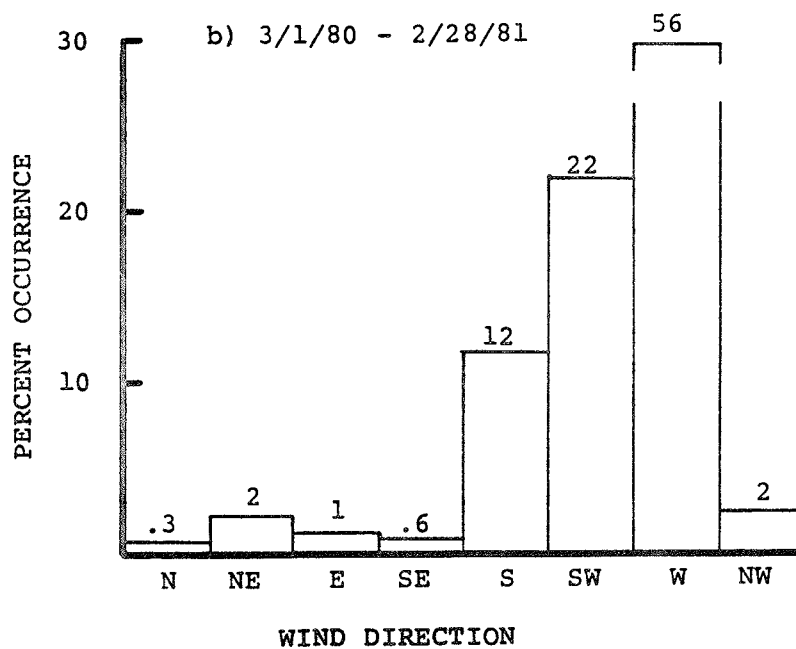
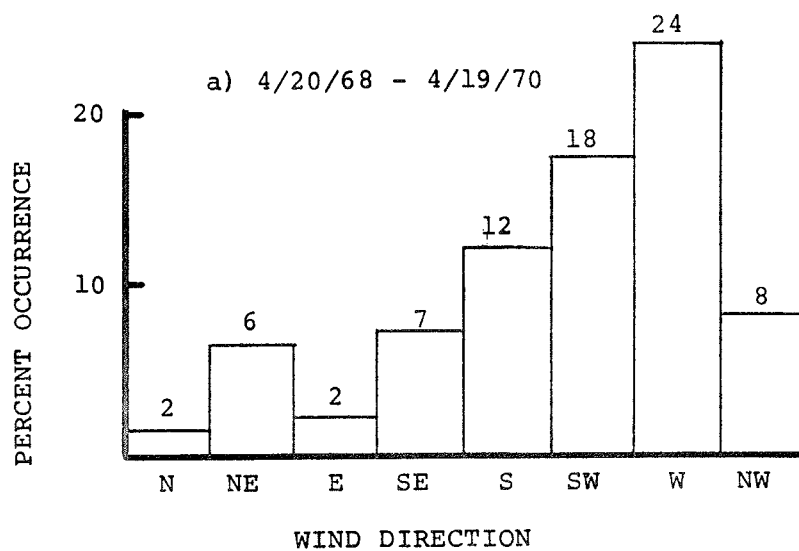


Figure D7. Histograms of wind direction.

Table D5
Percent Occurrence of Observed Breaker Types

a) April 20, 1968 - April 19, 1970			
<u>Spilling</u>	<u>Plunging</u>	<u>Surging</u>	
67%	18%	10%	
b) March 1, 1980 - February 28, 1981			
<u>Spilling</u>	<u>Spilling-Plunging</u>	<u>Plunging</u>	<u>Surging</u>
60%	29%	8%	2%

20. As mentioned above, the LEO data can be utilized to investigate the importance of wind on surfing conditions. From the observations of breaker height and mean wave period, along with a typical value for bottom slope, the statistics of the Irribarren Number can be generated for the Bolsa Chica site. Using Table D1, a prediction of the probability of occurrence of breaker type might then be made, with any significant differences from the observed statistics indicating effects of wind on the surf. Gravens (1988) provides several measured bottom profiles from Bolsa Chica, and a combined average is displayed in Figure D8. The average slope between MLLW and -5.0 ft MLLW is approximately 1/45. With this value for m along with LEO data, histograms of Irribarren Number (Eq. D1) can be generated, as shown in Figure D9. The first set has a mean Irribarren Number of 0.51, and shows that 37% of the waves fall within the spilling range and 60% in the plunging. The second set shows nearly identical behavior, with a mean value of 0.54, and 36% spilling and 63% plunging. No surging waves were predicted, most likely because these would only occur at high tide when the effective profile slope is much steeper than the average value chosen. By comparing these values to those from the observed breaker types (Table D5) it is noted that many more spilling breakers were observed than predicted. A crude estimate is that roughly half of the time the onshore winds are strong enough to shift the breaker type from plunging to spilling.

21. Relying on the observation that the surf at Bolsa Chica rarely closes out, criteria for surfable waves at the site can be established

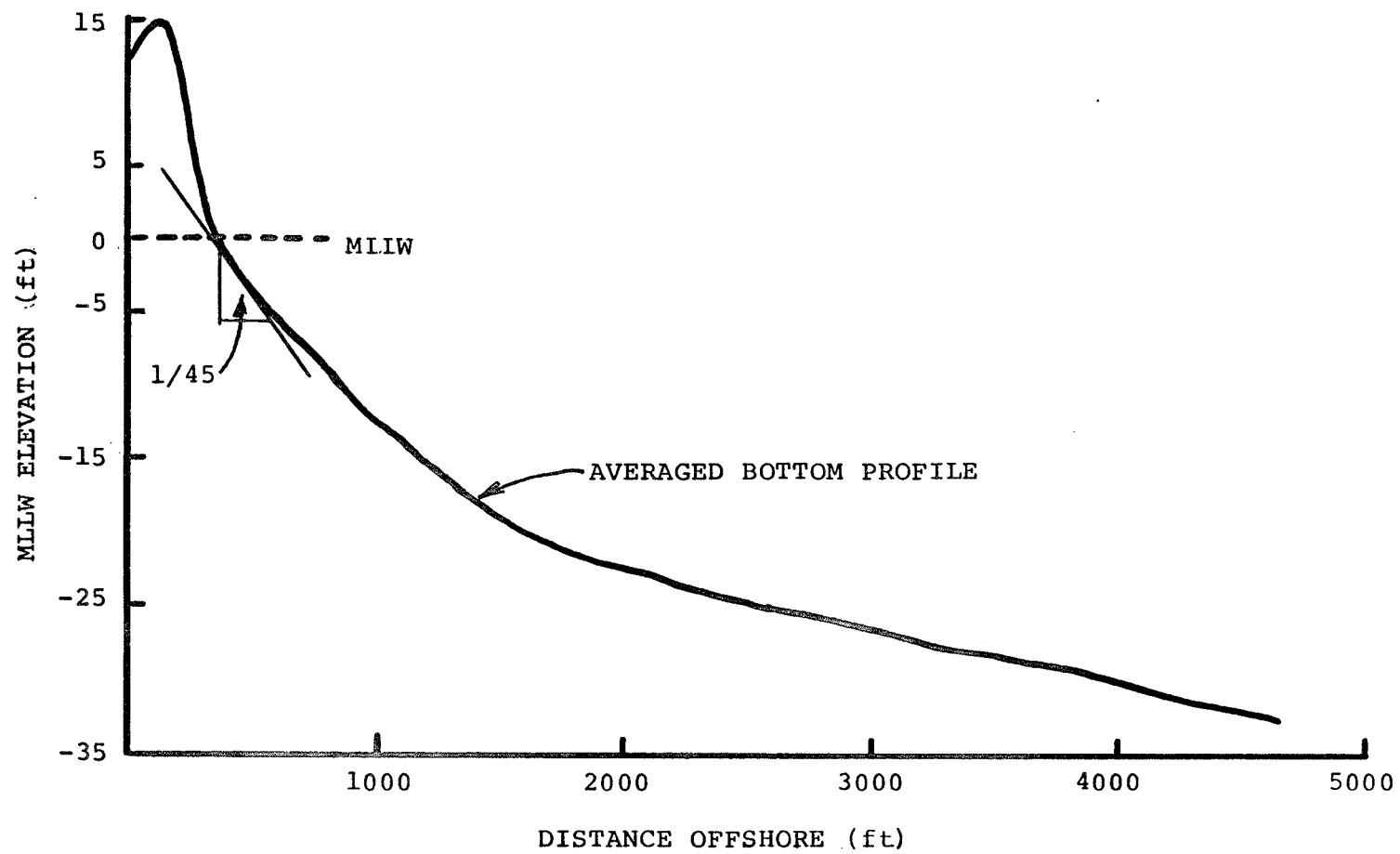


Figure D8. Averaged bottom profile for the beach at Bolsa Chica. Mean bottom slope between MLLW and -5.0 ft is approximately 1/45.

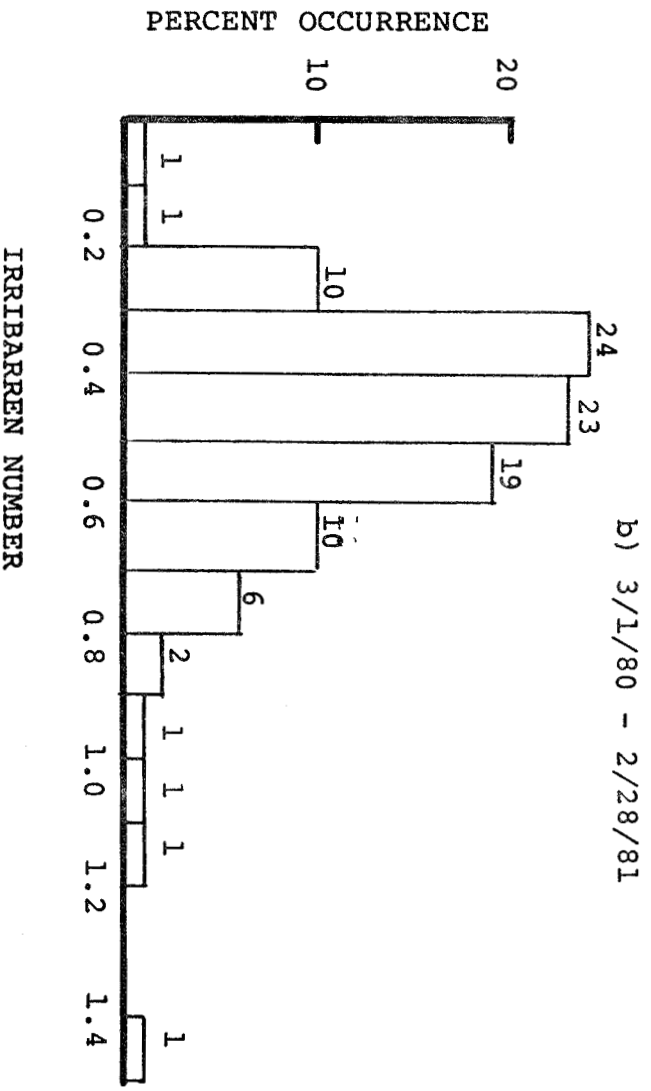
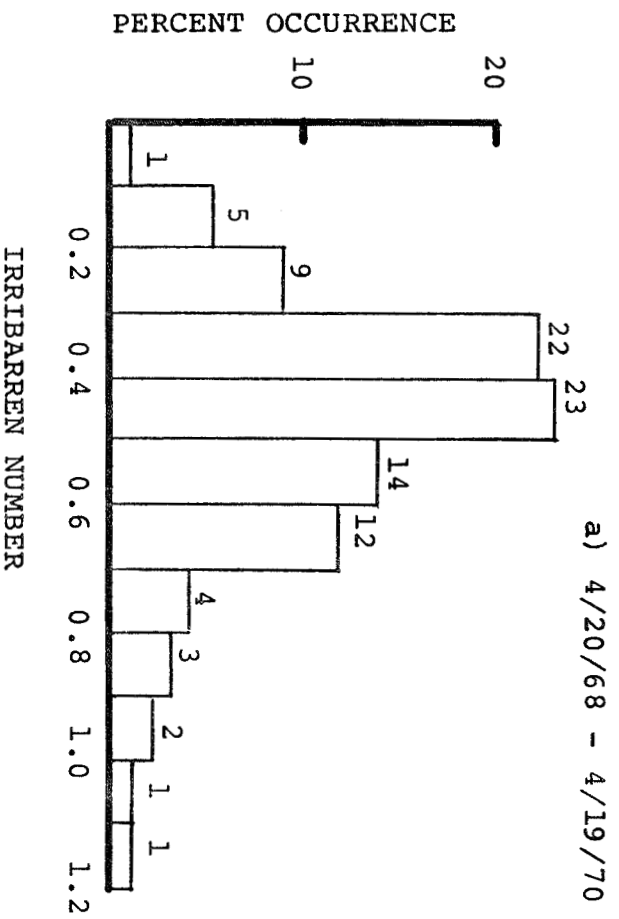


Figure D9. Histograms of Irribarren Number generated from LEO data. Most waves fall within the range of values for plunging breakers.

strictly in terms of observed breaker height, breaker type, and wind speed and direction. That is, if the height and shape of the breaker are suitable, it is assumed the peel rate is slow enough to preclude closing out. Conditions are considered to be unsurfable if any one of the following criteria are met:

- a. The observed breaker height is less than or equal to 2 ft.
- b. A surging breaker type is observed.
- c. The observed breaker type is spilling, the calculated Irribarren Number is less than 0.5, and the wind was out of the W, SW, or S at a speed greater than 10 mph.

Screening the data using these criteria, the first set of LEO observations indicates that existing conditions at Bolsa Chica are surfable 29% of the time, while the second set shows 39% occurrence of surfable conditions. This provides a reasonable number for the "surfability" of Bolsa Chica, i.e., surfable waves are present between 30 and 40 percent of the time.

Potential Impacts

22. With existing surfing conditions described, and quantified to a reasonable extent, potential impacts of the proposed project can now be identified and discussed in terms of the criteria set forth in the background section. Several configurations and lengths for the navigation structures have been examined during the course of the investigation of Bolsa Chica. The analysis provided below deals specifically with the original project design, which includes two jetties, extending to the 20 ft MLLW contour with a spacing of 800 ft, and an offshore breakwater, comprised of three sections with a total length of approximately 3200 ft. However, impacts of other variations of this design will be qualitatively the same, and could be quantified in a similar manner by utilizing the methodology described.

Primary Impacts

23. By far, the most salient impact of the proposed inlet project on surfing at Bolsa Chica will be the shadow zone cast by the offshore breakwater. Within most of this area, over most of the time, the requirement for sizeable waves will not be met. The size and position of this zone is easily determined to a suitable degree of accuracy by applying simple geometry,

whereby lines are extended towards shore from the two tips of the breakwater along the direction of the incident waves.

24. To determine wave direction at the proposed location of the offshore breakwater, conditions observed near the surf zone as provided by the LEO data must be transformed out to the appropriate water depth. Only the second data set contains measurements of wave angle of sufficient accuracy and resolution to accomplish this. Gravens (1988) performed these calculations, and transformed the wave observations out to a depth of 27 ft by utilizing linear wave theory to provide shoaling and refraction. This depth is just seaward of the proposed breakwater. Figure D10 displays the wave rose in its proper orientation and location with respect to the shoreline at the site. This rose has a mean wave direction that is almost directly onshore, but as expected has greater directional spread than the distribution observed near the surf zone, as indicated in Table D3b.

25. The projected geometric shadow zone for waves from the predominant direction is displayed in Figure D11, and shows:

- a. A region between the proposed jetties where there will be no opportunities for surfing.
- b. A region with a semicircular pattern of diffracted waves that will have smaller heights.
- c. A region outside the geometric shadow zone where surfing should be relatively unaffected.

26. Figure D12 shows that for the three most dominant directions, which account for a total of 80% of the incident waves, the shadow zone will be 3200 ft in length and will migrate over a total distance of approximately 4700 ft under this project configuration. For the more oblique directions the jetties begin to play a role, and for 10% of the time the project casts a total shadow approximately 3800 ft in length, as indicated in Figure D13.

Secondary Impacts

27. It is stressed that the numbers given above for the primary impacts provide a conservative estimate of lost surfing beach, because three secondary impacts can be identified that will serve to enhance the surfbreak to some degree. By its very nature, diffraction results in a gradient in wave height along the wave crest, which is the primary requirement for a peel rate suitable for surfing. In result the breakwater serves to improve the local surfbreak along the boundaries of the shadow zone. Also, the semicircular

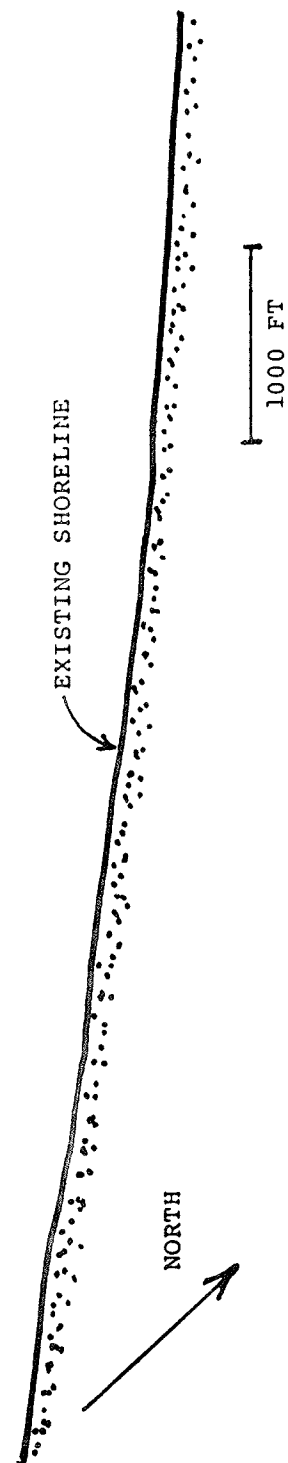
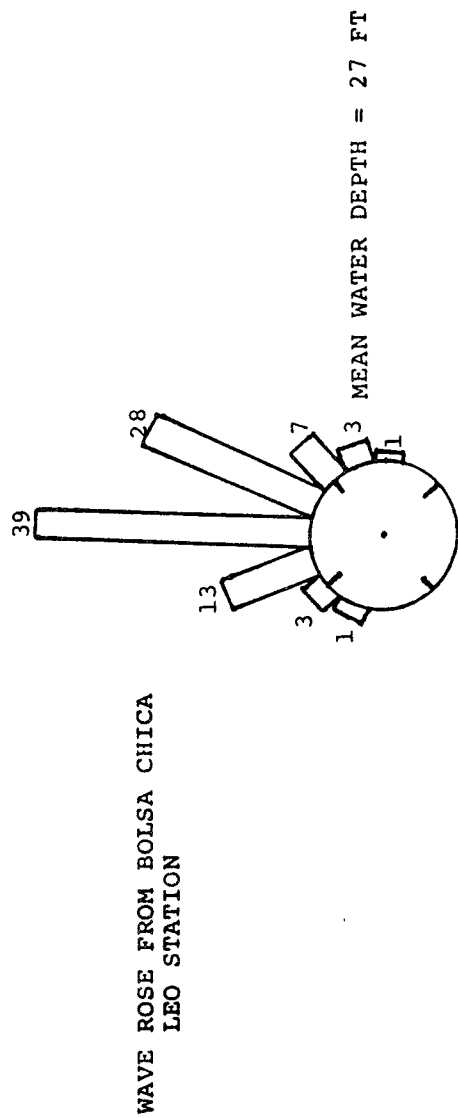


Figure D10. Wave rose oriented and positioned at 27 ft contour at site of proposed navigation project.
Generated from one year of LEO data and transformed using linear wave theory (after Gravens, 1988)

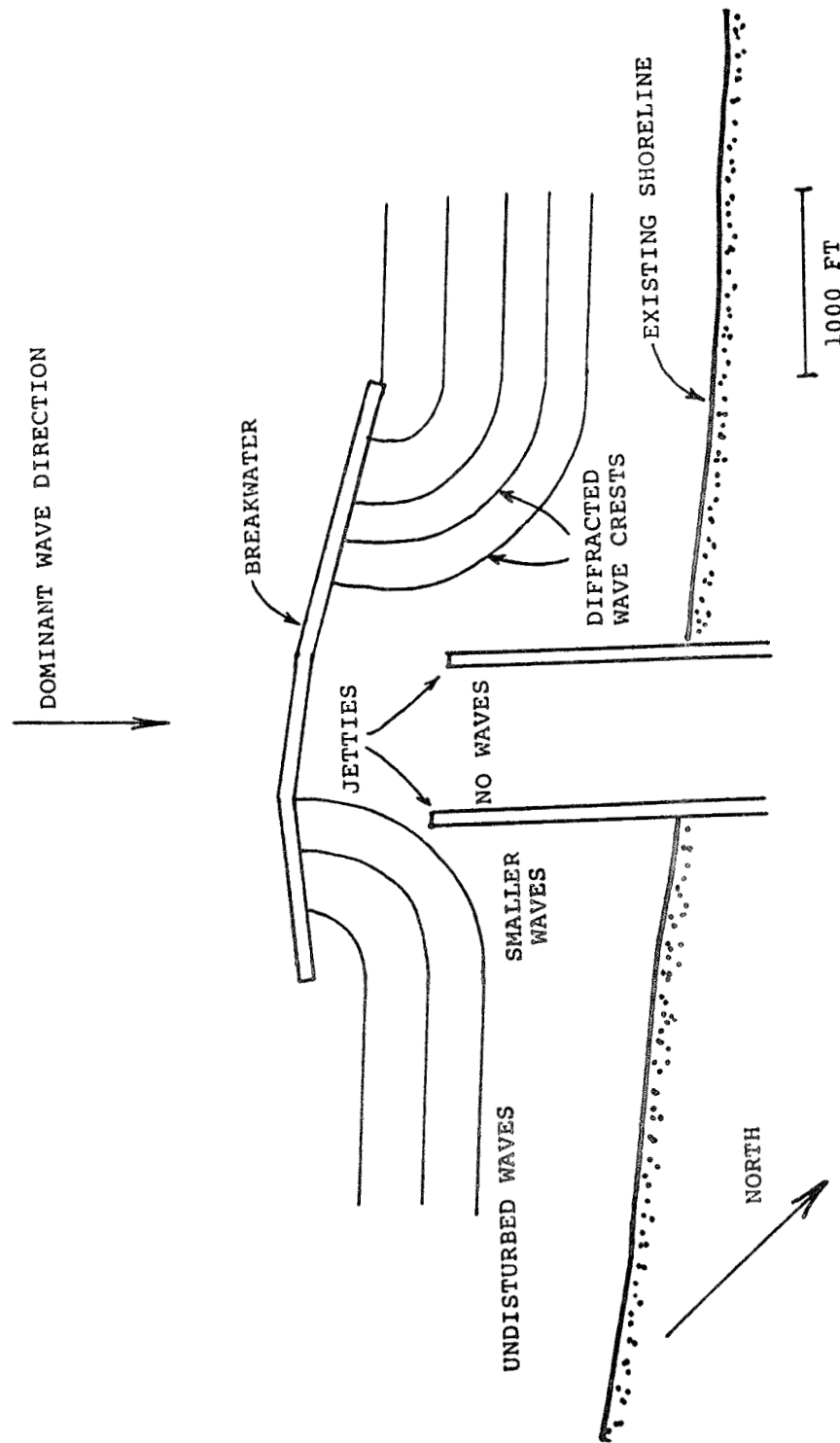


Figure D11. Schematic diagram of proposed navigation project and primary impacts on surf climate for dominant wave direction

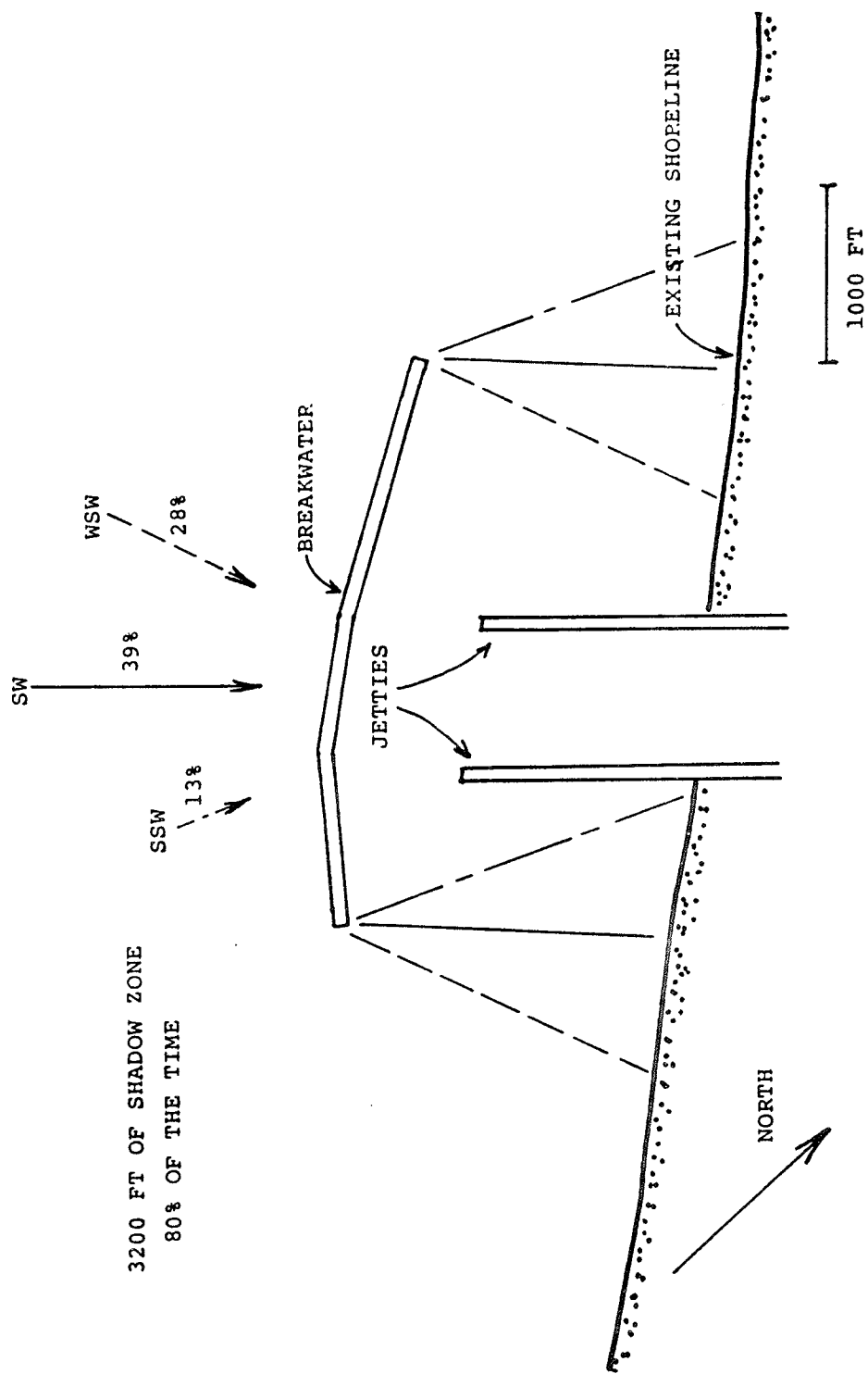


Figure D12. Shadow zone cast by offshore breakwater for the three dominant wave directions at Bolsa Chica.

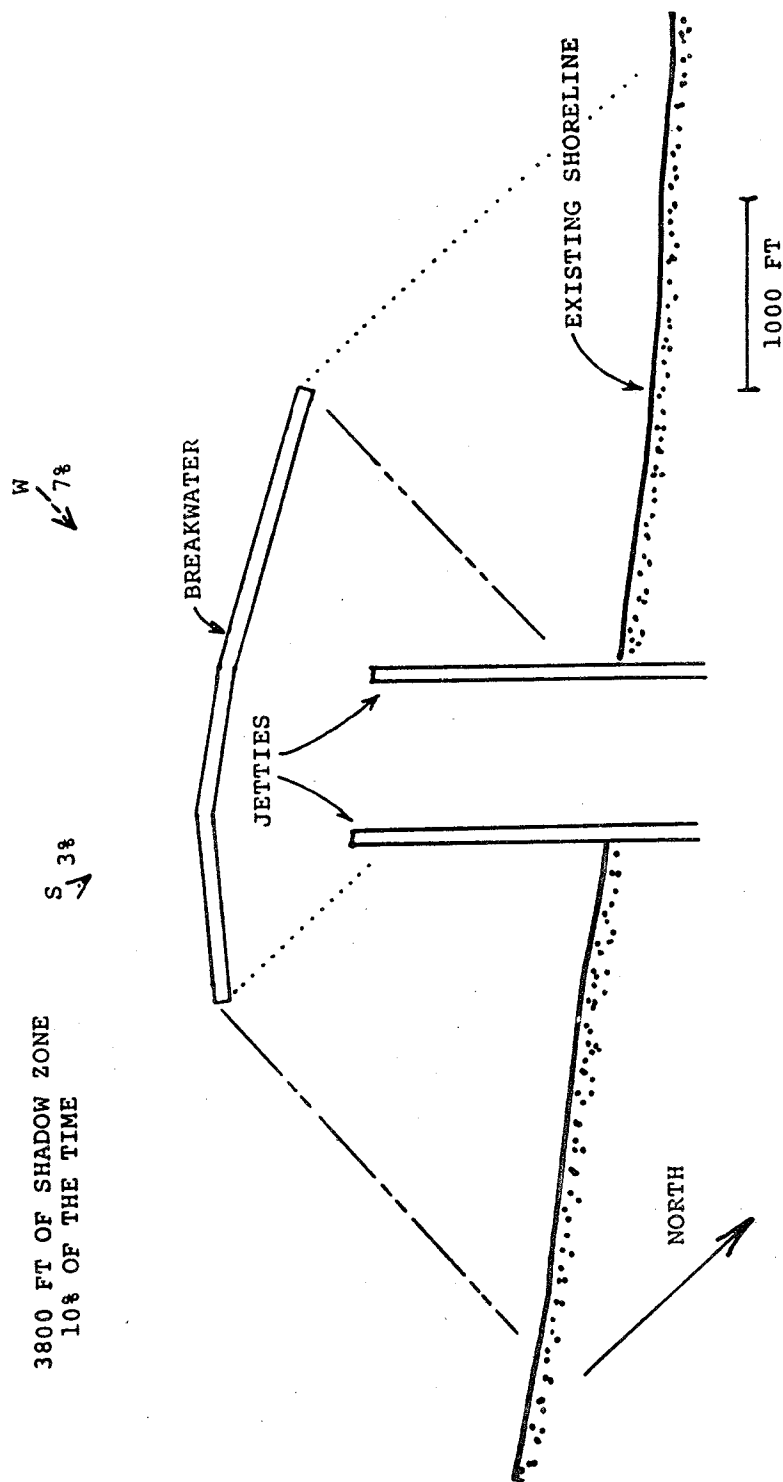


Figure D13. Shadow zone cast by offshore breakwater and jetties for the two secondary wave directions.

pattern of the diffracted wave crests tends to increase their obliqueness at breaking, further increasing the longcrest gradient in wave height and thereby enhancing the surfbreak.

28. In order to quantify to some extent the percent of time the diffracted waves will be surfable, the physical model at WES was operated under a variety of the more commonly occurring incident wave conditions. The diffracted breaking waves were videotaped and analyzed in slow motion/stop action to determine their peel rates. By applying Froude scaling, which dictates that the velocity scale between model and prototype is the square root of the length scale, the actual peel rates of breaking waves can be accurately predicted. Table D6 shows the conditions run, which encompass approximately 60% of the wave conditions found at the site, and the associated peel rates in model and prototype. In all but one of the tests, peel rates were documented at two different locations, usually on opposite sides of the inlet. As stated in the background section, the upper limit on attainable board speed is in the neighborhood of 38 ft/s (for larger waves), and so it appears that the diffracted waves will in many instances be surfable. It is important to note that these measurements were carried out with the existing bathymetry at the site in place. Bottom changes in response to the project may result in values for peel rates in the diffraction region different from those given in Table D6.

Table D6
Peel Rates for Diffracted Waves from Physical Model

Direction	Breaker Height (ft)	Period (s)	Peel Rate Model (ft/s)	Peel Rate Prototype (ft/s)
SW	2	12	3.0	26
SW (1st loc.)	4	14	4.9	42
SW (2nd loc.)	4	14	2.9	25
SW (1st loc.)	6	14	6.2	53
SW (2nd loc.)	6	14	2.8	24
WSW (1st loc.)	2	12	5.2	45
WSW (2nd loc.)	2	12	2.1	19
WSW (1st loc.)	4	14	3.3	29
WSW (2nd loc.)	4	14	2.2	19
WSW (1st loc.)	6	14	2.6	22
WSW (2nd loc.)	6	14	1.9	17

29. The second potential impact of the proposed navigation project on surfing at Bolsa Chica is in regards to wave reflection from the jetty structures. As described in the background section, the interaction of incident and reflected wave trains often serves to improve surfing due to a local increase in breaker height, steepening of the wave face, and formation of a bowl. This phenomenon was clearly evident during several tests of the physical model, especially during conditions of oblique incidence, and even with small incident heights. For higher waves with $H_b > 5$ ft (even those approaching directly onshore), diffraction and the associated semi-circular wave pattern would cause enough energy to penetrate the shadow zone and strike the jetty at an angle sufficient to create this type of break. The implication is that on days when waves are small or the faces of breakers are not steep enough to surf ("mushy" conditions), the triangular patch of enhanced surf next to one of the jetties may provide a rideable break. This occurs frequently at stabilized inlets such as Sebastian Inlet, Florida, which is one of the most popular surfing areas on the East Coast. Because the surf at Bolsa Chica is poor at least 60% of the time, mostly due to small wave heights, this patch of enhanced break could open the "window" for surfing conditions at the park considerably.

30. Finally, secondary impacts due to the shoreline response to the project are expected. At the present state-of-the-art, prediction of these impacts can only be qualitative at best, and relies on the accuracy of the modeling of the shoreline response immediately adjacent to the project. Figure D14 displays the predicted shoreline response from Test Case 1a reported in Gravens (1988). This prediction was made under the assumption that no sediment would be bypassed, and shows a region of sand deposition and shoreline advancement updrift (northwest) of the inlet, and a region of shoreline erosion downdrift. An increase in mean beach slope in the updrift region and a decrease in slope downdrift of the project will result. Waves updrift of the inlet will be slightly less affected by refraction before breaking takes place, and are likely to break at more oblique angles than under present conditions. The opposite is true for the downdrift area, with waves more closely aligned with the bottom contours as incipient breaking is attained.

31. The impacts of these shoreline changes can be inferred from the previous discussion of the criterion for a good surfbreak. Due to the changes

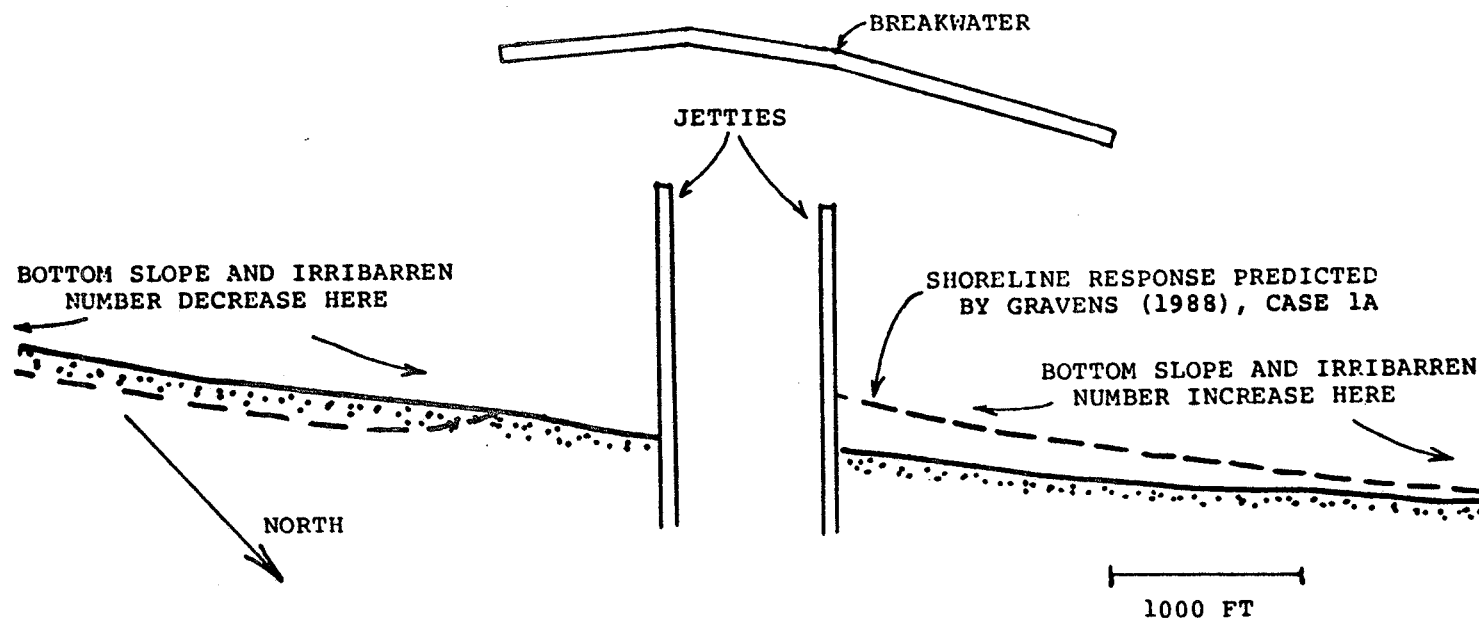


Figure D14. Projected shoreline response (Gravens, 1988) and expected changes in local Irribarren Number due to changes in mean bottom slope. Under this particular scenario, surfing conditions should improve updrift of the project

in mean beach slope, the Irribarren Number will increase updrift of the project and decrease in the downdrift region. Wave obliqueness at breaking should also increase updrift of the inlet due to steepening of the profile. Recalling that the predominant breaker type at the site is spilling, and the mean Irribarren Number under present conditions is at the lower end of the range for plunging breakers, it is expected that overall surfing conditions would improve updrift of the project. Following the same line of reasoning, one would expect surfing conditions to deteriorate in the downdrift region. The degree to which these impacts will occur cannot be quantified without a more detailed prediction of changes to the nearshore topography. More recent numerical shoreline response simulations, described in the main body of this report, indicate the project may be located near a nodal point in the littoral cell between the southern Anaheim jetty and the section of beach known as "the cliffs." If this is the case, sediment would deposit on both sides of the inlet in the shadow zone of the breakwater. Whatever the actual response, it can be concluded that in regions of shoreline advance the wave face shape will tend to be improved for surfing. In areas of retreat, conditions can be expected to deteriorate. It is not expected that improvements and detriments will exactly balance. Also, the role of smaller-scale bathymetric features on the existing surf break at the site has not been investigated. Vast and detailed bottom surveys with simultaneous observations of the surf break would be required to resolve this point. The effects of the proposed project on the nearshore bar system has not been established, and such a prediction is unfortunately beyond the present state-of-the-art.

32. As mentioned, it is quite possible that enhancement of surfing due to the secondary impacts will provide a greater window of opportunity for surfing at Bolsa Chica, i.e., incident wave conditions presently unsurfable due to small breaker heights, large peel rates, or poor wave face shape could become surfable. This will mitigate to some degree the loss of available space for surfing caused by the shadow zone. However, the enhancements cannot be completely quantified until 1) a complete sand management scheme is established, the resulting shoreline and bathymetric changes predicted, and the physical model operated with the shoreline in its altered state, and 2) basic measurements and research on the rudimentary mechanics of surfing are con-

ducted, e.g. study of board speed as a function wave shape, and wave shape as a function of Irribarren Number and wind conditions.

Summary, Conclusions, and Recommendations

33. The essence of the problem of quantifying the surfability of any beach lies in the determination of the joint statistics of 1) the peel rate of the breaking waves, and 2) the board speed attainable on these waves. Scientific investigations and predictive capabilities for these parameters are sorely lacking; however, they have been characterized herein in terms of the predicted or observed gradient in wave height along the wave crest, and the Irribarren Number. In general, surfbreak is improved as the Irribarren Number increases and the peel rate decreases.

34. Existing surfing conditions at Bolsa Chica can be classified as a typical beach break, with the quality of the surfbreak relatively uniform along the reach of the park. Waves are typically small (less than 3 ft) with periods between 11 and 13 s. Approximately 80% of the time they break nearly shore normal. However, inherent two-dimensionality in wave height (i.e. short-crested waves) provides peel rates slow enough to permit surfing. The average Irribarren Number is in the neighborhood of 0.5, which is in the transition between spilling and plunging breakers. Prevailing onshore winds often adversely effect the surfbreak by causing otherwise favorable conditions to form gently spilling breakers. From the analysis of three years of LEO data, it appears that surfable conditions can be found on the order of 40% of the time at Bolsa Chica.

35. The primary impact of the proposed navigable ocean entrance to surfing conditions at Bolsa Chica is the potential loss of approximately 3200 ft of surf break due to the shadow zone of the offshore breakwater. Approximately 3800 ft will be lost at times when the incident waves are strongly oblique. These conclusions are most likely to be conservative, as the secondary effects of the project will mitigate these losses to some degree. It is noted that the loss of surfbreak is incurred only at times when surfable waves would otherwise be present. Due to diffraction-induced wave obliqueness, surf enhanced by wave reflection from the jetties, and a predicted increase in the

Irribarren Number in the beach fillets created by the project, the percent of time rideable waves are found at Bolsa Chica is likely to increase.

36. The analyses presented indicate that adverse impacts on the surf break and on surfing recreation due to the navigation project at Bolsa Chica can be reduced by 1) minimizing the width of the inlet and the length of the offshore breakwater, and 2) including a sand bypassing system in the proposed project to control fillet size and lessen erosion of downdrift beaches and subsequent deterioration of the surfbreak. Sand bypassing should be conducted so as to avoid placing a large protruding deposit, or "lump", of sediment on the face of the downdrift beach. The extremely steep bottom slope associated with such features can force the Irribarren Number into the "unsurfable" range (greater than 2.0). On the other hand, placing bypassed material in the outer surf zone has been shown to enhance surfbreak, at least until the material is naturally redistributed.

References

- Battjes, J. A. 1974. "Surf Similarity," Proceedings of the 14th Conference on Coastal Engineering, American Society of Civil Engineers, Vol 1, pp 466-480.
- Galvin, C. J. 1968. "Breaker Type Classification on Three Laboratory Beaches," Journal of Geophysical Research, Vol 73, pp 3651-3659.
- Gravens, M. B. 1988. "Preliminary Shoreline Response Computer Simulation," Report 1: Bolsa Bay, California, Proposed Ocean Entrance System Study, unpublished draft report, US Army Engineer Waterways Experiment Station, Coastal Engineering Research Center, Vicksburg, MS.
- Sherlock, A. R., and Szuwalski, A. 1987. "A User's Guide to the Littoral Environment Observation Retrieval System," Instruction Report CERC-87-3, US Army Engineer Waterways Experiment Station, Coastal Engineering Research Center, Vicksburg, MS.

APPENDIX E: NOTATION

a	Sand porosity
A	Parameter determining equilibrium beach shape
BYP	Sand bypassing factor
C_{gb}	Wave group velocity at breaking given by linear wave theory
$\cot(\beta)$	Inverse beach slope
D	Wave energy dissipation in the surf zone
D_c	Depth of closure
D_{eq}	Equilibrium wave energy dissipation in the surf zone
D_g	Depth at seaward end of groin
DLT	Depth of littoral transport
F	Wave energy flux by linear wave theory
h	Water depth
H	Wave height
H_b	Breaking wave height
H_{mo}	Energy-based wave height
H_s	Significant wave height
H_{savg}	Average significant wave height
H_{smax}	Maximum significant wave height
k	Empirical coefficient in cross-shore transport rate equation
K_1, K_2	Calibration parameters in shoreline contour model
Q	Volume rate of longshore sand transport
Q_s	Volume rate of cross-shore sand transport
S	Ratio of sand density to water density
t	time
T_p	Peak spectral wave period
x	Coordinate direction
y	Coordinate direction
α_{bs}	Breaking wave angle to the shoreline